

STATE PREPARATION AND VERIFICATION IN
CONTINUOUSLY MEASURED QUANTUM SYSTEMS

Von der Fakultät für Mathematik und Physik
der Gottfried Wilhelm Leibniz Universität Hannover
zur Erlangung des akademischen Grades

Doktor der Naturwissenschaften
Dr. rer. nat.

genehmigte Dissertation von

M. Sc. Jonas Lammers

geboren am 6. Februar 1989 in Hannover

2018

Referent: Prof. Dr. Klemens Hammerer, Leibniz Universität Hannover
Korreferent: Dr. Hendrik Weimer, Leibniz Universität Hannover
Tag der Promotion: 21.09.2018

ABSTRACT

Time-continuous measurements are a well-established part and the foundation of many quantum optical experiments. This thesis explores possible approaches to use homodyne detection of light for the efficient preparation and verification of nontrivial quantum states in material systems. In the first part we employ a measurement-based feedback scheme using interferometric measurements of light and local feedback to generate an effective many-body interaction with inherent collective dissipation between N local quantum systems. Our ultimate goal is to use this conceptually simple scheme for the reliable preparation of entangled many-body states between distant non-interacting quantum systems, which is a prerequisite for a number of quantum information protocols. To gauge the feasibility of this endeavor we generalize a known feedback protocol from a pair to an array of N two-level systems, and show that it deterministically produces entangled many-body states. Another important application is quantum simulation where an easily accessible system is used to emulate a desired quantum dynamics that is too difficult to simulate otherwise. As a proof-of-principle we show how to realize an effective Ising interaction with arbitrary range and geometry between an array of two-level systems, and analyze the effect of the resulting dissipation.

In the second part we show how to use retrodiction, i. e., the inference of knowledge about the past state from future observations, to interpret a record of continuous observations as an instantaneous Positive-Operator Valued Measure (POVM) measurement on the initial state of a monitored system. Repeated POVM measurements on an ensemble of identical quantum states can be used to reconstruct the underlying density operator via state tomography. This allows to verify the presence of nontrivial quantum states given sufficient resolution of the POVM. We focus our approach on linear systems, derive the cumulant equations of motion of general quantum states and POVM elements, and show that stable dynamics cause any operator to collapse to a Gaussian operator in steady state. We apply retrodiction to an optomechanical system in the weak-coupling regime. Here we show that large cooperativity, $C_q > 1$, and efficient homodyne detection together enable sub-shot noise resolution of the retrodicted POVMs, just like it enables the conditional preparation of squeezed states.

Keywords: Measurement-based feedback, entanglement generation, quantum simulation, quantum state verification, retrodiction

ZUSAMMENFASSUNG

Zeitkontinuierliche Messungen sind ein etablierter Teil und Grundlage vieler quantenoptischer Experimente. Diese Arbeit untersucht mögliche Ansätze zur Verwendung von Homodyn-Detektion von Licht für die effiziente Erzeugung und Verifikation von nicht-trivialen Quantenzuständen in unterschiedlichen Systemen. Im ersten Teil verwenden wir ein Feedback-Schema basierend auf der interferometrischen Messung von Licht und lokalem Feedback, um eine effektive Vielteilchenwechselwirkung mit inhärenter kollektiver Dissipation zwischen N lokalen Quantensystemen zu generieren. Unser oberstes Ziel ist es, dieses konzeptuell einfache Schema für die zuverlässige Erzeugung von verschränkten Vielteilchenzuständen zwischen voneinander entfernten, nicht-wechselwirkenden Quantensystemen zu nutzen, was die Voraussetzung für eine Reihe von Quanteninformationsprotokollen ist. Um die Machbarkeit dieses Vorhabens einzuschätzen, verallgemeinern wir ein bekanntes Feedbackprotokoll von einem Paar auf N Zwei-Level-Systeme und zeigen, dass es in der Tat deterministisch verschränkte Vielteilchenzustände erzeugt. Eine weitere wichtige Anwendung ist Quantensimulation, bei der ein leicht zugängliches System verwendet wird, um eine gewünschte Quantendynamik zu emulieren, die sonst nur schwer zu simulieren ist. Als konkretes Fallbeispiel zeigen wir, wie man eine effektive Ising-Wechselwirkung mit beliebiger Reichweite und Geometrie zwischen N Zwei-Level-Systemen realisiert und wir untersuchen den Effekt der resultierenden Dissipation.

Im zweiten Teil zeigen wir, wie man Retrodiction verwendet, also der Rückschluss auf Eigenschaften eines vergangenen Zustands aus zukünftigen Beobachtungen, um eine Aufzeichnung kontinuierlicher Messungen als instantane POVM-Messung des Anfangszustands eines observierten Systems zu interpretieren. Wiederholte POVM-Messungen an einem Ensemble identischer Quantenzustände können verwendet werden, um den zugrunde liegenden Dichteoperator mittels Zustands-Tomographie zu rekonstruieren. Dies erlaubt es, vorliegende nicht-trivialen Quantenzustände bei ausreichender Auflösung der POVM nachzuweisen. Wir konzentrieren uns auf lineare Systeme, leiten die Bewegungsgleichungen der Kumulanten von allgemeinen Quantenzuständen und POVM-Elementen her und zeigen, dass stabile Dynamik jeden Operator dazu bringt, im stationären Zustand zu einem Gaußschen Operator zu werden. Wir wenden die Retrodiction auf ein optomechanisches System im Regime der schwachen Kopplung an. Hier zeigen wir, dass große Kooperativität, $C_q > 1$, und effiziente Homodyn-Detektion zusammen die Retrodiction einer quantenrauschaufgelösten POVM ermöglichen, so wie sie auch die Erzeugung konditionaler gequetschter Zustände erlauben.

Schlagwörter: Messbasiertes Feedback, Verschränkungserzeugung, Quantensimulation, Quantenzustandsverifikation, Retrodiction

If I have seen further it is by standing on the shoulders of Giants.

— Sir Isaac Newton

ACKNOWLEDGMENTS

First, foremost, and without much ado I want to thank Klemens Hammerer. Klemens, you have been a guide and mentor, an inspiration, and a shining example during all of my time in your group. You have earned my deepest respect for your continued patience and support, and I am very grateful for all the freedom and opportunities you have given me to grow both scientifically and as a person. I have always been able to look up to you without feeling looked down upon. I can only hope that I was able to justify the trust you placed in me.

Since physics is a truly collaborative science, I naturally met many amazing people along the way. I would especially like to thank Hendrik Weimer for teaching me about phase-transitions, many-body dynamics, and for agreeing to referee this thesis. My gratitude also goes to Michèle Heurs for many interesting conversations, for giving me a piece of chocolate despite not knowing the benefits of a ring resonator, and for agreeing to supervise my disputation. I would also like to thank Reinhard Werner for many insightful sessions on all parts of this thesis, which often resulted in a new angle at our work, and for being my RTG co-supervisor. I am also grateful to Stefan Danilishin for the numerous interesting discussions in Glasgow, Erlangen, and Hannover, for patiently sharing his insights into Wiener filtering, and for connecting this formalism to ours. Similarly, I thank David Reeb for his interest, input, and questions, and for patiently answering all of my questions on Bayesian estimation and machine learning. I also thank Wassilij Kopylov and the late Tobias Brandes for inviting me to Berlin for interesting discussions on feedback, and to Klaus Mølmer for sharing his insights into retrodiction.

This work would not have been possible without the efforts of Sebastian Hofer, who first introduced me to continuous measurements, stochastic calculus, and feedback master equations. I am grateful for all the discussions and critical questions that always deepened my understanding, and for agreeing to proofread parts of this thesis. I would also like to thank Lars Dammeier for agreeing to proofread parts of this work, and for being a fellow feedback sufferer. I am also grateful to Sahand Mahmoodian for providing constructive criticism despite suffering under the recent $> 30^\circ\text{C}$ heat wave, and to Corentin Gut for hunting down many elusive mistakes.

Another person who was instrumental from beginning to end of my PhD is Birgit Gemmeke, who somehow manages to juggle a number of different hats while still having time for a chat and a smile. The same goes for all past and present members of Klemens' group, in particular Marius, Jannis, Corentin, Sahand, and Ondřej, who suffered through my rants, provided distraction when needed, and were wonderful colleagues to work with, and to Denis, Niels, and Alexander for introduc-

ing me cryptography, QuTiP, and machine learning. No matter where life takes me, this friendly and open atmosphere will be difficult to find again.

I was lucky to have been associated with many institutions that allowed me to attend numerous talks, workshops, summer schools, and Christmas parties, including the ITP, AEI, QUEST, SFB1227, and RTG1991. Here I am particularly grateful to the Quantum Information group, especially to Lars Dammeier and Inken Siemon, for many interesting discussions and providing lots of moral support, and to the Quantum Control and 10m Prototype groups for being wonderful neighbors.

Last but not least I am grateful to all the people who make up my life outside the office. I want to thank Jan, Luise, and Sandra for all the moral support, and Roman, Rouven, Alex, and Philipp & Olga for the continued friendship. I would have never made it this far without the continued help of my family, Karla, Thomas, and Lisa, who encouraged me in all my endeavors. Most of all I want to thank Christina, who suffered with me and supported me through the numerous lows of scientific life.

CONTENTS

1	INTRODUCTION	1
2	MEASUREMENTS IN QUANTUM MECHANICS	7
2.1	Projective measurements	7
2.1.1	Pure states	7
2.1.2	Measurement postulate	7
2.1.3	Idealizations of the measurement postulate	8
2.1.4	Mixed states: density matrices	9
2.2	General measurements	10
2.2.1	Example: indirect measurement	10
2.2.2	General measurement postulate	11
2.2.3	Infinite-dimensional Hilbert spaces	12
I STATE PREPARATION THROUGH FEEDBACK		
3	FEEDBACK MASTER EQUATIONS	15
3.1	Derivation of an unconditional master equation	15
3.1.1	Introducing the setup	15
3.1.2	Coarse-graining of time	17
3.1.3	Interaction between system and bath mode	18
3.1.4	Tracing out the bath	20
3.2	Including measurement-based feedback	21
3.2.1	Adding phase plate and measurement	21
3.2.2	Applying feedback	23
3.2.3	Generalization to multiple systems	26
3.2.4	Generalization to multiple light modes	31
3.3	Parametrization of LOCC dynamics	32
4	DISSIPATIVE STATE PREPARATION	35
4.1	Entangling two-qubit protocol	35
4.2	Extension to multiple qubits	37
4.3	Analysis of the steady state	39
4.4	Outlook on preparation of general states	41
5	QUANTUM SIMULATION	43
5.1	Open Ising model with transverse fields	43
5.1.1	Engineering the Hamiltonian	43
5.1.2	Effect of the dissipation	45
5.2	Concrete example	46
5.3	Conclusion and Outlook	50
II STATE VERIFICATION THROUGH RETRODICTION		
6	STOCHASTIC MASTER AND EFFECT EQUATIONS	53
6.1	Derivation of a stochastic master equation	53
6.1.1	Expanding the conditional state	53
6.1.2	Statistics of the measurement current	54
6.1.3	Normalization of the state	56
6.1.4	Generalization to multiple baths	56
6.2	Backward effect equations	57
6.2.1	Quantum channels	58

6.2.2	Retrodiction	60
6.2.3	One-stop preparation and measurement	61
6.2.4	Time-continuous effect equations	62
6.3	Backward Itô integration	64
7	LINEAR SYSTEMS AND GAUSSIAN STATES	69
7.1	Linear systems	69
7.2	Quantum characteristic functions	70
7.2.1	Moments and cumulants	71
7.2.2	Unnormalized characteristic functions	72
7.3	Gaussian states and effect operators	73
7.3.1	Gaussian quantum states	73
7.3.2	Gaussian effect operators	74
7.4	Evolution of means and covariance matrix	76
7.4.1	Gaussian quantum states	76
7.4.2	Gaussian effect operators	78
7.4.3	Non-Gaussian operators	80
7.5	Stable dynamics leads to Gaussian operators	82
7.5.1	Stability of linear systems	82
7.5.2	Gaussification of arbitrary initial states	83
7.5.3	Gaussification of arbitrary effect operators	84
8	APPLICATIONS	85
8.1	Basic examples	85
8.1.1	Monitoring a decaying cavity	85
8.1.2	Beam splitter vs. squeezing interaction	88
8.2	Conditional state preparation and verification in optomechanics	89
8.2.1	Optomechanical setup	90
8.2.2	Optomechanical interaction	91
8.2.3	Mechanical master equation	92
8.2.4	Steady state: resonant drive	94
8.2.5	Steady state: detuned drive	100
8.2.6	Conclusion and generalization	101
9	CONCLUSION AND OUTLOOK	103
III APPENDIX		
A	HOMODYNE DETECTION	107
A.1	Intensity vs. quadrature measurement	107
A.2	Beam splitter	108
A.3	Detection efficiency	109
B	CUMULANT EQUATIONS OF MOTION	111
B.1	From operator to partial differential equation	111
B.2	Hamiltonian	112
B.3	Lindblad operators	114
B.4	Measurement terms	115
B.5	Combined evolution	117
B.6	Backward addition	119
C	OPTOMECHANICS: STEADY STATE VARIANCES AND MODE FUNCTIONS	121
C.1	Drive on resonance, detect sidebands	121
C.1.1	Blue sideband, $\Delta_{l_0} = +\omega_m$	121

c.1.2	Red sideband, $\Delta_{l_0} = -\omega_m$	123
c.2	Summary	124
c.2.1	Resonant detection, $\Delta_{l_0} = 0$	124
c.2.2	Blue, $\Delta_{l_0} = +\omega_m$	125
c.2.3	Red, $\Delta_{l_0} = -\omega_m$	126
c.3	Drive off-resonantly	126
c.3.1	Resonant detection, $\Delta_{l_0} = 0$	127
c.3.2	Blue sideband, $\Delta_{l_0} = +\omega_{\text{eff}}$	128
c.3.3	Red sideband, $\Delta_{l_0} = -\omega_{\text{eff}}$	129
c.4	Summary	131
c.4.1	Resonant detection, $\Delta_{l_0} = 0$	131
c.4.2	Blue, $\Delta_{l_0} = +\omega_m$	132
c.4.3	Red, $\Delta_{l_0} = -\omega_m$	133

BIBLIOGRAPHY	135
--------------	-----

CURRICULUM VITAE	145
------------------	-----

INTRODUCTION

Measurements in quantum mechanics are tricky business. In classical physics measuring a system may change an observer's state of knowledge, but does not necessarily have an effect on the physical state. In quantum mechanics measurements are described by the measurement postulate [1], which prescribes that the measurement of an *observable*, given by a Hermitian operator \hat{A} , projects or *collapses* the measured system into an eigenstate of \hat{A} . Unless it was already in an eigenstate, this necessarily changes the state of the system. This *measurement back action* is thus inherent to quantum theory.

The projective measurement postulate is in various ways an idealization of a physical measurement process. For example, the collapse occurs instantly whereas any physical measurement device will take some time to record and output a value. More importantly, the postulate assumes a direct measurements of the system without specifying how this is done. In practice the system of interest first needs to couple coherently to some detector, which then triggers a chain of events that eventually reaches the observer's mind. This is called a *von Neumann chain* [1], and an important question is where along this chain we can apply the measurement postulate and consider the measurement complete, known as *Heisenberg cut* [2].

Many physical systems are not directly measurable, but first need to be coupled to a probe. A highly effective and versatile probe is light. Optical measurements are well-described by making the Heisenberg cut at the photodetector, and applying the measurement postulate directly to the light field. Furthermore, many material systems are amenable to strong interactions with microwave and optical fields, which has led to the tremendous success of quantum optics. Nowadays the precision of measurement and control achieved by using photons has reached the quantum limit, which recently culminated in the Nobel prize being awarded jointly to David Wineland [3] and Serge Haroche [4].

An achievement of modern quantum theory is the description of indirect, non-projective measurements by a generalized measurement postulate. In place of projection operators one considers general measurement operators. These allow to describe weak measurements, which only partially collapse the system state, and to include uncertainty in the measurement, for example if an outcome may correspond to different states. A further generalization was the inclusion of continuous measurements, realized in the limit of both weak coupling and high repetition rate. This was made possible by the development of *quantum stochastic calculus* by Belavkin [5], and Hudson and Parthasarathy [6].

In recent years it has become possible to probe a range of platforms efficiently using continuous phase-sensitive measurements [7]. These include finite-dimensional systems such as superconducting qubits coupled to microwaves [8, 9] and atoms in optical cavities [10, 11], as well

as continuous-variable systems such as atomic ensembles in Holstein-Primakoff approximation [12, 13] and mechanical oscillators [14].

These developments have been made possible by the realization of large values of the *cooperativity* C_q , which captures the relative strength of the coherent system-light coupling compared to all unobserved dissipation channels. Reaching large $C_q > 1$ signifies that the system couples mostly to the observed channel, making it the dominant noise source. This results in entangled states between system and light, and thus between system and detector, which enables the observation of quantum features.

This thesis addresses questions that result from these developments. Our goal is two-fold. First, we use continuous measurements on an array of local systems to devise a simple feedback protocol, which enables the preparation of nontrivial quantum many-body states and the simulation of many-body Hamiltonians. Using only linear optics and homodyne measurements allows to project an array of non-interacting material systems into correlated quantum states – in the spirit of massive parallel entanglement swapping akin to protocols proposed in [15–18]. Subsequent application of Wiseman-Milburn Feedback [19, 20] to the systems generates effective many-body dynamics, which we show to go beyond Local Operations and Classical Communication (LOCC).

Second, we explore the possibility to use continuous measurements for the verification and tomography of quantum states. Monitoring a quantum system to infer knowledge about its past is a field of active research. Extensive work on this topic has been done by Mankei Tsang [21–23] who introduced a quantum theory of *time-symmetric smoothing*, which uses continuous measurements to estimate the past value of a classical parameter coupled to a quantum system. Gammelmark, Julsgaard and Mølmer [24] proposed a theory of *past quantum states* in which the usual quantum state is complemented by an *effect operator* \hat{E} that is conditioned on future observations. In their formalism \hat{E} provides a Bayesian update to the measurement probabilities of past observables. This theory was applied successfully to superconducting qubits [25], see also [26] for a review. Recently, Zhang and Mølmer [27] specialized the past quantum state formalism to Gaussian states in continuous variable systems. An alternative approach to quantum smoothing was suggested by Guevara and Wiseman [28]. Instead of applying a Bayesian update to the probabilities of past measurements as Mølmer and co-workers do, they introduce a smoothed quantum state, where the probabilities of the density matrix are conditioned.

We aim to complement this previous work on estimation of past states. Instead of applying a Bayesian update to either measurement results or density matrix, we interpret the continuous observation of a quantum system as an instantaneous Positive-Operator Valued Measure (POVM) measurement on its state in the past. We focus our approach on linear systems with Gaussian states, and demonstrate its effectiveness by applying it to the nontrivial example of an optomechanical system in the weak-coupling regime. We show that one can realize effective POVMs with sub-shot noise precision provided the cooperativity is sufficiently large, i. e., $C_q > 1$.

Outline

I begin in Chap. 2 with a brief review of the general theory of measurements in quantum mechanics, since these form the basis from which continuous measurements are derived. I start from the basic projective measurement postulate, and introduce classical uncertainty in the form of density matrices. I then show the effect of a projective measurement on part of a correlated state, composed of system and probe, which leads me to the general measurement postulate. This chapter is only a review of material found in standard text books.

Part I of this thesis treats a simple yet versatile feedback setup involving interferometric measurements and local feedback. It is mostly based on the article [29] for which I did the majority of the analytical and numerical computations, prepared the larger part of the manuscript, and most of the figures. Hendrik Weimer contributed to the manuscript, especially regarding the variational method presented and used in Sec. 4.3 that resulted in part of Fig. 4.4, and to the discussion of the Ising model in Sec. 5.1. The ideas for this article were developed jointly with Klemens Hammerer who also contributed to the manuscript, and to some computations.

In Chap. 3 I provide an intuitive derivation of an unconditional (i. e., deterministic) master equation for a single quantum system before adding continuous measurements and feedback to derive a Feedback Master Equation (FME). I do so while avoiding the use of quantum stochastic calculus to keep the derivation simple. After generalizing the equation to an array of N systems, I close with a classification of *local operation and classical communication* (LOCC) dynamics by providing a sufficient criterion for the FME to yield only LOCC dynamics.

Chapters 4 and 5 showcase some applications of the FME. In Chap. 4 I first review a known feedback protocol for a pair of two-level systems devised in [30], and shown to produce entanglement deterministically. I then generalize it to an array of N two-level systems, and show that it produces a steady state which is entangled independent of the number of involved systems. This is confirmed by the variational method of Hendrik Weimer.

In Chap. 5 I apply the FME to the problem of quantum simulation by considering a dissipative Ising model. After engineering a general Ising Hamiltonian I consider the jump operators that are inevitably part of the FME. Then I consider a concrete one-dimensional nearest-neighbor Ising model and investigate whether changing any of the remaining degrees of freedom of the FME allows to induce a phase transition. Hendrik Weimer contributed key ideas to the discussion of the phase transition.

Part II explores the possibility to use continuous measurements for the verification of quantum states through *retrodiction*. This is unpublished material to which I contributed a majority of the analytical computations, and created all figures. Ideas were developed jointly with Klemens Hammerer who also contributed to the calculations.

Chapter 6 begins by extending the derivation from Chap. 3 to conditional quantum states, and results in the general known Stochastic Master Equation (SME) for an arbitrary number of measurement and dissipation channels. I review the theory of Quantum Channels and POVMs

before showing that effect operators (POVM elements) satisfy a stochastic equation adjoint to the SME, and in particular that even the trivial effect operator $\hat{E} = \hat{1}$ will correspond to an effective measurement after conditional backpropagation. This summarizes the work of Gammelmark, Julsgaard and Mølmer [24], but differs from it by interpreting the retrodicted effect operator as an effective measurement on an unknown initial quantum state. I close the chapter by showing that the adjoint effect equation needs to be interpreted as a backward Itô equation. This was previously stated by Mankei Tsang [21–23] whose derivation is based on [31]. Our derivation is novel and only based on a recent result [32] on nested stochastic integrals.

I begin Chap. 7 with a review of linear systems, quantum characteristic functions, and Gaussian states, before deriving the equations of motion for the means and covariance matrix of Gaussian quantum states and Gaussian effect operators. These equations have previously been derived by Zhang and Mølmer [27]. I then go on to derive the equations of motion for cumulants of arbitrary (non-Gaussian) states and effect operators. In particular I show that in stable systems the unconditional cumulants decay exponentially, turning any state into a Gaussian state. I contributed both the derivation and the proof, and I am not aware of this result having appeared previously.

Chapter 8 presents applications of retrodiction, and opens with the basic example of a freely decaying cavity. I use this to explore the effects of different couplings between system and probe on the performance of retrodiction and conditional state preparation. I then consider the non-trivial example of an optomechanical system inside a cavity that can be adiabatically eliminated. This procedure is due to Sebastian Hofer and has appeared in [33, 34]. Using the resulting conditional mechanical master equation, I investigate how detecting different sidebands of the output affects the performance of preparation and retrodictive measurement of the mechanical state. I contributed the analytical computations, while ideas and discussions were developed jointly with Klemens Hammerer.

A FEW WORDS ON NOTATION

I will use hats, such as \hat{a} , to distinguish quantum operators from classical quantities, except the density operator ρ . Vectors are depicted as bold lower case letters, \mathbf{r} , while matrices are capital letters, M . An exception are the $N \times N$ -dimensional unit and null matrices depicted as $\mathbf{1}_N$ and $\mathbf{0}_N$. Brackets $[\hat{A}, \hat{B}] = \hat{A}\hat{B} - \hat{B}\hat{A}$ denote a commutator, while braces denote the anti-commutator, $\{\hat{A}, \hat{B}\} = \hat{A}\hat{B} + \hat{B}\hat{A}$. Complex conjugation is indicated by a star, r^* , while Hermitian conjugation of matrices and operators is indicated by a dagger, and the transpose by a T, so $M^\dagger = (M^*)^T$.

ACRONYMS

SME Stochastic Master Equation

CAO Creation and Annihilation Operator

FME Feedback Master Equation
BS Beam Splitter
TMS Two-Mode Squeezing
POVM Positive-Operator Valued Measure

In this section we review the theory of general measurements in quantum mechanics of which time-continuous diffusive measurements are a special case. Most of the material in this section can be found in standard textbooks [2, 35, 36] and the more comprehensive mathematical texts [37–40]. We include this review to introduce some notation and concepts that will be used throughout this thesis. Placing clarity above rigor, our treatment is bound to be incomplete. In particular we elaborate only briefly on the intricacies of infinite-dimensional Hilbert spaces.

2.1 PROJECTIVE MEASUREMENTS

2.1.1 Pure states

The state space of a quantum mechanical system \mathcal{S} may be represented as a Hilbert space \mathcal{H} , which is a d -dimensional complex vector space with a scalar product $\langle \cdot | \cdot \rangle : \mathcal{H} \times \mathcal{H} \rightarrow \mathbb{C}$. The dimension d may be finite or infinite and we comment on the difference below. Using Dirac notation we write elements of \mathcal{H} as *kets* $|\psi\rangle \in \mathcal{H}$. Unless noted otherwise any ket is a unit vector so $\| |\psi\rangle \|^2 = \langle \psi | \psi \rangle = 1$. These represent states of maximal knowledge of \mathcal{S} , also called *pure states*. The *dual* of $|\psi\rangle$, also called *bra*, is a linear map $\langle \psi | : \mathcal{H} \rightarrow \mathbb{C}$ that takes any $|\phi\rangle \in \mathcal{H}$ to the scalar product $\langle \psi | \phi \rangle$.

Pure states are suited for the description of *closed* systems. This assumes perfect knowledge of the dynamics, and that all interactions of \mathcal{S} are captured by a Hermitian *Hamiltonian operator* $\hat{H} : \mathcal{H} \rightarrow \mathcal{H}$. The Hamiltonian determines the time evolution of \mathcal{S} via the *Schrödinger equation*

$$i \frac{d}{dt} |\psi(t)\rangle = \hat{H} |\psi(t)\rangle, \quad (2.1)$$

which gives rise to a unitary time-evolution operator

$$\hat{U}(t_0, t_1) := \exp(-i\hat{H}(t_1 - t_0)). \quad (2.2)$$

This maps pure states to pure states, and propagates arbitrary initial states $|\psi(t_0)\rangle$ to a later time,

$$|\psi(t_1)\rangle = \hat{U}(t_0, t_1) |\psi(t_0)\rangle, \quad t_0 \leq t_1 \quad (2.3)$$

The evolution of closed systems is reversible. Given some $|\psi(t_1)\rangle$ we can always retrieve the unique initial state $|\psi(t_0)\rangle = \hat{U}^\dagger(t_0, t_1) |\psi(t_1)\rangle$.

2.1.2 Measurement postulate

The abstract state space of \mathcal{S} connects to physical reality through the measurement postulate. This states that an ideal measurement A on \mathcal{S}

is described by a collection $\{(y, |y\rangle), m \in \mathcal{M}\}$ of possible (discrete, non-degenerate) *measurement outcomes* $y \in \mathbb{R}$ and orthogonal states $|y\rangle$ which form a basis of \mathcal{H} . Performing the measurement essentially checks which one of these basis states the system is in. The device will output a result, y say, after which we *will* find \mathcal{S} in the state $|\psi_y\rangle = |y\rangle$, even though previously it was in the arbitrary state $|\psi\rangle$. Which result and state we obtain is random with probability $p(y|\psi) = |\langle y|\psi\rangle|^2 = \langle \psi|\hat{\Pi}_y|\psi\rangle$, where $\hat{\Pi}_y = |y\rangle\langle y|$ is a *projection operator*. Note that this randomness is inherent to quantum mechanical measurements and not due to uncertainty about the state. The procedure can also be written as

$$|\psi\rangle \xrightarrow{y} |\psi_y\rangle = \frac{\hat{\Pi}_y|\psi\rangle}{\sqrt{p(y|\psi)}}, \quad (2.4a)$$

$$p(y|\psi) = \langle \psi|\hat{\Pi}_y|\psi\rangle. \quad (2.4b)$$

Measurements of this type are called *von Neumann measurements* [1, Sec. III.5] or *projective measurements*, and the procedure (2.4) is known as *Born's rule*. If we construct a Hermitian *observable*

$$\hat{A} = \sum_y y \hat{\Pi}_y, \quad (2.5)$$

then the average or *expectation value* of the measurement A on the state $|\psi\rangle$ can be written as

$$\langle \hat{A} \rangle_\psi := \langle \psi|\hat{A}|\psi\rangle = \sum_y y p(y|\psi). \quad (2.6)$$

2.1.3 Idealizations of the measurement postulate

There are various ways in which both pure states and the measurement postulate are an idealization.

Classical uncertainty

In practice we never have perfect knowledge of a physical system, so pure states are always an idealization. Any physical model focuses only on some aspects of nature that are deemed relevant while neglecting others. This turns a closed into an open system, which dissipates into some *environment*, i. e., somewhere outside our model. In addition to technical imprecisions this inevitably lead to reduced certainty about the system state $|\psi\rangle$, but also about the post-measurement state $|\psi_y\rangle$ associated with outcome y of the measurement. Uncertainty about states can be incorporated into the theory by considering mixed instead of pure states, which we do in Sec. 2.1.4. But to describe a noisy measurement process we need to extend the measurement postulate (2.4), see Sec. 2.2.

Instantaneous collapse

The measurement occurs instantly so from one moment to the next the system *collapses* to a particular state, $|\psi\rangle \rightarrow |\psi_y\rangle$. However, any realistic measurement process, i. e., the reaction of a detection apparatus to a stimulant, takes a finite amount of time so this assumption can only be true in an approximate sense.

Direct measurement

The postulate assumes a direct measurement of the system which is never the case in practice [1, Sec. VI.1]. For example, consider trying to measure the internal state of an atom. There is no apparatus that directly reads out the atomic state. Instead the atom interacts with modes of the electromagnetic field which are observed through photodetection. Here a photon is absorbed by the active region of the photodetector, which causes a current to flow, which triggers a screen to emit more photons, which impinge on the experimenter's retina, and so on [2]. At some point along this chain one has to make a cut, known as Heisenberg's cut, to separate the quantum world from the classical and consider the measurement complete.

It turns out that one obtains quite useful predictions by treating the atom and light quantum mechanically, and making the cut at the level of the photodetector. Considering the light to be measured *directly and instantaneously* addresses the two previous concerns. The fact that measurements of the electromagnetic field are described so well by the measurement postulate is one of the main reasons for the success of quantum optics. However, to describe indirect measurements on quantum systems that can be measured only through interaction with light (or some other probe) we need to understand how quantum systems are coupled and to modify Eqs. (2.4). We do both in Sec. 2.2.

2.1.4 Mixed states: density matrices

A system \mathcal{S} is *open* if it interacts (i. e., becomes correlated) with some other system \mathcal{A} (called *environment*, *bath* or *probe*) that is not part of our description. This causes information about the state of \mathcal{S} to leak or *dissipate* into the environment, which reduces our (the "observers") certainty about the actual state of the system. To incorporate this uncertainty we need to replace pure state vectors $|\psi\rangle \in \mathcal{H}$ by *density operators* $\rho \in \mathcal{B}(\mathcal{H})$, which are bounded operators on \mathcal{H} . They are also called *density matrices*¹ or *mixed states*, and they provide a more general description of the system state than pure states: any $|\psi\rangle$ can be represented as $\rho = |\psi\rangle\langle\psi|$, and the dynamics of a closed system with Hamiltonian \hat{H} are given by

$$\frac{d}{dt}\rho(t) = -i[\hat{H}, \rho(t)] = -i(\hat{H}\rho(t) - \rho(t)\hat{H}), \quad (2.7)$$

which is equivalent to the Schrödinger equation (2.1), and gives rise to unitary time evolution analogous to Eqs. (2.2) and (2.3),

$$\rho(t_1) = \hat{U}(t_0, t_1)\rho(t_0)\hat{U}^\dagger(t_0, t_1). \quad (2.8)$$

However, beyond this ρ can also be any convex combination of pure states $|\phi_j\rangle$,

$$\rho = \sum_j p_j |\phi_j\rangle\langle\phi_j|, \quad (2.9)$$

with $p_j \geq 0$ and $\sum_j p_j = 1$, and in fact any convex combination of density matrices ρ_j is again a density matrix,

$$\rho = \sum_j p_j \rho_j. \quad (2.10)$$

¹ Technically it is not a matrix if $d = \infty$.

Density matrices are Hermitian positive semi-definite trace class operators with unit trace

$$\mathrm{Tr}\{\rho\} := \sum_y \langle y|\rho|y\rangle = \sum_j p_j = 1. \quad (2.11)$$

It is straightforward to check that the second equality holds regardless of whether ρ is of the form (2.9) or (2.10), and that it is independent of the choice of basis $\{|y\rangle\}$ as the trace should be [39].

The coefficients p_j are probabilities that represent our certainty about the actual state of the system. As long as all $p_j < 1$ we can, in principle, learn more about the system by gathering information². This is different from a pure superposition $|\psi\rangle = \sum_j \alpha_j |\phi_j\rangle$, which already is a zero entropy state that corresponds to $\rho = |\psi\rangle\langle\psi|$ with unit probability. There is nothing we can do to increase our knowledge about $|\psi\rangle$. A good measure of this classical uncertainty is the *purity*, defined as

$$\mathcal{P}(\rho) = \mathrm{Tr}\{\rho^2\}. \quad (2.12)$$

The purity of any state is bounded by $d^{-1} \leq \mathcal{P}(\rho) \leq 1$, with $\mathcal{P}(\rho) = 1$ if and only if we have maximal knowledge so ρ is a pure state, i. e., $p_j = 1$ for some j .

The measurement postulate from Eqs. (2.4) can be extended to mixed states through

$$\rho \xrightarrow{y} \rho_y = \frac{\hat{\Pi}_y \rho \hat{\Pi}_y}{p(y|\rho)}, \quad (2.13a)$$

$$p(y|\rho) = \mathrm{Tr}\{\hat{\Pi}_y \rho\}, \quad (2.13b)$$

and similarly we obtain averages of observables via

$$\langle \hat{A} \rangle_\rho = \mathrm{Tr}\{\hat{A} \rho\}. \quad (2.14)$$

2.2 GENERAL MEASUREMENTS

A more general measurement postulate than the one given in Sec. 2.1 is motivated by the following situation.

2.2.1 Example: indirect measurement

As alluded to in Sec. 2.1.3 many systems can only be measured indirectly by coupling to a probe. Consider a system \mathcal{S} (e. g., an atom) and a probe \mathcal{A} (e. g., an incoming field mode) that are described by the tensor product Hilbert space $\mathcal{H}^{\mathcal{S}\mathcal{A}} = \mathcal{H}^{\mathcal{S}} \otimes \mathcal{H}^{\mathcal{A}}$. Initially they are not correlated so their state is a product state $\rho^{\mathcal{S}\mathcal{A}}(t_0) = \rho^{\mathcal{S}}(t_0) \otimes \rho^{\mathcal{A}}(t_0)$. For simplicity we assume we have perfect knowledge of the probe, so it starts in a pure state $\rho^{\mathcal{A}}(t_0) = |\phi\rangle\langle\phi|$. We let \mathcal{S} and \mathcal{A} interact for some time $t = t_1 - t_0$ via a time-evolution operator $\hat{U} := \exp(-i\hat{H}^{\mathcal{S}\mathcal{A}}t)$. This generally produces an *entangled* state $\rho^{\mathcal{S}\mathcal{A}}(t_1) = \hat{U}\rho^{\mathcal{S}\mathcal{A}}(t_0)\hat{U}^\dagger$, which can no longer be written as a product state. A measurement of local properties of \mathcal{A} will thus be affected by the state of \mathcal{S} and vice versa.

² For example by continuously observing the environment, see Chap. 6.

We now measure some probe observable $\hat{A} = \sum_y y \hat{1} \otimes \hat{\Pi}_y$ and assume the measurement outputs a value y . Applying the projective measurement postulate (2.13) yields the state

$$\rho_y^{\mathcal{S}\mathcal{A}} \propto (\hat{1} \otimes \hat{\Pi}_y) \rho^{\mathcal{S}\mathcal{A}}(t_1) (\hat{1} \otimes \hat{\Pi}_y) \quad (2.15)$$

$$= |y\rangle\langle y| \left(\hat{U} \rho^{\mathcal{S}\mathcal{A}}(t_0) \hat{U}^\dagger \right) |y\rangle\langle y| \quad (2.16)$$

$$= \left(\langle y| \hat{U} |\phi\rangle \rho^{\mathcal{S}}(t_0) \langle \phi| \hat{U}^\dagger |y\rangle \right) \otimes |y\rangle\langle y| \quad (2.17)$$

$$= \left(\hat{M}_y \rho^{\mathcal{S}}(t_0) \hat{M}_y^\dagger \right) \otimes |y\rangle\langle y|, \quad (2.18)$$

with system operator $\hat{M}_y \equiv \hat{M}_y^{\mathcal{S}} := \langle y| \hat{U} |\phi\rangle$, and normalization given by the probability

$$p(y|\rho^{\mathcal{S}\mathcal{A}}(t_1)) = \text{Tr} \left\{ \hat{\Pi}_y \rho^{\mathcal{S}\mathcal{A}}(t_1) \right\} \quad (2.19)$$

$$= \text{Tr} \left\{ \hat{M}_y \rho^{\mathcal{S}}(t_0) \hat{M}_y^\dagger \right\} \quad (2.20)$$

$$= \text{Tr} \left\{ \hat{M}_y^\dagger \hat{M}_y \rho^{\mathcal{S}}(t_0) \right\}. \quad (2.21)$$

Because the probabilities sum to one,

$$1 \stackrel{!}{=} \sum_y p(y|\rho^{\mathcal{S}\mathcal{A}}(t_1)) = \text{Tr} \left\{ \sum_y \hat{M}_y^\dagger \hat{M}_y \rho^{\mathcal{S}}(t_0) \right\}, \quad (2.22)$$

for any state $\rho^{\mathcal{S}}(t_0)$ we can conclude that $\sum_y \hat{M}_y^\dagger \hat{M}_y \equiv \hat{1}$. Since we know both the initial probe state $|\phi\rangle$ and the dynamics \hat{U} , determining the probabilities $p(y|\rho^{\mathcal{S}\mathcal{A}}(t_1)) \equiv p(y|\rho^{\mathcal{S}}(t_0))$ actually reveals something about the initial *system* state. After the measurement \mathcal{S} and \mathcal{A} are in the uncorrelated product state (2.18) so we can take a partial trace over the probe which leaves us with the system state

$$\rho_y^{\mathcal{S}} = \frac{\hat{M}_y \rho^{\mathcal{S}}(t_0) \hat{M}_y^\dagger}{p(y|\rho^{\mathcal{S}}(t_0))}. \quad (2.23)$$

2.2.2 General measurement postulate

This example motivates the

General measurement postulate. A general measurement of a quantum system is described by a collection $\{(y, \hat{M}_y), y \in \mathcal{Y}\}$ of possible outcomes y and corresponding measurement operators $\hat{M}_y \in \mathcal{B}(\mathcal{H})$. If the system was in state ρ before the measurement, and the apparatus outputs a result y , the post-measurement state will be

$$\rho \xrightarrow{y} \rho_y = \frac{\hat{M}_y \rho \hat{M}_y^\dagger}{p(y|\rho)}, \quad (2.24a)$$

$$p(y|\rho) = \text{Tr} \{ \hat{M}_y^\dagger \hat{M}_y \rho \}. \quad (2.24b)$$

Conservation of probability requires $\sum_y \hat{M}_y^\dagger \hat{M}_y = \hat{1}$.

We retrieve the known projective measurement theory if we measure an observable with eigenvalues y and each $\hat{M}_y = \hat{\Pi}_y$ is a projection operator orthogonal to all others. Equation (2.24b) then requires a resolution of the identity, $\sum_y \hat{\Pi}_y = \hat{1}$. In general, however, the measurement operators need not be orthogonal.

The formalism can also describe *inefficient* measurements, for example if not all (or none) of the probe light is detected or the initial probe state is mixed. In that case a single result y may correspond to a number of different post-measurement states of the system and the total state

$$\rho_y = \frac{\sum_{k=0}^{K_y} \hat{M}_{k|y} \rho \hat{M}_{k|y}^\dagger}{p(y|\rho)}, \quad (2.25a)$$

$$p(y|\rho) = \text{Tr} \left\{ \sum_k \hat{M}_{k|y}^\dagger \hat{M}_{k|y} \rho \right\}, \quad (2.25b)$$

will be a mixture of these, depending on the number K_y of different measurement operators associated with y . The transition to a continuum of outcomes and measurement operators, replacing sums by integrals, is straightforward.

2.2.2.1 Positive-operator valued measures

Sometimes we are not interested in the post-measurement state $\rho_y = \hat{M}_y \rho \hat{M}_y^\dagger$, but only in the probabilities $p(y|\rho) \propto \text{Tr} \{ \hat{M}_y^\dagger \hat{M}_y \rho \}$. For example photodetection will always leave us with the vacuum state, but nonetheless lets us determine the statistics of the incoming field. In this case instead of the measurement operators \hat{M}_y it suffices to consider the positive self-adjoint *effect operators*

$$\hat{E}_y := \hat{M}_y^\dagger \hat{M}_y. \quad (2.26)$$

In fact, making no reference to the measurement operators at all we define any collection $\{ \hat{E}_y, y \in \mathcal{Y} \} \subset \mathcal{B}(\mathcal{H})$ of positive self-adjoint operators that resolve the identity, $\sum_y \hat{E}_y = \hat{1}$, as a Positive-Operator Valued Measure (POVM) [35, 41]. Note that if we are only given a POVM $\{ \hat{E}_y, y \in \mathcal{Y} \}$ there is not much sense in considering the post-measurement state since the decomposition (2.26) of effect operators into measurement operators is not unique.

2.2.3 Infinite-dimensional Hilbert spaces

If $d = \infty$ there are *unbounded* operators that are defined only on a domain $\mathcal{D} \subsetneq \mathcal{H}$ which is no longer the whole space \mathcal{H} [40]. Some of the statements in this section strictly apply only to finite-dimensional systems. But given the operational approach of this thesis, these are technicalities which shall not concern us. Ultimately, any physical system has limited energy and can thus be approximated arbitrarily well by a finite set of states.

Part I

STATE PREPARATION THROUGH FEEDBACK

In this part we are going to explore a simple yet versatile feedback setup involving interferometric measurements and local feedback operations. It is mostly based on the article [29] for which I did the majority of the analytical and numerical computations, prepared the larger part of the manuscript, and most of the figures. Hendrik Weimer contributed to the manuscript, especially regarding the variational method presented and used in Sec. 4.3 that resulted in part of Fig. 4.4, and to the discussion of the Ising model in Sec. 5.1. The ideas for this article were developed jointly with Klemens Hammerer who also contributed to the manuscript, and to some computations.

The description of quantum dynamics under continuous diffusive measurement (that is, in our context, homodyne detection of light) is thoroughly described in the formalism of stochastic Schrödinger and master equations, as pioneered by Belavkin [5] and Hudson and Parthasarathy [6]. Measurement-based feedback was incorporated by Wiseman and Milburn [19, 20, 42], and summarized comprehensively in textbooks of Wiseman and Milburn [2] and Jacobs [36]. This formalism provides stochastic equations of motion for quantum states *conditioned* on the measurement result (that is, the photocurrent³). The equation of motion for the *unconditional* quantum state can then easily be obtained in the ensemble average over all measurement results, which removes all stochastic terms. Following [2], we refer to the equation of motion describing unconditional, ensemble averaged quantum dynamics under continuous measurement and feedback as the Feedback Master Equation (FME). In this section we provide a derivation of the FME which is similar in spirit to the ones given in [43–45] but avoids the use of stochastic calculus [46] and quantum Langevin equations [45], and relies only on concepts from basic quantum mechanics. This necessarily comes at the expense of mathematical rigor, which we try to make up for by physically motivating any restrictions we impose. Similar derivations have been presented before [30, 33]. The following derivation has previously appeared in the article [29], and was adapted where necessary.

³ We also refer to processed detector outputs as “photocurrent,” such as a normalized homodyne signal.

3.1 DERIVATION OF AN UNCONDITIONAL MASTER EQUATION

We first consider the case of a single system coupled to a single light field in detail, see Fig. 3.1. The generalization to N systems coupled to $M \geq N$ beams of light and feedback fields is then straightforward, as depicted in Fig. 3.2.

3.1.1 Introducing the setup

We consider the setup depicted in Fig. 3.1 comprising a quantum system \mathcal{S} (“the system,” e. g., a cavity mode, an atom, or a mechanical oscillator) with associated Hilbert space $\mathcal{H}^{\mathcal{S}}$, which is coupled to a one-dimensional continuum of bosonic modes. These are collectively denoted \mathcal{A} with Hilbert space $\mathcal{H}^{\mathcal{A}}$ and in the following also referred to as “bath.” The Hamiltonian governing the joint evolution,

$$\hat{H} = \hat{H}_{\mathcal{S}} + \hat{H}_{\mathcal{A}} + \hat{H}_{\text{int}}, \quad (3.1a)$$

is composed of Hamiltonians for the system, the bath, and their interaction. These are given by

$$\hat{H}_{\mathcal{A}} = \int_0^\infty d\omega \omega \hat{a}_\omega^\dagger \hat{a}_\omega, \quad (3.1b)$$

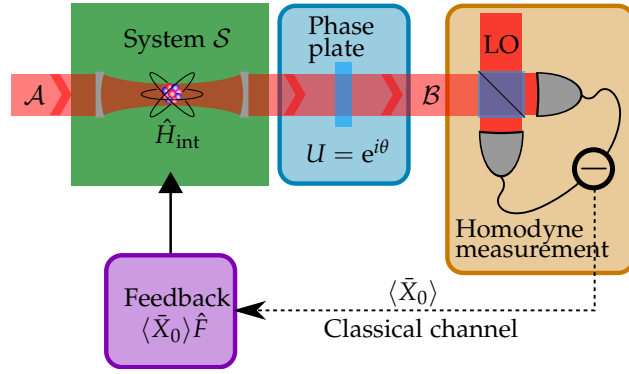


Figure 3.1: Feedback setup for a single system \mathcal{S} , such as an atom in a cavity (schematic). A one-dimensional light field \mathcal{A} couples to \mathcal{S} via \hat{H}_{int} , and passes through a phase plate $U = e^{i\theta}$. Subsequently, the transformed field $\mathcal{B} = U\mathcal{A}$ is combined with a strong local oscillator (LO) on a beam splitter. Two photodetectors measure the incident intensity, and the difference realizes a quadrature measurement, $\langle \bar{X}_0 \rangle$, implicitly depending on θ . This classical signal is transmitted back to the system (dotted line), where it is used to generate Hermitian feedback $\langle \bar{X}_0 \rangle \hat{F}$.

where $\hat{a}_\omega^\dagger, \hat{a}_\omega$ are the usual Creation and Annihilation Operators (CAOs) of the bath mode with frequency ω satisfying the commutation relations $[\hat{a}_\omega, \hat{a}_{\omega'}^\dagger] = \delta(\omega - \omega')$, and

$$\hat{H}_{\text{int}} = i \int_0^\infty d\omega \sqrt{\frac{\kappa(\omega)}{2\pi}} (\hat{S}\hat{a}_\omega^\dagger - \hat{S}^\dagger\hat{a}_\omega), \quad (3.1c)$$

which couples system and bath with strength $\kappa(\omega)$. This interaction is quite general because we do not further specify the system operator \hat{S} . We do impose the common restriction [45, 47] that \hat{H}_{int} is linear in \hat{a}_ω , but we will see below that this is satisfied by a number of relevant systems.

The precise form of the system Hamiltonian is not relevant as we go to an interaction frame [2] with respect to $\hat{H}_S + \hat{H}_A$, but we do make the following assumptions. First, the system-light interaction is constant in some large frequency bandwidth \mathcal{W} , that is $\kappa(\omega) \equiv \kappa$ for $\omega \in \mathcal{W}$ and negligible outside. This is known as the *first Markov approximation* and not unreasonable since constant coupling in frequency means the interaction is strongly localized in space [47]. Second, we assume the system operators merely acquire a time-dependent phase $\hat{S}(t) = \hat{S}e^{-i\Omega(t-t_0)}$ in the interaction picture⁴, which dominates the evolution. Any further time dependence is assumed to be negligible on the time scale set by the interaction $\tau_{\text{int}} \simeq \kappa^{-1}$. This assumption is made for simplicity and will later be dropped, e. g., in Sec. 8.2.

In the rotating frame and using these assumptions we write the interaction as

$$\hat{H}_{\text{int}}(t) = i\sqrt{\kappa} (\hat{S}\hat{a}^\dagger(t) - \hat{S}^\dagger\hat{a}(t)), \quad (3.2)$$

⁴ t_0 is the time where Schrödinger and interaction picture coincide.

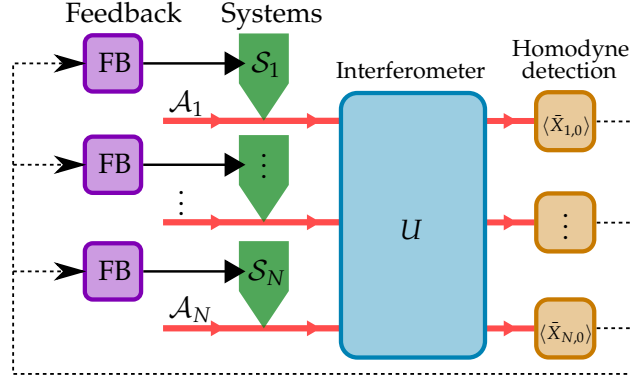


Figure 3.2: Proposed generalization of the simple feedback setup in Fig. 3.1 to N systems \mathcal{S}_j , $j = 1, \dots, N$, with corresponding light fields \mathcal{A}_j . After interacting with the systems, the fields traverse an N -port passive interferometer. Homodyne measurement of each beam yields quadratures $\langle \bar{X}_{\alpha,0} \rangle$, which together allow us to control the systems via local feedback.

with time-independent system operators \hat{S} , and time-dependent field operators

$$\hat{a}(t) := \frac{1}{\sqrt{2\pi}} \int_{\mathcal{W}} d\omega \hat{a}_\omega e^{-i(\omega-\Omega)(t-t_0)}. \quad (3.3)$$

Provided the bandwidth of constant coupling \mathcal{W} is sufficiently large, and the central frequency Ω is yet larger compared to \mathcal{W} , we can replace the integration area \mathcal{W} by \mathbb{R} [2, 43, 45] so the field operators $\hat{a}(t')$ from Eq. (3.3) satisfy the commutation relation $[\hat{a}(t'), \hat{a}^\dagger(t'')] = \delta(t' - t'')$.

To illustrate the interaction (3.2) we consider a few examples. First, let the system be a single cavity mode with annihilation operator \hat{a} . In that case coupling to the outside field is given by $\hat{S} \propto \hat{a}$. If the system is a simple two-level atom with raising and lowering operators $\hat{\sigma}_\pm$, the usual dipole coupling is given by $\hat{S} \propto \hat{\sigma}_+ + \hat{\sigma}_-$, which may simplify to $\hat{S} \propto \hat{\sigma}_-$ in the rotating wave approximation [2]. An (effective) spin- $\frac{1}{2}$ particle, such as a two-level atom inside a far-detuned cavity with a linearized field [48], may correspond to $\hat{S} \propto \hat{\sigma}_z$ with the usual Pauli operator $\hat{\sigma}_z$. Lastly, coupling a mechanical oscillator with position \hat{x} to light, and linearizing the interaction and field, yields a radiation pressure-interaction $\hat{S} \propto \hat{x}$ [49]. We will encounter this example again in Sec. 8.2. We emphasize that the assumptions leading to Eq. (3.2) hold in a broad range of systems, making this derivation applicable to a variety of physical realizations.

3.1.2 Coarse-graining of time

Let us now fix the time t and consider how a combined system-bath state $\rho^{\mathcal{S}\mathcal{A}}(t)$ evolves (in the interaction frame) during a time step $t \rightarrow t + \delta t$. For a perturbative treatment we need δt to be smaller than all other time scales which in this frame means $\delta t / \tau_{\text{int}} \sim \kappa \delta t \ll 1$. In that case we can eventually treat $\delta t \rightarrow dt$ as infinitesimal to obtain a time-continuous master equation for \mathcal{S} . For given δt the perturbative errors become smaller the weaker system and bath are coupled.

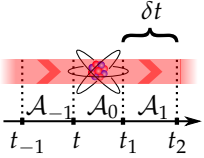


Figure 3.3: Discrete temporal modes interacting with the system in a conveyor belt fashion.

For any $\delta t > 0$ the evolution is governed by an interaction of the system with a discrete temporal mode of the light of duration δt (or spatial mode of length $c \delta t$ where c is the speed of light). Using t as a reference we set $t_n := t + n\delta t$ for $n \in \mathbb{Z}$. For simplicity we write t instead of t_0 , but emphasize again that for now t is fixed. We divide time into disjoint slices $[t_n, t_n + \delta t)$ of length δt as in Fig. 3.3. To each slice we associate a coarse-grained operator

$$\bar{A}_n := \frac{1}{\sqrt{\delta t}} \int_{t_n}^{t_n + \delta t} \hat{a}(t') dt'. \quad (3.4)$$

These are dimensionless and satisfy the commutation relation

$$\begin{aligned} [\bar{A}_n, \bar{A}_m^\dagger] &= \frac{1}{\delta t} \int_{t_n}^{t_n + \delta t} dt' \int_{t_m}^{t_m + \delta t} dt'' [\hat{a}(t'), \hat{a}^\dagger(t'')] \\ &= \delta_{nm}. \end{aligned} \quad (3.5)$$

Importantly, the normalization of \bar{A}_n ensures that Eq. (3.5) holds regardless of the arbitrary time δt . These operators thus give rise to the aforementioned discrete modes, which we denote \mathcal{A}_n and which exist on Hilbert spaces \mathcal{H}_n^A such that $\mathcal{H}^A = \bigotimes_{n \in \mathbb{Z}} \mathcal{H}_n^A$. We introduce the shorthand $\mathcal{A}_{n>0}$ to refer to all modes moving away from \mathcal{S} and $\mathcal{A}_{n \leq 0}$ for all modes coming in.

During every temporal slice the system is presented with a different bath mode (e. g., \mathcal{A}_0 from t to $t + \delta t$) in a “conveyor belt” fashion, as depicted in Fig. 3.3. A part of the field moves in, interacts with the system, and then escapes to infinity, never to return. This corresponds to the usual *Markov approximation* [2] where the evolution of the system does not depend on its history but only on its present state. So while the $\mathcal{A}_{n>0}$ may be correlated with \mathcal{S} they do not affect its future evolution, and the modes $\mathcal{A}_{n \leq 0}$ have not yet interacted with the system. Thus we can ignore all correlations between system and bath for now, and consider only those arising during $[t, t + \delta t)$. In that case, even though the joint system-bath state $\rho^{\mathcal{S}A}(t)$ in principle lives on a large Hilbert space

$$\mathcal{H}^{\mathcal{S}A} = \mathcal{H}^{\mathcal{S}} \bigotimes_{n \in \mathbb{Z}} \mathcal{H}_n^A \quad (3.6)$$

$$= \dots \otimes \mathcal{H}_{-2}^A \otimes \mathcal{H}_{-1}^A \otimes [\mathcal{H}^{\mathcal{S}} \otimes \mathcal{H}_0^A] \otimes \mathcal{H}_1^A \otimes \dots, \quad (3.7)$$

it suffices to consider only the bracketed part, and we denote this reduced state by $\rho_0^{\mathcal{S}A}(t) \in \mathcal{H}^{\mathcal{S}} \otimes \mathcal{H}_0^A$.

3.1.3 Interaction between system and bath mode

Initially system and bath are in a product state $\rho_0^{\mathcal{S}A}(t) = \rho^{\mathcal{S}}(t) \otimes \rho_0^A$ because \mathcal{A}_0 has just moved in and is not yet correlated with \mathcal{S} . This trivially implements the usual *Born* or *weak coupling approximation*, which assumes that interaction with the system does not change the state of the bath: if all incoming $\mathcal{A}_{n \leq 0}$ are in the same initial state then from the system’s point of view the bath is indeed reset after every step. We assume the system state $\rho^{\mathcal{S}}(t)$ is known and $\rho_0^A = |0\rangle\langle 0|$ is in the vacuum state

of \mathcal{A}_0 . This does not necessarily mean that there are no photons impinging on the system. For example, the system may be driven by a strong coherent $|\alpha_t\rangle$ (or squeezed) field which can be treated semi-classically (e. g., [47, Ch. 4], [49]). The effect of the large amplitude α is simply to displace all bath CAOs. This changes the coupling rates and equilibria of the joint system, but not the quantum mechanical interaction which is still fully captured by a (possibly squeezed) vacuum state of the bath.

We now let the interaction (3.2) act on the state

$$\rho_0^{SA}(t) = \rho^S(t) \otimes |0\rangle\langle 0|. \quad (3.8)$$

with duration δt . This generates

$$\rho_{\text{int}}^{SA} := \hat{U}(t, t + \delta t) \rho_0^{SA}(t) \hat{U}^\dagger(t, t + \delta t), \quad (3.9)$$

where \hat{U} is the usual time-ordered evolution operator,

$$\hat{U}(t, t + \delta t) := \mathcal{T} \exp\left(-i \int_t^{t+\delta t} dt' \hat{H}_{\text{int}}(t')\right). \quad (3.10)$$

To understand how this operator acts on the vacuum bath we assume $\epsilon := \sqrt{\kappa \delta t} \ll 1$ is a small parameter to expand \hat{U} in a power series in ϵ (see, e. g., [50, Chapter 4.2]),

$$\hat{U}(t, t + \delta t) = 1 + \hat{U}^{(1)} + \hat{U}^{(2)} + \mathcal{O}(\delta t^{3/2}), \quad (3.11)$$

with (non-unitary) operators

$$\hat{U}^{(1)} = -i \int_t^{t+\delta t} dt_1 \hat{H}_{\text{int}}(t_1), \quad (3.11a)$$

$$\hat{U}^{(2)} = - \int_t^{t+\delta t} dt_1 \int_t^{t_1} dt_2 \hat{H}_{\text{int}}(t_1) \hat{H}_{\text{int}}(t_2). \quad (3.11b)$$

Due to the singular nature¹ of $\hat{a}(t')$ and $\hat{a}^\dagger(t')$ we have to consider the first *two* components of the series to capture all terms of order $\delta t \sim \epsilon^2$. We rewrite the integrand of $\hat{U}^{(2)}$ using $\hat{H}_{\text{int}}(t_1) \hat{H}_{\text{int}}(t_2) = \hat{H}_{\text{int}}(t_1) \hat{H}_{\text{int}}(t_2) / 2 + \hat{H}_{\text{int}}(t_2) \hat{H}_{\text{int}}(t_1) / 2 + [\hat{H}_{\text{int}}(t_1), \hat{H}_{\text{int}}(t_2)] / 2$, and we find that the commutator vanishes on the vacuum state. Being left with an integrand symmetric in t_1 and t_2 we may change the integration boundaries to obtain

$$\hat{U}^{(2)}|0\rangle = -\frac{1}{2} \int_t^{t+\delta t} dt_1 \int_t^{t+\delta t} dt_2 \hat{H}_{\text{int}}(t_1) \hat{H}_{\text{int}}(t_2) |0\rangle. \quad (3.12)$$

Defining the coarse-grained Hamiltonian

$$\bar{H}_{\text{int}} := i \left(\hat{S} \bar{A}_0^\dagger - \hat{S}^\dagger \bar{A}_0 \right) \quad (3.13)$$

the effect of \hat{U} on the vacuum can be written as

$$\hat{U}(t, t + \delta t) |0\rangle = \exp(-i\epsilon \bar{H}_{\text{int}}) |0\rangle + \mathcal{O}(\epsilon^3), \quad (3.14)$$

¹ Intuitively, in discrete time we have to treat δt as the smallest possible time increment. Each term of the expansion then goes as a power of $\sqrt{\kappa \delta t}$: every factor of \hat{a} goes as $\delta t^{-1/2}$ (since $[\hat{a}(t), \hat{a}^\dagger(t)] = \delta(0) \sim 1/\delta t$ [2]) while each integration $\int^{\delta t} dt' \dots$ contributes a factor of δt , and every Hamiltonian scales as $\sqrt{\kappa}$.

which holds if we neglect terms of order $\mathcal{O}(\epsilon^3)$. The evolved system-light state, normalized to the same order, is then given by

$$\rho_{\text{int}}^{\mathcal{S}\mathcal{A}} = \exp(-i\epsilon\bar{H}_{\text{int}})\rho_0^{\mathcal{S}\mathcal{A}}(t)\exp(i\epsilon\bar{H}_{\text{int}}) + \mathcal{O}(\epsilon^3). \quad (3.15)$$

Again the effect of \bar{H}_{int} is independent of the step size δt , like an average.

Due to the interaction the system has built up correlations with the bath. So if we were to measure \mathcal{A}_0 we would also obtain some information about the state of the system. We will do so in Sec. 3.2.2 to perform measurement-based feedback on the system, and to track the conditional system state in Chap. 6. But for now we let \mathcal{A}_0 simply escape to infinity.

3.1.4 Tracing out the bath

The mode \mathcal{A}_0 simply escapes to infinity, has no further effect on the system, and can be purged from our description. This also means it takes away any information it may have carried about $\rho^{\mathcal{S}}(t)$. We model this ignorance by averaging over all possible states of the bath, which is done by taking a *partial trace* (see [39, Ch. 2]) over the bath degrees of freedom. This is denoted as

$$\rho^{\mathcal{S}}(t + \delta t) = \text{Tr}_{\mathcal{A}}\left\{\rho_{\text{int}}^{\mathcal{S}\mathcal{A}}\right\} \quad (3.16)$$

which leaves us with the unconditional system state $\rho^{\mathcal{S}}(t + \delta t)$. To evaluate this expression we expand $\rho_{\text{int}}^{\mathcal{S}\mathcal{A}}$ in the small parameter $\epsilon = \sqrt{\kappa\delta t}$. We will later see that we need to go to order $\mathcal{O}(\epsilon^2)$ to see nontrivial behavior, so we need to consider

$$\exp(-i\epsilon\bar{H}_{\text{int}}) = 1 - i\epsilon\bar{H}_{\text{int}} - \frac{1}{2}\epsilon^2\bar{H}_{\text{int}}^2 + \mathcal{O}(\epsilon^3), \quad (3.17)$$

and by dropping terms of order $\mathcal{O}(\epsilon^3)$ we obtain

$$\begin{aligned} \rho^{\mathcal{S}}(t + \delta t) &\approx \text{Tr}_{\mathcal{A}}\left\{\rho_0^{\mathcal{S}\mathcal{A}}(t)\right\} - i\epsilon\text{Tr}_{\mathcal{A}}\left\{[\bar{H}_{\text{int}}, \rho_0^{\mathcal{S}\mathcal{A}}(t)]\right\} \\ &\quad + \frac{\epsilon^2}{2}\text{Tr}_{\mathcal{A}}\left\{2\bar{H}_{\text{int}}\rho_0^{\mathcal{S}\mathcal{A}}(t)\bar{H}_{\text{int}} - \{\bar{H}_{\text{int}}^2, \rho_0^{\mathcal{S}\mathcal{A}}(t)\}\right\}, \end{aligned} \quad (3.18)$$

with commutator $[\hat{A}, \hat{B}] = \hat{A}\hat{B} - \hat{B}\hat{A}$ and anti-commutator $\{\hat{A}, \hat{B}\} = \hat{A}\hat{B} + \hat{B}\hat{A}$. Computing the trace then yields, for example,

$$\text{Tr}_{\mathcal{A}}\left\{\rho_0^{\mathcal{S}\mathcal{A}}(t)\right\} = \text{Tr}_{\mathcal{A}}\left\{\rho^{\mathcal{S}}(t) \otimes |0\rangle\langle 0|\right\} \quad (3.19)$$

$$= \rho^{\mathcal{S}}(t)\text{Tr}_{\mathcal{A}}\{|0\rangle\langle 0|\} = \rho^{\mathcal{S}}(t), \quad (3.20)$$

and for the term linear in ϵ ,

$$\text{Tr}_{\mathcal{A}}\left\{\bar{H}_{\text{int}}\rho_0^{\mathcal{S}\mathcal{A}}(t)\right\} = i\text{Tr}_{\mathcal{A}}\left\{\left(\hat{Z}\bar{A}_0^\dagger - \hat{Z}^\dagger\bar{A}_0\right)\rho^{\mathcal{S}}(t) \otimes |0\rangle\langle 0|\right\} \quad (3.21)$$

$$\begin{aligned} &= i\text{Tr}_{\mathcal{A}}\left\{\left(\hat{Z}\rho^{\mathcal{S}}(t)\right) \otimes \left(\bar{A}_0^\dagger|0\rangle\langle 0|\right)\right\} \\ &\quad - i\text{Tr}_{\mathcal{A}}\left\{\left(\hat{Z}^\dagger\rho^{\mathcal{S}}(t)\right) \otimes \left(\bar{A}_0|0\rangle\langle 0|\right)\right\} \end{aligned} \quad (3.22)$$

$$= i\hat{Z}\rho^{\mathcal{S}}(t)\text{Tr}\left\{\bar{A}_0^\dagger|0\rangle\langle 0|\right\} \quad (3.23)$$

$$\begin{aligned} &\quad - i\hat{Z}^\dagger\rho^{\mathcal{S}}(t)\text{Tr}\left\{\bar{A}_0|0\rangle\langle 0|\right\} \\ &= 0, \end{aligned} \quad (3.24)$$

where we used that CAOs have vanishing expectation value on the vacuum. Similar evaluation of the other terms yields

$$\rho^S(t + \delta t) = \rho^S(t) + \epsilon^2 \mathcal{D}[\hat{S}] \rho^S(t) \quad (3.25)$$

where we introduced the *Lindblad superoperator*

$$\mathcal{D}[\hat{S}] \rho^S(t) := \hat{S} \rho^S(t) \hat{S}^\dagger - \frac{1}{2} \hat{S}^\dagger \hat{S} \rho^S(t) - \frac{1}{2} \rho^S(t) \hat{S}^\dagger \hat{S}. \quad (3.26)$$

The term superoperator is used to distinguish regular operators, which act on vectors in Hilbert space, from operators that act on those operators, such as \mathcal{D} acting on ρ . The argument \hat{S} of the Lindblad operator is also called a *jump operator* since in quantum optics $\hat{S} \propto \hat{\sigma}_\pm$ or $\hat{S} \propto \hat{a}$ often describes the “jumps” of a system that emits or absorbs photons from the bath and thus abruptly transitions to a different state. But the name is also used when \hat{S} describes a continuous operation, such as $\hat{S} \propto \hat{\sigma}_z$ for the rotation of a spin.

Equation (3.25) shows that it was indeed necessary to keep terms of order $\epsilon^2 = \kappa \delta t$ to see nontrivial effects. We find the time-continuous evolution of $\rho^S(t)$ by considering the increment

$$\delta \rho^S(t) := \rho^S(t + \delta t) - \rho^S(t) = \kappa \mathcal{D}[\hat{S}] \rho^S(t) \delta t. \quad (3.27)$$

Taking the limit of an infinitesimal step, $\delta t \rightarrow dt$, is straightforward because all of the operators are independent of δt . We can then treat $\delta \rho^S(t) \rightarrow d\rho^S(t)$ itself as infinitesimal so

$$d\rho^S(t) = \kappa \mathcal{D}[\hat{S}] \rho^S(t) dt. \quad (3.28)$$

This equation is indeed the quantum master equation for a system weakly coupled via \hat{S} to a heat bath of zero temperature [2, 36, 45, 47]. More generally, by including an additional system Hamiltonian \hat{H}_S or by leaving the rotating frame, we would find

$$d\rho^S(t) = -i[\hat{H}_S, \rho^S(t)] dt + \kappa \mathcal{D}[\hat{S}] \rho^S(t) dt. \quad (3.29)$$

3.2 INCLUDING MEASUREMENT-BASED FEEDBACK

3.2.1 Adding phase plate and measurement

Let us return to the joint system-light state ρ_{int}^{SA} after the interaction. Instead of letting the light escape we will measure it to obtain information about \mathcal{S} . For greater flexibility in the measurements we can perform, we let \mathcal{A}_0 first traverse a passive optical element, which for a single one-dimensional field simply corresponds to a phase plate (light blue box in Fig. 3.1 (a)). In later sections we will consider setups involving several fields in which case the passive element corresponds to a linear interferometer. We assume that compared to the interaction time δt both the optics and measurement act instantaneously (with negligible delay) on the field.

In order to pave the way for generalization to multiple fields we give here an overly elaborate description of the action of a phase plate.

We assume the optics to be independent of frequency in the relevant bandwidth. The plate then imprints an additional phase θ on \mathcal{A}_0 , so $\bar{A}_0 \mapsto U\bar{A}_0$ with the complex scalar $U = e^{i\theta}$. It will be useful to view this phase-shifted field as a new field \mathcal{B} with CAOs given by $\hat{b}(t) := U\hat{a}(t)$ so the coarse-grained slice \mathcal{B}_0 comes with $\bar{B}_0 := U\bar{A}_0$. These operators still satisfy $[\bar{B}_0, \bar{B}_0^\dagger] = 1$ and have the same vacuum state $|0\rangle$ as \mathcal{A}_0 . Simultaneously defining a new system operator

$$\hat{Z} := U\hat{S} = e^{i\theta}\hat{S} \quad (3.30)$$

allows us to write $\bar{H}_{\text{int}} = i(\hat{Z}\bar{B}_0^\dagger - \hat{Z}^\dagger\bar{B}_0)$ so

$$\rho_{\text{int}}^{SB} = \exp(-i\epsilon\bar{H}_{\text{int}})\rho_0^{SB}(t)\exp(i\epsilon\bar{H}_{\text{int}}) + \mathcal{O}(\epsilon^3) \quad (3.31)$$

still holds but with $\hat{S} \rightarrow \hat{Z}$.

The next step in our scheme is a homodyne quadrature measurement of the outgoing beam, enclosed in the dark orange box in Fig. 3.1 (a), and further explained in App. A. The quadrature operators of \mathcal{B}_0 are given by

$$\bar{X}_0 := \frac{1}{\sqrt{2}}(\bar{B}_0 + \bar{B}_0^\dagger), \quad (3.32a)$$

$$\bar{P}_0 := -\frac{i}{\sqrt{2}}(\bar{B}_0 - \bar{B}_0^\dagger), \quad (3.32b)$$

with commutation relation $[\bar{X}_0, \bar{P}_0] = i$. Without loss of generality we restrict ourselves to measuring only \bar{X}_0 since \bar{B}_0 implicitly depends on θ so we can always change the quadrature by choosing a different phase. The \bar{X}_0 -quadrature eigenstates $|\bar{x}\rangle$ of the field \mathcal{B}_0 are defined through $\bar{X}_0|\bar{x}\rangle = \bar{x}|\bar{x}\rangle$ for $\bar{x} \in \mathbb{R}$, where the bar emphasizes that these states correspond to coarse-grained operators \bar{X}_0 .

Assuming the homodyne detector outputs a specific value, \bar{x} say, the light is projected into the corresponding eigenstate, and the state of \mathcal{S} after interaction and measurement is given by

$$\tilde{\rho}_{\bar{x}}^{\mathcal{S}}(t + \delta t) := \langle \bar{x} | \rho_{\text{int}}^{SB} | \bar{x} \rangle, \quad (3.33)$$

where the subscript indicates that the state is *conditioned* on the outcome \bar{x} . Note that $\tilde{\rho}_{\bar{x}}^{\mathcal{S}}(t + \delta t)$ does not have unit trace, denoted by the tilde, and so is not a density operator in a strict sense. After normalization we find

$$\rho_{\bar{x}}^{\mathcal{S}}(t + \delta t) := \frac{1}{p(\bar{x})} \langle \bar{x} | \rho_{\text{int}}^{SB} | \bar{x} \rangle, \quad (3.34a)$$

$$p(\bar{x}) = \text{Tr}_{\mathcal{S}} \left\{ \langle \bar{x} | \rho_{\text{int}}^{SB} | \bar{x} \rangle \right\} = \text{Tr} \left\{ |\bar{x}\rangle \langle \bar{x}| \rho_{\text{int}}^{SB} \right\}. \quad (3.34b)$$

where $\text{Tr}_{\mathcal{S}}\{\dots\}$ denotes a partial trace over the system degrees of freedom. Equation (3.34b) is important because it tells us that the normalization $p(\bar{x})$ is just the probability to measure \bar{x} given ρ_{int}^{SB} .

Obtaining the result \bar{x} has revealed some information about the state of \mathcal{S} . We can use this knowledge to apply measurement-based feedback (in Sec. 3.2.2) and to derive a stochastic master equation (in Chap. 6) for the conditional state. But first we will check for consistency by seeing

what happens if we simply ignore the measurement result. This corresponds to averaging over all possible conditional states weighted with their respective probabilities,

$$\rho^S(t + \delta t) = \int_{\mathbb{R}} p(\bar{x}) \rho_{\bar{x}}^S(t + \delta t) d\bar{x} \quad (3.35)$$

$$= \int_{\mathbb{R}} \langle \bar{x} | \rho_{\text{int}}^{SB} | \bar{x} \rangle d\bar{x} \quad (3.36)$$

$$= \text{Tr}_{\mathcal{B}} \{ \rho_{\text{int}}^{SB} \}, \quad (3.37)$$

where the integral $\int d\bar{x} \langle \bar{x} | \dots | \bar{x} \rangle = \text{Tr}_{\mathcal{B}} \{ \dots \}$ is one possible way to compute the partial trace over the bath. This corresponds precisely to the expression found in Sec. 3.1.4, but with \hat{Z} instead of \hat{S} . Following the same procedure as before we find the master equation

$$d\rho^S(t) = \kappa \mathcal{D}[\hat{Z}] \rho^S(t) dt = \kappa \mathcal{D}[\hat{S}] \rho^S(t) dt, \quad (3.38)$$

where we used that $\hat{Z} = e^{i\theta} \hat{S}$ and $\mathcal{D}[\alpha \hat{S}] = |\alpha|^2 \mathcal{D}[\hat{S}]$ for complex scalars α .

3.2.2 Applying feedback

In this section we will use the the measurement result to apply instantaneous Markovian feedback to the conditional state $\rho_{\bar{x}}^S(t + \delta t)$ from Eq. (3.34), depicted by the purple box in Fig. 3.1 (a). *Instantaneous* here means that all possible delay τ_{delay} is negligible on the time scale δt so it acts back on the system before the succeeding time step. In particular, because $\tau_{\text{delay}} \ll \delta t \ll \tau_{\text{int}}$ this requires the delay to be much smaller than the interaction time. The feedback is *Markovian* in the sense that it depends only on the measured signal at a specific time and not on a record of previous measurements.

3.2.2.1 Hamiltonian feedback

We aim to keep the feedback simple to alleviate experimental difficulties. To this end we choose *Hamiltonian feedback* [19, 20] (also known as *Wiseman-Milburn Markovian feedback* [36]), which is linear⁵ in the measurement current. It is effected by modifying the Hamiltonian proportional to the unprocessed measurement signal, so in a time-continuous picture we would naively include

$$\hat{H}_{\text{fb}}(t) = \sqrt{\kappa_{\text{fb}}} \hat{F} Y(t) \quad (3.39)$$

in the evolution where \hat{F} is some Hermitian operator and $Y(t) \propto \langle \hat{x}(t) \rangle = \langle \hat{b}(t) + \hat{b}^\dagger(t) \rangle / \sqrt{2}$ is the instantaneous homodyne current, see also App. A. One has to take care not to violate causality when applying the feedback since it must act *after* interaction and measurement. So simply adding $\hat{H}_{\text{fb}}(t)$ to the original interaction $\hat{H}_{\text{int}}(t)$ in (3.2) yields nonsensical results². However, in our stroboscopic picture the system evolves sequen-

⁵ The singular nature of the measurement current makes higher orders ill-defined [19].

² A rigorous way to add time-continuous feedback is to start with finite delay of the feedback, deriving a proper equation of motion and then letting the delay go to zero [19, 20].

tially anyway so we first complete the measurement of \bar{X}_0 with result \bar{x} to prepare the coarse-grained feedback Hamiltonian

$$\bar{H}_{\text{fb}} = \sqrt{2\kappa}\hat{F}\bar{x}. \quad (3.40)$$

Here we rescaled \hat{F} to replace κ_{fb} by 2κ in order to obtain a more convenient master equation later on. Applying \bar{H}_{fb} to $\rho_{\bar{x}}^{\mathcal{S}}(t + \delta t)$ as in Eq. (3.15) generates (recall $\epsilon = \sqrt{\kappa\delta t}$)

$$\rho_{\text{fb}}^{\mathcal{S}}(\bar{x}) := \exp\left(-i\sqrt{2\epsilon}\bar{x}\hat{F}\right)\rho_{\bar{x}}^{\mathcal{S}}(t + \delta t)\exp\left(i\sqrt{2\epsilon}\bar{x}\hat{F}\right). \quad (3.41)$$

We did not further specify \hat{F} to keep the feedback general. For example, the system could be a single mode cavity with CAOs \hat{c}^\dagger, \hat{c} . Then $\hat{F} \propto \hat{c}^\dagger \hat{c}$ shifts the frequency of the cavity mode [51], whereas $\hat{F} \propto i(\hat{c} - \hat{c}^\dagger)$ affects the cavity drive [42]. Physically, these operations may be realized by modulating either the refractive index inside the cavity or its transmission. On the other hand, if the system is a particle with (effective) spin- $\frac{1}{2}$, we may rotate its spin through $\hat{F} \propto \hat{\sigma}_y$ with Pauli operator $\hat{\sigma}_y$. This is realized, for example, for a two-level atom inside a cavity by suitable external driving fields, e. g., optical pulses or magnetic radio-frequency fields [48]. Further examples of feedback operators are provided in the applications in Chaps. 4 and 5 (see, for instance, Eqs. (4.4), (4.10), and (5.3)).

Let us express the conditional system state $\rho_{\text{fb}}^{\mathcal{S}}(\bar{x})$ in terms of the initial states of \mathcal{S} and \mathcal{B} . Plugging in the definitions of $\rho_{\bar{x}}^{\mathcal{S}}$ and $\rho_{\text{int}}^{\mathcal{SB}}$ from Eqs. (3.34) and (3.31) into (3.41), and using the fact that $|\bar{x}\rangle$ is an eigenstate of \bar{X}_0 , we find

$$\rho_{\text{fb}}^{\mathcal{S}}(\bar{x}) = \frac{1}{p(\bar{x})} \langle \bar{x} | e^{-i\sqrt{2\epsilon}\bar{X}_0\hat{F}} \rho_{\text{int}}^{\mathcal{SB}} e^{i\sqrt{2\epsilon}\bar{X}_0\hat{F}} | \bar{x} \rangle \quad (3.42)$$

$$= \frac{1}{p(\bar{x})} \langle \bar{x} | \hat{K} \left(\rho^{\mathcal{S}}(t) \otimes |0\rangle\langle 0| \right) \hat{K}^\dagger | \bar{x} \rangle, \quad (3.43)$$

where

$$\hat{K} := \exp(-i\sqrt{2\epsilon}\bar{X}_0\hat{F}) \exp(-i\epsilon\bar{H}_{\text{int}}). \quad (3.44)$$

In contrast to coherent feedback, where the output of the quantum system is directly fed back, measurement-based feedback does not require any quantum information to be transmitted, only the measurement result, which can be processed classically. This may be a practical advantage because it allows for (digital) processing and amplification of the signal. But it has the great disadvantage that we are restricted to actions of the form above. The feedback also always has to follow some interaction and measurement procedure which takes additional time compared to an equivalent coherent scheme [36, Sec. 5.2].

3.2.2.2 Feedback master equation

By definition the feedback, and thus $\rho_{\text{fb}}^{\mathcal{S}}(\bar{x})$, is conditioned on a particular measurement result. If we do not want to constantly monitor the detector output to keep track of the state, we need to understand the *unconditional* evolution, i. e., we need to know how the system behaves

on average. To this end we have to proceed as in Sec. 3.1.4: we sum $\rho_{\text{fb}}^S(\bar{x})$ over all possible results \bar{x} weighted with their respective probabilities $p(\bar{x}) = \text{Tr}\{|\bar{x}\rangle\langle\bar{x}|\rho_{\text{int}}^{SB}\}$. Again this gives us a partial trace over the light field

$$\rho^S(t + \delta t) = \int_{-\infty}^{\infty} d\bar{x} p(\bar{x}) \rho_{\text{fb}}^S(\bar{x}) \quad (3.45)$$

$$= \text{Tr}_B \left\{ \hat{K} \left(\rho^S(t) \otimes |0\rangle\langle 0| \right) \hat{K}^\dagger \right\}, \quad (3.46)$$

which we evaluate by expanding \hat{K} in powers of ϵ and neglecting terms of order $\mathcal{O}(\epsilon^3)$. This yields

$$\begin{aligned} \rho^S(t + \delta t) &= \rho^S(t) - \frac{\epsilon^2}{2} \left\{ (\hat{Z}^\dagger \hat{Z} + \hat{Z}^2) \rho^S(t) + \text{h.c.} \right\} \\ &\quad + \sqrt{2}\epsilon \langle \bar{X}_0 \rangle \left\{ (\hat{Z} - i\hat{F}) \rho^S(t) + \text{h.c.} \right\} \\ &\quad + \epsilon^2 \langle \bar{X}_0^2 \rangle \left\{ (\hat{Z}^2 - \hat{F}^2 - 2i\hat{F}\hat{Z}) \rho^S(t) + \text{h.c.} \right\} \\ &\quad + 2\epsilon^2 \langle \bar{X}_0^2 \rangle (\hat{Z} - i\hat{F}) \rho^S(t) (\hat{Z}^\dagger + iF), \end{aligned} \quad (3.47)$$

with system operators \hat{F} and $\hat{Z} = U\hat{S} = e^{i\theta}\hat{S}$, and where the expectation value is taken with respect to the vacuum state, e.g., $\langle \bar{X}_0 \rangle = \text{Tr}_B \{ \bar{X}_0 |0\rangle\langle 0| \} = \langle 0 | \bar{X}_0 |0 \rangle$. We can use the vacuum statistics of \bar{X}_0 , namely $\langle 0 | \bar{X}_0 |0 \rangle = 0$ and $\langle 0 | \bar{X}_0^2 |0 \rangle = 1/2$, and $\epsilon = \sqrt{\kappa\delta t}$ to obtain the unconditional system state

$$\begin{aligned} \rho^S(t + \delta t) &= \rho^S(t) - \frac{i}{2} \kappa [\hat{F}\hat{Z} + \hat{Z}^\dagger \hat{F}, \rho^S(t)] \delta t \\ &\quad + \kappa \mathcal{D}[\hat{Z} - i\hat{F}] \rho^S(t) \delta t, \end{aligned} \quad (3.48)$$

with Lindblad operator \mathcal{D} from Eq. (3.26). It is clear that the time scale of the corresponding quantum dynamics is set by the strength of the light-matter interaction κ . Taking the limit $\delta t \rightarrow dt$ is as straightforward as in Eq. (3.28) so we find the FME

$$d\rho^S(t) = -\frac{i}{2} \kappa [\hat{F}\hat{Z} + \hat{Z}^\dagger \hat{F}, \rho^S(t)] dt + \kappa \mathcal{D}[\hat{Z} - i\hat{F}] \rho^S(t) dt \quad (3.49a)$$

$$= -i[\hat{H}, \rho^S(t)] dt + \mathcal{D}[\hat{L}] \rho^S(t) dt \quad (3.49b)$$

with Hamiltonian \hat{H} and jump operator \hat{L} respectively given by

$$\hat{H} := \frac{1}{2} \kappa (\hat{F}\hat{Z} + \hat{Z}^\dagger \hat{F}), \quad \text{and} \quad \hat{L} := \sqrt{\kappa} (\hat{Z} - i\hat{F}). \quad (3.49c)$$

To check for consistency, we note that without feedback, $\hat{F} = 0$, we obtain the unconditional master equation (3.28), as we should.

We arrived at this important result, Eqs. (3.49), using only basic rules of quantum mechanics, but emphasize that one obtains the same result [2, 20] by employing stochastic calculus [5] to treat measurement and feedback rigorously. On an individual system measurement-based feedback can be used, for example, to stabilize the output [19], avoid back action [52] or protect quantum states from decoherence [51]. But if collectively applied to multiple systems it can be used to engineer effective many-body interactions. To this end we will now generalize the formalism to a collection of quantum systems.

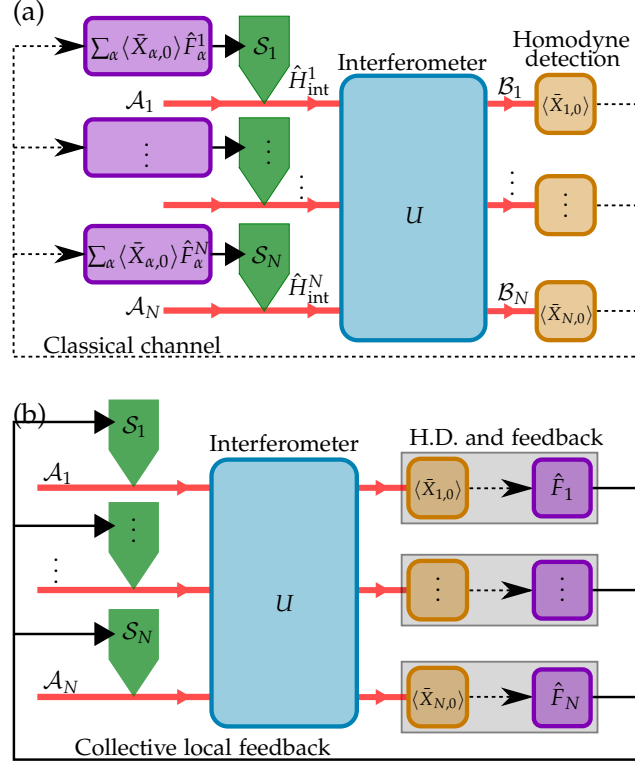


Figure 3.4: (a) Schematic layout of the feedback scheme for N systems \mathcal{S}_1 through \mathcal{S}_N . Each system interacts locally with a single light field \mathcal{A}_k via \hat{H}_{int}^k . The fields traverse an interferometer given by an $N \times N$ unitary matrix U . Homodyne detection of the outgoing fields \mathcal{B}_α yields the quadratures $\langle \bar{X}_{\alpha,0} \rangle$. Each signal is transmitted back to the systems via classical channels (dotted line), and generates local feedback of the form $\langle \bar{X}_{\alpha,0} \rangle \hat{F}_\alpha^j$ on each \mathcal{S}_j . The total feedback on \mathcal{S}_j is generated by $\sum_{\alpha=1}^N \langle \bar{X}_{\alpha,0} \rangle \hat{F}_\alpha^j$. (b) A different schematic of the same setup. It emphasizes how each measurement $\langle \bar{X}_\alpha \rangle$ is used to generate collective feedback $\hat{F}_\alpha = \sum_{j=1}^N \hat{F}_\alpha^j$ on all systems. This represents the same scheme as in (a) but viewing the feedback as collective simplifies our calculations.

3.2.3 Generalization to multiple systems

Instead of a single system we now consider an array of systems \mathcal{S}_j , $j = 1, \dots, N$, each coupled to a corresponding bath \mathcal{A}_j as in Fig. 3.4 (a). Note that the systems need not be identical, and that there is no direct interaction between them, so the collective system Hamiltonian decomposes into a sum of local terms, $\hat{H}_S = \sum_j \hat{H}_S^j$.

3.2.3.1 Setup and coarse-graining

As in the previous section we assume that the relevant system and light Hamiltonians allow us to change to an interaction frame in which the total system-light coupling can be expressed as

$$\hat{H}_{\text{int}}(t) = \sum_{j=1}^N \hat{H}_{\text{int}}^j(t). \quad (3.50)$$

The Hamiltonians $\hat{H}_{\text{int}}^j(t)$ generate the coupling of \mathcal{S}_j to \mathcal{B}_j and are given by

$$\hat{H}_{\text{int}}^j(t) = i\sqrt{\kappa}(\hat{S}_j\hat{a}_j^\dagger(t) - \hat{S}_j^\dagger\hat{a}_j(t)) \quad (3.51)$$

for every j . We assume here a common coupling strength κ for all of the N systems. Inhomogeneities of the coupling constants can be absorbed into the system operators \hat{S}_j . Each \hat{S}_j is a local operator, meaning that it acts nontrivially only on system \mathcal{S}_j , and $\hat{a}_j(t)$ are bosonic annihilation operators as in Eq. (3.2), obeying the usual relation

$$[\hat{a}_j(t), \hat{a}_k^\dagger(t')] = \delta_{jk}\delta(t - t'). \quad (3.52)$$

As in Sec. 3.1.2, we fix the time t and coarse-grain the evolution by introducing the discrete time step δt . We can adopt the corresponding coarse-grained CAO from Eq. (3.4),

$$\bar{A}_{j,n} := \frac{1}{\sqrt{\delta t}} \int_{t_n}^{t_n+\delta t} \hat{a}_j(t') dt', \quad (3.53)$$

for discrete times $t_n = t + n\delta t$. These satisfy $[\bar{A}_{j,n}, \bar{A}_{k,m}] = \delta_{jk}\delta_{nm}$ so each $\bar{A}_{j,n}$ corresponds to a discrete bosonic mode $\mathcal{A}_{j,n}$, where the first index labels the systems and the second denotes how far the mode is from the interaction region. During the considered time step only $\mathcal{A}_{j,0}$ contributes to the system evolution so we drop all others.

As before we assume we know the joint system state $\rho^S(t)$ and have all incoming light fields in the vacuum state, so $\rho^{S,A}(t) = \rho^S(t) \otimes |0\rangle\langle 0|$, where $|0\rangle\langle 0|$ is the collective vacuum of all light modes. Thus as in Eq. (3.15) the combined system-light state after the interaction will be

$$\rho_{\text{int}}^{S,A} = \exp(-i\epsilon\bar{H}_{\text{int}})\rho^{S,A}(t)\exp(i\epsilon\bar{H}_{\text{int}}) + \mathcal{O}(\epsilon^3) \quad (3.54)$$

where $\epsilon = \sqrt{\kappa\delta t}$ and

$$\bar{H}_{\text{int}} = i \sum_{j=1}^N (\hat{S}_j \bar{A}_{j,0}^\dagger - \hat{S}_j^\dagger \bar{A}_{j,0}). \quad (3.55)$$

For ease of notation we combine the operators $\bar{A}_{j,0}$ and \hat{S}_j into N -dimensional vectors \bar{A}_0 and \hat{S} respectively, so $\bar{H}_{\text{int}} = i(\hat{S} \cdot \bar{A}_0^\dagger - \hat{S}^\dagger \cdot \bar{A}_0)$ with the dot-product $\hat{S} \cdot \bar{A}_0^\dagger := \sum_j \hat{S}_j \bar{A}_{j,0}^\dagger$.

As before, letting the light escape after the interaction will lead to a master equation

$$d\rho^S(t) = \kappa \sum_{j=1}^N \mathcal{D}[\hat{S}_j]\rho^S(t) dt \quad (3.56)$$

for the collective system state, and we see that each \mathcal{S}_j couples to a local jump operator \hat{S}_j . In order to generate nontrivial dynamics we thus have to measure the outgoing modes.

3.2.3.2 Interferometer and measurement

Before the measurement we send the light through a set of optics. The simple phase plate from Sec. 3.2.1 is replaced by an interferometer, which mixes the $\mathcal{A}_{j,0}$ via a unitary $N \times N$ matrix U , depicted as a blue box in Fig. 3.4 (a). The interferometer yields outgoing fields $\mathcal{B}_{1,0}, \dots, \mathcal{B}_{N,0}$ with corresponding annihilation operators

$$\bar{\mathcal{B}}_0 := U\bar{\mathcal{A}}_0 \quad \Leftrightarrow \quad \bar{\mathcal{B}}_{\alpha,0} := \sum_{j=1}^N U_{\alpha j} \bar{\mathcal{A}}_{j,0}. \quad (3.57)$$

To avoid confusion between the systems \mathcal{S}_j and incoming fields $\mathcal{A}_{j,0}$ on one hand, and the measured fields $\mathcal{B}_{\alpha,0}$ on the other we use greek indices for the latter. Because the passive interferometer does not mix annihilation and creation operators we find $[\bar{\mathcal{B}}_{\alpha,0}, \bar{\mathcal{B}}_{\beta,0}^\dagger] = \delta_{\alpha,\beta}$. The optics thus output a combination of the former fields $\mathcal{A}_{j,0}$, which make up new independent bosonic modes $\mathcal{B}_{\alpha,0}$. Changing the system operators in the same manner, so that

$$\hat{\mathcal{Z}} := U\hat{\mathcal{S}} \quad \Leftrightarrow \quad \hat{\mathcal{Z}}_\alpha := \sum_{j=1}^N U_{\alpha j} \hat{\mathcal{S}}_j, \quad (3.58)$$

allows us to rewrite the interaction,

$$\bar{H}_{\text{int}} = i(\hat{\mathcal{Z}} \cdot \bar{\mathcal{B}}_0^\dagger - \hat{\mathcal{Z}}^\dagger \cdot \bar{\mathcal{B}}_0). \quad (3.59)$$

We now perform a homodyne measurement of each \mathcal{B}_α . As before, we introduce the coarse-grained quadrature operators

$$\bar{\mathcal{X}}_0 := \frac{1}{\sqrt{2}}(\bar{\mathcal{B}}_0 + \bar{\mathcal{B}}_0^\dagger), \quad (3.60a)$$

$$\bar{\mathcal{P}}_0 := -\frac{i}{\sqrt{2}}(\bar{\mathcal{B}}_0 - \bar{\mathcal{B}}_0^\dagger). \quad (3.60b)$$

Without loss of generality we measure only the $\bar{\mathcal{X}}_{\alpha,0}$ -quadratures. Any other quadrature can be measured by inserting phase plates before the detectors, which amounts to multiplying U by a diagonal phase matrix, $D = \text{diag}(e^{i\theta_1}, \dots, e^{i\theta_N})$, from the left. Since all $\bar{\mathcal{X}}_{\alpha,0}$ commute, we may define common eigenstates $|\bar{\mathbf{x}}\rangle := |\bar{x}_1, \dots, \bar{x}_N\rangle$ as usual through

$$\bar{\mathcal{X}}_{\alpha,0}|\bar{\mathbf{x}}\rangle = \bar{x}_\alpha|\bar{\mathbf{x}}\rangle. \quad (3.61)$$

The conditional system state after the measurement carries over from Eq. (3.34),

$$\rho_{\bar{\mathbf{x}}}^{\mathcal{S}}(t + \delta t) := \frac{1}{p(\bar{\mathbf{x}})} \langle \bar{\mathbf{x}} | \rho_{\text{int}}^{\mathcal{S}\mathcal{B}} | \bar{\mathbf{x}} \rangle, \quad (3.62a)$$

$$p(\bar{\mathbf{x}}) = \text{Tr}_S \left\{ \langle \bar{\mathbf{x}} | \rho_{\text{int}}^{\mathcal{S}\mathcal{B}} | \bar{\mathbf{x}} \rangle \right\} = \text{Tr} \left\{ |\bar{\mathbf{x}}\rangle \langle \bar{\mathbf{x}} | \rho_{\text{int}}^{\mathcal{S}\mathcal{B}} \right\}, \quad (3.62b)$$

with normalization given by the joint probability density function $p(\bar{\mathbf{x}})$.

3.2.3.3 Applying local feedback

As in Eq. (3.41), we apply Hamiltonian feedback to the conditional state,

$$\rho_{\text{fb}}^{\mathcal{S}}(\bar{\mathbf{x}}) = \exp\left(-i\sqrt{2}\epsilon\hat{G}(\bar{\mathbf{x}})\right)\rho_{\bar{\mathbf{x}}}^{\mathcal{S}}(t + \delta t)\exp\left(i\sqrt{2}\epsilon\hat{G}(\bar{\mathbf{x}})\right), \quad (3.63)$$

with some Hermitian generator $\hat{G}(\bar{\mathbf{x}})$ acting on the N systems that depends on the measurement outcomes $\bar{\mathbf{x}}$. It is crucial to specify at this point the resources which are assumed in the feedback operations: in order to maintain the assumption that there is no direct physical interaction between the systems we restrict ourselves to local feedback operations, each affecting only individual systems as depicted in Fig. 3.4 (a). This means we can write $\hat{G}(\bar{\mathbf{x}}) = \sum_{j=1}^N \hat{G}_j(\bar{\mathbf{x}})$ with local operators $\hat{G}_j(\bar{\mathbf{x}})$ acting (nontrivially) on \mathcal{S}_j only. We still assume feedback linear in the measurement signal, so we can write $\hat{G}_j(\bar{\mathbf{x}}) = \sum_{\alpha=1}^N \bar{x}_\alpha \hat{F}_\alpha^j$, where \hat{F}_α^j are local Hermitian operators that use the measurement of $\mathcal{B}_{\alpha,0}$ to produce feedback on \mathcal{S}_j . Consequently, the total feedback on all systems yields

$$\hat{G}(\bar{\mathbf{x}}) = \sum_{\alpha,j=1}^N \bar{x}_\alpha \hat{F}_\alpha^j. \quad (3.64)$$

Our choice of \hat{G} effects *simultaneous* action of all feedback operations. This is justified because, as we will show below Eq. (3.70), different feedback operations commute up to $\mathcal{O}(\epsilon^3)$ due to the independent statistics of the light fields.

To simplify the notation, let us collect the feedback corresponding to measurement signal \bar{x}_α ,

$$\hat{F}_\alpha := \sum_{j=1}^N \hat{F}_\alpha^j, \quad (3.65)$$

as shown in Fig. 3.4 (b). If we combine all \hat{F}_α into a vector $\hat{\mathbf{F}}$, we can write $\hat{G}(\bar{\mathbf{x}}) = \bar{\mathbf{x}} \cdot \hat{\mathbf{F}}$ to obtain the conditional feedback state

$$\rho_{\text{fb}}^{\mathcal{S}}(\bar{\mathbf{x}}) = \exp\left(-i\sqrt{2}\epsilon\bar{\mathbf{x}} \cdot \hat{\mathbf{F}}\right)\rho_{\bar{\mathbf{x}}}^{\mathcal{S}}(t + \delta t)\exp\left(i\sqrt{2}\epsilon\bar{\mathbf{x}} \cdot \hat{\mathbf{F}}\right). \quad (3.66)$$

Note that Figs. 3.4 (a) and 3.4 (b) describe the same setup, with only a slight change in notation and a different view on the feedback.

As in Eq. (3.43), we express $\rho_{\text{fb}}^{\mathcal{S}}(\bar{\mathbf{x}})$ in terms of the initial states of system and light,

$$\rho_{\text{fb}}^{\mathcal{S}}(\bar{\mathbf{x}}) = \frac{1}{p(\bar{\mathbf{x}})} \langle \bar{\mathbf{x}} | \hat{K} \left(\rho^{\mathcal{S}}(t) \otimes |0\rangle\langle 0| \right) \hat{K}^\dagger | \bar{\mathbf{x}} \rangle, \quad (3.67)$$

with

$$\hat{K} := \exp\left(-i\sqrt{2}\epsilon\bar{\mathbf{X}}_0 \cdot \hat{\mathbf{F}}\right)\exp(-i\epsilon\bar{H}_{\text{int}}). \quad (3.68)$$

3.2.3.4 Averaging the dynamics

To obtain the unconditional system evolution we average the conditional state from Eq. (3.67) with respect to all light fields. This yields the familiar expression

$$\rho^{\mathcal{S}}(t + \delta t) = \int_{\mathbb{R}^N} d\bar{x}_1 \dots d\bar{x}_N p(\bar{\mathbf{x}}) \rho_{\text{fb}}^{\mathcal{S}}(\bar{\mathbf{x}}) \quad (3.69)$$

$$= \text{Tr}_{\mathcal{B}} \left\{ \hat{K} \left(\rho^{\mathcal{S}}(t) \otimes |0\rangle\langle 0| \right) \hat{K}^\dagger \right\}, \quad (3.70)$$

where $\text{Tr}_{\mathcal{B}}\{\dots\}$ now denotes a partial trace over *all* baths. We expand \hat{K} and drop terms of order $\mathcal{O}(\epsilon^3)$ to evaluate the trace. Using that operators of different baths commute, and $\langle 0|\bar{X}_{\alpha,0}|0\rangle = 0$ and $\langle 0|\bar{X}_{\alpha,0}\bar{X}_{\beta,0}|0\rangle = \delta_{\alpha,\beta}/2$, yields the density matrix

$$\begin{aligned} \rho^S(t + \delta t) &= \rho^S(t) - \frac{i}{2} \kappa \sum_{\alpha=1}^N [\hat{F}_\alpha \hat{Z}_\alpha + \hat{Z}_\alpha^\dagger \hat{F}_\alpha, \rho^S(t)] \delta t \\ &\quad + \kappa \sum_{\alpha=1}^N \mathcal{D}[\hat{Z}_\alpha - i\hat{F}_\alpha] \rho^S(t) \delta t. \end{aligned} \quad (3.71)$$

At this point we can justify the choice of simultaneous feedback in Eq. (3.66). The order in which the feedback is applied is irrelevant for our purposes, as can be seen as follows: consider two generic feedback terms, $\epsilon \bar{x}_\alpha \hat{F}_\alpha$ and $\epsilon \bar{x}_\beta \hat{F}_\beta$. The results $\bar{x}_{\alpha/\beta}$ are promoted to operators in the formulation of (3.67). Comparing sequential to simultaneous application of the feedback using the Baker-Campbell-Hausdorff formula one finds

$$\begin{aligned} &\exp(\epsilon \bar{X}_{\alpha,0} \hat{F}_\alpha) \exp(\epsilon \bar{X}_{\beta,0} \hat{F}_\beta) \\ &= \exp\left(\epsilon \bar{X}_{\alpha,0} \hat{F}_\alpha + \epsilon \bar{X}_{\beta,0} \hat{F}_\beta + \frac{\epsilon^2}{2} \bar{X}_{\alpha,0} \bar{X}_{\beta,0} [\hat{F}_\alpha, \hat{F}_\beta]\right) + \mathcal{O}(\epsilon^3). \end{aligned} \quad (3.72)$$

When taking the partial trace in Eq. (3.70) the additional commutators $\bar{X}_{\alpha,0} \bar{X}_{\beta,0} [\hat{F}_\alpha, \hat{F}_\beta]$ contribute only vacuum expectation values of the form $\langle \bar{X}_{\alpha,0} \bar{X}_{\beta,0} \rangle$ for $\alpha \neq \beta$. These vanish due to the independence of the fields, and our choice of simultaneous feedback in Eq. (3.64) is justified.

3.2.3.5 General feedback master equation

As before, combining $\kappa \delta t \mapsto \delta t$ into dimensionless time in Eq. (3.71) and taking the limit $\delta t \rightarrow dt$, we can read off the Feedback Master Equation (FME)

$$\begin{aligned} d\rho^S(t) &= -\frac{i}{2} \sum_{\alpha=1}^N [\hat{F}_\alpha \hat{Z}_\alpha + \hat{Z}_\alpha^\dagger \hat{F}_\alpha, \rho^S(t)] dt \\ &\quad + \sum_{\alpha=1}^N \mathcal{D}[\hat{Z}_\alpha - i\hat{F}_\alpha] \rho^S(t) dt \end{aligned} \quad (3.73a)$$

$$= -i[\hat{H}, \rho^S(t)] dt + \sum_{\alpha=1}^N \mathcal{D}[\hat{L}_\alpha] \rho^S(t) dt, \quad (3.73b)$$

with an effective Hamiltonian and jump operators

$$\hat{H} := \frac{1}{2} \sum_{\alpha=1}^N (\hat{F}_\alpha \hat{Z}_\alpha + \hat{Z}_\alpha^\dagger \hat{F}_\alpha), \quad \text{and} \quad \hat{L}_\alpha := \hat{Z}_\alpha - i\hat{F}_\alpha, \quad (3.73c)$$

each comprising sums of local operators⁶

$$\hat{Z}_\alpha = \sum_{j=1}^N U_{\alpha j} \hat{S}_j, \quad \text{and} \quad \hat{F}_\alpha = \sum_{j=1}^N \hat{F}_\alpha^j. \quad (3.73c)$$

⁶ Recall: Latin indices (j) denote the system the operator acts on; Greek indices (α) indicate which measurement signal is used for the feedback.

The FME (3.73) for N systems under continuous, diffusive, interferometric measurement and local feedback is the main result of this section. The resulting open-system many-body dynamics is determined by a Hamiltonian \hat{H} and a set of jump operators \hat{L}_α . The Hamiltonian exhibits pairwise interactions of, in principle, arbitrary range. The jump operators are sums of strictly local terms but comprising, in principle, operators of each system, and therefore act collectively on all systems. Thus the FME describes a fairly general class of open and interacting many-body systems without requiring any direct physical interaction among them: all interactions are mediated by the interferometric measurement and feedback. These can be engineered almost arbitrarily in range or geometry by a proper choice of (i) the system-light interactions characterized by the system operators \hat{S}_j , cf. Eq. (3.51), (ii) the interferometer U , and (iii) the feedback scheme determined by the operators \hat{F}_α^j , cf. Eq. (3.64).

Before we identify conditions for achieving nontrivial quantum dynamics in Sec. 3.3, and consider possible choices for $\{\hat{S}_j, U, \hat{F}_\alpha^j\}$ in Chaps. 4 and 5, we perform the useful generalization of the formalism to multiple baths per system.

3.2.4 Generalization to multiple light modes

As in the previous section, consider N systems \mathcal{S}_j coupled to baths \mathcal{A}_j , and let us denote the feedback dynamics from Eq. (3.73) by a Liouvillian $\mathcal{L}^{\mathcal{A}}$, so

$$d\rho^{\mathcal{S}}(t) = -i[\hat{H}^{\mathcal{A}}, \rho^{\mathcal{S}}(t)]dt + \sum_{\alpha=1}^N \mathcal{D}[\hat{L}_\alpha^{\mathcal{A}}]\rho^{\mathcal{S}}(t)dt \quad (3.74)$$

$$=: \mathcal{L}^{\mathcal{A}}\rho^{\mathcal{S}}(t). \quad (3.75)$$

Now assume that each \mathcal{S}_j can simultaneously interact with a second field \mathcal{B}_k . These may correspond to different frequencies, polarizations, or spatial modes. We can construct a second interferometer $U^{\mathcal{B}}$ for the \mathcal{B} -fields, and perform additional measurements and feedback to drive the systems. Turning off the \mathcal{A} -fields and considering only the dynamics generated by the \mathcal{B} -fields will generate an analogous feedback master equation

$$d\rho^{\mathcal{S}}(t) = -i[\hat{H}^{\mathcal{B}}, \rho^{\mathcal{S}}(t)]dt + \sum_{\alpha=1}^N \mathcal{D}[\hat{L}_\alpha^{\mathcal{B}}]\rho^{\mathcal{S}}(t)dt \quad (3.76)$$

$$=: \mathcal{L}^{\mathcal{B}}\rho^{\mathcal{S}}(t). \quad (3.77)$$

If we take into account both \mathcal{A} - and \mathcal{B} -fields we find that the Liouvillians simply add up,

$$d\rho^{\mathcal{S}}(t) = \mathcal{L}^{\mathcal{B}}\rho + \mathcal{L}^{\mathcal{A}}\rho. \quad (3.78)$$

The reason for this is the additive structure of the Hamiltonian and jump operators in Eqs. (3.73). To see this combine the system and feedback operators each into a single vector, $\hat{S} = (\hat{S}^{\mathcal{A}}, \hat{S}^{\mathcal{B}})^{\text{T}}$ and $\hat{F} = (\hat{F}^{\mathcal{A}}, \hat{F}^{\mathcal{B}})^{\text{T}}$, as

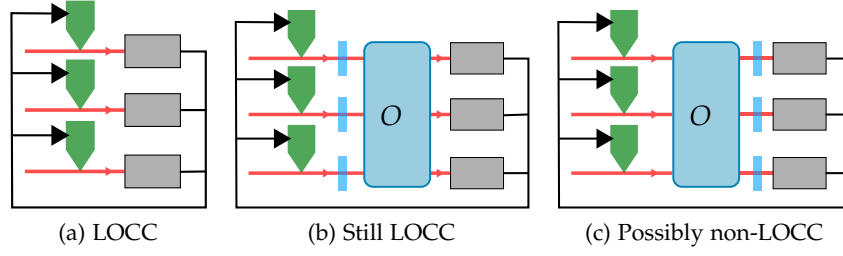


Figure 3.5: (a) Without an interferometer we can perform only local measurements. In combination with local feedback, the scheme will generate only LOCC dynamics. (b) Local phase plates before an LOCC setup, such as a real orthogonal interferometer O , will not enable any non-local operations. This is an example that does not necessarily satisfy Eq. (3.85). (c) Phase plates before the detectors, on the other hand, change the homodyne measurement basis. They may enable non-LOCC dynamics, even if the preceding setup is LOCC.

if we had $2N$ systems. The new system operators after the interferometer are then given by $\hat{\mathbf{Z}} = (\hat{\mathbf{Z}}^A, \hat{\mathbf{Z}}^B)^T := U\hat{\mathbf{S}}$, with a block diagonal matrix

$$U = \begin{bmatrix} U^A & \mathbf{0} \\ \mathbf{0} & U^B \end{bmatrix}. \quad (3.79)$$

Inserting this into Eqs. (3.73) will yield a Hamiltonian $\hat{H} = \hat{H}^A + \hat{H}^B$, and two sets of jump operators \hat{L}_k^A, \hat{L}_k^B , which results in the additive Liouvillians above. Obviously this line of reasoning can be extended to an arbitrary number of fields.

3.3 PARAMETRIZATION OF LOCC DYNAMICS

Without an interferometer we would measure each mode separately and then perform local feedback on the systems through classical channels. Schemes of this type are known to generate only *local operations and classical communication* (LOCC) dynamics [35, 53], which may transform, but not produce any quantum correlations. Thus an interferometer is required if we wish to create entanglement. However, as we will show in this chapter, not any setup will do as one might end up in the LOCC regime even for a nontrivial interferometer.

A setup without interferometer, as in Fig. 3.5a, corresponds to setting U equal to the $N \times N$ identity matrix, $U = \mathbf{1}_N$. The resulting Feedback Master Equation (FME) from Eq. (3.73) reads

$$\dot{\rho} = -\frac{i}{2} \sum_{k=1}^N [\hat{F}_k \hat{S}_k + \hat{S}_k^\dagger \hat{F}_k, \rho] + \sum_{k=1}^N \mathcal{D}[\hat{S}_k - i\hat{F}_k]\rho, \quad (3.80)$$

with local operators \hat{S}_k and feedback operators $\hat{F}_k = \sum_{l=1}^N \hat{F}_k^l$. Although the FME retains its apparently non-local form, we know from the underlying setup that it will generate only LOCC dynamics, as will any master equation which can be written in this way.

Now consider the case of a nontrivial interferometer, $U \neq \mathbf{1}_N$. We can always rewrite the general FME,

$$\begin{aligned}\dot{\rho} &= -\frac{i}{2} \sum_{k=1}^N [\hat{F}_k \hat{Z}_k + \hat{Z}_k^\dagger \hat{F}_k, \rho] + \sum_{k=1}^N \mathcal{D}[\hat{Z}_k - i\hat{F}_k] \rho \\ &= -\frac{i}{2} \sum_{j=1}^N [\hat{G}_j \hat{S}_j + \hat{S}_j^\dagger \hat{G}_j, \rho] + \sum_{j=1}^N \mathcal{D}[\hat{S}_j - i\hat{G}_j] \rho,\end{aligned}\quad (3.81)$$

by introducing (generally non-Hermitian) feedback operators

$$\hat{G}_j = \sum_{k=1}^N U_{kj} \hat{F}_k, \quad (3.82)$$

and using the invariance of Lindblad operators under multiplication by unitary matrices,

$$\sum_k \mathcal{D}[\hat{L}_k] \rho = \sum_k \mathcal{D} \left[\sum_l U_{kl} \hat{L}_l \right] \rho. \quad (3.83)$$

If the \hat{G}_j all happen to be Hermitian, the rewritten master equation is equivalent to Eq. (3.80), and thus also gives rise to LOCC dynamics. Hermiticity of \hat{G}_j can be formulated as

$$\begin{aligned}0 &= \hat{G}_j - \hat{G}_j^\dagger \\ &= \sum_{k=1}^N (U_{kj} - U_{kj}^*) \hat{F}_k \\ &= \sum_{l=1}^N \left[\sum_{k=1}^N (U_{kj} - U_{kj}^*) \hat{F}_k \right].\end{aligned}\quad (3.84)$$

Since each term in the sum over l acts on a different system, they are linearly independent and must vanish individually. Thus a sufficient condition for LOCC dynamics reads

$$\sum_{k=1}^N \text{Im}[U_{kj}] \hat{F}_k^l = 0, \quad \text{for all } j, l = 1, \dots, N. \quad (3.85)$$

In particular, this condition is satisfied for any real orthogonal interferometer $U = O$, which mixes beams without introducing a relative phase shift. The reason is that a general complex U mixes \hat{x} - and \hat{p} -quadratures, which creates non-commuting observables in the outputs, while a real orthogonal $U = O$ does not.

However, Eq. (3.85) is not a necessary condition for LOCC dynamics. For example, consider the complex diagonal matrix $U = \Lambda := \text{diag}(e^{i\theta_1}, \dots, e^{i\theta_N})$, which causes local phase shifts without mixing the fields, or any real orthogonal matrix O with phases multiplied from the right, $U = O\Lambda$, see Fig. 3.5b. In both configurations, absolute phases are imprinted on the incoming fields which can be absorbed into the system operators \hat{S}_k . They constitute LOCC setups that need not satisfy Eq. (3.85). In fact, if some unitary matrix U_0 fulfills Eq. (3.85) then any $U = U_0\Lambda$ will also generate LOCC dynamics even if it does not satisfy (3.85).

On the other hand, the seemingly similar case of multiplication of O with phases from the left, $U = \Lambda O$, depicted in Fig. 3.5c, actually changes the homodyne measurement basis. This may facilitate non-LOCC dynamics, even if the interferometer alone does not. This fact is made use of in the protocol presented in Sec. 4.1.

DISSIPATIVE STATE PREPARATION

In this chapter we examine the feedback scheme with regard to dissipative state engineering [54]. Here the goal is to generate nontrivial quantum correlations in the stationary state achieved in the long-time limit of the general feedback scheme presented in Sec. 3.2. One particular example of this kind has been given by Hofer et al. [30, 33, 34] who showed that it is possible to design a feedback master equation which deterministically drives a pair of two-level-systems (qubits) into an entangled state. We begin in Sec. 4.1 by reviewing this two-qubit protocol, which serves as a prime illustration of how we might employ the general Feedback Master Equation (FME) given in Eq. (3.73). In Sec. 4.2 we extend it to include more than two qubits, and show in Sec. 4.3 that it can produce entangled many-body states.

4.1 ENTANGLING TWO-QUBIT PROTOCOL

The two-qubit protocol from [30] is depicted in Fig. 4.1. It comprises two physical qubits, \mathcal{S}_1 and \mathcal{S}_2 , with corresponding light fields, \mathcal{A}_1 and \mathcal{A}_2 , and a balanced beam splitter mixing the beams. Subsequently, a phase plate shifts the phase of one field by $\pi/2$. Together with homodyne detection this realizes a continuous-variable Bell measurement. The fields are time-continuously projected into maximally entangled Einstein-Podolsky-Rosen (EPR) states by measuring the operators $\hat{X}_1 = \hat{X}_{\mathcal{A}_1} + \hat{X}_{\mathcal{A}_2}$ and $\hat{X}_2 = \hat{P}_{\mathcal{A}_1} - \hat{P}_{\mathcal{A}_2}$ in the top and bottom detector, respectively. Here, $\hat{X}_{\mathcal{A}_j}$ ($\hat{P}_{\mathcal{A}_j}$) denotes the amplitude (phase) quadrature of incoming field \mathcal{A}_j . Choosing appropriate feedback operators then drives the two qubits into the state $|\psi(z)\rangle \propto |00\rangle - z|11\rangle$. The parameter $z \in (0, 1)$ is chosen beforehand to fix the system-light coupling and feedback gains, which then determine $|\psi(z)\rangle$.

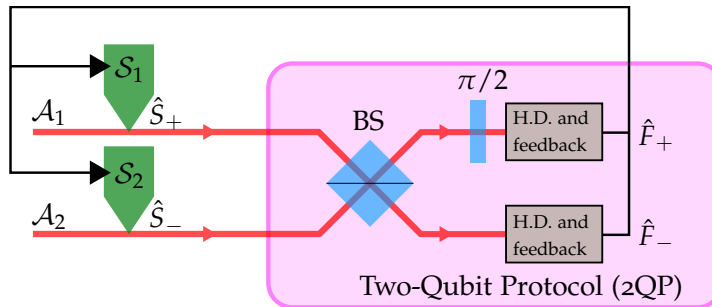


Figure 4.1: Illustration of the two-qubit protocol (2QP). Both qubits \mathcal{S}_j interact with light fields via \hat{S}_+ or \hat{S}_- respectively. The fields are superposed on a balanced beam splitter (BS), after which one beam is phase-shifted by $\pi/2$. We perform a homodyne measurement (HM) of each field, and apply feedback \hat{F}_\pm proportional to the measured signal. The qubits will eventually relax into the steady state $|\psi(z)\rangle$.

The system-light coupling is generated by the system operators

$$\hat{S}_+ = s_+ \hat{\sigma}_+^1 + s_- \hat{\sigma}_-^1, \quad \hat{S}_- = s_+ \hat{\sigma}_+^2 - s_- \hat{\sigma}_-^2, \quad (4.1)$$

with $s_+ = \sqrt{z(1+z)}$ and $s_- = \sqrt{1-z}$ ¹. Here, $\hat{\sigma}_\pm^j$ denote the standard Pauli raising and lowering operators acting on the j th qubit. We differ slightly from the notation of Sec. 3.2.3, replacing the system operators \hat{S}_1 and \hat{S}_2 with \hat{S}_+ and \hat{S}_- respectively, to more easily include multiple qubits in the following section.

The beam splitter and subsequent phase plate are represented by

$$U = \frac{1}{\sqrt{2}} \begin{bmatrix} 1 & 0 \\ 0 & i \end{bmatrix} \begin{bmatrix} 1 & 1 \\ 1 & -1 \end{bmatrix} = \frac{1}{\sqrt{2}} \begin{bmatrix} 1 & 1 \\ i & -i \end{bmatrix}, \quad (4.2)$$

so that the new system operators read

$$\hat{Z}_+ = \frac{1}{\sqrt{2}}(\hat{S}_+ + \hat{S}_-), \quad \hat{Z}_- = \frac{i}{\sqrt{2}}(\hat{S}_+ - \hat{S}_-). \quad (4.3)$$

We choose the feedback operators

$$\hat{F}_+ = g_+ \hat{\sigma}_y^1 + g_- \hat{\sigma}_y^2, \quad \hat{F}_- = g_- \hat{\sigma}_x^1 - g_+ \hat{\sigma}_x^2, \quad (4.4)$$

with gain coefficients $g_\pm = z(s_- \pm s_+)/(\sqrt{2}s_+s_-)$. The system master equation that results from plugging these choices into the general FME (3.73) reads

$$\dot{\rho} = \mathcal{L}\rho := -\frac{i}{2}[\hat{F}_+\hat{Z}_+ + \hat{F}_-\hat{Z}_- + \text{h.c.}, \rho] + \mathcal{D}[\hat{J}_+]\rho + \mathcal{D}[\hat{J}_-]\rho, \quad (4.5)$$

with jump operators $\hat{J}_\pm = \hat{Z}_\pm - i\hat{F}_\pm$.

The operators \hat{F}_\pm and \hat{Z}_\pm were chosen such that the master equation has the unique stationary state

$$|\psi(z)\rangle = \frac{1}{\sqrt{1+z^2}}(|00\rangle - z|11\rangle), \quad (4.6)$$

which can be seen as follows. The jump operators in Eq. (4.5) are

$$\hat{J}_+ \propto \hat{K}_1 + \lambda(z)\hat{K}_2, \quad \hat{J}_- \propto \lambda(z)\hat{K}_1 - \hat{K}_2, \quad (4.7)$$

with $\hat{K}_1 = \hat{\sigma}_-^1 + z\hat{\sigma}_+^2$ and $\hat{K}_2 = \hat{\sigma}_-^2 + z\hat{\sigma}_+^1$ for some $\lambda(z) \in \mathbb{R}$. It is straightforward to check that \hat{K}_1 and \hat{K}_2 have $|\psi(z)\rangle$ as their common *dark state* [54], i. e., as eigenstate with eigenvalue 0, and thus as dark state of \hat{J}_+ and \hat{J}_- . The particular combinations of \hat{Z}_\pm and \hat{F}_\pm that make up the jump operators were also chosen such that $|\psi(z)\rangle$ is an eigenstate of the Hamiltonian in Eq. (4.5). These two properties place $|\psi(z)\rangle\langle\psi(z)|$ in the kernel of Liouvillian \mathcal{L} , and make it a steady state of the system [54]. Further investigation, e. g., by diagonalizing the Liouvillian, shows that $|\psi(z)\rangle$ is the *only* steady state, which entails that regardless of the initial state the qubits will eventually be driven into $|\psi(z)\rangle$. In other

¹ How this specific system-light coupling might be achieved experimentally in an atomic system is outlined in Appendix D of [30].

words $|\psi(z)\rangle$ is prepared deterministically after some finite relaxation time.

In the following we will treat z as a variable rather than as a constant to be fixed at the start. This is justified because when z is changed, $z \rightarrow z'$ say, the qubits will relax into the new steady state $|\psi(z')\rangle$. If the variation of z is sufficiently slow compared to the relaxation time, we expect the qubits to adiabatically follow the state space trajectory $\{|\psi(z)\rangle, z \in [0, 1]\}$.

The interesting result of [30], which also inspired the present work, was the deterministic preparation of entanglement. For any $0 < z < 1$ we see that $|\psi(z)\rangle$ is entangled, and will ideally approach the maximally entangled Bell state $|\Phi^-\rangle \propto |00\rangle - |11\rangle$ as $z \rightarrow 1$. This ideal limit can never be realized exactly since it leads to infinite feedback gains, $|g_{\pm}| \rightarrow \infty$. But using a more realistic description of the dynamics including passive photon loss [30, 33] (see also App. A.3), the highest possible degree of entanglement is always obtained for $z < 1$. Keeping s_{\pm} as above while optimizing g_{\pm} to maximize the amount of entanglement in the steady state for every z , the optimal gains g_{\pm} always remain finite, and one finds an entangled steady state for up to 50% photon loss.

The opposite limit of $z = 0$ corresponds to a setup without feedback, which entails $\hat{H} = 0$. With jump operators $\hat{J}_k \sim \hat{S}_k = \hat{\sigma}_-^k$, the qubits are incoherently pumped into the trivial state $|00\rangle$.

4.2 EXTENSION TO MULTIPLE QUBITS

Motivated by this deterministic preparation of a nontrivial quantum state of qubits, we examined whether and how the scheme could be extended to generate multipartite entangled states. To begin, consider a third qubit S_3 added to the existing setup, and coupled to S_2 via a replica of the original protocol with the same parameter z , shown in Fig. 4.2. This is realized by letting S_2 simultaneously interact with two light fields, \mathcal{A}_2 and \mathcal{B}_2 , e. g., different polarizations of the same field or different spatial modes, as discussed in Sec. 3.2.4.

We now generalize the operators \hat{S}_{\pm} and \hat{F}_{\pm} from the previous section. Let the index $j = 1, 2$ label the different two-qubit-setups, each coupling a pair $S_j S_{j+1}$. The system operators for the j th setup read

$$\hat{S}_{j,+} = s_+ \hat{\sigma}_+^j + s_- \hat{\sigma}_-^j, \quad \hat{S}_{j,-} = s_+ \hat{\sigma}_+^{j+1} - s_- \hat{\sigma}_-^{j+1}, \quad (4.8)$$

and are mixed by the beam splitter and phase plate of each setup to yield

$$\hat{Z}_{j,+} = \frac{1}{\sqrt{2}}(\hat{S}_{j,+} + \hat{S}_{j,-}), \quad \hat{Z}_{j,-} = \frac{i}{\sqrt{2}}(\hat{S}_{j,+} - \hat{S}_{j,-}). \quad (4.9)$$

The feedback is mediated via operators

$$\hat{F}_{j,+} = g_+ \hat{\sigma}_y^j + g_- \hat{\sigma}_y^{j+1}, \quad \hat{F}_{j,-} = g_- \hat{\sigma}_x^j - g_+ \hat{\sigma}_x^{j+1}. \quad (4.10)$$

The resulting Liouvillian $\mathcal{L}_{j,j+1}$ acts on the pair $S_j S_{j+1}$ as indicated on the right in Fig. 4.2. It takes the same form as in Eq. (4.5),

$$\mathcal{L}_{j,j+1}\rho := -\frac{i}{2}[\hat{F}_{j,+}\hat{Z}_{j,+} + \hat{F}_{j,-}\hat{Z}_{j,-} + \text{h.c.}, \rho] + \mathcal{D}[\hat{J}_{j,+}]\rho + \mathcal{D}[\hat{J}_{j,-}]\rho, \quad (4.11)$$

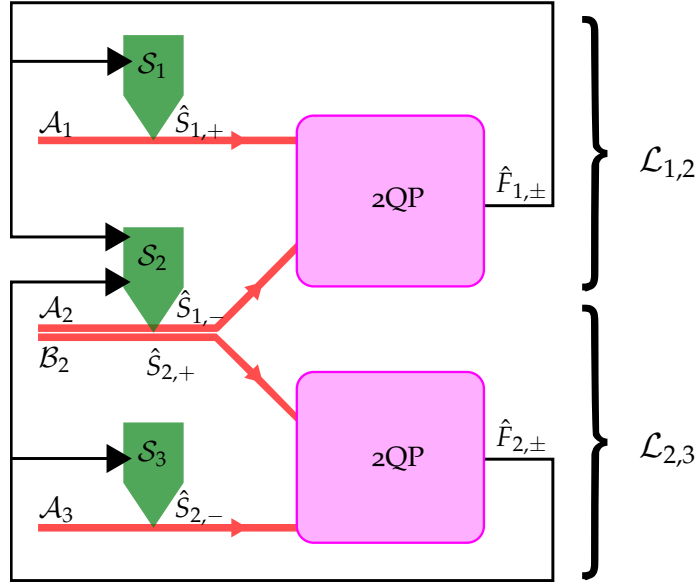


Figure 4.2: The Two-Qubit Protocol (2QP) is extended to 3 qubits. This is done by letting two light fields, \mathcal{A}_2 and \mathcal{B}_2 , interact with \mathcal{S}_2 , and using a second copy of the 2QP. \mathcal{A}_2 interacts via $\hat{S}_{1,-}$ and then enters the first 2QP with light coming from \mathcal{S}_1 . This generates feedback $\hat{F}_{1,\pm}$ on $\mathcal{S}_1\mathcal{S}_2$ which gives rise to the Liouvillian $\mathcal{L}_{1,2}$. Analogously, \mathcal{B}_2 interacts with \mathcal{S}_2 via $\hat{S}_{2,+}$ and then enters the second 2QP together with \mathcal{A}_3 coming from \mathcal{S}_3 . This results in feedback $\hat{F}_{2,\pm}$ on $\mathcal{S}_2\mathcal{S}_3$ and Liouvillian $\mathcal{L}_{2,3}$.

with the proper system and feedback operators, and jump operators $\hat{J}_{j,\pm} = \hat{Z}_{j,\pm} - i\hat{F}_{j,\pm}$. The total feedback master equation for all three qubits then comprises both Liouvillians,

$$\dot{\rho} = \mathcal{L}_{1,2}\rho + \mathcal{L}_{2,3}\rho. \quad (4.12)$$

It is now straightforward to extend the setup and formalism to N qubits $\mathcal{S}_1, \dots, \mathcal{S}_N$ with corresponding $\mathcal{L}_{j,j+1}$ for $j = 1, \dots, N-1$. This represents an open-ended chain with nearest-neighbor interaction. We can turn this chain into a ring by also coupling \mathcal{S}_N to \mathcal{S}_1 via $\mathcal{L}_{N,N+1} \equiv \mathcal{L}_{N,1}$. This gives rise to the master equation

$$\dot{\rho} = \sum_{j=1}^N \mathcal{L}_{j,j+1}\rho, \quad (4.13)$$

which generates periodic and translationally invariant dynamics. The steady state should inherit these symmetries.

Recall that the non-periodic two-qubit version of the protocol prepares the state $|\psi(z)\rangle$ from Eq. (4.6), which goes from a product state for $z = 0$ to a maximally entangled state as $z \rightarrow 1$. It was shown that bipartite entanglement in a system of qubits is monogamous [55, 56]. Consequently, highly entangling two qubits, \mathcal{S}_1 and \mathcal{S}_2 say, places an upper bound on the possible entanglement between \mathcal{S}_2 and \mathcal{S}_3 (and so on). Hence we expect some competition between the pairwise dynamics generated by each $\mathcal{L}_{j,j+1}$, reminiscent of a frustrated spin chain.

4.3 ANALYSIS OF THE STEADY STATE

The competing Liouvillians $\mathcal{L}_{j,j+1}$ give rise to a nontrivial collective steady state of the qubits. To investigate it we use the Python package “QuTiP” [57, 58] to obtain exact results for small numbers of systems ($N \leq 7$), and a recently established variational procedure [59] in the limit of a large number of systems.

The central element of the variational procedure is a variational principle for the steady state of an open quantum system. After restricting the steady state ansatz to a certain variational manifold, the steady state equation $(d/dt)\rho = 0$ can no longer be solved, as the true steady state will generically lie outside the variational manifold. Therefore, the variational norm $\|(d/dt)\rho\|$ is minimized instead to obtain an approximation for the steady state. Importantly, the choice of the variational norm is not arbitrary, but has to be the trace norm $\|(d/dt)\rho\|_1 = \text{Tr}\{|(d/dt)\rho|\}$ [59, 60], i. e., the sum of singular values of $(d/dt)\rho$.

Here, we parametrize the density operator according to

$$\begin{aligned} \rho = & \rho_0 \otimes \rho_0 \otimes \cdots + \sum_i \rho_0 \otimes \cdots \otimes C_{i,i+1} \otimes \rho_0 \cdots \\ & + \sum_{i,j} \rho_0 \otimes \cdots \otimes C_{i,i+1} \otimes \rho_0 \cdots \otimes C_{j,j+1} \otimes \rho_0 \cdots + \dots \end{aligned} \quad (4.14)$$

The first term is simply a product state of all qubits being in the state ρ_0 . The other terms involve the nearest-neighbor correlation matrices $C_{i,i+1}$ and allow to describe nonclassical correlations such as entanglement. As the calculation of the exact variational norm is in general still an intractable problem, we resort to an upper bound to the norm that can be efficiently calculated, and is given by a sum of three-qubit problems, $\|(d/dt)\rho\| \leq \sum_i \|(d/dt)\rho_{i-1,i,i+1}\|$, where $\rho_{i-1,i,i+1}$ is the reduced density operator involving three qubits [59, 60]. As we consider a translationally invariant problem, minimizing a single three-qubit term minimizes the full sum as well.

Results

As before, turning off the feedback ($z = 0$) yields the trivial pure state

$$|\psi(z = 0)\rangle = \bigotimes_{j=1}^N |0\rangle_j, \quad (4.15)$$

obtained by incoherent pumping of the individual systems. With feedback ($z > 0$), however, the competing dynamics immediately take effect. This can be seen in Fig. 4.3, where we plot the purity $\mathcal{P}(\rho(z)) = \text{Tr}\{(\rho(z))^2\}$ for different values of z . As z grows, $\rho(z)$ becomes increasingly mixed and approaches the maximally mixed state for $z \rightarrow 1$, where the feedback gains become infinite. Thus we expect to find no quantum correlations in either of the limits $z \rightarrow 0$ or $z \rightarrow 1$.

In the regime $0 < z < 1$, on the other hand, entanglement does form, as can be seen in Figs. 4.4 and 4.5. A simple indicator for bipartite entanglement is the *concurrence* $\mathcal{C}(\rho_{kl}(z))$ [55, 56, 61], which is related to the entanglement of formation for two-qubit states. It can be computed for

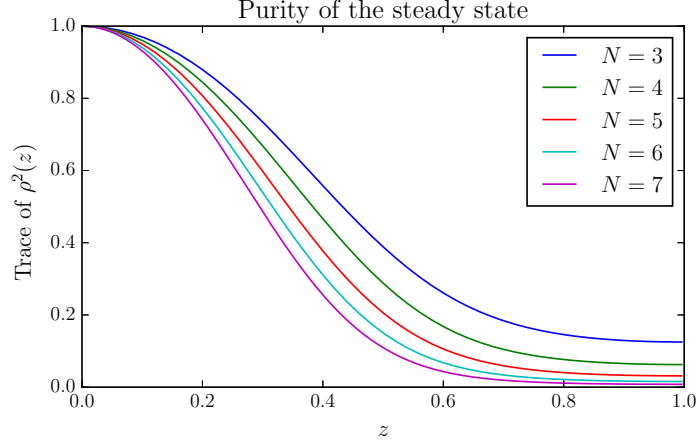


Figure 4.3: The purity of the steady state varies with z . Without feedback ($z = 0$) all systems are incoherently pumped into $|0\rangle$. As z grows, however, competition between the pairwise dynamics increasingly mixes the steady state. The maximally mixed state is approached with $\mathcal{P}(\rho) = \text{Tr}(\rho(z))^2 \rightarrow 2^{-N}$ as $z \rightarrow 1$. The curves in the legend are shown from top to bottom in the figure.

arbitrary pairs of qubits $\mathcal{S}_k\mathcal{S}_l$ after taking the partial trace over all other systems,

$$\rho_{kl}(z) := \text{Tr}_{\neq \mathcal{S}_k, \mathcal{S}_l} \{\rho(z)\}. \quad (4.16)$$

For the two-qubit state ρ_{kl} the concurrence is then defined as

$$\mathcal{C}(\rho_{kl}) = \max\{0, \lambda_1 - \lambda_2 - \lambda_3 - \lambda_4\}, \quad (4.17)$$

where the λ_j are the square roots of the eigenvalues of $\rho_{kl}(\hat{\sigma}_y \otimes \hat{\sigma}_y)\rho_{kl}^*(\hat{\sigma}_y \otimes \hat{\sigma}_y)$ in decreasing order.

Since the dynamics, and hence the steady state, is translationally invariant and periodic the concurrence only depends on the distance between two qubits on the ring. Our analysis revealed that the concurrence of nearest neighbors is non-zero in the region $0 < z \lesssim 0.4$, see Fig. 4.4. Thus the steady state is indeed entangled in this regime. We found that the concurrence is independent of the number of systems for $N \leq 7$, and qualitatively agrees with the variational results. On the other hand, the concurrence between non-neighboring qubits vanishes everywhere, which may be because each Liouvillian $\mathcal{L}_{j,j+1}$ acts only on neighboring pairs.

To better understand the results obtained using the concurrence we also considered the *logarithmic negativity* E_N [61–63]. This is defined as

$$E_N(\rho_{\mathcal{X}\mathcal{Y}}) = \log_2 \|\rho_{\mathcal{X}\mathcal{Y}}^{\text{T}_{\mathcal{X}}}\|_1, \quad (4.18)$$

where $\rho_{\mathcal{X}\mathcal{Y}}$ is the state of a bipartite system $\mathcal{X}|\mathcal{Y}$, the operation $\text{T}_{\mathcal{X}}$ denotes the partial transpose with respect to subsystem \mathcal{X} , and $\|\rho\|_1$ is trace norm as above. Neither of the subsystems, \mathcal{X} or \mathcal{Y} , need to be qubits, and may each constitute multipartite systems themselves. If $E_N(\rho_{\mathcal{X}\mathcal{Y}})$ is non-zero, systems \mathcal{X} and \mathcal{Y} are entangled, so it provides a sufficient (but not necessary [62, 63]) condition for the presence of quantum correlations. The results of our study can be seen in Fig. 4.5. The

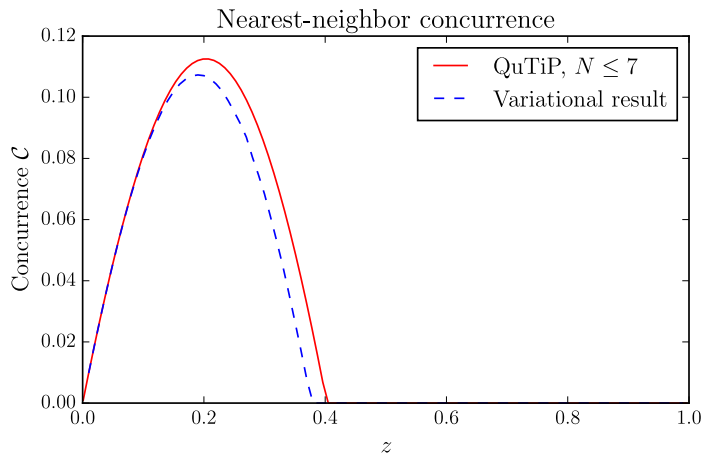


Figure 4.4: The concurrence $\mathcal{C}(\rho_{k,k+1}(z))$ of neighboring qubits in the steady state is non-zero for $0 < z \lesssim 0.4$, showing the presence of entanglement. We computed the steady state directly using the Python package QuTiP [57, 58] for small system size ($N \leq 7$ qubits), and found the concurrence to be independent of N (solid red line). For large N we analyzed the steady state using a variational approach [59]. While the variational concurrence (dotted blue line) takes on slightly different values, it is still in good qualitative agreement with our exact results. We found the concurrence between non-neighboring qubits to vanish everywhere.

largest region in which we were able to detect entanglement in this way was for up to $z \approx 0.6$. Out of all possible bipartitions, the entanglement always extended furthest for the “odd|even”-partition with subsystems $\mathcal{X} = \mathcal{S}_1\mathcal{S}_3\mathcal{S}_5\dots$ and $\mathcal{Y} = \mathcal{S}_2\mathcal{S}_4\mathcal{S}_6\dots$

It is interesting that the entanglement as measured by E_N not only extends further but also peaks at larger z than the concurrence. This may be attributed to the fact that the concurrence is, in a sense, a more local quantity since it detects only correlations between two qubits, while the logarithmic negativity takes into account the collective N -qubit state. This difference in behavior might indicate that the quantum correlations are not simply destroyed as z grows, but instead manifest in more complex or long-ranged form, such as true multipartite entanglement [61, 62].

These results settle the question of whether the feedback scheme can reliably produce entangled many-body states. Both the concurrence and the logarithmic negativity provide clear evidence for quantum correlations in the steady state, which could not necessarily be expected from the underlying setup or the master equation alone. Furthermore, the entanglement appears to be present independent of the number of systems, which is backed by the results of the variational ansatz.

4.4 OUTLOOK ON PREPARATION OF GENERAL STATES

In the previous sections we first designed the dynamics and then checked for interesting features of the resulting steady state. A complementary approach is to first choose a state of interest and then tailor the dynam-

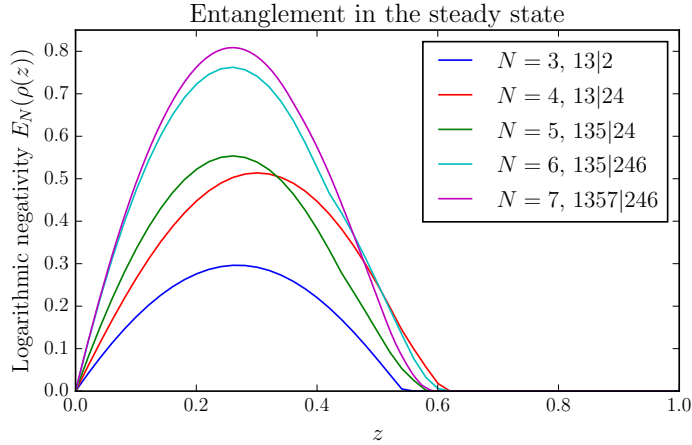


Figure 4.5: The logarithmic negativity $E_N(\rho(z))$ in the steady state for “odd|even”-bipartitions of setups comprising $N = 3, \dots, 7$ qubits. Increasing the system size causes a larger peak negativity. Notably, the entanglement persists for values of around $z \approx 0.6$, where the concurrence has long vanished. The curves in the legend are shown from bottom to top in the figure.

ics such that this state is realized as steady state [54]. However, there are a few pitfalls one has to be aware of.

Without imposing physical or other constraints there are a large number of (redundant) degrees of freedom in the setup. We can in principle freely choose the system operators \hat{S}_j , the interferometer U , and the feedback operators \hat{F}_α . Considering N systems with local Hilbert space dimension d , each system operator \hat{S}_j is determined by $2d^2$ real parameters, the interferometer by N^2 , and each feedback operator by d^2 , which yields a total of $N^2 + 3Nd^2$ real numbers. Even for the simple case of three qubits one ostensibly has 45 parameters. Of course these are not independent. As discussed in Sec. 3.3, the system operators can always be redefined to absorb phases from the interferometer, and the feedback operators can absorb any real matrix. Identifying these redundant degrees of freedom would be paramount to a complete and efficient parametrization of the realizable dynamics.

It is an open question to classify, at least partially, the set of reachable steady states. It is known [64, 65] that to produce a state with entanglement between k parties as the steady state of some dissipative dynamics, the Liouvillian that generates these dynamics must have at least one jump term that is at least k -local, i. e., acts irreducibly on k subsystems. Master equations such as the FME (3.73) are not unique since one can always redefine the Hamiltonian and jump operators while generating the same evolution (see, e. g., Eq. (3.83)). Translating the restrictions of the possible feedback setups into restrictions on the locality of the dynamics would be quite useful to confine the set of possible steady states.

We now approach the feedback setup from the perspective of quantum simulation. It can be difficult to design and control many-body quantum systems in experiments because of their complex interaction, and it is often not feasible to simulate them on classical computers due to their large state space. A full-scale quantum computer might relieve these issues, but is still out of reach. This gap is filled by quantum simulation [66–73], where a complex physical many-body system is emulated using a more easily controllable setup.

Our feedback scheme may prove useful in this regard since it realizes pairwise interaction and collective dissipation between distant systems, while using only standard techniques of quantum optics. To gauge its scope we realize a dissipative Ising spin model with local transverse fields. Such models are the subject of active research because of their relation to ultracold Rydberg atoms [74–78].

5.1 OPEN ISING MODEL WITH TRANSVERSE FIELDS

The system we wish to emulate comprises N interacting spin-1/2 particles with Hamiltonian

$$\hat{H}_{\text{Ising}} = \sum_{k \neq l}^N \delta_{kl} \hat{\sigma}_x^k \hat{\sigma}_x^l - \sum_{k=1}^N B_k \hat{\sigma}_z^k, \quad (5.1)$$

where $\hat{\sigma}_u^j$ ($u = x, y, z$) denotes a Pauli operator acting on the j th system. The parameters $\delta_{kl} \in \mathbb{R}$ determine the interaction between systems k and l , while $B_k \in \mathbb{R}$ is the strength of local magnetic fields. If we set $\delta_{kk} = -B_k$, all parameters can be encoded in a real matrix $\Delta = (\delta_{kl})$. Note that we do not make assumptions about the range or geometry of the interaction, so \hat{H}_{Ising} may apply to, e.g., a chain, a ring, or a d -dimensional lattice, depending solely on the choice of Δ .

5.1.1 Engineering the Hamiltonian

To generate this Hamiltonian using our feedback scheme we consider an ensemble of N two-level systems, $\mathcal{S}_1, \dots, \mathcal{S}_N$, as in the previous chapter. Each \mathcal{S}_k is coupled to two light fields, \mathcal{A}_k and \mathcal{B}_k , as shown in Fig. 5.1. We choose identical system-light coupling for both fields via system operators

$$\hat{S}_k^{\mathcal{A}} = \hat{S}_k^{\mathcal{B}} =: \hat{S}_k = \hat{\sigma}_-, \quad (5.2)$$

as well as identical feedback operators

$$\hat{F}_k^{\mathcal{A}} = \hat{F}_k^{\mathcal{B}} =: \hat{F}_k = \sum_{j=1}^N g_{jk} \hat{\sigma}_x^j, \quad (5.3)$$

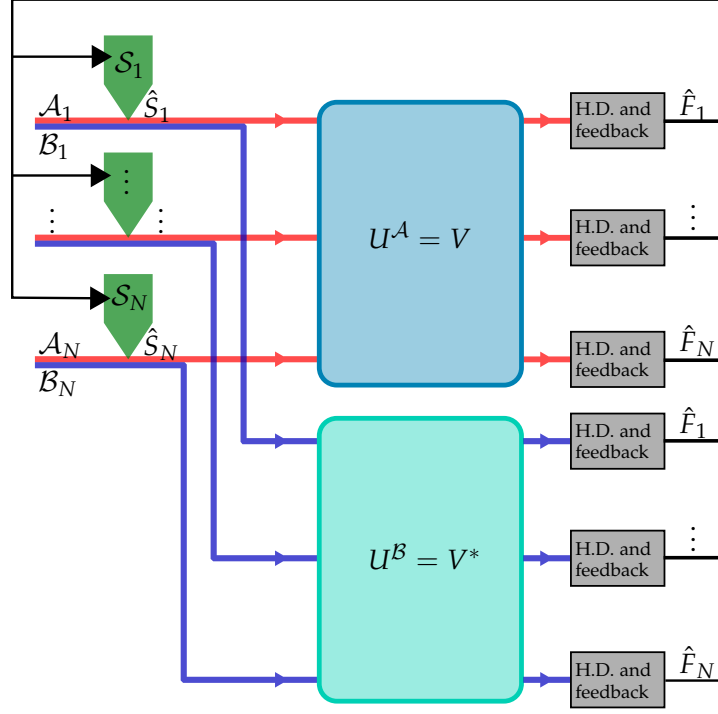


Figure 5.1: A feedback scheme to realize an open Ising model. Each two-level system \mathcal{S}_k couples to two light fields, \mathcal{A}_k (red) and \mathcal{B}_k (blue). The \mathcal{A} -fields traverse an interferometer V , while the \mathcal{B} -fields pass the complex conjugate V^* . Homodyne detection of each field then allows for feedback via operators \hat{F}_k . This way one can realize the dynamics of a dissipative Ising model.

with some feedback gains $G = (g_{jk}) \in \mathbb{R}^{N \times N}$. Note that even though system and feedback operators are the same, the setups may still generate different dynamics if their interferometers U^A and U^B are different.

We first neglect the \mathcal{B} -fields, and consider only the dynamics generated by the \mathcal{A} -fields. We fix the interferometer U^A to be some $N \times N$ unitary matrix, $U^A = V$. Together with the operators \hat{S}_k and \hat{F}_k chosen as above, we find the feedback Hamiltonian

$$\begin{aligned} \hat{H}^A = & \frac{1}{2} \sum_{k \neq l} \left(\text{Re}[K_{kl}] \hat{\sigma}_x^l + \text{Im}[K_{kl}] \hat{\sigma}_y^l \right) \hat{\sigma}_x^k \\ & + \frac{1}{2} \sum_{k=1}^N \text{Re}[K_{kk}] (\hat{1} + \hat{\sigma}_z^k), \end{aligned} \quad (5.4)$$

where we defined the matrix $K = (K_{kl}) := GV$, comprising gains and interferometer, and $\text{Re}[\cdot]$ and $\text{Im}[\cdot]$ denote real and imaginary part respectively. The Hamiltonian \hat{H}^A already resembles \hat{H}_{Ising} from Eq. (5.1), up to terms creating a $\hat{\sigma}_x \hat{\sigma}_y$ -interaction. We use the second feedback setup to eliminate these.

For the moment let us consider only the dynamics generated by the \mathcal{B} -fields. We choose the second interferometer to be the complex conjugate

of the first, $U^{\mathcal{B}} = V^*$. Thus we obtain a second feedback Hamiltonian $\hat{H}^{\mathcal{B}}$ with K^* instead of K , so

$$\begin{aligned} \hat{H}^{\mathcal{B}} &= \frac{1}{2} \sum_{k \neq l} \left(\text{Re}[K_{kl}] \hat{\sigma}_x^l - \text{Im}[K_{kl}] \hat{\sigma}_y^l \right) \hat{\sigma}_x^k \\ &\quad + \frac{1}{2} \sum_{k=1}^N \text{Re}[K_{kk}] (\hat{1} + \hat{\sigma}_z^k). \end{aligned} \quad (5.5)$$

As explained in Sec. 3.2.4 we obtain the combined evolution of both schemes by adding their Liouvillians. Thus, the total Hamiltonian $\hat{H} = \hat{H}^{\mathcal{A}} + \hat{H}^{\mathcal{B}}$ will be

$$\hat{H} = \sum_{k \neq l} \text{Re}[K_{kl}] \hat{\sigma}_x^k \hat{\sigma}_x^l + \sum_{k=1}^N \text{Re}[K_{kk}] (\hat{1} + \hat{\sigma}_z^k). \quad (5.6)$$

The interaction and local fields in this model are entirely governed by the matrix $\text{Re}[K] = \text{Re}[GV] = G\text{Re}[V]$. Recall that we are free to choose both the feedback gains G and the interferometer V . Assuming $\text{Re}[V]$ can be inverted, we can realize a given set of couplings Δ by setting the gains as

$$G = \Delta \text{Re}[V]^{-1}. \quad (5.7)$$

This will yield the desired Hamiltonian from Eq. (5.1),

$$\hat{H} = \sum_{k \neq l} \delta_{kl} \hat{\sigma}_x^k \hat{\sigma}_x^l - \sum_{k=1}^N B_k (\hat{\sigma}_z^k + \hat{1}), \quad (5.8)$$

up to negligible constants.

A generic unitary V is not guaranteed to have a non-singular real part. However, writing

$$\text{Re}[V] = \frac{1}{2}(V^* + V) = \frac{1}{2}V^*(\mathbf{1}_N + V^T V) \quad (5.9)$$

shows that invertibility of $\text{Re}[V]$ is equivalent to that of $\mathbf{1}_N + V^T V$. Thus the necessary and sufficient condition is that all eigenvalues of $V^T V$ are different from -1 . Note also that V does not need to reflect the geometry of the physical model as given by Δ .

5.1.2 Effect of the dissipation

Recall from the Feedback Master Equation (FME) (3.73) that our scheme naturally introduces jump operators of the form

$$\hat{Z}_k - i\hat{F}_k = \sum_{l=1}^N U_{kl} \hat{S}_l - i\hat{F}_k \quad (5.10)$$

for each light field. In this case there will be two sets of jump operators, corresponding to the \mathcal{A} - and \mathcal{B} -setup respectively.

As mentioned in Sec. 3.3 a collection of jump operators is always invariant under unitary transformations,

$$\sum_k \mathcal{D}[\hat{J}_k] \rho = \sum_k \mathcal{D} \left[\sum_l U_{kl} \hat{J}_l \right] \rho, \quad (5.11)$$

and we use this to define a new set of jump operators,

$$\hat{J}_k := \sum_{l=1}^N (U^\dagger)_{kl} (\hat{Z}_l - i\hat{F}_l) = \hat{S}_k - i \sum_{l=1}^N U_{lk}^* \hat{F}_l, \quad (5.12)$$

equivalent to the former. These are given by

$$J_k^A := \hat{S}_k - i \sum_{j=1}^N V_{jk}^* \hat{F}_j = \hat{\sigma}_-^k - i \sum_{j=1}^N \Gamma_{jk} \hat{\sigma}_x^j, \quad (5.13)$$

$$J_k^B := \hat{S}_k - i \sum_{j=1}^N V_{jk} \hat{F}_j = \hat{\sigma}_-^k - i \sum_{j=1}^N \Gamma_{jk}^* \hat{\sigma}_x^j, \quad (5.14)$$

with the complex matrix

$$\Gamma := \Delta \text{Re}[V]^{-1} V^* = 2\Delta(\mathbf{1}_N + V^T V)^{-1}. \quad (5.15)$$

Together with the Hamiltonian from Eq. (5.8) these jump operators yield the dynamics of an open system of interacting spins with master equation

$$\dot{\rho} = -i[\hat{H}, \rho] + \sum_{k=1}^N \mathcal{D}[J_k^A] \rho + \sum_{k=1}^N \mathcal{D}[J_k^B] \rho. \quad (5.16)$$

An important observation is that the coupling matrix Δ appears in Γ and thus also in the jump operators. Hence, fixing the interaction and local fields of the physical model encoded in the Hamiltonian (5.8) also determines the structure and strength of the dissipation. In particular, both Δ and V will determine the range of the jump operators, i. e., how many systems couple to the same bath.

Note that there are degrees of freedom we have not used. One parameter we could change is the relative strength of the system-light interaction and feedback. We can change the interaction by a factor $r \in \mathbb{R}$, i. e., $\hat{S} \mapsto r\hat{S}$, while inversely changing the feedback, $\hat{F} \mapsto \hat{F}/r$. This will not affect the Hamiltonian since it only comprises products of the form $\hat{S}\hat{F}$. On the other hand, it will cause either $\hat{\sigma}_-$ (for $r \gg 1$) or $\hat{\sigma}_x$ (for $r \ll 1$) to dominate the jump operators, and also increase the overall strength of the dissipation compared to \hat{H} .

Another free parameter is asymmetry of Δ . Let us set $\Delta_\pm := (\Delta \pm \Delta^T)/2$ as the symmetric and skew-symmetric part of $\Delta = \Delta_+ + \Delta_-$ respectively. The symmetric part is fixed by the physical couplings δ and B in the Hamiltonian from Eq. (5.1). However, Δ_- does not enter the Hamiltonian, so we are free to choose it at will. It only affects the jump operators. For simplicity, we set $\Delta_- = \mathbf{0}_N$ in the following example.

5.2 CONCRETE EXAMPLE

To demonstrate how to realize a specific model we consider a translationally invariant one-dimensional Ising chain with nearest-neighbor interaction and periodic boundary conditions. The corresponding physical Hamiltonian is

$$\hat{H}_{\text{Ising}} = \delta \sum_{k=1}^N \hat{\sigma}_x^k \hat{\sigma}_x^{k+1} - B \sum_{j=1}^N \hat{\sigma}_z^j, \quad (5.17)$$

with periodicity implemented by setting $\hat{\sigma}_x^{N+1} \equiv \hat{\sigma}_x^1$. We can read off the interaction matrix Δ ,

$$\Delta = B\mathbf{1}_N + \frac{\delta}{2}(S + S^T), \quad (5.18)$$

where $S = (s_{kl})$ is the periodic shift matrix with elements $s_{N,1} = s_{k,k+1} = 1 \forall k$ and $s_{kl} = 0$ otherwise, i. e.,

$$S = \begin{bmatrix} 0 & 1 & 0 & \dots & 0 \\ 0 & 0 & 1 & \dots & 0 \\ \vdots & \vdots & & \ddots & \\ 0 & 0 & \dots & 0 & 1 \\ 1 & 0 & \dots & 0 & 0 \end{bmatrix}. \quad (5.19)$$

We would now like to engineer translationally invariant jump operators in order not to break the symmetry of the model. To this end we must choose V such that the coefficient matrix from the jump operators, $\Gamma = 2\Delta(\mathbf{1}_N + V^T V)^{-1}$, is also translationally invariant. This is the case if and only if $[V^T V, S] = 0$, so $V^T V$ and S must be simultaneously diagonalizable. We know that the discrete Fourier transform $F = (F_{jk})$ [79] with

$$F_{jk} = \frac{1}{\sqrt{N}} e^{2\pi i \frac{jk}{N}}, \quad j, k = 0, \dots, N-1, \quad (5.20)$$

diagonalizes the shift matrix with $S = F\Omega F^\dagger$ where $\Omega = \text{diag}(\omega_0, \dots, \omega_{N-1})$ and $\omega_k = e^{2\pi i \frac{k}{N}}$. Thus we must choose V such that $V^T V$ can be diagonalized as

$$V^T V = F\Lambda^2 F^\dagger \quad (5.21)$$

with some diagonal unitary matrix $\Lambda = \text{diag}(\lambda_0, \lambda_1, \dots, \lambda_{N-1})$. The combination $V^T V$ is symmetric, which requires $\lambda_k = \lambda_{N-k}$ for all k . A possible solution is to set

$$V = F\Lambda F^\dagger, \quad (5.22)$$

which is also symmetric because Λ^2 and Λ have the same structure. This leads to the correct expression $V^T V = V^2 = F\Lambda^2 F^\dagger$. Since $\mathbf{1}_N + V^T V$ needs to be non-singular we require that $\lambda_k \neq \pm i$ for all λ_k (cf. the discussion around Eq. (5.9)).

The independent eigenvalues λ_k can still be used to change the structure and range of the jump operators. We set

$$\lambda_k^2 = \frac{1 - 2i \cos(2\pi k/N)}{1 + 2i \cos(2\pi k/N)}, \quad (5.23)$$

for $k = 0, \dots, N-1$, to obtain a tridiagonal matrix

$$(\mathbf{1}_N + V^T V)^{-1} = \frac{1}{2}(\mathbf{1}_N + iS + iS^T). \quad (5.24)$$

Recall that $\Delta = B\mathbf{1}_N + \frac{\delta}{2}(S + S^T)$ is also tridiagonal, so we find the coefficient matrix of the jump operators to be

$$\Gamma = (B + i\delta)\mathbf{1}_N + \left(\frac{\delta}{2} + iB\right)(S + S^T) + i\frac{\delta}{2}(S^2 + (S^T)^2). \quad (5.25)$$

This matrix couples only nearest and next-nearest neighbors, so each jump operator \hat{J}_k will act on the five systems $\mathcal{S}_{k-2}, \dots, \mathcal{S}_{k+2}$ for any k . Nearest-neighbor-only jump operators would require a diagonal $V^T V$, which in turn implies $V = O\Lambda$ for some real orthogonal matrix O and diagonal phase matrix $\Lambda = \text{diag}(e^{i\theta_1}, \dots, e^{i\theta_N})$. This, however, places us in the LOCC regime discussed in Sec. 3.3, which would erase possible quantum features from the model.

In addition to restricting the range of the jump operators, we can change the relative strength of system and feedback operators, as mentioned in the previous section. This will leave \hat{H} invariant but introduce a parameter $r \in \mathbb{R}$ in the jump operators,

$$J_k^A = r\hat{\sigma}_-^k - \frac{i}{r} \sum_{j=1}^N \Gamma_{jk} \hat{\sigma}_x^j, \quad J_k^B = r\hat{\sigma}_-^k - \frac{i}{r} \sum_{j=1}^N \Gamma_{jk}^* \hat{\sigma}_x^j. \quad (5.26)$$

For large $r \gg 1$ the dissipation will be dominated by local $\hat{\sigma}_-$ -decay, driving each spin into the $|\downarrow_z\rangle$ -state. In the limit of small $r \ll 1$ the $\hat{\sigma}_x$ -dephasing takes over. Note that the sum

$$\hat{\Sigma}_x^k := \sum_{j=1}^N \Gamma_{jk}^* \hat{\sigma}_x^j \quad (5.27)$$

may in principle generate interesting quantum states. For instance, when applied to the trivial state $\otimes_j |\downarrow_z\rangle_j$ it will create a kind of $|W\rangle$ state with weights Γ_{jk} . On the other hand, in the case of strong dissipation governed by $\hat{\Sigma}_x$ the systems will likely be driven into a mixed state since $[\hat{\Sigma}_x, \hat{\Sigma}_x^\dagger] = 0$, so the maximally mixed state $\rho = \hat{1}$ is a dark state, $\mathcal{D}[\hat{\Sigma}_x]\hat{1} = 0$

Results

We set $g := B/\delta$ and $\alpha := r/|\delta|^{1/2}$ to examine the steady state of the master equation for different values of g and α . We can distinguish the following limiting cases.

When $g \ll 1$, the Hamiltonian \hat{H} will be governed by the interaction term, $\hat{H} \sim \sum_k \hat{\sigma}_x^k \hat{\sigma}_x^{k+1}$. We find that the dominant elements of the jump operator coefficients Γ are of order $\mathcal{O}(1)$ when $g \ll 1$, so the dissipation only depends on our choice of α . For $\alpha \gg 1$, the local $\hat{\sigma}_-$ -decay will dominate the master equation, and all spins align in the $|\downarrow_z\rangle$ -state. For $\alpha \ll 1$ we expect the $\hat{\Sigma}_x$ -dephasing to generate a highly mixed steady state.

In the limit of $g \gg 1$ and $\alpha \ll 1$, the main contribution to the Hamiltonian will come from the local fields proportional to g , so $\hat{H} \sim -g \sum_k \hat{\sigma}_z^k$. However, the total master equation will again be dominated by $\hat{\Sigma}_x$ -dephasing, creating a mixed steady state. The reason is that the dominant elements

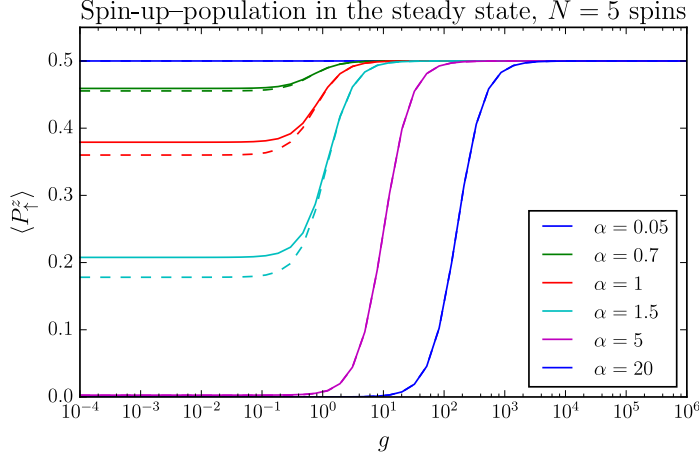


Figure 5.2: We plot the spin-up-density in the steady state of the dissipative Ising model against $g = B/\delta$ (continuous lines) for $N = 5$ spins. We consider different values of the asymmetry parameter $\alpha = r/|\delta|^{1/2}$. For comparison we also plot the results of the purely dissipative steady states obtained by setting $\hat{H} = 0$ in the dynamics (dashed lines). Good agreement between the full and purely dissipative steady states occurs only when α is close to unity.

of Γ are now also of order $\mathcal{O}(g)$, which enhances the dissipation rate by $g^2/\alpha^2 \gg g$.

For $g, \alpha \gg 1$ we can distinguish two different cases. When $\alpha^2 \gg g \gg 1$, the jump operators are dominated by $\alpha \hat{\sigma}_-^k$, since the largest elements of Γ are of order $\mathcal{O}(g)$ so the $\hat{\Sigma}_x$ -dephasing goes as $g/\alpha \ll \alpha$. Conversely, for $g \gg \alpha^2 \gg 1$ the dephasing takes over and creates a mixed steady state.

Notably, in both limiting cases, $\alpha \gg 1$ and $\alpha \ll 1$, the dissipation dominates the dynamics, independent of g . We expect the Hamiltonian to play a role only when α is close to unity. To see this effect, we computed the steady state using QuTiP [57, 58] for $N = 5$ spins. We chose the density of spins in the up-state $|\uparrow_z\rangle$,

$$\langle \hat{P}_{\uparrow}^z \rangle := \frac{1}{N} \sum_{j=1}^N \frac{1 + \langle \hat{\sigma}_z^j \rangle}{2}, \quad (5.28)$$

as an order parameter.

The results of the full dynamics are shown as solid lines in Fig. 5.2. They behave as expected in the limits we just discussed. The plots also illustrate the crossover in the intermediate regime for $\alpha \approx 1$ and $g \ll 1$, where $\hat{\sigma}_-$ and $\hat{\Sigma}_x$ compete. To isolate the effect of the Hamiltonian, we also computed the steady state of the purely dissipative dynamics, setting $\hat{H} = 0$ (dashed lines in Fig. 5.2). As expected, the dissipation is dominant whenever α is different from unity, and there is only a slight deviation when $\alpha \approx 1$.

In the regime $g, \alpha \gg 1$, the systems behave qualitatively similar to a dissipative Rydberg gas [74–78]. This is not entirely surprising: in both cases, the dissipation breaks the \mathbb{Z}_2 symmetry of the Ising Hamiltonian, hinting that both models could fall into the same universality class. The dissipative Rydberg gas exhibits a liquid-gas transition for sufficiently

strong driving [59], corresponding to the steep increase in Fig. 5.2. However, as the liquid-gas transition belongs to the universality class of the classical Ising model [77], we cannot expect to observe a true phase transition in our 1D simulations.

5.3 CONCLUSION AND OUTLOOK

The aim of this work was to identify the different types of quantum dynamics encompassed by the interferometric feedback setup in Chap. 3. The specific realizations studied in this (and the previous) chapter demonstrate that the general FME comprises nontrivial dynamics for appropriate choices of system and feedback operators. In particular with regard to the concrete Ising model considered in the previous section we were surprised by the (sometimes overwhelming) number of degrees of freedom available in the setup. These allow to easily tweak the dynamics, but also make it difficult to fully gauge the scope of the FME. For example, identifying the complete class of physical models that are realizable by the FME is an outstanding problem.

Part II

STATE VERIFICATION THROUGH RETRODICTION

In this part we employ continuous measurements to infer information about a system in the past, known as *retrodiction*. We explore the possibility to use it for the experimental verification of quantum states. This is unpublished material to which I contributed a majority of the analytical computations, and created all figures. Ideas were developed jointly with Klemens Hammerer who also contributed to the calculations.

In this chapter we show that time-continuously monitoring a system can be used to gain knowledge about its past state. In Sec. 6.1 we are going to derive the Stochastic Master Equation (SME) of a monitored quantum system, aiming for an intuitive rather than rigorous presentation as in Chap. 3. SMEs yield states that are conditioned on the measurement record. In Sec. 6.2 we show that instead of conditioning the state, this record lets us infer information about the past state of the system. This is known as *retrodiction*. We close with a brief introduction to backward Itô integration, necessary to perform retrodiction, in Sec. 6.3.

6.1 DERIVATION OF A STOCHASTIC MASTER EQUATION

We still consider the generic quantum optical setup from Sec. 3.1 of a system weakly coupled to a bosonic bath which we observe through homodyne detection (see App. A). Instead of applying measurement-based feedback, we are going to use the measurement record in this section to keep track of the state of the system. The measurement process in quantum mechanics is inherently random, and conditioning the evolution introduces this randomness to the dynamics. Thus a rigorous treatment of monitored quantum systems, such as in [7, 45], requires the use of quantum stochastic calculus, as pioneered in [5, 6], which extends classical stochastic calculus [46] to non-commuting noise processes.

There are a number of excellent texts [2, 7, 36, 43, 47, 80, 81] deriving *stochastic* (or *conditional*) master and Schrödinger equations of quantum optical systems with varying degrees of rigor. The derivation presented in this section strives to stay true to the goal of Chap. 3 to be as intuitive as possible. We thus make do without the intricacies of quantum stochastic calculus, which are necessary for a rigorous treatment and can be found in [5, 6].

6.1.1 Expanding the conditional state

We start our derivation with the state of some system \mathcal{S} that has interacted with a light field \mathcal{B} . Homodyne detection of the field revealed outcome \bar{x} . This lead us to the conditional system state in Eq. (3.33),

$$\tilde{\rho}_{\bar{x}}^{\mathcal{S}}(t + \delta t) = \langle \bar{x} | \rho_{\text{int}}^{\mathcal{S}\mathcal{B}} | \bar{x} \rangle, \quad (6.1a)$$

with the post-interaction state

$$\rho_{\text{int}}^{\mathcal{S}\mathcal{B}} = \exp\left(-i\sqrt{\delta t}\bar{H}_{\text{int}}\right)\rho_0^{\mathcal{S}\mathcal{B}}(t)\exp\left(i\sqrt{\delta t}\bar{H}_{\text{int}}\right) + \mathcal{O}(\delta t^{3/2}), \quad (6.1b)$$

$$\bar{H}_{\text{int}} = i\left(\hat{S}\bar{B}_0^\dagger - \hat{S}^\dagger\bar{B}_0\right), \quad (6.1c)$$

where \hat{S} is a system operator, \bar{B}_0 is the annihilation operator of the incoming light mode, and δt is dimensionless time measured in units of

the interaction time $\tau_{\text{int}} = \kappa^{-1}$. We eventually want to let $\delta t \rightarrow dt$ to derive a time-continuous equation of motion conditioned on a stream of measurement results. Assuming $\delta t \ll 1$ we expand the exponential and find analogously to Eq. (3.18) the expression

$$\begin{aligned} \tilde{\rho}_{\bar{x}}^S(t + \delta t) &\approx \langle \bar{x} | \rho_0^{SB}(t) | \bar{x} \rangle - i\sqrt{\delta t} \langle \bar{x} | [\bar{H}_{\text{int}}, \rho_0^{SB}(t)] | \bar{x} \rangle \\ &\quad + \frac{\delta t}{2} \langle \bar{x} | \left(2\bar{H}_{\text{int}} \rho_0^{SB}(t) \bar{H}_{\text{int}} - \{ \bar{H}_{\text{int}}^2, \rho_0^{SB}(t) \} \right) | \bar{x} \rangle, \end{aligned} \quad (6.2)$$

where we neglected terms of order $\mathcal{O}(\delta t^{3/2})$. To evaluate the expectation values we use that the incoming field is in the vacuum state, $\rho_0^{SB}(t) = \rho^S(t) \otimes |0\rangle\langle 0|$. Since $\bar{B}_0|0\rangle = 0$ we can replace

$$\bar{H}_{\text{int}}|0\rangle \equiv i\sqrt{2}\hat{S}\bar{X}_0|0\rangle, \quad \bar{H}_{\text{int}}^2|0\rangle \equiv (\hat{S}^+\hat{S} - \hat{S}^2(2\bar{X}_0^2 - 1))|0\rangle. \quad (6.3)$$

With these relations we find

$$\begin{aligned} \tilde{\rho}_{\bar{x}}^S(t + \delta t) &\approx p_0(\bar{x}) \left(\rho^S(t) + \sqrt{2\delta t} \bar{x} (\hat{S}\rho^S(t) + \rho^S(t)\hat{S}^+) \right) \\ &\quad + 2\delta t \bar{x}^2 p_0(\bar{x}) \hat{S}\rho^S(t)\hat{S}^+ - \frac{\delta t}{2} p_0(\bar{x}) \{ \hat{S}^+\hat{S}, \rho^S(t) \} \\ &\quad + \frac{\delta t}{2} p_0(\bar{x}) (2\bar{x}^2 - 1) (\hat{S}^2\rho^S(t) + \rho^S(t)(\hat{S}^+)^2), \end{aligned} \quad (6.4)$$

where we introduced the probability density

$$p_0(\bar{x}) = |\langle \bar{x} | 0 \rangle|^2 = \frac{1}{\sqrt{\pi}} e^{-\bar{x}^2} \quad (6.5)$$

of obtaining a result \bar{x} by measuring the vacuum directly.

6.1.2 Statistics of the measurement current

To proceed recall that \bar{x} is the outcome of the homodyne measurement averaged over $[t, t + \delta t)$. As such it is a random variable comprising a sum of measurement results \bar{x}_k of smaller time slices $[\tau_k, \tau_{k+1})$ with $\tau_k = t + k\delta t/N$ with $k = 0, \dots, N-1$. We can employ the central limit theorem [82] which states that the distribution of a sum of N independently⁷ distributed random variables (with finite means and variance) approaches a normal (i. e., Gaussian) distribution as N becomes large. To find the mean and variance of \bar{x} we consider the probability to measure a particular \bar{x} given by Eq. (3.34b),

$$p(\bar{x}) = \text{Tr}\{\tilde{\rho}_{\bar{x}}^S(t + \delta t)\} \quad (6.6)$$

$$= p_0(\bar{x}) \left(1 + \sqrt{2\delta t} \bar{x} \langle \hat{S} + \hat{S}^+ \rangle_\rho + \mathcal{O}(\delta t) \right) \quad (6.7)$$

$$\propto \exp \left(- \left(\bar{x} - \frac{\sqrt{2\delta t}}{2} \langle \hat{S} + \hat{S}^+ \rangle_\rho \right)^2 \right) + \mathcal{O}(\delta t), \quad (6.8)$$

where $\langle \hat{S} \rangle_\rho := \text{Tr}\{\hat{S}\rho^S(t)\}$. We read off that \bar{x} has mean and variance given by

$$\text{E}[\bar{x}] = \frac{\sqrt{2\delta t}}{2} \langle \hat{S} + \hat{S}^+ \rangle_\rho, \quad \text{Var}[\bar{x}] = \frac{1}{2}. \quad (6.9)$$

⁷ This is only satisfied as long as the Markov property holds: $\delta t/N$ must be larger than the bath correlation time.

To separate the deterministic component (the mean) from stochastic fluctuations let us define a new random variable

$$\bar{w} := \sqrt{2}\bar{x} - \sqrt{\delta t}\langle\hat{S} + \hat{S}^+\rangle_\rho \quad (6.10)$$

such that $E[\bar{w}] = 0$ and $\text{Var}[\bar{w}] = 1$ independent of the measurement time δt . Thus to take the limit $\delta t \rightarrow dt$ in a sensible way we need to find a properly scaled $\delta\bar{w} \propto \bar{w}$ such that $\delta\bar{w} \rightarrow dW$ yields the right increment. Note that the origin of \bar{w} is the quantum noise of the incoming light, present even when we measure only vacuum. We assume this to be *white noise* [2, 36, 47], and we want the resulting *Wiener increment* dW to reflect this by satisfying the white noise statistics

$$E[dW] = 0, \quad \text{Var}[dW] = E[dW^2] = dt. \quad (6.11)$$

Thus the proper scaling is $\delta\bar{w} = \sqrt{\delta t}\bar{w}$, and consequently $\delta\bar{x} = \sqrt{2\delta t}\bar{x} \rightarrow dY(t)$ such that

$$dY(t) = \langle\hat{S} + \hat{S}^+\rangle_\rho dt + dW(t), \quad (6.12)$$

where we introduced the (*homodyne*) *measurement current* $Y(t)$ as continuous limit of the discrete outcomes \bar{x} . The increment $dY(t)$ then satisfies

$$E[dY(t)] = \langle\hat{S} + \hat{S}^+\rangle_\rho dt, \quad E[dY(t)^2] = dt. \quad (6.13)$$

The most important property of white noise is that it is independent from one moment to next,

$$E[dW(t)dW(t')] = \delta(t - t')dt dt', \quad (6.14)$$

so any average over finite time will actually be equivalent to an ensemble average $E[\dots]$ [2, App. B]. With this in mind we can take the relations

$$dW(t)^2 = dY(t)^2 = dt, \quad (6.15a)$$

$$dW(t)dW(t') = dY(t)dY(t') = 0, \quad \forall t \neq t', \quad (6.15b)$$

to hold without an explicit expectation value. These are called *Itô rules*, and they make it necessary to include second order terms in any series expansion because a second order stochastic increment will yield a first order time increment.

Let us now return to the conditional state from Eq. (6.4). We subtract the constant contribution $\rho^S(t)$, and take the limit $\delta t \rightarrow dt$ by making the aforementioned replacements, in particular $2\delta t\bar{x}^2 \rightarrow dY(t)^2 \equiv dt$. We then obtain an unnormalized Conditional or Stochastic Master Equation (SME) for the system state,

$$\begin{aligned} \text{(I)} \quad d\tilde{\rho}_c^S(t) &= (\hat{S}\tilde{\rho}_c^S(t) + \tilde{\rho}_c^S(t)\hat{S}^+)dY(t) \\ &\quad + \hat{S}\tilde{\rho}_c^S(t)\hat{S}^+ - \frac{1}{2}\{\hat{S}^+\hat{S}, \tilde{\rho}_c^S(t)\}dt \end{aligned} \quad (6.16)$$

$$= (\hat{S}\tilde{\rho}_c^S(t) + \tilde{\rho}_c^S(t)\hat{S}^+)dY(t) + \mathcal{D}[\hat{S}]\tilde{\rho}_c^S(t)dt, \quad (6.17)$$

where the subscript indicates that ρ_c is a conditional state. The (I) in front of the equation emphasizes that this is a stochastic Itô differential equation. This is important because standard rules of calculus have to be

replaced by Ito rules such as (6.15), and standard integrals are replaced by stochastic Itô integrals, see Sec. 6.3. Conditioning the evolution of the system on a continuous measurement record is also known as *filtering*, see, e. g., [83] and references therein. In the following we will drop the superscript \mathcal{S} , but keep the subscript which indicates that $\tilde{\rho}_c$ is a conditional state.

6.1.3 Normalization of the state

Equation (6.17) is not trace-preserving so the solution $\tilde{\rho}_c(t)$ will no longer have unit trace. This can be remedied by explicit normalization of $\tilde{\rho}_c(t + dt) = \rho_c(t) + d\tilde{\rho}_c(t)$, i. e.,

$$\rho_c(t + dt) = \frac{\tilde{\rho}_c(t + dt)}{\text{Tr}\{\tilde{\rho}_c(t + dt)\}}. \quad (6.18)$$

After a series expansion of $\text{Tr}\{\tilde{\rho}_c(t + dt)\}^{-1} = (1 + \text{Tr}\{d\tilde{\rho}_c(t)\})^{-1}$ and using the Itô rules (6.15) one finds

$$(I) \, d\rho_c(t) = \mathcal{D}[\hat{S}]\rho_c(t)dt + \mathcal{H}[\hat{S}]\rho_c(t)dW(t) \quad (6.19a)$$

with the Wiener increment $dW(t)$ from Eq. (6.12), and the Lindblad and measurement superoperators

$$\mathcal{D}[\hat{S}]\rho := \hat{S}\rho\hat{S}^\dagger - \frac{1}{2}\{\hat{S}^\dagger\hat{S}, \rho\}, \quad (6.19b)$$

$$\mathcal{H}[\hat{S}]\rho := (\hat{S} - \langle\hat{S}\rangle_\rho)\rho + \rho(\hat{S}^\dagger - \langle\hat{S}^\dagger\rangle_\rho). \quad (6.19c)$$

Note that $\mathcal{H}[\hat{S}]\rho$ is linear in \hat{S} but nonlinear in ρ because of the expectation values. We would like to point out that Eqs. (6.17) and (6.19a) generate equivalent dynamics. One has to decide whether it is more convenient to either solve a nonlinear equation with a normalized state at every step in time, or a linear equation followed by explicit renormalization of the final ρ . Or if the optimal solution is actually a hybrid of both [84].

6.1.4 Generalization to multiple baths

If we include a system Hamiltonian \hat{H} , and finite efficiency $\eta \in [0, 1]$ of the homodyne detection (cf. App. A.3), we obtain

$$(I) \, d\rho_c(t) = -i[\hat{H}, \rho_c(t)]dt + \mathcal{D}[\hat{S}]\rho_c(t)dt + \sqrt{\eta}\mathcal{H}[\hat{S}]\rho_c(t)dW(t). \quad (6.20)$$

We see that without detections ($\eta = 0$) or by taking an ensemble average we retrieve the unconditional master equation (3.29)⁸. We can also change the measurement by varying the phase θ of the local oscillator with respect to the signal, see App. A. This affects the measurement operator $\hat{C} := \sqrt{\eta}e^{i\theta}\hat{S}$ but not the jump operator $\hat{L} := \hat{S}$, so a more general form of the master equation reads

$$(I) \, d\rho_c(t) = -i[\hat{H}, \rho_c(t)]dt + \mathcal{D}[\hat{L}]\rho_c(t)dt + \mathcal{H}[\hat{C}]\rho_c(t)dW(t). \quad (6.21)$$

⁸ Only true for Itô equations where ρ_c is independent of dW .

We generalize this further by considering not just a single but N_L bosonic baths \mathcal{B}_j that couple to \mathcal{S} via jump operators \hat{L}_j . We assume that $N_C \leq N_L$ of these are subject to homodyne detection producing independent Wiener increments $dW_k(t)$ with corresponding measurement operators \hat{C}_k . This yields the general SME

$$\begin{aligned} \text{(I)} \quad d\rho_c(t) = & -i[\hat{H}, \rho_c(t)]dt + \sum_{j=1}^{N_L} \mathcal{D}[\hat{L}_j]\rho_c(t)dt \\ & + \sum_{k=1}^{N_C} \mathcal{H}[\hat{C}_k]\rho_c(t)dW_k(t). \end{aligned} \quad (6.22)$$

The equivalent unnormalized SME reads

$$\begin{aligned} \text{(I)} \quad d\tilde{\rho}_c(t) = & -i[\hat{H}, \tilde{\rho}_c(t)]dt + \sum_{j=1}^{N_L} \mathcal{D}[\hat{L}_j]\tilde{\rho}_c(t)dt \\ & + \sum_{k=1}^{N_C} \left(\hat{C}_k \tilde{\rho}_c(t) + \tilde{\rho}_c(t) \hat{C}_k^\dagger \right) dY_k(t), \end{aligned} \quad (6.23)$$

while averaging over all measurement results leads to the corresponding unconditional master equation

$$d\rho(t) = -i[\hat{H}, \rho(t)]dt + \sum_{j=1}^{N_L} \mathcal{D}[\hat{L}_j]\rho(t)dt. \quad (6.24)$$

If the master equation is derived in a different way than sketched above (see, e. g., Sec. 8.2), the measurement operators do not need to correspond one-to-one to the jump operators. In fact, in Sec. 8.2 we will see an example where effectively $N_C > N_L$. However, since any information recorded by the detectors must have previously leaked from the system it holds that

$$\sum_{j=1}^{N_L} \hat{L}_j^\dagger \hat{L}_j - \sum_{k=1}^{N_C} \hat{C}_k^\dagger \hat{C}_k \geq 0 \quad (6.25)$$

with equality only for unit detection efficiency.

6.2 BACKWARD EFFECT EQUATIONS

In the previous section we saw that a continuous measurement record can be used to condition the evolution of the quantum state. In this section we are going to show that it can instead also be used to infer information about the past state of the system, known as *retrodiction*. To this end we need to recall the concept of effect operators from section 2.2.2.1: an effect operator \hat{E}_x , belonging to some Positive-Operator Valued Measure (POVM), is a positive Hermitian operator that yields the probability for some outcome x to be measured on $\rho(t)$ via $p(x|\rho(t)) = \text{Tr}\{\hat{E}_x\rho(t)\}$.

We will interpret $\hat{E}_x \equiv \hat{E}_x(t)$ itself as a dynamical object. It may seem odd that $\hat{E}_x(t)$, which is associated with a particular measurement event at fixed time t , can propagate through time, so let us provide a simple example. We consider a classical particle moving freely through space at

velocity v . We measure it at time t to be at position x . Now we know that if we had measured at some time t' we would have found it at $x + v(t' - t)$, so we find a relation between the possible effects at t and at t' given by $E_x(t) = E_{x+v(t'-t)}(t')$. Finding a result at one time is equivalent to finding a different result at a different time. Now in a quantum setting there is of course uncertainty in our knowledge of both v and x , which needs to be propagated as well, but the idea remains essentially the same. Our goal is first to find the relationship between effect operators at different times, and then to show that continuous measurements actually improve the resolution of past POVMs.

Let us briefly mention some related work. Barnett, Pegg, and Jeffers [85–87] considered backpropagation of effect operators in closed and open quantum systems, but did not treat continuous measurements. Together with work by Yanagisawa [88] on estimation of initial Gaussian states, this was developed by Mankei Tsang [21–23] into a quantum theory of *time-symmetric smoothing*. Here, monitoring is used to estimate the past value of a classical parameter coupled to a quantum system. More recently [89] he also suggested an alternative approach to weak value estimation of the past of a quantum observable using subsequent measurements.

Gammelmark, Julsgaard and Mølmer [24] proposed a theory of *past quantum states*, in which the state ρ and effect operator \hat{E} are conditioned on the past and future observation records, respectively. If $\rho(t)$ is considered as a collection of probabilities for measurement outcomes at time t , then $\hat{E}(t)$ provides a Bayesian update of these probabilities which yields more decisive, less entropic distributions. This theory was specialized to Gaussian states in continuous variable systems by Zhang and Mølmer [27]. An alternative approach to smoothing in quantum systems was suggested by Guevara and Wiseman [28]. Instead of applying a Bayesian update to the probabilities of past measurements as Mølmer and co-workers do, they define a smoothed quantum state, where the probabilities of the density matrix are conditioned on the continuous measurement results.

Our approach aims to complement this previous work. Instead of providing a Bayesian update to either measurement results or the density matrix, we are going to interpret the continuous observation of a quantum system as an effective instantaneous POVM measurement on its state in the past. To do so we will first recapitulate the concept of quantum channels $\mathcal{N}_{t_0,t}$ in Sec. 6.2.1 because they allow to derive the dynamics of \hat{E}_x elegantly. In Sec. 6.2.2 we derive the time evolution of effect operators in arbitrary monitored systems. In Sec. 6.2.3 we provide a brief motivation for this work before we focus on dynamics generated by a SME in Sec. 6.2.4.

6.2.1 Quantum channels

Quantum channels constitute a general description of quantum operations including the types of evolution and measurement described so far. A quantum channel $\mathcal{N} : \mathcal{B}(\mathcal{H}) \rightarrow \mathcal{B}(\mathcal{H})$ is a linear map that is com-

pletely positive¹ and trace-preserving (CPTP). These conditions are necessary to ensure physically meaningful evolution of propagated states $\rho(t_1) = \mathcal{N}_{t_0,t_1}[\rho(t_0)]$. Quantum channels describe Markovian (memoryless) evolution of closed and open quantum systems. For a more comprehensive introduction to quantum channels we refer to [39, 41].

A further generalization are *conditional* or *stochastic* quantum channels $\mathcal{N}_{t_0,t_1|y}$, also called quantum instruments, that describe evolution conditioned on the outcome y of an arbitrary measurement, and produce conditional states $\rho_y(t_1) = \mathcal{N}_{t_0,t_1|y}[\rho(t_0)]$. It will be convenient to drop the trace-preserving condition, and to consider channels $\tilde{\mathcal{N}}_{t_0,t_1|y}$ that are only *trace non-increasing*, i. e., $\text{Tr}\{\tilde{\mathcal{N}}_{t_0,t_1|y}[\hat{A}]\} \leq \text{Tr}\{\hat{A}\}$. An important feature is that if an initial state is propagated, $\tilde{\rho}_y(t_1) = \tilde{\mathcal{N}}_{t_0,t_1|y}[\rho(t_0)]$, its trace will yield the probability

$$p(y|\rho(t_0)) = \text{Tr}\{\tilde{\mathcal{N}}_{t_0,t_1|y}[\rho(t_0)]\} \quad (6.26)$$

that the operation corresponding to outcome y occurs given $\rho(t_0)$.

An important role in retrodiction is also played by the adjoint channel \mathcal{N}^\dagger which denotes the Hilbert-Schmidt adjoint of \mathcal{N} defined by the relation

$$\text{Tr}\{\hat{B}\mathcal{N}[\hat{A}]\} = \text{Tr}\{\mathcal{N}^\dagger[\hat{B}]\hat{A}\} \quad \forall \hat{A}, \hat{B} \in \mathcal{B}(\mathcal{H}). \quad (6.27)$$

The trace-preserving property of \mathcal{N} implies *unitality* of \mathcal{N}^\dagger , which means that the identity is preserved, $\mathcal{N}^\dagger[\hat{1}] = \hat{1}$. Trace non-increasing channels yield adjoints with $\mathcal{N}^\dagger[\hat{1}] \leq \hat{1}$.

6.2.1.1 Kraus decomposition of arbitrary channels

An important theorem (see, e. g., [41, Thm. 2.1]) connecting the idea of quantum channels to the general measurement postulate in Sec. 2.2.2 is that any linear map $\tilde{\mathcal{N}}_y$ is completely positive if and only if it admits a *Kraus decomposition*

$$\tilde{\mathcal{N}}_y[\hat{A}] = \sum_{k \in \mathcal{K}_y} \hat{M}_{k|y} \hat{A} \hat{M}_{k|y}^\dagger \quad (6.28)$$

where the operators $\hat{M}_{k|y}$ are called *Kraus operators*, and the set \mathcal{K}_y may depend on the measurement outcome. The Kraus operators satisfy

$$\sum_y \sum_{k \in \mathcal{K}_y} \hat{M}_{k|y}^\dagger \hat{M}_{k|y} = \hat{1}, \quad (6.29)$$

which is equivalent to the condition that $\sum_y \tilde{\mathcal{N}}_y = \mathcal{N}$ constitutes a trace-preserving channel. Any completely positive quantum evolution can be represented in this way, possibly dropping the measurement outcome y , the sum over k , or both. For example, a closed system would evolve with a single unitary Kraus operator $\hat{M} = \hat{U}$ which obviously satisfies $\hat{U}^\dagger \hat{U} = \hat{1}$ and thus produces the trivial single-outcome POVM $\hat{E} = \hat{1}$. On the other hand, a projective measurement comes with projection operators $\hat{M}_y = \hat{\Pi}_y$ (so no sum over k).

¹ Complete positivity means that $\mathcal{N} \otimes \hat{1}_n$ maps positive operators to positive operators for all $n \in \mathbb{N}_0$. This ensures that systems which are initially entangled with some auxiliary system still undergo positive evolution if the ancilla is ignored.

While $\tilde{\mathcal{N}}_{t_0, t_1|y}[\rho]$ ostensibly describes only discrete evolution where the state “hops” from t_0 to t_1 , quantum channels can also describe infinitesimal (and thus continuous) evolution. For example, the SME (6.17) corresponds to a quantum channel $\tilde{\mathcal{N}}_{t, t+dY|dY}$ comprising Kraus operators [2, 24, 84]

$$\hat{M}_{dY} \propto \left(1 - \frac{1}{2} \hat{S}^\dagger \hat{S} dt + \hat{S} dY \right), \quad (6.30)$$

with normalization to ensure that

$$\int_{\mathbb{R}} d(dY) \hat{M}_{dY}^\dagger \hat{M}_{dY} = \hat{1}. \quad (6.31)$$

Note that from conditional channels we can derive both unconditional channels and POVMs, cf. section 2.2.2.1. Ignoring the result y by averaging over all possible outcomes yields an unconditional channel $\tilde{\mathcal{N}}_{t_0, t_1} := \sum_y \tilde{\mathcal{N}}_{t_0, t_1|y}$ that is again trace-preserving. On the other hand, ignoring the output state $\tilde{\mathcal{N}}_{t_0, t_1|y}[\rho]$ still leaves us with effect operators $\hat{E}_y = \hat{M}_y^\dagger \hat{M}_y$ that constitute a POVM.

6.2.2 Retrodiction

In this section we will show that continuously monitoring a quantum system \mathcal{S} actually effects an instantaneous POVM measurement on the initial state. To this end assume that \mathcal{S} evolves according to a conditional quantum channel $\tilde{\mathcal{N}}_{t_0, t_1|Y}$ from t_0 to t_1 such that

$$\tilde{\rho}_Y(t_1) = \tilde{\mathcal{N}}_{t_0, t_1|Y}[\rho(t_0)], \quad (6.32)$$

which depends on the particular measurement record $\mathcal{Y} := \{Y(s), t_0 \leq s < t_1\}$ obtained during a single run of the experiment. This conditional state $\tilde{\rho}_Y(t)$ is what we obtain, for example, by integrating a SME such as Eq. (6.23) with initial condition $\rho(t_0)$ and the particular homodyne record \mathcal{Y} . Recall that the trace of the conditional state carries the probability for \mathcal{Y} to have occurred given $\rho(t_0)$, cf. Eq. (6.26),

$$p(\mathcal{Y}|\rho(t_0)) = \text{Tr}\{\tilde{\rho}_Y(t_1)\}. \quad (6.33)$$

Suppose we perform a POVM measurement $\{\hat{E}_x|x \in \mathfrak{X}\}$ with outcome set \mathfrak{X} and effect operators \hat{E}_x on the (normalized) state $\rho_Y(t_1)$. We expect outcome x to occur with conditional probability

$$p(x|\mathcal{Y}, \rho(t_0)) = \text{Tr}\{\hat{E}_x \rho_Y(t_1)\} = \frac{\text{Tr}\{\hat{E}_x \tilde{\rho}_Y(t_1)\}}{p(\mathcal{Y}|\rho(t_0))}. \quad (6.34)$$

Rewriting the conditional probability on the left-hand side as

$$p(x|\mathcal{Y}, \rho(t_0)) = \frac{p(x, \mathcal{Y}|\rho(t_0))}{p(\mathcal{Y}|\rho(t_0))}, \quad (6.35)$$

we find that the joint probability to obtain result x and record \mathcal{Y} is given by a POVM measurement on the unnormalized conditional state,

$$p(x, \mathcal{Y}|\rho(t_0)) = \text{Tr}\{\hat{E}_x \tilde{\rho}_Y(t_1)\}. \quad (6.36)$$

If we plug Eq. (6.32) into this expression, we can use the definition of the adjoint channel $\tilde{\mathcal{N}}_{t_0, t_1 | \mathcal{Y}}^+$ to obtain

$$\begin{aligned} p(x, \mathcal{Y} | \rho(t_0)) &= \text{Tr}\{\hat{E}_x \tilde{\mathcal{N}}_{t_0, t_1 | \mathcal{Y}}[\rho(t_0)]\} \\ &= \text{Tr}\{\tilde{\mathcal{N}}_{t_0, t_1 | \mathcal{Y}}^+[\hat{E}_x] \rho(t_0)\}, \end{aligned} \quad (6.37)$$

Making the identification

$$\hat{E}_{x, \mathcal{Y}}(t_0) := \tilde{\mathcal{N}}_{t_0, t_1 | \mathcal{Y}}^+[\hat{E}_x], \quad (6.38)$$

we can rewrite the probability as

$$p(x, \mathcal{Y} | \rho(t_0)) = \text{Tr}\{\hat{E}_{x, \mathcal{Y}}(t_0) \rho(t_0)\}, \quad (6.39)$$

which suggests that $\hat{E}_{x, \mathcal{Y}}(t_0)$ actually plays the role of an effect operator and $\{\hat{E}_{x, \mathcal{Y}}(t_0) | x \in \mathfrak{X}, \mathcal{Y} \in \mathfrak{Y}\}$ constitutes a POVM on the initial state $\rho(t_0)$, where \mathfrak{Y} denotes the set of all possible monitoring records. This shows that a POVM measurement at t_1 is equivalent to an effective POVM at some previous time t_0 . This observation-assisted backpropagation of effect operators is what we refer to as *retrodiction*.

An even more profound observation is that this result also holds if we consider the trivial single-element POVM $\hat{E}(t_1) = \hat{1}$ at t_1 . This corresponds to making a measurement with only a single possible outcome, and thus not a measurement at all. In that case we find effect operators

$$\hat{E}_{\mathcal{Y}}(t_0) := \tilde{\mathcal{N}}_{t_0, t_1 | \mathcal{Y}}^+[\hat{1}] \quad (6.40)$$

which depend solely on the measurement record \mathcal{Y} . In this sense time-continuously monitoring a quantum system from t_0 to t_1 is equivalent to performing an instantaneous POVM measurement at the initial time t_0 . It does not depend on some final effect operator $\hat{E}_x(t_1)$ to yield nontrivial effect operators $\hat{E}_{\mathcal{Y}}(t_0)$ in the past. Note that this result crucially depends on using the unnormalized channel $\tilde{\mathcal{N}}^+$ since $\mathcal{N}^+[\hat{1}] = \hat{1}$. Because averaging over (i. e., ignoring) the measurement results always yields a unital channel, this shows that $\sum_{\mathcal{Y} \in \mathfrak{Y}} p(\mathcal{Y} | \rho(t_0)) = 1$ and thus $\sum_{\mathcal{Y} \in \mathfrak{Y}} \hat{E}_{\mathcal{Y}} = \hat{1}$, so $\{\hat{E}_{\mathcal{Y}}(t_0) | \mathcal{Y} \in \mathfrak{Y}\}$ really does constitute a POVM.

To anticipate a possible source of confusion we emphasize again that POVMs are a sub-class of general measurements because they yield probabilities for measurement outcomes but make no statement about the post-measurement state. This makes sense when the state (i. e., wave function or density operator) is interpreted simply as a means to compute probabilities for the outcomes of possible measurements one could make on the system. Since the observation record is used in Eq. (6.39) to reveal information about a system in the past that has long since moved on (and possibly does not even exist anymore), there is not much sense in making statements about the post-measurement state.

6.2.3 One-stop preparation and measurement

One of the main motivations of this work is that continuous measurements are routinely used in various platforms to prepare quantum systems in nontrivial conditional states. This usually requires large cooperativities ($C > 1$), i. e., strong coherent coupling to the observed bath mode

compared to all other dissipation channels. However, the subsequent readout of these states remains a challenge, see, e. g., the phenomenological approaches in [90] for massive mechanical oscillators, and in [8, 91] for superconducting qubits. But as has recently been shown in [9, 25] for superconducting qubits (see also [26] for a review) retrodiction can assist in the verification of these states.

A typical situation we have in mind is that a monitored system evolves conditionally from t_0 to t , producing a record $\mathcal{I} := \{Y(s), t_0 \leq s < t\}$. Using filtering this prepares the system in the conditional state $\rho_{\mathcal{I}}(t)$. To read out this state we let the system evolve further until some time $t_1 > t$, producing another measurement record $\mathcal{J} := \{Y(s), t \leq s < t_1\}$. Using the method presented in the previous section this record tells us that we effectively measured the effect operator $\hat{E}_{\mathcal{J}}$ on $\rho_{\mathcal{I}}(t)$. We thus perform state preparation and verification with the same setup by using disjoint sets of data.

6.2.4 Time-continuous effect equations

We now consider the special case of a system \mathcal{S} governed by SME (6.23), restricted to a single measurement and jump operator for simplicity,

$$\begin{aligned} \text{(I)} \quad d\tilde{\rho}_c(t) &= -i[\hat{H}, \tilde{\rho}_c(t)]dt + \mathcal{D}[\hat{L}]\tilde{\rho}_c(t)dt \\ &+ (\hat{C}\tilde{\rho}_c(t) + \tilde{\rho}_c(t)\hat{C})dY(t). \end{aligned} \quad (6.41)$$

To derive the effect equation adjoint to this master equation consider again Eq. (6.37), which can be written as

$$\text{Tr}\{\hat{E}(t_1)\tilde{\rho}_{\mathcal{Y}}(t_1)\} = \text{Tr}\{\hat{E}_{\mathcal{Y}}(t_0)\rho(t_0)\} \quad (6.42)$$

$$= \text{Tr}\{\hat{E}_{\mathcal{J}}(t)\tilde{\rho}_{\mathcal{I}}(t)\}, \quad (6.43)$$

where we split the measurement record $\mathcal{Y} = \mathcal{I} \cup \mathcal{J}$ at some arbitrary time $t \in (t_0, t_1)$. In the following we drop the subscripts of ρ and \hat{E} and remember that both are conditioned on respective parts of \mathcal{Y} . Obviously the first line does not depend on t , so when we take a variation with respect to t [24, 85–87] we find

$$0 = d_t \text{Tr}\{\hat{E}(t)\tilde{\rho}(t)\} \quad (6.44)$$

$$= \text{Tr}\{\hat{E}(t+dt)\tilde{\rho}(t+dt) - \hat{E}(t)\tilde{\rho}(t)\}. \quad (6.45)$$

We know that $\tilde{\rho}(t+dt) = \tilde{\rho}(t) + d\tilde{\rho}(t)$ with $d\tilde{\rho}(t)$ given by Eq. (6.41), and we similarly assume we can write⁹ $\hat{E}(t) = \hat{E}(t+dt) - d\hat{E}(t+dt)$. We determine $d\hat{E}(t+dt)$ from inserting these relation into the equation above,

$$0 = \text{Tr}\{\hat{E}(t+dt)d\tilde{\rho}(t) + d\hat{E}(t+dt)\tilde{\rho}(t)\}. \quad (6.46)$$

Looking at the first term in conjunction with (6.41), and suppressing the bulky time dependence of $\hat{E}(t+dt) \equiv \hat{E}$ for the moment, we see the trace decomposes into three parts,

$$\text{Tr}\{\hat{E}d\tilde{\rho}(t)\} = (A)dt + (B)dt + (C)dY(t), \quad (6.47)$$

⁹ This convention of a forward-pointing increment follows Tsang [21, 22], but differs from Mølmer et al. [24, 27].

for the Hamiltonian, jump, and measurement operators respectively. For example

$$(A) = -i\text{Tr}\{\hat{E}[\hat{H}, \tilde{\rho}(t)]\} \quad (6.48)$$

$$= -i\text{Tr}\{\hat{E}(\hat{H}\tilde{\rho}(t) - \tilde{\rho}(t)\hat{H})\} \quad (6.49)$$

$$= -i\text{Tr}\{\hat{E}\hat{H}\tilde{\rho}(t) - \hat{H}\hat{E}\tilde{\rho}(t)\} \quad (6.50)$$

$$= i\text{Tr}\{[\hat{H}, \hat{E}]\tilde{\rho}(t)\}, \quad (6.51)$$

where from the second to third line we made use of the cyclic property of the trace. Similarly we find for the jump operator with $\mathcal{D}[\hat{L}]\rho = \hat{L}\rho\hat{L}^\dagger - (\hat{L}^\dagger\hat{L}\rho + \rho\hat{L}^\dagger\hat{L})/2$ that

$$(B) = \text{Tr}\{\hat{E}(\mathcal{D}[\hat{L}]\tilde{\rho}(t))\} \quad (6.52)$$

$$= \text{Tr}\left\{\left(\mathcal{D}^\dagger[\hat{L}]\hat{E}\right)\tilde{\rho}(t)\right\}, \quad (6.53)$$

with $\mathcal{D}^\dagger[\hat{L}]\hat{E} = \hat{L}^\dagger\hat{E}\hat{L} - (\hat{L}^\dagger\hat{L}\hat{E} + \hat{E}\hat{L}^\dagger\hat{L})/2$, and for the measurement term

$$(C) = \text{Tr}\{\hat{E}(\hat{C}\tilde{\rho}(t) + \tilde{\rho}(t)\hat{C})\} \quad (6.54)$$

$$= \text{Tr}\{(\hat{C}^\dagger\hat{E} + \hat{E}\hat{C})\tilde{\rho}(t)\}. \quad (6.55)$$

Putting all three contributions together yields

$$0 = \text{Tr}\left\{\left(\text{d}\hat{E} + i[\hat{H}, \hat{E}]\text{d}t + \mathcal{D}^\dagger[\hat{L}]\hat{E}\text{d}t + (\hat{C}^\dagger\hat{E} + \hat{E}\hat{C})\text{d}Y(t)\right)\tilde{\rho}(t)\right\}. \quad (6.56)$$

Note that we made no assumptions about $\tilde{\rho}$ so this equation has to hold for arbitrary density operators. Recalling that $\hat{E} \equiv \hat{E}(t + \text{d}t)$ we shift the time argument, $t + \text{d}t \rightarrow t$, to arrive at the *backward* or *adjoint effect equation*

$$-\text{d}\hat{E}(t) = i[\hat{H}, \hat{E}(t)]\text{d}t + \mathcal{D}^\dagger[\hat{L}]\hat{E}(t)\text{d}t + (\hat{C}^\dagger\hat{E}(t) + \hat{E}(t)\hat{C})\text{d}Y(t - \text{d}t). \quad (6.57)$$

Comparing the effect equation to the corresponding forward master equation (6.41) we observe the following differences. The sign of the Hamiltonian changes which we expect from the usual time-reversal in closed systems. The Lindblad superoperators \mathcal{D} are replaced by their adjoint \mathcal{D}^\dagger which are no longer trace-preserving but vanish when applied to the identity. Each measurement operator \hat{C}_k is replaced by its adjoint.

To understand the unusual argument of $\text{d}Y(t - \text{d}t)$ note that we started with a stochastic Itô equation denoted by (I) in Eq. (6.41), but we did not say how to interpret the effect equation we just obtained. It turns out that it is a stochastic *backward Itô equation*, which we denote by (BI). This just means that when expressing an integral involving $\text{d}\hat{E}$ as a Riemann sum, the stochastic increment needs to be evaluated at the *upper* limit of each subinterval. We will elaborate on this in the following section.

Generalization of the backward equation to N_L decay channels and N_C measurement processes is straightforward and yields

$$(BI) \quad -\text{d}\hat{E}(t) = i[\hat{H}, \hat{E}(t)]\text{d}t + \sum_{j=1}^{N_L} \mathcal{D}^\dagger[\hat{L}_j]\hat{E}(t)\text{d}t + \sum_{k=1}^{N_C} (\hat{C}_k^\dagger\hat{E}(t) + \hat{E}(t)\hat{C}_k)\text{d}Y_k(t). \quad (6.58)$$

In principle Eq. (6.58) can also be normalized to generate nonlinear but trace-preserving evolution [24], provided the system is finite-dimensional or \hat{E} is a trace class operator.

6.3 BACKWARD ITÔ INTEGRATION

Because the effect equation for \hat{E} is a stochastic backward Itô equation, which is perhaps less common than the Itô equation, we will use this section to clarify the distinction. For a general introduction to stochastic differential and integral equations we recommend [46, 92].

Deterministic integrals of integrable functions defined as limits of Riemann-Stieltjes sums do not depend on whether their integrands are evaluated at the lower or upper end of their subintervals. The upper and lower Riemann sums converge in the limit of vanishing subinterval length. For integrals of stochastic functions this is not the case as the integrand may fluctuate rapidly [46, 47, 92]. Thus there are different ways to integrate a random process depending on where one evaluates the integrand.

A common type in physics is the Itô stochastic integral with the integrand evaluated at the lower end of each subinterval. Another well-known type is the Stratonovich integral with evaluation at the mid-point [46, 92]. A third, lesser known type is the backward Itô integral with the integrand evaluated at the upper limit of each subinterval [32]. We denote Itô integrals and differentials by a prepended (I) and backward Itô integrals by (BI). Everything to the right of (I) (or (BI)) is an Itô (or backward Itô) integral. It is possible to mix different integral types [32]. But since we never do this it should always be clear which type of integral is being used.

To clarify the distinction between (I) and (BI) let us recall the definition of Itô integrals [46, 92]. Consider an interval $[t_0, t_1]$ and partitions $P_n = \{\tau_j : j = 0, \dots, n\}$ such that

$$t_0 = \tau_0 < \tau_1 < \dots < \tau_n = t_1. \quad (6.59)$$

We consider only sequences of P_n such that

$$\text{mesh}(P_n) := \max_{j=1, \dots, n} (\tau_j - \tau_{j-1}) \rightarrow 0 \quad (6.60)$$

as $n \rightarrow \infty$. Provided it exists and is independent of the partition sequence, the Itô integral of some function (or stochastic process) $f(t)$ with respect to a white noise process $W_t (\equiv W(t))$ is defined as the mean-square limit

$$(I) \int_{t_0}^{t_1} f(\tau) dW_\tau := \lim_{n \rightarrow \infty} \sum_{j=1}^n f(\tau_{j-1}) (W_{\tau_j} - W_{\tau_{j-1}}). \quad (6.61)$$

The corresponding backward Itô integral is defined as

$$(BI) \int_{t_0}^{t_1} f(\tau) dW_\tau := \lim_{n \rightarrow \infty} \sum_{j=1}^n f(\tau_j) (W_{\tau_j} - W_{\tau_{j-1}}). \quad (6.62)$$

Given a stochastic process $X(t)$ with Itô equation

$$(I) dX_t = f(X_t, t)dt + g(X_t, t)dW_t, \quad (6.63)$$

the corresponding backward Itô equation reads

$$(BI) dX_t = [f(X_t, t) - g(X_t, t)g'(X_t, t)]dt + g(X_t, t)dW_t \quad (6.64)$$

with $g'(X_t, t) = (\partial g(x, t)/\partial x)|_{x=X_t}$.

We need backward Itô integrals because they naturally govern the evolution of the effect operator, as derived in the previous section. Let us illustrate this by considering a simple Itô stochastic process $X(t)$ driven only by white noise,

$$(I) dX(t) = M_t X(t) dW_t, \quad (6.65)$$

with Wiener increment dW_t and some linear map M_t acting on $X(t)$, which may itself be scalar-, vector-, matrix- or operator-valued. Integrating both sides we obtain an equivalent integro-differential equation²,

$$X(t) = X(t_0) + (I) \int_{t_0}^t M_\tau X(\tau) dW_\tau. \quad (6.66)$$

If we continue replacing $X(\tau)$ on the right-hand side by this expression we find

$$X(t) = \sum_{n=0}^{\infty} \mathcal{M}_{t,t_0}^{(n)} X(t_0) \quad (6.67)$$

with the operators $\mathcal{M}_{t,t_0}^{(n)}$ defined recursively via

$$\mathcal{M}_{t,t_0}^{(0)} = \mathbb{1}, \quad \mathcal{M}_{t,t_0}^{(n)} = (I) \int_{t_0}^t M_\tau \mathcal{M}_{\tau,t_0}^{(n-1)} dW_\tau. \quad (6.68)$$

We retrieve the Itô equation of $X(t)$ through variation with respect to t since

$$d_t \mathcal{M}_{t,t_0}^{(0)} = 0, \quad (6.69)$$

$$d_t \mathcal{M}_{t,t_0}^{(n)} = (I) d_t \int_{t_0}^t M_{\tau_1} dW_{\tau_1} \int_{t_0}^{\tau_1} M_{\tau_2} dW_{\tau_2} \cdots \int_{t_0}^{\tau_{n-1}} M_{\tau_n} dW_{\tau_n} \quad (6.70)$$

$$= (I) M_t dW_t \int_{t_0}^t M_{\tau_2} dW_{\tau_2} \cdots \int_{t_0}^{\tau_{n-1}} M_{\tau_n} dW_{\tau_n} \quad (6.71)$$

$$= (I) M_t \mathcal{M}_{t,t_0}^{(n-1)} dW_t, \quad (6.72)$$

so as expected we find

$$d_t X(t) = \sum_{n=0}^{\infty} d_t \mathcal{M}_{t,t_0}^{(n)} X(t_0) \quad (6.73)$$

$$= (I) M_t \sum_{n=1}^{\infty} \mathcal{M}_{t,t_0}^{(n-1)} X(t_0) dW_t \quad (6.74)$$

$$= (I) M_t X(t) dW_t. \quad (6.75)$$

² Equation (6.66) is actually the proper form of Eq. (6.65), which is often taken as a short-hand but mathematically ill-defined.

Now consider a second process $E(t)$ which starts at $t_1 > t$ and evolves as the adjoint of $X(t)$ with respect to some scalar product $\langle \cdot | \cdot \rangle$, such that

$$\langle E(t_1) | X(t_1) \rangle = \left\langle E(t_1) \left| \sum_{n=0}^{\infty} \mathcal{M}_{t_1, t_0}^{(n)} X(t_0) \right. \right\rangle \quad (6.76)$$

$$= \left\langle \sum_{n=0}^{\infty} (\mathcal{M}_{t_1, t_0}^{(n)})^\dagger E(t_1) \left| X(t_0) \right. \right\rangle \quad (6.77)$$

$$= \langle E(t_0) | X(t_0) \rangle \quad (6.78)$$

for arbitrary t_0 , so

$$E(t) = \sum_{n=0}^{\infty} (\mathcal{M}_{t_1, t}^{(n)})^\dagger E(t_1). \quad (6.79)$$

To obtain a differential equation analogous to (6.65) for $E(t)$ we need to take a derivative with respect to t . It is not immediately clear how to do this from

$$\begin{aligned} (\mathcal{M}_{t_1, t}^{(n)})^\dagger E(t_1) &= (\mathbf{I}) \int_t^{t_1} dW_{\tau_1} \int_t^{\tau_1} dW_{\tau_2} \dots \\ &\dots \int_t^{\tau_{n-1}} dW_{\tau_n} M_{\tau_n}^\dagger \dots M_{\tau_2}^\dagger M_{\tau_1}^\dagger E(t_1), \end{aligned} \quad (6.80)$$

since t appears in every integral.

If the integrals were regular deterministic integrals we could simply re-order the integration boundaries. For example, for an integrable deterministic function $f(t, s)$ one finds

$$\int_0^1 dt \int_0^t ds f(t, s) = \int_0^1 ds \int_s^1 dt f(t, s). \quad (6.81)$$

Here, the left-hand side corresponds to the scheme depicted in Fig. 6.1 (a), while the right-hand side corresponds to the scheme in Fig. 6.1 (b), where the arrows indicate the direction of the inner integral. An equivalent result for stochastic integrals was proven by Kuznetsov [32, Ch. 7]. He showed that one can swap the order of integration provided one simultaneously changes from regular Itô to backward Itô integrals, so proceeding inductively we find

$$\begin{aligned} (\mathcal{M}_{t_1, t}^{(n)})^\dagger E(t_1) &= (\mathbf{I}) \int_t^{t_1} dW_{\tau_1} \int_t^{\tau_1} dW_{\tau_2} \dots \\ &\dots \int_t^{\tau_{n-1}} dW_{\tau_n} M_{\tau_n}^\dagger \dots M_{\tau_2}^\dagger M_{\tau_1}^\dagger E(t_1) \end{aligned} \quad (6.82)$$

$$\begin{aligned} &= (\text{BI}) \int_t^{t_1} dW_{\tau_n} \dots \int_{\tau_3}^{t_1} dW_{\tau_2} \times \\ &\quad \times \int_{\tau_2}^{t_1} dW_{\tau_1} M_{\tau_n}^\dagger \dots M_{\tau_2}^\dagger M_{\tau_1}^\dagger E(t_1) \end{aligned} \quad (6.83)$$

$$\begin{aligned} &= (\text{BI}) \int_t^{t_1} M_{\tau_n}^\dagger dW_{\tau_n} \dots \int_{\tau_3}^{t_1} M_{\tau_2}^\dagger dW_{\tau_2} \times \\ &\quad \times \int_{\tau_2}^{t_1} M_{\tau_1}^\dagger dW_{\tau_1} E(t_1) \end{aligned} \quad (6.84)$$

$$= (\text{BI}) \int_t^{t_1} M_{\tau}^\dagger (\mathcal{M}_{t_1, \tau}^{(n-1)})^\dagger dW_{\tau} E(t_1), \quad (6.85)$$

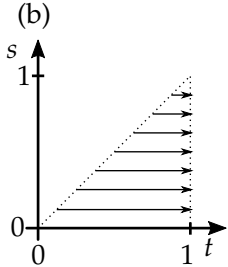
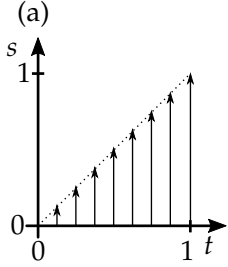


Figure 6.1: Changing the order of integration.

where all nested integrals in the last three equations are backward Itô integrals. Taking a variation with respect to the lower limit of an integral yields a negative sign, so we find

$$-d_t(\mathcal{M}_{t_1,t}^{(n)})^\dagger = (\text{BI}) M_t^\dagger(\mathcal{M}_{t_1,t}^{(n-1)})^\dagger dW_t, \quad (6.86)$$

and consequently

$$-d_t E(t) = (\text{BI}) M_t^\dagger E(t) dW_t. \quad (6.87)$$

We are going to apply retrodiction to Gaussian systems, which are linear systems with Gaussian states. Linear dynamics are ubiquitous in physics for a number of reasons. Many prototypical physical systems, such as harmonic oscillators, are linear. These allow for exact and analytical solutions. Thus even if the actual dynamics are nonlinear (anharmonic), a linear approximation may serve as a good starting point for further studies. Important examples include optical and microwave cavities, mesoscopic mechanical resonators, and any hybrid setup where these are linearly coupled [2, 47, 49, 93]. Gaussian states in turn are ubiquitous in linear systems because they remain Gaussian under linear dynamics, allow for a simple representation in phase space, and in fact stable linear dynamics cause any initial state to become Gaussian, as we will show in Sec. 7.5. To set the scene we recall some basic definitions about linear systems, quantum characteristic functions, and Gaussian states, which also serves to introduce our notation. We then consider the evolution of the means and covariance matrix of the filtered state and retrodicted effect operators.

From now on we always consider bosonic quantum systems with M modes and $2M$ associated canonical operators $\hat{r} = (\hat{r}_j)_{j=1,\dots,2M}$. The \hat{r}_j satisfy canonical commutation relations

$$i\sigma_{jk} := [\hat{r}_j, \hat{r}_k], \quad (7.1)$$

giving rise to a skew-symmetric symplectic matrix $\sigma \in \mathbb{R}^{2M \times 2M}$. For example, the usual choice for a harmonic oscillator would be

$$\hat{r} = \begin{bmatrix} \hat{x}^T & \hat{p}^T \end{bmatrix}^T = \begin{bmatrix} \hat{x}_1 & \dots & \hat{x}_M & \hat{p}_1 & \dots & \hat{p}_M \end{bmatrix}^T, \quad (7.2)$$

which entails

$$\sigma = \begin{bmatrix} \mathbf{0}_M & \mathbf{1}_M \\ -\mathbf{1}_M & \mathbf{0}_M \end{bmatrix}. \quad (7.3)$$

7.1 LINEAR SYSTEMS

A linear system is a dynamical system whose canonical operators evolve according to linear Heisenberg equations of motion. We consider dynamics governed by the general Itô Stochastic Master Equation (SME) (6.22),

$$\begin{aligned} \text{(I)} \quad d\rho(t) = & -i[\hat{H}, \rho(t)]dt + \sum_{j=1}^{N_L} \mathcal{D}[\hat{L}_j]\rho(t)dt \\ & + \sum_{k=1}^{N_C} \mathcal{H}[\hat{C}_k]\rho(t)dW_k(t), \end{aligned} \quad (7.4)$$

as derived in Sec. 6.1. The dW_k are independent stochastic Wiener increments, so they are zero-mean Gaussian-distributed random variables with variance dt satisfying the Itô table

$$dW_j(t)dW_k(t) = \delta_{jk}dt. \quad (7.5)$$

They are related to corresponding measurement currents $Y_j(t)$ as

$$dY_j(t) = \langle \hat{C}_j + \hat{C}_j^\dagger \rangle_\rho dt + dW_j(t). \quad (7.6)$$

In linear systems the Hamiltonian is at most quadratic in the canonical operators while the jump and measurement operators are at most linear. In the Hamiltonian we neglect constants and absorb possible linear terms by redefining the canonical operators. Then \hat{H} can be expressed as

$$\hat{H} = \frac{1}{2} \hat{\mathbf{r}}^T H \hat{\mathbf{r}}, \quad (7.7)$$

with a symmetric matrix $H \in \mathbb{R}^{2M \times 2M}$. The N_C linear measurement operators we write as

$$\hat{C} = (A + iB) \hat{\mathbf{r}}, \quad (7.8)$$

with $A, B \in \mathbb{R}^{N_C \times 2M}$, and the N_L jump operators, also linear in $\hat{\mathbf{r}}$, can be written as

$$\hat{L} = \Lambda \hat{\mathbf{r}}, \quad (7.9)$$

$$\Lambda^\dagger \Lambda =: \Delta + i\Omega, \quad (7.10)$$

with complex $\Lambda \in \mathbb{C}^{N_L \times 2M}$ and $\Delta, \Omega \in \mathbb{R}^{2M \times 2M}$ symmetric and skew-symmetric respectively. Since any information recorded by the observer must have previously left the system (cf. Eq. (6.25)) it must hold that

$$\sum_j \hat{L}_j^\dagger \hat{L}_j - \sum_k \hat{C}_k^\dagger \hat{C}_k \geq 0 \quad \Leftrightarrow \quad \Delta - A^T A - B^T B \geq 0. \quad (7.11)$$

7.2 QUANTUM CHARACTERISTIC FUNCTIONS

A useful tool in classical probability theory are characteristic functions. The characteristic function of a random variable R is defined as the (classical) expectation value $\chi(\xi) := \mathbb{E}[e^{i\xi R}]$. This is well-defined even when R admits no probability density function $p_R(r)$. But if $p_R(r)$ does exist then χ is its Fourier transform. It is normalized as $\chi(0) = \mathbb{E}[1] = 1$. The characteristic function is a moment-generating function for R which means the n^{th} moment μ_n is obtained from the n^{th} derivative of χ at the origin,

$$\mu_n = \mathbb{E}[R^n] = \left(-i \frac{\partial}{\partial \xi} \right)^n \chi(\xi) \Big|_{\xi=0}. \quad (7.12)$$

Thus given χ one has access to all statistics of R .

In quantum systems operators \hat{r}_j are random variables whose statistics are determined by the state ρ with the classical expectation value $\mathbb{E}[R]$

replaced by $\langle \hat{r}_j \rangle = \text{Tr}\{\hat{r}_j \rho\}$. An extension of classical probability distributions to continuous-variable quantum systems are phase space quasi-probability distributions, such as the Wigner function [94]. Its Fourier transform is the *quantum characteristic function* [47, 95–97]

$$\chi_\rho(\boldsymbol{\xi}, t) := \langle \mathcal{W}(\boldsymbol{\xi}) \rangle_\rho = \text{Tr}\{\mathcal{W}(\boldsymbol{\xi}) \rho(t)\}, \quad (7.13)$$

which we define as the expectation value of the unitary Weyl operator [98–100],

$$\mathcal{W}(\boldsymbol{\xi}) := \exp(-i\boldsymbol{\xi}^T \sigma \hat{\boldsymbol{r}}) = \exp(i(\boldsymbol{p}^T \hat{\boldsymbol{x}} - \boldsymbol{q}^T \hat{\boldsymbol{p}})). \quad (7.14)$$

Since every mode of the system is associated with two canonical operators we always have an even number of operators $\hat{r}_1, \dots, \hat{r}_{2M}$ and phase space variables $\boldsymbol{\xi} = [q_1, \dots, q_M, p_1, \dots, p_M]^T \in \mathbb{R}^{2M}$. Note that because $\mathcal{W}(0) = \hat{1}$, the characteristic function of a normalized state satisfies $\chi_\rho(0) = \text{Tr}\{\rho\} = 1$, but we elaborate on this condition in Sec. 7.2.2. The characteristic function provides a description of the system state that is equivalent to ρ : we can always retrieve the full density matrix from [98, 99]

$$\rho = \frac{1}{(2\pi)^M} \int d^{2M} \boldsymbol{\xi} \chi_\rho(\boldsymbol{\xi}) \mathcal{W}(-\boldsymbol{\xi}). \quad (7.15)$$

7.2.1 Moments and cumulants

Like its classical counterpart, χ_ρ allows to calculate arbitrary moments and cumulants of the canonical operators through appropriate derivatives at the origin. One must take care because the definition of χ_ρ is not unique: since operators do not commute as in classical probability theory there are different orderings of χ_ρ . Throughout this thesis we choose symmetric ordering, so all moments we obtain from χ_ρ will also be symmetrically ordered (see below).

We write the moments as

$$\mu_{m_1, \dots, m_{2M}}^\rho := \langle (\hat{r}_1)^{m_1} \dots (\hat{r}_{2M})^{m_{2M}} \rangle_\rho^{(s)}, \quad (7.16)$$

where the superscript (s) denotes symmetric ordering, meaning a simple geometric average over all possible orderings of the operators. Note that the moments depend on t through $\rho(t)$, which we suppress for simplicity. Index m_j tells us how often the operator \hat{r}_j appears in each product. For example, for a single-mode system with $M = 1$ and $\hat{r}_1 = \hat{x}$, $\hat{r}_2 = \hat{p}$ this means

$$\mu_{2,0}^\rho = \langle \hat{x}^2 \rangle_\rho^{(s)} = \langle \hat{x}^2 \rangle_\rho, \quad (7.17)$$

$$\mu_{1,1}^\rho = \langle \hat{x} \hat{p} \rangle_\rho^{(s)} = \frac{1}{2} \langle \hat{x} \hat{p} + \hat{p} \hat{x} \rangle_\rho, \quad (7.18)$$

$$\mu_{2,1}^\rho = \langle \hat{x}^2 \hat{p} \rangle_\rho^{(s)} = \frac{1}{3} \langle \hat{x}^2 \hat{p} + \hat{x} \hat{p} \hat{x} + \hat{p} \hat{x}^2 \rangle_\rho. \quad (7.19)$$

If we introduce the *twisted derivative*

$$\tilde{\partial}_j := \sum_{k=1}^{2M} \sigma_{jk} \frac{\partial}{\partial \xi_k} \quad (7.20)$$

to take into account the commutation relations, we obtain the moments from χ_ρ via

$$\mu_{m_1, \dots, m_{2M}}^\rho = (-i\tilde{\partial}_1)^{m_1} \dots (-i\tilde{\partial}_{2M})^{m_{2M}} \chi_\rho(\xi) \Big|_{\xi=0}. \quad (7.21)$$

An alternative to moments are *cumulants* $\kappa_{m_1, \dots, m_{2M}}^\rho$ (see [101, 102] or [103] and references therein) which we also obtain (symmetrically ordered) from χ_ρ through

$$\kappa_{m_1, \dots, m_{2M}}^\rho = (-i\tilde{\partial}_1)^{m_1} \dots (-i\tilde{\partial}_{2M})^{m_{2M}} \ln[\chi_\rho(\xi)] \Big|_{\xi=0}. \quad (7.22)$$

Hence we can express the characteristic function as [102]

$$\chi_\rho(\xi) = \sum_{m_1, \dots, m_{2M}=0}^{\infty} \frac{(i\tilde{\xi}_1)^{m_1}}{m_1!} \dots \frac{(i\tilde{\xi}_{2M})^{m_{2M}}}{m_{2M}!} \mu_{m_1, \dots, m_{2M}}^\rho \quad (7.23)$$

$$= \exp \left(\sum_{m_1, \dots, m_{2M}=0}^{\infty} \frac{(i\tilde{\xi}_1)^{m_1}}{m_1!} \dots \frac{(i\tilde{\xi}_{2M})^{m_{2M}}}{m_{2M}!} \kappa_{m_1, \dots, m_{2M}}^\rho \right), \quad (7.24)$$

where we introduced $\tilde{\xi}_j = \sum_k \sigma_{jk} \xi_k$. Note that the lowest order moment and cumulant give the normalization, so $\mu_{0, \dots, 0}^\rho = 1$ and $\kappa_{0, \dots, 0}^\rho = 0$ for normalized states. We will see in Sec. 7.3 that cumulants play a special role in the description of Gaussian states since all cumulants of order greater than two vanish.

7.2.2 Unnormalized characteristic functions

The normalization of the characteristic function follows directly from the normalization of the density operator since $\chi_\rho(0) = \text{Tr}\{\rho\} = 1$. Thus if we consider an unnormalized operator \hat{E} with $\text{Tr}\{\hat{E}\} \neq 1$, the corresponding phase space function

$$\tilde{\chi}_E(\xi) = \text{Tr}\{\mathcal{W}(\xi)\hat{E}\} \quad (7.25)$$

must be explicitly normalized to obtain a proper characteristic function

$$\chi_E(\xi) = \frac{\tilde{\chi}_E(\xi)}{\tilde{\chi}_E(0)}. \quad (7.26)$$

This is relevant when computing the moments from χ_E . But using this expression to obtain the cumulants instead of the moments we see that all except $\kappa_{0, \dots, 0}^E$ satisfy

$$\kappa_{m_1, \dots, m_{2M}}^E = (-i\tilde{\partial}_1)^{m_1} \dots (-i\tilde{\partial}_{2M})^{m_{2M}} (\ln[\tilde{\chi}_E(\xi)] - \ln[\tilde{\chi}_E(0)]) \Big|_{\xi=0} \quad (7.27)$$

$$\equiv (-i\tilde{\partial}_1)^{m_1} \dots (-i\tilde{\partial}_{2M})^{m_{2M}} \ln[\tilde{\chi}_E(\xi)] \Big|_{\xi=0} \quad (7.28)$$

This shows that at the level of the cumulants the normalization of \hat{E} is irrelevant (as long as $\tilde{\chi}_E(0) = \text{Tr}\{\hat{E}\}$ exists).

7.3 GAUSSIAN STATES AND EFFECT OPERATORS

7.3.1 Gaussian quantum states

A *Gaussian state* [96, 99–101, 104–108] is any quantum state $\rho(t)$ whose characteristic function is a Gaussian function,

$$\chi_\rho(\boldsymbol{\xi}, t) = \exp\left(-\frac{1}{2}\boldsymbol{\xi}^T \sigma^T V_\rho(t) \sigma \boldsymbol{\xi} + i\boldsymbol{\xi}^T \sigma^T \mathbf{r}_\rho(t)\right). \quad (7.29)$$

This implies that all other quasi-probability distributions, such as the Wigner function, are Gaussian as well, since they are related to one another and to χ_ρ via Fourier and Weierstrass transforms, which preserve their Gaussian form. A Gaussian characteristic function is fully determined by a vector of means $\mathbf{r}_\rho(t) \in \mathbb{R}^{2M}$ and a symmetric covariance matrix $V_\rho(t) \in \mathbb{R}^{2M \times 2M}$. Since in turn χ_ρ fully determines ρ according to (7.15), this is a very economical representation of the state. We emphasize that it is also an *exact* representation and not an approximation.

Comparing (7.29) to the expression of χ_ρ in terms of cumulants, Eq. (7.24), we can read off that mean and covariance matrix

$$r_j^\rho = \langle \hat{r}_j \rangle_\rho = \kappa_{0, \dots, \underset{j}{1}, \dots, 0}^\rho \quad (7.30)$$

$$V_{jk}^\rho = \frac{1}{2} \langle \{ \hat{r}_j - r_j^\rho, \hat{r}_k - r_k^\rho \} \rangle_\rho = \kappa_{0, \dots, \underset{j}{1}, \dots, \underset{k}{1}, \dots, 0}^\rho \quad (7.31)$$

are precisely the cumulants of first and second order. Here the arrows indicate the position of the respective indices. This is confirmed by plugging (7.29) into Eq. (7.22) to compute the cumulants, which also shows that all third and higher orders vanish identically. Beside this sparse representation Gaussian states have the tremendously useful property to remain Gaussian under linear dynamics, which we will see and use in Sec. 7.4. Thus the evolution of $\rho(t)$ is fully determined by the evolution of $\mathbf{r}_\rho(t)$ and $V_\rho(t)$. These properties make Gaussian states and their description through cumulants particularly attractive.

Purity of Gaussian states

An important measure of the quality of any state preparation scheme is the purity $\mathcal{P}(\rho) = \text{Tr}\{\rho^2\} \leq 1$ of the prepared state. It quantifies the amount of classical uncertainty in ρ . For a Gaussian state it depends only on the covariance matrix, and for a state of M modes it reads [109]

$$\mathcal{P}(\rho) = 1/\sqrt{\det(2V_\rho)} = 1/\left(2^M \sqrt{\det(V_\rho)}\right). \quad (7.32)$$

Unobserved dissipation tends to reduce the purity during evolution, while monitoring the dynamics and conditioning the state increases the purity. Ideally, perfect detection allows to prepare pure states with $\mathcal{P}(\rho) = 1$. The bound $\mathcal{P} \leq 1$ implies $\det(V_\rho) \geq 2^{-M}$, which is also imposed by Heisenberg's uncertainty relation, and saturated only by pure states.

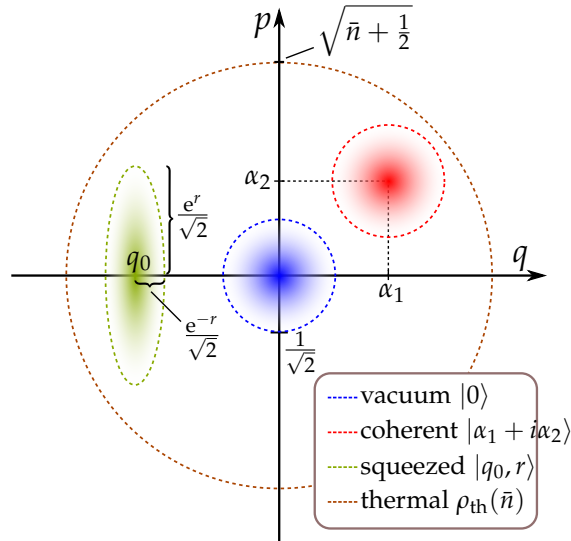


Figure 7.1: A plot of Wigner functions of different Gaussian states in phase space. Dashed lines bound the noise ellipses corresponding to a given covariance matrix V , centered at the means of \hat{x} and \hat{p} . Vacuum (blue) and coherent (red) states have variance $1/2$ (*shot noise*) and thus standard deviation $1/\sqrt{2}$ in each quadrature. The displaced squeezed (green) state has sub-shot noise variance in \hat{x} for an increased variance in \hat{p} . The centered thermal (unfilled brown) state has equal variances $\sqrt{\bar{n} + 1/2}$ in \hat{x} and \hat{p} for mean excitation number \bar{n} . Vacuum, coherent and squeezed states are pure, i. e., quantum-limited states, saturating Heisenberg's uncertainty relation, while the thermal state is a mixed state for $\bar{n} > 0$.

Important Gaussian states, which are depicted for a single mode in Fig. 7.1, are coherent, squeezed, and thermal states. Coherent states $|\alpha\rangle$ are pure states with equal variances $V_{xx} = V_{pp} = 1/2$ (the *shot-noise limit*) and vanishing covariance, and means given by the real and imaginary part of α . The vacuum $|0\rangle$ is a special coherent state with vanishing means. Squeezed states [95] are also pure, and have the variance in one quadrature reduced below shot noise. The conjugate quadrature is then necessarily anti-squeezed to satisfy Heisenberg's uncertainty relation. An important class of mixed Gaussian states are thermal states. These have vanishing means, vanishing covariance, and equal variances $V_{xx} = V_{pp} = \bar{n} + 1/2$, where $\bar{n} \geq 0$ is the mean number of excitations. Importantly, $\mathcal{P} = 1/(2\bar{n} + 1)$ decreases as \bar{n} grows.

7.3.2 Gaussian effect operators

The definition above can of course be extended to arbitrary operators. In particular, we assume all effect operators \hat{E} realized through retrodiction (cf. Sec. 6.2) to be Gaussian operators as done in [27, 110]. Typical examples of direct Gaussian measurements in quantum optics are homodyne and heterodyne detection, see also App. A. A homodyne measurement corresponds to Positive-Operator Valued Measures (POVMs) comprising projections onto squeezed states that in the ideal limit of infinite squeezing¹⁰ measure only a single quadrature, $\hat{E}_x = |x\rangle\langle x|$. Heterodyne detection, on the other hand, yields information about both quadratures

¹⁰ Obviously these are not proper states, but they can be approximated arbitrarily well by squeezed Gaussians.

simultaneously at reduced certainty of each, and thus projects onto coherent states, $\hat{E}_\alpha = |\alpha\rangle\langle\alpha|/\pi$.

We can also assume any retrodicted effect operators to be Gaussian if the backward dynamics are *stable*, which we will explain in Sec. 7.5. Note that just like the forward dynamics the linear backward dynamics causes any Gaussian operator (and any Gaussian POVM) to remain Gaussian for all past times. In case no measurement was performed at t_1 the natural POVM to start our backpropagation is $\hat{E}(t_1) = \hat{1}$, which is not Gaussian, but should collapse to a Gaussian in stable systems. To avoid using the identity (for example in simulations [110]) one could start with a two-element POVM $\{\hat{E}_\beta, \hat{1} - \hat{E}_\beta\}$, where

$$\hat{E}_\beta \propto e^{-\beta\hat{H}} \quad (7.33)$$

is proportional to a thermal state [95, 106] with inverse temperature $\beta > 0$. Let us set $\hat{E}(t_1) = \hat{E}_\beta$ for arbitrarily small but fixed β . Stable dynamics cause the long-time evolution to become independent of β , and in fact independent of the choice of initial POVM altogether. Another way [22, 110], which we did not explore, is the following: the problem with the identity operator is that it has infinite variances. A possible solution is to consider instead the *information matrix* $P := V^{-1}$, which is the inverse of the covariance matrix that simply vanishes as $V \rightarrow \infty$.

Restricting ourselves to Gaussian POVMs in this way we find that, just like ρ , the effect operator is fully characterized by its means and covariance matrix for all times,

$$r_j^E = \langle \hat{r}_j \rangle_E := \frac{\text{Tr}\{\hat{r}_j \hat{E}\}}{\text{Tr}\{\hat{E}\}}, \quad (7.34)$$

$$V_{jk}^E = \frac{1}{2} \langle \{\hat{r}_j - r_j^E, \hat{r}_k - r_k^E\} \rangle_E, \quad (7.35)$$

and we can represent \hat{E} in phase space through its characteristic function

$$\chi_E(\boldsymbol{\xi}, t) = \exp\left(-\frac{1}{2}\boldsymbol{\xi}^T \sigma^T V_E(t) \sigma \boldsymbol{\xi} + i\boldsymbol{\xi}^T \sigma^T \mathbf{r}_E(t)\right). \quad (7.36)$$

Purity of Gaussian effect operators

The purity of effect operators tells us something about the quality of the corresponding measurement. Unit purity means a given POVM actually corresponds to projections onto pure states, constituting a quantum-limited measurement. Equal variances then belong to projections onto coherent states, while asymmetric variances indicate projections onto squeezed states. Reduced purity means additional uncertainty and thus lower resolution of the measurement.

We will see in the examples in Sections 8.1 and 8.2 that the purity of retrodicted effect operators decreases quickly when the detection efficiency is low or there is coupling to unobserved baths. To make this quantitative consider a system that is continuously measured with rate Γ , and is also coupled to further unobserved decay channels at rate γ . We will find that the purity of both the conditional state and the retrodicted effect operator depend crucially on the quantum cooperativity

$C_q = \Gamma/\gamma$. We will show in Sec. 8.2 that only in the regime $C_q > 1$ it is possible to retrodict quantum-limited (i. e., pure) effect operators, and to prepare quantum-limited conditional states.

7.4 EVOLUTION OF MEANS AND COVARIANCE MATRIX

7.4.1 Gaussian quantum states

A master equation for ρ can be translated directly into a differential equation for χ_ρ [95]. We only need to replace the canonical operators by corresponding differential operators on χ_ρ as detailed in App. B. For a general quantum state with arbitrary cumulants we find that the means evolve as

$$\text{(I)} \quad d\mathbf{r}_\rho(t) = Q\mathbf{r}_\rho(t)dt + (2V_\rho(t)A^\text{T} - \sigma B^\text{T})d\mathbf{W}(t), \quad (7.37)$$

with the *drift matrix*

$$Q := \sigma(H + \Omega), \quad (7.38)$$

comprising unitary and dissipative terms. If we reintroduce the actually measured homodyne signal from Eq. (7.6),

$$\text{(I)} \quad d\mathbf{Y}(t) = 2A\mathbf{r}_\rho(t)dt + d\mathbf{W}(t), \quad (7.39)$$

we can write

$$\text{(I)} \quad d\mathbf{r}_\rho(t) = M_\rho(t)\mathbf{r}_\rho(t)dt + (2V_\rho(t)A^\text{T} - \sigma B^\text{T})d\mathbf{Y}(t), \quad (7.40)$$

with the *measurement-enhanced drift matrix*

$$M_\rho(t) := Q + 2\sigma B^\text{T}A - 4V_\rho(t)A^\text{T}A. \quad (7.41)$$

We call it enhanced because the additional measurement matrices A and B help to stabilize the dynamics. The measurement currents enter the evolution of the means in Eq. (7.40) only through multiplication with the measurement matrices. Reducing the detection efficiency, which corresponds to $A, B \rightarrow 0$, thus causes the stochastic increment to disappear as it should. Note that the covariance matrix $V_\rho(t)$ twice enters the evolution, once through the drift matrix M_ρ and once directly coupled to the photocurrent. A consequence of the latter term is that a large variance, corresponding to large uncertainty about the state, boosts the effect that a bit of gathered information has on the evolution of the conditional means.

Assuming a Gaussian state we show in App. B that the covariance matrix itself satisfies the deterministic equation

$$\begin{aligned} \dot{V}_\rho(t) &= QV_\rho(t) + V_\rho(t)Q^\text{T} + \sigma\Delta\sigma^\text{T} \\ &\quad - \left(2V_\rho(t)A^\text{T} - \sigma B^\text{T}\right)\left(2V_\rho(t)A^\text{T} - \sigma B^\text{T}\right)^\text{T} \end{aligned} \quad (7.42a)$$

$$\begin{aligned} &= (Q + 2\sigma B^\text{T}A)V_\rho(t) + V_\rho(t)(Q + 2\sigma B^\text{T}A)^\text{T} \\ &\quad + \sigma\tilde{\Delta}\sigma^\text{T} - 4V_\rho(t)A^\text{T}AV_\rho(t) \end{aligned} \quad (7.42b)$$

$$\begin{aligned} &= M_\rho(t)V_\rho(t) + V_\rho(t)M_\rho^\text{T}(t) \\ &\quad + \sigma\tilde{\Delta}\sigma^\text{T} + 4V_\rho(t)A^\text{T}AV_\rho(t). \end{aligned} \quad (7.42c)$$

with the *diffusion matrix* (cf. Eq. (7.11))

$$\tilde{\Delta} := \Delta - B^T B \geq 0. \quad (7.42d)$$

The evolution of $V_\rho(t)$ is deterministic, and independent of the means $\mathbf{r}_\rho(t)$ and all other cumulants, which is a peculiarity of Gaussian dynamics, and not generally true, as we will see in Sec. 7.4.3. However, although it is independent of the measurement record and not a stochastic equation, it does depend on the measurement device through matrices A and B . This is reasonable since the information gained from observations of the system helps condition the state, reducing the uncertainty in at least some of its quadratures.

Steady state solution

We assume stable dynamics (see [2, Chapters 6.4, 6.6] and Sec. 7.5.1 for more details) so the covariance matrix of any initial (Gaussian) state will collapse to a steady state V_ρ^{ss} . We find V_ρ^{ss} by solving the algebraic Riccati equation $\dot{V}_\rho = 0$ which implies

$$M_\rho^{\text{ss}} V_\rho^{\text{ss}} + V_\rho^{\text{ss}} (M_\rho^{\text{ss}})^T = -\sigma \tilde{\Delta} \sigma^T - 4V_\rho^{\text{ss}} A^T A V_\rho^{\text{ss}}, \quad (7.43)$$

where M_ρ^{ss} is the drift matrix $M_\rho(t)$ with $V_\rho(t) \equiv V_\rho^{\text{ss}}$. The right-hand side is negative semi-definite (negative definite if there is some unobserved dissipation) and the covariance matrix is positive definite for physical (finitely squeezed) states, so M_ρ^{ss} is *stable*, i. e., has only eigenvalues with non-positive real part. In practice, assuming sub-unit detection efficiency, M_ρ^{ss} is *strictly stable*, i. e., has only eigenvalues with negative real parts.

Now if the experiment has been running sufficiently long for the covariance matrix to have collapsed to its fixed point, we can simply plug V_ρ^{ss} and M_ρ^{ss} into Eq. (7.40) to find the evolution of the means,

$$\text{(I)} \quad \mathbf{r}_\rho(t) = e^{M_\rho^{\text{ss}}(t-t_0)} \mathbf{r}_\rho(t_0) + \int_{t_0}^t e^{M_\rho^{\text{ss}}(t-\tau)} (2V_\rho^{\text{ss}} A^T - \sigma B^T) d\mathbf{Y}(\tau). \quad (7.44)$$

Importantly, because M_ρ^{ss} is stable both the initial condition $\mathbf{r}_\rho(t_0)$ and the integrand are damped exponentially. Writing λ_{max} for the eigenvalue of M_ρ^{ss} with largest (still negative) real part, we expect that for times $t - t_0 \gg |\text{Re}[\lambda_{\text{max}}]|^{-1}$ the means will be driven only by the measurement current,

$$\text{(I)} \quad \mathbf{r}_\rho(t) \sim \int_{t_0}^t e^{M_\rho^{\text{ss}}(t-\tau)} (2V_\rho^{\text{ss}} A^T - \sigma B^T) d\mathbf{Y}(\tau). \quad (7.45)$$

Thus we obtain a conditional state whose shape is fixed, and which moves around phase space driven by the measurement current.

Temporal mode functions

Note that the means (and thus the whole state) do not depend on the entire continuous measurement record $\{\mathbf{Y}(s) | t_0 \leq s < t\}$, but only on

an integral of the photocurrent, which is a simple vector of $2M$ real numbers. In fact, the $2M \times N_C$ -dimensional integral kernel

$$F_\rho(t) = (f_{jk}^\rho(t)) := e^{M_{\rho}^{\text{ss}}t} (2V_{\rho}^{\text{ss}}A^T - \sigma B^T) \quad (7.46)$$

picks out a set of *temporal modes* of the monitored fields $Y(\tau)$ which then drive the quadratures $r(t)$. Each (unnormalized) temporal mode function (or *filter function*) $f_{jk}^\rho(t - \tau)$ is convoluted with a corresponding measurement current $Y_k(\tau)$,

$$(I) X_j(t) := \int_{t_0}^t f_{jk}^\rho(t - \tau) dY_k(\tau), \quad (7.47)$$

to enter the evolution of $r_j(t)$. Recall that $Y_k(\tau) \propto \langle \hat{x}_k(\tau) \rangle$ is the result of a quadrature measurement of some outgoing light field. Thus integration with f_{jk}^ρ can be interpreted as the measurement of a different quadrature operator

$$\hat{X}_j(t) \propto \int f_{jk}^\rho(t - \tau) \hat{x}_k(\tau) d\tau \quad (7.48)$$

with outcome $X_j(t)$. Of course the mode functions f_{jk}^ρ are not normalized, and will generally not be orthogonal.

7.4.2 Gaussian effect operators

Assuming that the effect operators we realize through retrodiction are Gaussian operators, we can analogously to the previous section derive a set of differential backward equations for the means and covariance matrix. Let us recall the unnormalized effect equation Eq. (6.58),

$$(BI) -d\hat{E}(t) = i[\hat{H}, \hat{E}(t)]dt + \sum_{j=1}^{N_L} \mathcal{D}^\dagger[\hat{L}_j] \hat{E}(t)dt + \sum_{k=1}^{N_C} (\hat{C}_k^\dagger \hat{E}(t) + \hat{E}(t) \hat{C}_k) dY_k(t), \quad (7.49)$$

with the adjoint Lindblad operator

$$\mathcal{D}^\dagger[\hat{L}] \hat{E} := \hat{L}^\dagger \hat{E} \hat{L} - \frac{1}{2} \hat{L}^\dagger \hat{L} \hat{E} - \frac{1}{2} \hat{E} \hat{L}^\dagger \hat{L}. \quad (7.50)$$

To be able to adapt the results of the previous section we rewrite Eq. (7.49) as

$$(BI) -d\hat{E}(t) = -i[-\hat{H}, \hat{E}(t)]dt + \sum_{j=1}^{N_L} \mathcal{D}[\hat{L}_j] \hat{E}(t) + \sum_{j=1}^{N_L} (\hat{L}_j^\dagger \hat{E}(t) \hat{L}_j - \hat{L}_j \hat{E}(t) \hat{L}_j^\dagger) dt + \sum_{k=1}^{N_C} (\hat{C}_k^\dagger \hat{E}(t) + \hat{E}(t) \hat{C}_k) dY_k(t), \quad (7.51)$$

where the second line compensates for the replacement of \mathcal{D}^\dagger by \mathcal{D} . We see that this equation is structurally very similar to the usual unnormalized master equation (6.22), so the expressions for dr_ρ and \dot{V}_ρ in Eqs. (7.40) and (7.42) serve as a good starting point with the following changes: (i) Time-reversal requires us to treat them as backward Itô equations, cf. Sec. 6.3. (ii) The sign flip of \hat{H} causes $H \rightarrow -H$ and replacing the measurement operators \hat{C}_k by their adjoint entails $B \rightarrow -B$. (iii) Working out the change stemming from the sandwich and normalization terms in the second line we find in App. B.6 that it contributes terms $-2\sigma\Omega r_E$ and $-2(\sigma\Omega V_E + (\sigma\Omega V_E)^\top)$ to the evolution of the means and covariance matrix, respectively. Together with $H \rightarrow -H$ this simply changes the sign of the unconditional drift matrix $Q \rightarrow -Q$. Hence the backward Itô equation for the means reads

$$(BI) -dr_E(t) := r_E(t - dt) - r_E(t) \quad (7.52a)$$

$$= -Qr_E(t)dt + (2V_E(t)A^\top + \sigma B^\top)dW(t) \quad (7.52b)$$

$$= M_E(t)r_E(t)dt + (2V_E(t)A^\top + \sigma B^\top)dY(t), \quad (7.52c)$$

with the measurement-enhanced backward drift matrix

$$M_E(t) := -Q - 2\sigma B^\top A - 4V_E(t)A^\top A. \quad (7.53)$$

The deterministic backward Riccati equation for the covariance matrix is similar to Eq. (7.42),

$$-\dot{V}_E := V_E(t - dt) - V_E(t) \quad (7.54a)$$

$$= M_E(t)V_E(t) + V_E(t)M_E^\top(t) + \sigma\tilde{\Delta}\sigma^\top + 4V_E(t)A^\top AV_E(t). \quad (7.54b)$$

We now clearly see the importance of continuous measurements for retrodiction. Without observations, $A = B = \mathbf{0}$, the drift matrices would be equal up to a sign, $M_\rho(t) = -M_E(t) = Q$. At the same time the quadratic Riccati equations for V_ρ and V_E would turn into linear Lyapunov equations. Assuming stable forward dynamics with a positive steady state solution $V_\rho^{\text{ss}} > 0$ of Eq. (7.43),

$$QV_\rho^{\text{ss}} + V_\rho^{\text{ss}}Q^\top = -\sigma\tilde{\Delta}\sigma^\top, \quad (7.55)$$

would preclude stable backward dynamics: there cannot simultaneously be a steady state $V_E^{\text{ss}} > 0$ that satisfies

$$-QV_E^{\text{ss}} - V_E^{\text{ss}}Q^\top = -\sigma\tilde{\Delta}\sigma^\top. \quad (7.56)$$

Only the presence of a sufficiently large quadratic $A^\top A$ -term in Eq. (7.54), corresponding to sufficiently efficient measurements, allows us to find an equilibrium backward covariance matrix $V_E^{\text{ss}} > 0$. As in the previous section this implies a stable M_E^{ss} whose eigenvalues have non-positive real part.

Assuming stable backward dynamics we can plug the steady state matrices V_E^{ss} and M_E^{ss} into the equation for the means. As in the forward case we find the solution

$$(BI) r_E(t) = e^{(t_1-t)M_E^{\text{ss}}} r_E(t_1) + \int_t^{t_1} e^{(\tau-t)M_E^{\text{ss}}} (2V_E^{\text{ss}}A^\top + \sigma B^\top)dY(\tau), \quad (7.57)$$

where the integral is a backward Itô integral as explained in Sec. 6.3. Stability of M_E^{ss} again implies exponential damping of the final condition $r_E(t_1)$ and of the integrand.

The backward temporal mode functions defined by the integral kernel in (7.57) will generally be different from the forward modes, in particular because the exponential envelope decays in the future, not in the past. But otherwise the discussion would follow similar lines.

7.4.3 Non-Gaussian operators

In App. B we derive the equations of motion for the cumulants of *general* quantum operators under linear dynamics. Since any state that is not Gaussian automatically has infinitely many non-vanishing cumulants [101], one obtains an infinite hierarchy of coupled differential equations. Because the cumulants defined in Eq. (7.22) are more difficult to work with, we provide an alternative definition. Let us write the cumulants of N^{th} order, i. e., of products of N canonical operators, as

$$V_{m_1, \dots, m_N}^{(N)} := \langle \hat{r}_{m_1} \dots \hat{r}_{m_N} \rangle^c. \quad (7.58)$$

In this section we drop the superscripts $V^\rho, V^E \equiv V$ of individual elements for better readability. The indices $1 \leq m_k \leq 2M$ indicate that operator \hat{r}_{m_k} is at position k in the cumulant. Since we consider only symmetrically ordered cumulants the position is actually irrelevant and the V are symmetric under permutations of indices. At first and second order these relate to the means and covariance matrix as

$$r_j = \langle \hat{r}_j \rangle = V_j^{(1)}, \quad (7.59)$$

$$V_{jk} = \frac{1}{2} \langle \{ \hat{r}_j - r_j, \hat{r}_k - r_k \} \rangle = V_{jk}^{(2)}. \quad (7.60)$$

7.4.3.1 Non-Gaussian quantum state

In App. B.5 we find that the evolution of the means of general states ρ is no different from that of Gaussian states, and given by Eq. (7.40). The covariance matrix, however, generally becomes stochastic and satisfies,

$$\begin{aligned} \text{(I)} \quad dV_{m_1, m_2}^{(2)} = & \left[M_\rho V_\rho^{(2)} + V_\rho^{(2)} M_\rho^T \right. \\ & \left. + \sigma \tilde{\Delta} \sigma^T + 4V_\rho^{(2)} A^T A V_\rho^{(2)} \right]_{m_1, m_2} dt \\ & + 2 \sum_{j=1}^{2M} V_{m_1, m_2, j}^{(3)} (A^T dW)_j. \end{aligned} \quad (7.61)$$

The first two lines are the same as Eq. (7.42), but additionally a Wiener increment is introduced through coupling to the third order cumulants $V_\rho^{(3)}$. The evolution of arbitrary cumulants of order $N \geq 3$ is given by

$$\begin{aligned}
\text{(I)} \quad dV_{m_1, \dots, m_N}^{(N)} &= \sum_{\tau \in \mathcal{S}^{\text{cycl}}(N)} M_{m_{\tau(1)}, k}^\rho V_{k, m_{\tau(2)}, \dots, m_{\tau(N)}}^{(N)} dt \\
&\quad - 2 \sum_{n=2}^{N-2} \sum_{\substack{p \in \text{Bipart}(N) \\ |p|=n}} V_{m_{p(1)}, \dots, m_{p(n)}, j}^{(n+1)} (A^T A)_{jk} V_{k, m_{q(1)}, \dots, m_{q(N-n)}}^{(N-n+1)} dt \\
&\quad + 2V_{m_1, \dots, m_N, k}^{(N+1)} (A^T d\mathbf{W})_{k'}
\end{aligned} \tag{7.62}$$

with implicit sums over repeated indices j and k . The sum over $\tau \in \mathcal{S}^{\text{cycl}}(N)$ runs through all cyclic permutations of $\{1, \dots, N\}$, and $p \in \text{Bipart}(N)$ with $|p| = n$ are all bipartitions of $\{1, \dots, N\}$, such that one part contains n elements $p(1), \dots, p(n)$ while its complement contains $q(1), \dots, q(N-n)$. It is interesting to note here that all cumulants couple to the next higher order only through the stochastic term, and deterministically only to lower orders.

7.4.3.2 Non-Gaussian effect operator

In App. B.6 we also compute the backward equations of motion of general (non-Gaussian) effect operators. Again the evolution of the means is the same as for Gaussian operators given by Eq. (7.52). The evolution of the covariance matrix also only changes by becoming a stochastic backward Itô equation,

$$\begin{aligned}
\text{(BI)} \quad -dV_{m_1, m_2}^{(2)} &= \left[M_E V_E^{(2)} + V_E^{(2)} M_E^T \right. \\
&\quad \left. + \sigma \tilde{\Delta} \sigma^T + 4V_E^{(2)} A^T A V_E^{(2)} \right]_{m_1, m_2} dt \\
&\quad + 2 \sum_{j=1}^{2M} V_{m_1, m_2, j}^{(3)} (A^T d\mathbf{W})_j.
\end{aligned} \tag{7.63}$$

where again the first two lines are the same as for Gaussian effect operators, and higher-order cumulants with $N \geq 3$ evolve as

$$\begin{aligned}
\text{(BI)} \quad -dV_{m_1, \dots, m_N}^{(N)} &= \sum_{\tau \in \mathcal{S}^{\text{cycl}}(N)} M_{m_{\tau(1)}, k}^E V_{k, m_{\tau(2)}, \dots, m_{\tau(N)}}^{(N)} dt \\
&\quad - 2 \sum_{n=2}^{N-2} \sum_{\substack{p \in \text{Bipart}(N) \\ |p|=n}} V_{m_{p(1)}, \dots, m_{p(n)}, j}^{(n+1)} (A^T A)_{jk} V_{k, m_{q(1)}, \dots, m_{q(N-n)}}^{(N-n+1)} dt \\
&\quad + 2V_{m_1, \dots, m_N, k}^{(N+1)} (A^T d\mathbf{W})_k.
\end{aligned} \tag{7.64}$$

7.5 STABLE DYNAMICS LEADS TO GAUSSIAN OPERATORS

7.5.1 Stability of linear systems

Stability in dynamical systems is the idea that observers with different initial states of knowledge about the system state but access to the same measurement record will come to an agreement about the state for sufficiently long observation times [2, Ch. 6]. This requires the state to deterministically approach a *steady state*, which is a notion that needs to be modified when considering *conditional* dynamics. Even in equilibrium the system still experiences quantum fluctuations that make the conditional means move around phase space, cf. (7.45). Only the covariance matrix, which (for Gaussian states) is not driven by the measurement current, may have a stable fixed point V^{ss} . Thus when we refer to a system in steady state we always mean that the covariance matrix has collapsed to V^{ss} . Linear systems for which the covariance matrix deterministically collapses to some V^{ss} such that the unconditional means decay to zero are called (*asymptotically*) *stable* [93]. This is the case if and only if the pair $(Q^T, 2A^T)$ is *stabilizable* [2], which means there exists a real matrix F such that $Q + 2FA$ has only eigenvalues with negative real parts.

Now the assumption of a Gaussian initial state $\rho(t_0)$ is reasonable from a physical viewpoint since Gaussian measurements [36, 81, 111] and Gaussian baths [112] tend to “Gaussify” the state of the system. Mathematically Gaussification means that if we start with an arbitrary initial state $\rho(t_0)$, its higher-order cumulants ($N \geq 3$) are exponentially damped by the dynamics, and it collapses to a Gaussian steady state. We show below that the deterministic parts of the equations of motion cause such a decay, which leads us to conjecture that this Gaussification indeed takes place assuming the evolution is stable in the traditional sense. In other words, if the dynamics are such that arbitrary initial Gaussians collapse to a particular steady state V^{ss} , which stabilizes the evolution of the means (makes them decay), then also non-Gaussian states will become Gaussian and collapse to V^{ss} . Thus in stable systems we can choose t_0 such that any transient non-Gaussian components have decayed to safely assume that $\rho(t_0)$ is Gaussian.

An analogous stability criterion applies to effect operators. We conjecture that arbitrary $\hat{E}(t_1)$ will become Gaussian as long as the backward dynamics are stable, which is the case if and only if $(-Q^T, 2A^T)$ is stabilizable. Having both stable forward and backward dynamics requires that one observes the right combination of modes, and that the observations are sufficiently efficient compared to all other decoherence channels, cf. the discussion around Eq. (7.55). The decaying cavity considered in Sec. 8.1 is a basic example of a system with stable forward dynamics but non-stabilizable backward evolution. This is because only one of the quadratures is monitored, so uncertainty about the other will grow indefinitely.

7.5.2 *Gaussification of arbitrary initial states*

We now show that in stable systems the deterministic part of the evolution of the cumulants, i. e., with $dW \equiv 0$, leads to a decay of higher orders ($N \geq 3$). Assuming stable dynamics causes the second cumulants $V_\rho^{(2)}$ of any Gaussian state to be driven deterministically into a steady state V_ρ^{ss} , such that the resulting drift matrix M_ρ^{ss} is stable, i. e., has only eigenvalues with negative real part (see the discussion surrounding Eq. (7.43)). If we consider some non-Gaussian state with $V_\rho^{(3)} \neq 0$, then $V_\rho^{(2)}$ itself becomes a random process, which in addition to a deterministic drift towards V_ρ^{ss} will experience some diffusion induced by the additive white noise dependent on $V_\rho^{(3)}$. Thus we expect the second cumulants to collapse to V_ρ^{ss} asymptotically, and then experience stochastic fluctuations about this stable fixed point. In the following we assume this collapse has already occurred, and show that this also stabilizes the deterministic evolution of all higher-order cumulants. The relevant part of their dynamics is given by

$$\begin{aligned} \dot{V}_{m_1, \dots, m_N}^{(N)} &= \sum_{\tau \in \mathcal{S}^{\text{cycl}}(N)} M_{m_{\tau(1)}, k}^{ss} V_{k, m_{\tau(2)}, \dots, m_{\tau(N)}}^{(N)} \\ &\quad - 2 \sum_{n=2}^{N-2} \sum_{\substack{p \in \text{Bipart}(N) \\ |p|=n}} V_{m_{p(1)}, \dots, m_{p(n)}, j}^{(n+1)} (A^T A)_{jk} V_{k, m_{q(1)}, \dots, m_{q(N-n)}}^{(N-n)}. \end{aligned} \quad (7.65)$$

so coupling occurs only to orders N and below. In particular, $V_\rho^{(3)}$ only couples to itself. We assume for the moment that all cumulants of orders $3, \dots, N-1$ have decayed to zero, so the second line vanishes. The evolution is then simply given by

$$\dot{V}_{m_1, \dots, m_N}^{(N)} = \sum_{\tau \in \mathcal{S}^{\text{cycl}}(N)} M_{m_{\tau(1)}, k}^{ss} V_{k, m_{\tau(2)}, \dots, m_{\tau(N)}}^{(N)}. \quad (7.66)$$

To analyze the stability of this linear dynamical system we assume that $M_\rho^{ss} = T^{-1} \Lambda T$ can be diagonalized¹¹ with eigenvalues

$$\Lambda = \text{diag}(\lambda_1, \dots, \lambda_{2M}). \quad (7.67)$$

We can then consider an equivalent dynamical system comprising

$$\tilde{V}_{m_1, \dots, m_N}^{(N)} = T_{m_1, m'_1} \dots T_{m_N, m'_N} V_{m'_1, \dots, m'_N}^{(N)} \quad (7.68)$$

with summation over repeated indices. The $\tilde{V}_{m_1, \dots, m_N}^{(N)}$ are still symmetric under permutations of indices, so the equations of motion become

$$\dot{\tilde{V}}_{m_1, \dots, m_N}^{(N)} = \sum_{\tau \in \mathcal{S}^{\text{cycl}}(N)} \Lambda_{m_{\tau(1)}, k} \tilde{V}_{k, m_{\tau(2)}, \dots, m_{\tau(N)}}^{(N)} \quad (7.69)$$

$$= \sum_{\tau \in \mathcal{S}^{\text{cycl}}(N)} \lambda_{m_{\tau(1)}} \tilde{V}_{m_{\tau(1)}, m_{\tau(2)}, \dots, m_{\tau(N)}}^{(N)} \quad (7.70)$$

$$= (\lambda_{m_1} + \lambda_{m_2} + \dots + \lambda_{m_N}) \tilde{V}_{m_1, m_2, \dots, m_N}^{(N)}, \quad (7.71)$$

¹¹ This corresponds to switching to the dynamical modes of the system [2, Ch. 6].

where in the second and third line there are *no* implicit sums over the m_j . Since the transformation (7.68) is just a change of basis, the eigenvalues of the dynamical map defined by Eq. (7.66) are the same as those of Eq. (7.71), which we can read off directly: they are given by $v_{n_1, \dots, n_{2M}} := n_1 \lambda_1 + \dots + n_{2M} \lambda_{2M}$ where the n_j are all possible partitions of N , i. e., $n_j \geq 0$ and $\sum_j n_j = N$. Due to the assumed stability, all λ_j (eigenvalues of M_ρ^{ss}) have negative real part, and so do the $v_{n_1, \dots, n_{2M}}$ (eigenvalues of the map (7.66)). More explicitly, let λ_{\max} (λ_{\min}) denote the eigenvalue of M_ρ^{ss} with largest (smallest) real part. Then the eigenvalue of (7.66) with the largest (smallest) real part is given by $N\lambda_{\max}$ ($N\lambda_{\min}$).

The assumption we made to obtain Eq. (7.66) was that all $\tilde{V}_\rho^{(n)}$ with $3 \leq n < N$ have already vanished. Thus we first note that (7.66) holds without any assumptions for $\tilde{V}_\rho^{(3)}$, which consequently decays to zero. We then proceed inductively to higher orders. This shows that in stable systems the deterministic evolution of the $\tilde{V}_\rho^{(N)}$ causes exponential decay to zero.

7.5.3 Gaussification of arbitrary effect operators

As mentioned before, the stability of the backward dynamics can be analyzed in exactly the same way as the forward evolution. Thus we conjecture that any initial effect operator will collapse to a Gaussian operator as long as the unconditional backward dynamics are stable in the sense discussed in Sec. 7.5.1, i. e., that the covariance matrix approaches a stable fixed point V_E^{ss} such that the drift matrix

$$M_E^{\text{ss}} = -Q - 2\sigma B^T A - 4V_E^{\text{ss}} A^T A \quad (7.72)$$

has only eigenvalues with negative real part.

APPLICATIONS

To illustrate the usefulness of retrodiction as developed in the previous chapters, we are going to apply it in two different settings. First we explore two simple toy models to gauge the fundamental limits of the method, and then we will apply it to a realistic optomechanical system in Sec. 8.2.

8.1 BASIC EXAMPLES

8.1.1 Monitoring a decaying cavity

Let us start with the simple example of a decaying cavity undergoing homodyne detection, depicted in Fig. 8.1. This setup was considered by Zhang and Mølmer [27] who showed that past Gaussian state estimates are improved when future observations are taken into account. It was also used by Wiseman [84] to illustrate linear quantum trajectories. He reproduced the known result that with an ideal detector and infinite observation time one can perform a projective measurement of the initial state onto a quadrature eigenstate without ever preparing a squeezed state of the cavity field. We will confirm this using retrodiction on Gaussian states.

We consider an ideal freely damped cavity in a rotating frame, such that $\hat{H} = 0$, with decay rate Γ , and we perform homodyne detection with homodyne angle θ and efficiency $\eta \in [0, 1]$ (cf. App. A). The corresponding Stochastic Master Equation (SME) for the conditional cavity state reads (cf. Sec. 6.1)

$$(I) \, d\rho(t) = \Gamma \mathcal{D}[\hat{a}]\rho(t)dt + \sqrt{\eta\Gamma} \mathcal{H}[e^{-i\theta}\hat{a}]\rho(t)dW(t), \quad (8.1)$$

where \hat{a}^\dagger, \hat{a} are the cavity Creation and Annihilation Operators (CAOs). The canonical quadrature operators are $\hat{x} = (\hat{a} + \hat{a}^\dagger)/\sqrt{2}$ and $\hat{p} = -i(\hat{a} - \hat{a}^\dagger)/\sqrt{2}$, which we collect into a vector $\hat{r} = [\hat{x}, \hat{p}]^T$. Then the Wiener increment $dW(t)$ is related to the detector output $dY(t)$ as

$$dY(t) = \sqrt{2\eta\Gamma} \langle \hat{x}_\theta \rangle_\rho dt + dW(t), \quad (8.2)$$

with $\hat{x}_\theta := \cos(\theta)\hat{x} + \sin(\theta)\hat{p}$. Due to the symmetry of the problem we choose $\theta = 0$ without loss of generality, observing only the \hat{x} -quadrature of the cavity.

8.1.1.1 Conditional state evolution

Before we perform retrodiction we consider the monitored evolution of a Gaussian cavity state. As we showed in Sec. 7.5 assuming a Gaussian state is not a strong restriction as long as the dynamics are stable. We know this is the case because even without measurements the cavity will decay to the vacuum, which is a Gaussian state. But we can

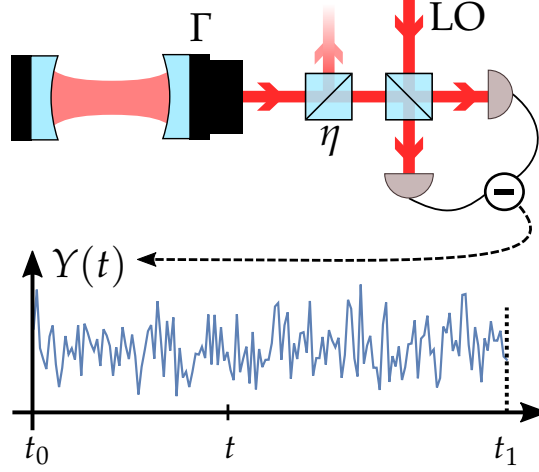


Figure 8.1: Schematic of a freely decaying cavity monitored from time t_0 to t_1 . Light leaving the cavity at rate Γ is superposed on a balanced beam splitter with a strong local oscillator (LO). Two photodetectors monitor the output ports and their photocurrents are subtracted to yield a time-continuous homodyne measurement signal $Y(t)$. Imperfect detection is modeled as photon loss induced by a second beam splitter which only transmits a fraction η of the signal light. See also App. A.

confirm this using the stabilizability criterion of Sec. 7.5.1. Using the formalism of Sec. 7.4 we read off the matrices $H = \mathbf{0}_2$ for the Hamiltonian, and $\Delta = (\Gamma/2)\mathbf{1}_2$ and $\Omega = (\Gamma/2)\sigma$ for the dissipation, where σ is the 2×2 symplectic matrix. The resulting drift matrix $Q = \sigma(H + \Omega) = -(\Gamma/2)\mathbf{1}_2$ has only negative eigenvalues, so the dynamics are indeed trivially stable. The measurement matrices are $A = \sqrt{\eta\Gamma/2} \begin{bmatrix} 1 & 0 \end{bmatrix}$ and $B = \sqrt{\eta\Gamma/2} \begin{bmatrix} 0 & 1 \end{bmatrix}$.

Spelling out Eqs. (7.37) and (7.42) for dr_ρ and \dot{V}_ρ , and dropping the subscript to improve readability, we find

$$\text{(I)} \quad dx(t) = -\frac{\Gamma}{2}xdt + \sqrt{\frac{\eta\Gamma}{2}}(2V_{xx}(t) - 1)dW(t), \quad (8.3a)$$

$$\text{(I)} \quad dp(t) = -\frac{\Gamma}{2}pdt + \sqrt{\frac{\eta\Gamma}{2}}2V_{xp}(t)dW(t), \quad (8.3b)$$

and

$$\dot{V}_{xx} = -(1 - 2\eta)\Gamma V_{xx} + (1 - \eta)\frac{\Gamma}{2} - 2\eta\Gamma V_{xx}^2, \quad (8.4a)$$

$$\dot{V}_{xp} = -(1 - \eta)\Gamma V_{xp} - 2\eta\Gamma V_{xx}V_{xp}, \quad (8.4b)$$

$$\dot{V}_{pp} = -\Gamma V_{pp} + \frac{\Gamma}{2} - 2\eta\Gamma V_{xp}^2. \quad (8.4c)$$

The steady state solution to the Riccati equation $\dot{V} = 0$ is simply

$$V_{xx}^{\text{ss}} = V_{pp}^{\text{ss}} = \frac{1}{2}, \quad V_{xp}^{\text{ss}} = 0. \quad (8.5)$$

Computing the purity $\mathcal{P}(\rho) = 1/(2\sqrt{\det(V^{\text{ss}})}) = 1$ shows that the prepared steady state is a pure coherent state. Plugging V^{ss} into the equations for the means makes dW drop out, so the long-term forward evolution does not depend on the monitored output. Both mean values decay

exponentially, affirming the known result that for long times a decaying cavity will simply collapse to the vacuum state, $\rho_{\text{ss}} = |0\rangle\langle 0|$.

This insight is important. It shows that the covariance matrix alone does not let us judge the effectiveness of a given preparation (or retrodiction) scheme. If the unconditional dynamics produce some mixed steady state we can increase our knowledge by monitoring the output. At long times the conditional dynamics will produce a state with fixed covariance and measurement-dependent means that moves around phase space, such that the averaged conditional dynamics agree with the unconditional dynamics. However, if the unconditional dynamics already yield a quantum-limited state (such as the vacuum in the present example) then there is nothing to be gained from observing the output. These statements apply to both quantum states and effect operators.

While the observations cannot aid the (long-term) state preparation we will now see that they let us infer information about the *initial* state of the cavity.

8.1.1.2 Retrodiction of POVM elements

In [84] Wiseman constructed an explicit effect operator from the (ideal) continuous measurement record and showed that monitoring the cavity is equivalent to a quadrature measurement on its initial state. The effect equation adjoint to Eq. (8.1) reads

$$\text{(BI)} \quad -d\hat{E}(t) = \Gamma \mathcal{D}^\dagger[\hat{a}]\hat{E}(t)dt + \sqrt{\eta\Gamma}(\hat{a}^\dagger \hat{E}(t) + \hat{E}(t)\hat{a})dY(t). \quad (8.6)$$

Restricting ourselves to Gaussian Positive-Operator Valued Measures (POVMs) we can directly write down the equations of motion of means and covariance matrix, Eqs. (7.52) and (7.54). Again we drop the subscript E to improve readability, so

$$\text{(BI)} \quad -dx(t) = \frac{\Gamma}{2}xdt + \sqrt{\frac{\eta\Gamma}{2}}(2V_{xx}(t) + 1)dW(t), \quad (8.7a)$$

$$\text{(BI)} \quad -dp(t) = \frac{\Gamma}{2}pdt + \sqrt{\frac{\eta\Gamma}{2}}2V_{xp}(t)dW(t), \quad (8.7b)$$

and

$$-\dot{V}_{xx} = (1 - 2\eta)\Gamma V_{xx} + (1 - \eta)\frac{\Gamma}{2} - 2\eta\Gamma V_{xx}^2, \quad (8.8a)$$

$$-\dot{V}_{xp} = (1 - \eta)\Gamma V_{xp} - 2\eta\Gamma V_{xx}V_{xp}, \quad (8.8b)$$

$$-\dot{V}_{pp} = \Gamma V_{pp} + \frac{\Gamma}{2} - 2\eta\Gamma V_{xp}^2. \quad (8.8c)$$

The equation for V_{xx} is decoupled so we solve $\dot{V}_{xx} = 0$ to find

$$V_{xx}^{\text{ss}} = \frac{1 - \eta}{2\eta}, \quad (8.9)$$

which entails constant covariance, $\dot{V}_{xp} \equiv 0$, independent of its current value. Note that the \hat{x} -variance vanishes, $V_{xx}^{\text{ss}} \rightarrow 0$, as $\eta \rightarrow 1$ which shows that the corresponding effect operator measures \hat{x} with arbitrary precision. The effect operator will be squeezed in \hat{x} for any $\eta > 1/2$.

On the other hand, $V_{xx}^{\text{ss}} \rightarrow \infty$ as $\eta \rightarrow 0$ emphasizing that retrodiction crucially depends on observations. When attempting to solve $\dot{V}_{pp} = 0$ we find that there is no solution, V_{xp}^{ss} and V_{pp}^{ss} , which simultaneously satisfies $V_{pp}^{\text{ss}} \geq 0$ and $\det[V^{\text{ss}}] \geq 0$, which are necessary requirements for a proper covariance matrix. Thus V_{pp} does not have a steady state and grows beyond all bounds as time runs backwards. This is in line with the fact that our setup only gathers information about \hat{x} . Thus, retrodiction allows to effectively perform a projective measurement of a quadrature operator on the initial state of the cavity. By changing the homodyne angle analogous results can be obtained for any quadrature \hat{x}_θ . This agrees with the finding of Wiseman [84] who used an explicit operator representation to find the effect operator. It is not difficult to check¹ that the effect operator constructed in [84] indeed satisfies the equation of motion (8.6).

We can now also derive the temporal modes which have to be extracted from the photocurrent. Plugging V_{xx}^{ss} into the equation for x we find

$$\text{(BI)} \quad -dx(t) = \frac{\Gamma}{2}xdt + \sqrt{\frac{\Gamma}{2\eta}}dW(t) \quad (8.10)$$

$$= -\frac{\Gamma}{2}xdt + \sqrt{\frac{\Gamma}{2\eta}}dY(t). \quad (8.11)$$

The solution to this equation is given by

$$\text{(BI)} \quad x(t) = e^{-\Gamma(t_1-t)/2}x(t_1) + \sqrt{\frac{\Gamma}{2\eta}} \int_t^{t_1} e^{-\Gamma(t_1-\tau)/2}dY(\tau), \quad (8.12)$$

for $t \leq t_1$ so the initial value $x(t_1)$ is exponentially damped, and far into the past the mean \hat{x} -quadrature of the retrodicted effect operator will depend only on the integrated measurement current with mode function

$$f(t) = \sqrt{\frac{\Gamma}{2\eta}}e^{-\Gamma t/2}. \quad (8.13)$$

8.1.2 Beam splitter vs. squeezing interaction

We will now examine why we can prepare only a coherent state (the vacuum) but are able to measure squeezed states. This is due to the Beam Splitter (BS) coupling between the cavity and the field outside,

$$\hat{H}_{\text{int}}^{\text{BS}} = \Gamma(\hat{a}\hat{c}_{\text{out}}^\dagger + \hat{a}^\dagger\hat{c}_{\text{out}}), \quad (8.14)$$

where $\hat{c}_{\text{out}}^\dagger, \hat{c}_{\text{out}}$ are the CAOs corresponding to the outgoing mode being measured. This interaction causes a state swap between the intracavity and outside fields. To illustrate this further let us replace the BS coupling by a Two-Mode Squeezing (TMS) interaction,

$$\hat{H}_{\text{int}}^{\text{TMS}} = \Gamma(\hat{a}^\dagger\hat{c}_{\text{out}}^\dagger + \hat{a}\hat{c}_{\text{out}}). \quad (8.15)$$

¹ When computing $d\hat{E}(t)$ of the effect operator in [84] it is important to reintroduce the initial time which was set to zero there, and to take the derivative with respect to this time.

For our simple cavity this is obviously unrealistic but we will encounter the TMS interaction again in the optomechanical system of the next section, so it is worthwhile understanding the effect this has on the dynamics. The corresponding master equation reads

$$(I) \, d\rho(t) = \Gamma \mathcal{D}[\hat{a}^\dagger]\rho(t)dt + \sqrt{\eta\Gamma}\mathcal{H}[\hat{a}^\dagger]\rho(t)dW(t). \quad (8.16)$$

This yields equations of motion for the means and (co)variances of the conditional state,

$$(I) \, dx(t) = \frac{\Gamma}{2}xdt + \sqrt{\frac{\eta\Gamma}{2}}(2V_{xx}(t) + 1)dW(t), \quad (8.17)$$

$$(I) \, dp(t) = \frac{\Gamma}{2}pdt + \sqrt{\frac{\eta\Gamma}{2}}2V_{xp}(t)dW(t), \quad (8.18)$$

and

$$\dot{V}_{xx} = (1 - 2\eta)\Gamma V_{xx} + (1 - \eta)\frac{\Gamma}{2} - 2\eta\Gamma V_{xx}^2, \quad (8.19)$$

$$\dot{V}_{xp} = (1 - \eta)\Gamma V_{xp} - 2\eta\Gamma V_{xx}V_{xp}, \quad (8.20)$$

$$\dot{V}_{pp} = \Gamma V_{pp} + \frac{\Gamma}{2} - 2\eta\Gamma V_{xp}^2, \quad (8.21)$$

which are exactly the same as the backward Eqs. (8.7) and (8.8) for the BS interaction. So we know that V_{pp} will grow beyond all bounds in the long time limit, but we can condition the \hat{x} -quadrature to arbitrary precision limited only by our detection efficiency η , meaning we can prepare arbitrarily squeezed states. Similarly, the situation is reversed for the backward effect equation, which yields equations for the means and covariance matrix given by the forward equations Eqs. (8.3) and (8.4). Hence the retrodicted effect operators will become independent of the photocurrent in the long-time limit and project only on the vacuum state.

To understand this role reversal note that $\hat{H}_{\text{int}}^{\text{TMS}}$ creates entangled pairs of photons so detecting the outgoing light will reveal information about the current state of the cavity (“What *is* the state?”) while light generated by the state-swapping BS interaction contains information about the state of the oscillator before the interaction (“What *was* the state?”). The effect each coupling has on the performance of both pre- and retrodiction is summarized in the following table.

	Prediction ρ	Retrodiction \hat{E}
TMS	Squeezed	Coherent
BS	Coherent	Squeezed

8.2 CONDITIONAL STATE PREPARATION AND VERIFICATION IN OPTOMECHANICS

The illustrative examples studied in the previous sections provide the background for the application of the formalism to time-continuous measurements of optomechanical systems [49, 113]. The system of interest is

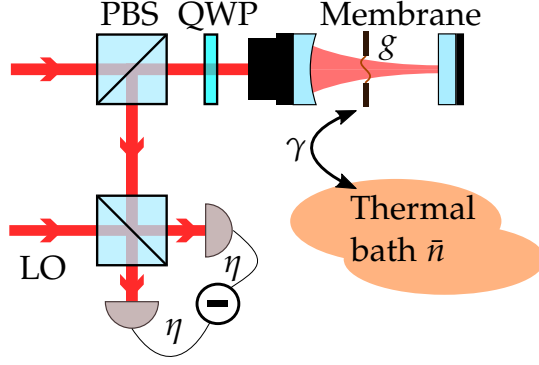


Figure 8.2: Schematic of a micromechanical membrane coupled to a driven cavity with coupling strength g . Before entering the cavity the linearly polarized driving field is transmitted through a polarizing beam splitter (PBS) and quarter-wave plate (QWP). After interaction with the cavity and membrane the outgoing light again passes the QWP, such that it becomes orthogonally polarized to the incoming light. It is reflected off the PBS and superposed on a second beam splitter with a strong local oscillator (LO) to perform homodyne or heterodyne detection with detection efficiency η . The membrane is additionally coupled to a thermal bath with rate γ and mean phonon number \bar{n} .

a single mode of a mechanical oscillator, such as a membrane depicted in Fig. 8.2, which couples to the light field inside a resonantly driven cavity. The cavity output is measured through homodyne or heterodyne detection, see App. A. We will be interested in the weak coupling limit of optomechanics, where the cavity can be adiabatically eliminated, and the time-continuous measurement effectively concerns the mechanical system only. It is important to note that this weak coupling limit does not exclude the regime of strong quantum cooperativity where the measurement back action noise process effectively becomes stronger than all other noise processes acting on the oscillator. Quantum cooperativities on the order of 100 have been demonstrated in recent optomechanical systems [14]. It is clear that the tools of quantum state pre- and retrodiction become especially powerful in such a regime.

The adiabatic limit of the conditional optomechanical master equation has been treated in great detail in [33, 34]. We summarize here the main aspects, and then apply it to discuss preparation and verification of the mechanical state.

8.2.1 Optomechanical setup

We consider a mechanical mode with frequency ω_m coupled to a cavity (ω_c), driven by a strong coherent field with frequency ω_0 . We move to a rotating frame with respect to the drive ω_0 , and assume the intra-cavity amplitude α_c is large so we can linearize the interaction [49], which yields

$$\hat{H}_{\text{lin}} = \hat{H}_0 + g(\hat{a} + \hat{a}^\dagger)(\hat{a}_c + \hat{a}_c^\dagger), \quad (8.22a)$$

$$\hat{H}_0 = \omega_m \hat{a}^\dagger \hat{a} - \Delta_c \hat{a}_c^\dagger \hat{a}_c, \quad (8.22b)$$

where \hat{H}_0 comprises the local Hamiltonians of cavity and mechanics with $\Delta_c = \omega_0 - \omega_c$, and $g \propto g_0 \alpha_c$ is the cavity-enhanced optomechanical

coupling strength. \hat{a} and \hat{a}_c are the annihilation operators of the mechanical and cavity mode, respectively.

The cavity field leaks out at a full width at half maximum (FWHM) decay rate κ . The (unconditional) master equation of the joint state ρ_{mc} of mechanical and cavity mode reads

$$\dot{\rho}_{mc}(t) = -i[\hat{H}_{lin}, \rho_{mc}(t)] + \kappa \mathcal{D}[\hat{a}_c] \rho_{mc}(t) + \mathcal{L}_{th} \rho_{mc}(t), \quad (8.23)$$

where we have also included a thermal bath,

$$\mathcal{L}_{th} \rho_{mc}(t) = \gamma(\bar{n} + 1) \mathcal{D}[\hat{a}] \rho_{mc}(t) + \gamma \bar{n} \mathcal{D}[\hat{a}^\dagger] \rho_{mc}(t), \quad (8.24)$$

with mean phonon number \bar{n} which couples to the mechanical oscillator at rate γ (FWHM of the mechanical mode).

We monitor the field that leaks from the cavity using homodyne or heterodyne detection, depicted in the bottom left of Fig. 8.2. As compared to the SME (8.1) of the decaying cavity studied in Sec. 8.1, we consider here a slightly more general setup where the local oscillator frequency ω_{lo} may be detuned from the driving frequency ω_0 , captured by $\Delta_{lo} = \omega_{lo} - \omega_0$. This realizes a measurement of the outgoing field quadrature operator $\hat{a}_{out}(t)e^{-i\Delta_{lo}t+i\theta_{lo}} + \hat{a}_{out}^\dagger(t)e^{i\Delta_{lo}t-i\theta_{lo}}$, where θ_{lo} is the tunable phase of the local oscillator. The relations between the different frequencies and detunings are visualized in Fig. 8.3. The resulting SME for cavity and mechanics reads

$$\begin{aligned} \text{(I)} \quad d\rho(t) = & -i[\hat{H}_{lin}, \rho_{mc}(t)]dt + \kappa \mathcal{D}[\hat{a}_c] \rho_{mc}(t)dt \\ & + \mathcal{L}_{th} \rho_{mc}(t)dt \\ & + \sqrt{\eta\kappa} \mathcal{H}[\hat{a}_c e^{i(\Delta_c + \Delta_{lo})t - i\theta_{lo}}] \rho_{mc}(t) dW(t), \end{aligned} \quad (8.25)$$

where $\eta \in [0, 1]$ is the detection efficiency.

We would like an effective master equation for the mechanics alone. To this end one can start from the combined master equation (8.25) and move to an interaction picture with respect to \hat{H}_0 . Assuming the cavity field decays fast on the time scale set by the optomechanical interaction, $g/\kappa \ll 1$, one can adiabatically eliminate the cavity dynamics from the description. For details of this procedure see [33, 34]. Before we state the result let us take a closer look at the optomechanical interaction.

8.2.2 Optomechanical interaction

The linearized radiation pressure interaction is given by the last term in Eq. (8.22). The interaction decomposes into two terms: (i) a Beam Splitter (BS) coupling

$$\hat{H}_{BS} = g(\hat{a}\hat{a}_c^\dagger + \hat{a}^\dagger\hat{a}_c), \quad (8.26)$$

and (ii) a Two-Mode Squeezing (TMS) interaction

$$\hat{H}_{TMS} = g(\hat{a}\hat{a}_c + \hat{a}^\dagger\hat{a}_c^\dagger), \quad (8.27)$$

which give rise to Stokes and anti-Stokes scattering processes depicted in Fig. 8.4. If we work in an interaction picture with respect to \hat{H}_0 then

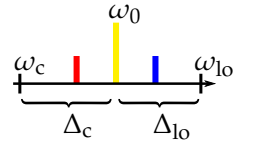


Figure 8.3: Involved frequencies and detunings, depicted for $\Delta_{c/lo} > 0$. Red/blue sidebands of the drive at $\omega_0 \pm \omega_m$.

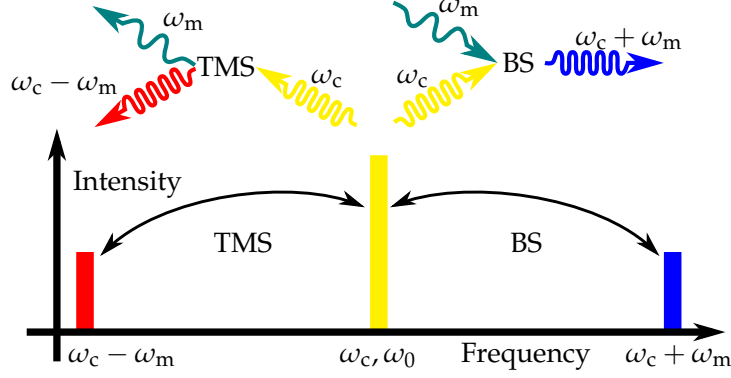


Figure 8.4: Top: schematic conversion processes occurring in the optomechanical setup depicted in Fig. 8.2, driven on resonance $\omega_0 = \omega_c$. Cavity photons at frequency ω_c are scattered into the sidebands while creating or annihilating a mechanical phonon at frequency ω_m . Bottom: the spectrum of the outgoing light (not to scale). As discussed in Sec. 8.2.2 the linearized optomechanical interaction facilitates two processes: The BS interaction converts a cavity photon into a phonon and an outgoing photon in the lower (red) sideband at $\omega_c - \omega_m$. TMS combines a cavity photon and a phonon to produce an outgoing photon in the upper (blue) sideband at $\omega_c + \omega_m$.

\hat{H}_{BS} and \hat{H}_{TMS} will oscillate at frequencies $\omega_m \pm \Delta_c$, respectively. For a *red-detuned* drive, $\Delta_c = -\omega_m$, the BS interaction becomes resonant and is thus enhanced while the TMS interaction oscillates quickly at $2\omega_m$ and is suppressed. For a *blue-detuned* drive, $\Delta_c = \omega_m$, the situation is reversed so the TMS interaction is enhanced and the BS interaction suppressed. The entangling and state-swap dynamics corresponding to resonant \hat{H}_{TMS} or \hat{H}_{BS} have been demonstrated experimentally in a circuit QED setup [114, 115]. For a resonant drive, $\Delta_c = 0$, both processes contribute equally.

As we have seen in the initial example in Sec. 8.1, the entangling TMS interaction enhances our ability to prepare a conditional mechanical state. Because the outgoing light at $\omega_0 - \omega_m$ is entangled with the mechanics, performing a quantum-limited squeezed detection on that sideband will also project the oscillator onto a squeezed state. On the other hand, the BS interaction generates light at $\omega_0 + \omega_m$ with the mechanical state swapped onto it. Observing it lets us determine what the state was before the interaction but will not enable the preparation of squeezed states. For retrodiction the situation is reversed. Extracting information about the system in the past from BS light produces squeezed effect operators (sharp measurements) on the past state, while entangled TMS light lets us retrodict coherent effect operators at best. Thus TMS (blue drive) enhances our ability to prepare while the BS interaction (red drive) enhances our ability to retrodict.

8.2.3 Mechanical master equation

In [33, 34] the master equation (8.25) is turned into an effective evolution equation for the mechanical state $\rho_m \equiv \rho$ through adiabatic elimination

of the cavity mode. Since the result is not a proper Lindblad master equation one needs to perform a rotating wave approximation for which we integrate the dynamics over a short time,

$$\delta\rho(t) := \int_t^{t+\delta t} d\rho(\tau). \quad (8.28)$$

We assume ω_m is much larger than other system frequencies set by the optomechanical interaction and decoherence, i. e., $\omega_m \gg g^2/\kappa$, $\bar{n}\gamma$. In fact, ω_m is so much larger that we can choose δt such that $\omega_m \gg 1/\delta t \gg g^2/\kappa$, $\bar{n}\gamma$, which allows us to pull $\rho(t)$ out of all deterministic time integrals since it is approximately constant on this time scale. We can then perform the rotating wave approximation by dropping all off-resonant terms oscillating at $\pm 2\omega_m$. Let us set

$$\theta_{\pm} := \arctan\left(\frac{-\Delta_c \pm \omega_m}{\kappa/2}\right). \quad (8.29)$$

In terms of these we choose the local oscillator phase and rotate to a new quadrature frame,

$$\theta_{\text{lo}} = \frac{\pi - \theta_+ - \theta_-}{2}, \quad \hat{a} \mapsto \hat{a}e^{i(\theta_+ - \theta_-)/2}, \quad (8.30)$$

to find the averaged master equation

$$\begin{aligned} \text{(I)} \quad \delta\rho(t) = & \Gamma_- \mathcal{D}[\hat{a}]\rho(t)\delta t + \Gamma_+ \mathcal{D}[\hat{a}^\dagger]\rho(t)\delta t + \mathcal{L}_{\text{th}}\rho(t)\delta t \\ & + \sqrt{\eta} \int_t^{t+\delta t} \mathcal{H} \left[\sqrt{\Gamma_-} \hat{a} e^{-i(\omega_{\text{eff}} - \Delta_{\text{lo}})\tau} \right. \\ & \left. + \sqrt{\Gamma_+} \hat{a}^\dagger e^{i(\omega_{\text{eff}} + \Delta_{\text{lo}})\tau} \right] \rho(\tau) dW(\tau). \end{aligned} \quad (8.31)$$

The effective mechanical frequency

$$\omega_{\text{eff}} := \omega_m - \sqrt{2}g^2(\beta_+ + \beta_-), \quad (8.32a)$$

$$\beta_{\pm} := \frac{\Delta_c \pm \omega_m}{(\kappa/2)^2 + (\Delta_c \pm \omega_m)^2} \quad (8.32b)$$

results from a shift of ω_m due to the optical spring effect, and the rates

$$\Gamma_{\pm} := \frac{g^2\kappa}{(\kappa/2)^2 + (-\Delta_c \pm \omega_m)^2} \quad (8.33)$$

are the usual Stokes and anti-Stokes rates known from sideband cooling. From these we can define two effective cooperativities

$$C_{\pm} := \Gamma_{\pm}/\gamma = C_{\text{cl}} \frac{\kappa^2}{\kappa^2 + 4(-\Delta_c \pm \omega_m)^2}, \quad (8.34)$$

in terms of the classical cooperativity

$$C_{\text{cl}} = \frac{4g^2}{\kappa\gamma}. \quad (8.35)$$

Each C_{\pm} compares the rate of the respective (anti-)Stokes process to the incoherent coupling rate of the thermal bath. In the bad-cavity regime²

² We assumed $\omega_m \gg g^2/\kappa$ for the rotating wave approximation which imposes $\omega_m/\kappa \gg (g/\kappa)^2$. However, we also used $g/\kappa \ll 1$ to eliminate the cavity so $(g/\kappa)^2$ is a small parameter and the derivation holds for a range of linewidths from the sideband-resolved ($\kappa \ll \omega_m$) to the bad-cavity ($\kappa \gg \omega_m$) regime.

$\kappa \gg \omega_m$ and assuming $\kappa \gg \Delta_c$ the cooperativities reduce to the classical cooperativity, $C_{\pm} \approx C_{\text{cl}}$.

To obtain a proper master equation we still need to perform the integral over the measurement term in Eq. (8.31) which depends on the choice of Δ_{lo} . But Eq. (8.31) already illustrates the point we made in Sec. 8.2.2: detuning the driving field affects the optomechanical interaction. Driving on resonance, $\Delta_c = 0$, TMS and BS interaction occur with equal strength which is reflected by $\Gamma_+ = \Gamma_-$. A blue drive, $\Delta_c = \omega_m$, enhances TMS and causes $\Gamma_+ > \Gamma_-$, while a red drive, $\Delta_c = -\omega_m$, enhances the BS interaction and causes $\Gamma_- > \Gamma_+$.

8.2.4 Steady state: resonant drive

We begin by exploring in detail the case of a resonantly driven cavity $\Delta_c = 0$, so we find $\omega_{\text{eff}} = \omega_m$, equal rates $\Gamma_+ = \Gamma_- =: \Gamma$, and equal cooperativities $C := C_+ = C_-$ with

$$C = C_{\text{cl}} \frac{\kappa^2}{\kappa^2 + 4\omega_m^2}. \quad (8.36)$$

8.2.4.1 Detect on resonance

The first detection scheme we consider is homodyne detection on resonance, $\Delta_{\text{lo}} = 0$. Plugging this into Eq. (8.31) and using again that we can pull $\rho(t)$ out of the integrals we find

$$\begin{aligned} \text{(I)} \quad \delta\rho(t) &= \mathcal{L}_{\text{th}}\rho(t) + \Gamma\mathcal{D}[\hat{a}]\rho(t)\delta t + \Gamma\mathcal{D}[\hat{a}^\dagger]\rho(t)\delta t \\ &\quad + \sqrt{\eta\Gamma}\mathcal{H}[\hat{x}]\rho(t)\delta W_c(t) + \sqrt{\eta\Gamma}\mathcal{H}[\hat{p}]\rho(t)\delta W_s(t) \end{aligned} \quad (8.37)$$

with $\hat{x} = (\hat{a} + \hat{a}^\dagger)/\sqrt{2}$ and $\hat{p} = -i(\hat{a} - \hat{a}^\dagger)/\sqrt{2}$, and the coarse-grained Wiener increments

$$\text{(I)} \quad \delta W_c(t) := \sqrt{2} \int_t^{t+\delta t} \cos(\omega_m\tau) dW(\tau), \quad (8.38a)$$

$$\text{(I)} \quad \delta W_s(t) := \sqrt{2} \int_t^{t+\delta t} \sin(\omega_m\tau) dW(\tau). \quad (8.38b)$$

With the usual Itô rules we find that these are approximately normalized, $\delta W_c^2(t) = \delta t(1 + \mathcal{O}(\omega_m\delta t)^{-1})$ and $\delta W_s^2(t) = \delta t(1 + \mathcal{O}(\omega_m\delta t)^{-1})$, and independent $\delta W_c(t)\delta W_s(t) = \delta t\mathcal{O}(\omega_m\delta t)^{-1}$. Thus we can replace $\delta t \rightarrow dt$, $\delta\rho \rightarrow d\rho$ and $\delta W_{c/s} \rightarrow dW_{c/s}$ to obtain the effective system dynamics

$$\begin{aligned} \text{(I)} \quad d\rho(t) &= \mathcal{L}_{\text{th}}\rho(t) + \Gamma\mathcal{D}[\hat{x}]\rho(t)dt + \Gamma\mathcal{D}[\hat{p}]\rho(t)dt \\ &\quad + \sqrt{\eta\Gamma}\mathcal{H}[\hat{x}]dW_c(t) + \sqrt{\eta\Gamma}\mathcal{H}[\hat{p}]dW_s(t) \end{aligned} \quad (8.39)$$

with independent Wiener increments $dW_c(t)$ and $dW_s(t)$.

Conditional state evolution

Using the notation of Sec. 7.4 we find $H = \mathbf{0}_2$, $\Delta = (\Gamma + \frac{1}{2}\gamma(2\bar{n} + 1))\mathbf{1}_2$ and $\Omega = \frac{1}{2}\gamma\sigma$, as well as the measurement matrices $A = \sqrt{\eta\Gamma}\mathbf{1}_2$, and $B = \mathbf{0}_2$. Again this system is trivially stable as long as there is some

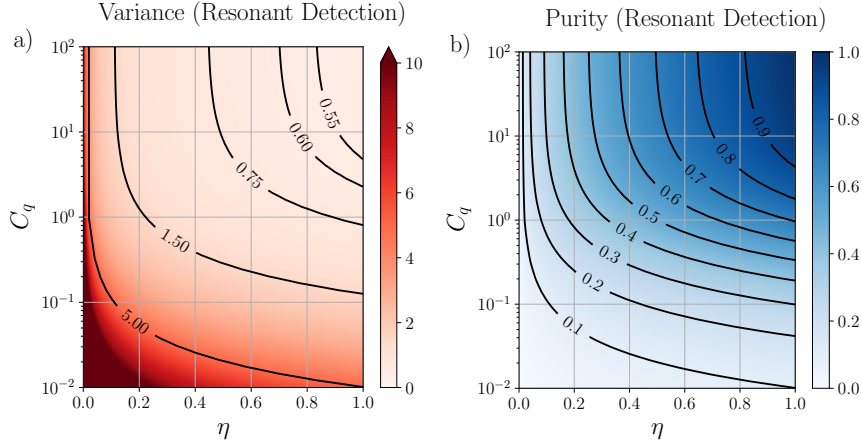


Figure 8.5: (a) Log-linear plot of the steady state variance V_{ss} from Eq. (8.40) obtained for homodyne detection on resonance, plotted against detection efficiency η and quantum cooperativity $C_q = C/(\bar{n} + 1)$. We chose a bath occupation of $\bar{n} \sim 10^5$ [14], which entails $C \sim 10^3 \dots 10^7$ in the plotted regime. The exact variance is virtually indistinguishable from its approximate value (8.45) because the difference goes as $\sim 1/C$. The plot is also indistinguishable from the exact and approximate variances \bar{V}_{ss} of the effect operator in Eqs. (8.48) and (8.49). (b) The purity of the covariance matrix corresponding to the variance in (a).

dissipation, but since $A \propto \mathbf{1}_2$ it is also stabilizable. As before we solve $\dot{V}^\rho = 0$ to obtain the steady state covariance matrix V_ρ^{ss} . To simplify the notation we will drop the superscript, and keep in mind that we always consider states (and later effect operators) in steady state. We thus find vanishing covariance $V_{xp}^\rho = 0$ and equal variances

$$V_\rho := V_{xx}^\rho = V_{pp}^\rho = \frac{1}{8\eta C} \left(\sqrt{1 + 8\eta C(2C + 2\bar{n} + 1)} - 1 \right) \quad (8.40)$$

in terms of the cooperativity (8.36). The purity is simply the inverse of the variance, $\mathcal{P}(\rho) = 1/(2V_\rho)$ so to judge the effectiveness of the preparation it suffices to consider V_ρ . Note that as $\eta \rightarrow 0$ the variance approaches the usual thermal steady state value $V_\rho \rightarrow \bar{n} + \frac{1}{2} + C$, where C is due to measurement back action noise. From the covariance matrix we can compute the enhanced drift matrix M_ρ from Eq. (7.41) which turns out to be diagonal,

$$M_\rho = \lambda_\rho \mathbf{1}_2, \quad \lambda_\rho = -\frac{\gamma}{2} \sqrt{1 + 8\eta C(2C + 2\bar{n} + 1)}. \quad (8.41)$$

The degenerate eigenvalue λ_ρ is always real, and negative as long as γ or $\eta\Gamma$ are non-zero and thus guarantees stable dynamics. We obtain the mode functions $F_\rho(t)$ from Eq. (7.46) with which dW_c and dW_s are convoluted by evaluating the kernel

$$F_\rho(t) = \begin{bmatrix} f_{xc}^\rho(t) & f_{xs}^\rho(t) \\ f_{pc}^\rho(t) & f_{ps}^\rho(t) \end{bmatrix} = e^{M_\rho t} (2V_\rho A^T - \sigma B^T). \quad (8.42)$$

We find that $f_{xs}^\rho(t) = f_{pc}^\rho(t) = 0$ and

$$f^\rho(t) := f_{xc}^\rho(t) = f_{ps}^\rho(t) = 2\sqrt{\eta\Gamma} V_\rho e^{-\lambda_\rho t}, \quad (8.43)$$

which shows that the cosine and sine components of the measurement current each only enter the corresponding (\hat{x} or \hat{p}) quadrature.

In the following we assume that $\eta C \gg 1$ and $\bar{n} \gg 1$ so $\bar{n} + 1 \approx \bar{n}$. In terms of the *quantum cooperativity* [49]

$$C_q = \frac{C}{\bar{n} + 1} \approx \frac{C}{\bar{n}} \quad (8.44)$$

the variance becomes approximately

$$V_\rho \approx \frac{1}{2} \sqrt{\frac{C_q + 1}{\eta C_q}} = \frac{1}{2\sqrt{\eta}} \sqrt{1 + \frac{1}{C_q}}, \quad (8.45)$$

plotted in Fig. 8.5 (a), and the mode function damping rate is given by

$$\lambda_\rho \approx -2\eta\Gamma \sqrt{\frac{C_q + 1}{\eta C_q}}. \quad (8.46)$$

Finding equal variances (cf. Eq. (8.40)) and vanishing covariance indicates that we prepared a thermal steady state, which approaches a pure coherent state as $\eta \rightarrow 1$ and $C_q \rightarrow \infty$ as we see from the limiting V_ρ in (8.45) and also from the purity plot in Fig. 8.5 (b). This makes sense because splitting the measurement current into cosine and sine components in Eq. (8.37) allows to measure simultaneously both mechanical quadratures, like heterodyne detection of the mechanical mode.

The exponent λ_ρ determines how fast the mode functions (8.43) decay, and thereby the “memory time” of the conditional state, i. e., how far the conditioning extends into the past. In the regime where $C_q \gg 1 \Leftrightarrow \Gamma \gg \gamma(\bar{n} + 1)$ we find $\lambda_\rho \approx -2\Gamma/\sqrt{\eta}$ so the mode function is only determined by the measurement rate. As Γ approaches the time scale of the evolution the mode function becomes more concentrated at t , so the state follows the measurement almost in real time. However, Γ cannot get too close to ω_m without violating our coarse-graining assumption. In the opposite regime of $C_q \ll 1 \Leftrightarrow \Gamma \ll \gamma(\bar{n} + 1)$ the exponent is given by $\lambda_\rho \approx -2\sqrt{\Gamma\gamma(\bar{n} + 1)}/2$. As $\Gamma \rightarrow 0$ the mode function becomes essentially flat and also goes to zero itself. In this limit, the detection will yield mostly noise and only little signal, so the evolution becomes effectively unconditional.

Retrodiction of effect operators

We obtain the backward steady state by solving the Riccati equation corresponding to Eq. (7.54). Again this yields a vanishing covariance, $V_{xp}^E = 0$, and equal variances

$$V_E := V_{xx}^E = V_{pp}^E \quad (8.47)$$

$$= \frac{1}{8\eta C} \left(\sqrt{1 + 8\eta C(2C + 2\bar{n} + 1)} + 1 \right) \quad (8.48)$$

$$\approx \frac{1}{2} \sqrt{\frac{C_q + 1}{\eta C_q}}, \quad (8.49)$$

so we find effect operators with equal variance, which corresponds to a POVM realizing a heterodyne measurement.

The backward variance is greater than the forward variance, $V_E - V_\rho = 1/(4\eta C)$. The difference vanishes as $C \rightarrow \infty$ so the limits (8.45) and (8.49) are the same, and the plot in Fig. 8.5 (a) also holds for V_E . As expected, the exact V_E in Eq. (8.48) diverges without observations: $V_E \sim 1/(4\eta C)$ as $\eta \rightarrow 0$. Otherwise the forward and backward dynamics are very similar: we find the same drift matrix as in (8.41) with a degenerate negative eigenvalue $\lambda_E = \lambda_\rho$, and the mode function takes the same form as before,

$$f_E(t) = 2\sqrt{\eta\Gamma}V_E e^{-\lambda_E t}, \quad (8.50)$$

with the increased variance V_E placing greater weight on the photocurrent compared to the forward mode, and pointing to the future instead of the past. Assuming $C, \bar{n} \gg 1$, forward and backward mode functions become identical.

For both preparation and retrodiction we see that we can never measure or prepare states with sub-shot noise resolution. In fact, in the ideal limit of perfect detection, $\eta \rightarrow 1$, and large cooperativity, $C_q \rightarrow \infty$, both V_ρ and V_E approach $1/2$ so we can at best measure and prepare coherent states. This symmetry is not surprising since detecting on resonance means both TMS and BS interaction contribute equally to the observed light. The situation is different when the local oscillator is resonant with either of the sidebands.

8.2.4.2 Detecting the sidebands

We now detune the local oscillator with respect to the driving laser, $\Delta_{\text{lo}} = \pm\omega_m$, to resolve the information contained in the sidebands located at $\omega_c \pm \omega_m$. Recalling the general coarse-grained SME (8.31), we see that detecting the blue sideband, $\Delta_{\text{lo}} = \omega_m$, makes the measurement operator \hat{a} resonant while \hat{a}^\dagger now oscillates at $2\omega_m$ (and vice versa on the red sideband). Thus we expect to better resolve the effect of the BS interaction on the blue sideband, and of the TMS interaction on the red sideband.

To evaluate the integrals in the SME (8.31) we introduce

$$(I) \delta W_0(t) := \int_t^{t+\delta t} dW(\tau), \quad (8.51a)$$

$$(I) \delta W_{c,2}(t) := \sqrt{2} \int_t^{t+\delta t} \cos(2\omega_m \tau) dW(\tau), \quad (8.51b)$$

$$(I) \delta W_{s,2}(t) := \sqrt{2} \int_t^{t+\delta t} \sin(2\omega_m \tau) dW(\tau), \quad (8.51c)$$

analogous to Eqs. (8.38), which separate the photocurrent oscillating at twice the mechanical frequency from its DC component (at the given sideband frequency). As before these are approximately normalized and independent of one another (up to $\mathcal{O}(\omega_m \delta t)^{-1}$) so we treat them as independent Wiener increments. Making the replacements $\delta t \rightarrow dt$ and

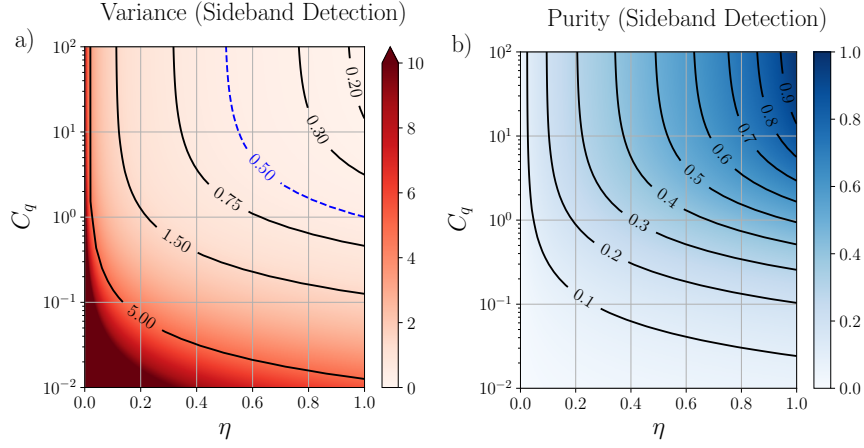


Figure 8.6: (a) Linear-logarithmic plot of the approximate steady state variances V_{xx}^p and V_{xx}^E from Eqs. (8.54a) and (8.58c), plotted against detection efficiency η and quantum cooperativity C_q in the limit of large cooperativity $C \gg 1$. The dashed line denotes the shot noise-limited variance of the vacuum state at $V_{xx} = 1/2$. (b) The purity of the covariance matrices corresponding to the variances in Eqs. (8.54a-b) and (8.58c-d). Squeezing occurs for purities of about $\mathcal{P}(\rho) \gtrsim 1/2$.

$\delta W_\alpha \rightarrow dW_\alpha$ we obtain two coarse-grained master equations depending on the choice of Δ_{l_0} . Detecting the red sideband, $\Delta_{l_0} = -\omega_m$, yields

$$\begin{aligned}
 \text{(I)} \quad d\rho(t) = & \mathcal{L}_{\text{th}}\rho(t) + \Gamma\mathcal{D}[\hat{a}^\dagger]\rho(t)dt + \Gamma\mathcal{D}[\hat{a}]\rho(t)dt \\
 & + \sqrt{\eta\Gamma}\mathcal{H}[\hat{a}^\dagger]\rho(t)dW_0(t) \\
 & + \sqrt{\frac{\eta\Gamma}{2}}\mathcal{H}[\hat{a}]\rho(t)dW_{c,2}(t) + \sqrt{\frac{\eta\Gamma}{2}}\mathcal{H}[-i\hat{a}]\rho(t)dW_{s,2}(t),
 \end{aligned} \tag{8.52}$$

while detecting the blue sideband, $\Delta_{l_0} = +\omega_m$, results in

$$\begin{aligned}
 \text{(I)} \quad d\rho(t) = & \mathcal{L}_{\text{th}}\rho(t) + \Gamma\mathcal{D}[\hat{a}^\dagger]\rho(t)dt + \Gamma\mathcal{D}[\hat{a}]\rho(t)dt \\
 & + \sqrt{\eta\Gamma}\mathcal{H}[\hat{a}]\rho(t)dW_0(t) \\
 & + \sqrt{\frac{\eta\Gamma}{2}}\mathcal{H}[\hat{a}^\dagger]\rho(t)dW_{c,2}(t) + \sqrt{\frac{\eta\Gamma}{2}}\mathcal{H}[i\hat{a}^\dagger]\rho(t)dW_{s,2}(t).
 \end{aligned} \tag{8.53}$$

A more detailed analysis of the Gaussian dynamics resulting from these equation can be found in App. C. Below we will only state the results.

Detecting the red sideband

We first consider the local oscillator tuned to the red sideband, $\Delta_{\text{lo}} = -\omega_m$. Analogously to the case of resonant detection we can use the Gaussian formalism to compute the conditional steady state variances,

$$V_{xx}^{\rho} \approx \frac{1}{3} \sqrt{\frac{(3-2\eta)C_q + 3}{\eta C_q}} - \frac{1}{6}, \quad (8.54a)$$

$$V_{pp}^{\rho} \approx \sqrt{\frac{C_q + 1}{\eta C_q}} + \frac{1}{2}, \quad (8.54b)$$

$$V_{xx}^E \approx \frac{1}{3} \sqrt{\frac{(3-2\eta)C_q + 3}{\eta C_q}} + \frac{1}{6}, \quad (8.54c)$$

$$V_{pp}^E \approx \frac{1}{2} \sqrt{\frac{C_q + 1}{\eta C_q}} - \frac{1}{2}. \quad (8.54d)$$

Considering the ideal limit $\eta \rightarrow 1$ and $C_q \rightarrow \infty$ we find

$$V_{xx}^E \rightarrow \frac{1}{2}, \quad V_{pp}^E \rightarrow \frac{1}{2} \quad (8.55)$$

for the effect operator, so at best we retrodict POVMs that project onto coherent states. On the other hand, we find

$$V_{xx}^{\rho} \rightarrow \frac{1}{6}, \quad V_{pp}^{\rho} \rightarrow \frac{3}{2} \quad (8.56)$$

for the conditional steady state, showing that we can in principle prepare squeezed states. Necessary conditions for going below shot noise are $C_q > 1$ and $\eta > 1/2$ since

$$V_{xx}^{\rho} < \frac{1}{2} \Leftrightarrow \eta > \frac{C + \bar{n}}{2C} \approx \frac{1}{2} \left(1 + \frac{1}{C_q} \right), \quad (8.57)$$

which is confirmed by the plot of V_{xx}^{ρ} in Fig. 8.6 (a). Even for $\eta = 1$ and with one quadrature below shot noise the conditional state will be mixed as seen in Fig. 8.6 (b), and only asymptotically become pure as $C_q \rightarrow \infty$.

Detecting the blue sideband

Tuning the local oscillator to the blue sideband, for $\Delta_{\text{lo}} = +\omega_m$, we find

$$V_{xx}^{\rho} \approx \frac{1}{3} \sqrt{\frac{(3-2\eta)C_q + 3}{\eta C_q}} + \frac{1}{6}, \quad (8.58a)$$

$$V_{pp}^{\rho} \approx \sqrt{\frac{C_q + 1}{\eta C_q}} - \frac{1}{2}, \quad (8.58b)$$

$$V_{xx}^E \approx \frac{1}{3} \sqrt{\frac{(3-2\eta)C_q + 3}{\eta C_q}} - \frac{1}{6}, \quad (8.58c)$$

$$V_{pp}^E \approx \sqrt{\frac{C_q + 1}{\eta C_q}} + \frac{1}{2}, \quad (8.58d)$$

so the situation is exactly reversed: in the limit $\eta \rightarrow 1$ and $C_q \rightarrow \infty$ the effect operators can in principle project onto squeezed states,

$$V_{xx}^E \rightarrow \frac{1}{6}, \quad V_{pp}^E \rightarrow \frac{3}{2}, \quad (8.59)$$

while the prepared conditional states are at best coherent,

$$V_{xx}^\rho \rightarrow \frac{1}{2}, \quad V_{pp}^\rho \rightarrow \frac{1}{2}. \quad (8.60)$$

Retrodictive squeezing in this regime again requires $C_q > 1$ and $\eta > 1/2$ because

$$V_{xx}^E < \frac{1}{2} \Leftrightarrow \eta > \frac{C + \bar{n} + 1}{2C} = \frac{1}{2} \left(1 + \frac{1}{C_q} \right). \quad (8.61)$$

Since both the limiting \hat{x} -variances (8.54a) and (8.58c) and corresponding \hat{p} -variances agree, the plots in Fig. 8.6 also hold for the effect operators retrodicted by observing the blue sideband.

These results are summarized in Tab. 8.1, which confirms the simple considerations from Sec. 8.2.2. We showed that in the regime $C_q > 1$ it is possible to prepare conditional states and retrodict effect operators with sub-shot noise variance by monitoring the sidebands of the cavity drive.

	Detuning	Sideband	Preparation ρ	Retrodiction \hat{E}
TMS	Blue, $\Delta_c = \omega_m$	Red, $\Delta_{lo} = -\omega_m$	Squeezed	Coherent
BS	Red, $\Delta_c = -\omega_m$	Blue, $\Delta_{lo} = \omega_m$	Coherent	Squeezed

Table 8.1: For a given interaction this table shows the optimal detuning of the cavity drive to enhance it, the optimal sideband to detect its effects, and the ideal outcome of conditional preparation and retrodiction. Note that a detuned drive ($\Delta_c \neq 0$) is beneficial but not necessary to obtain squeezed states and effect operators. Detecting sidebands ($\Delta_{lo} = \pm\omega_m$), on the other hand, *is* necessary.

8.2.5 Steady state: detuned drive

Very relevant in experiments is also the case of a detuned drive, $\Delta_c \neq 0$. In particular to perform sideband cooling and to stabilize the dynamics, but also to prepare squeezed mechanical states [33, 34]. In the same way, non-zero detuning also allows for much richer retrodictive dynamics since it enables the selective enhancement of the BS and TMS interaction as is apparent from the master equation (8.31). In App. C we provide analytical results for the steady state variances and mode functions for arbitrary detuning of the drive, and for resonant and sideband detection. As expected we find that the conditional state and retrodicted effect operator are further squeezed if an appropriate detuning (and detection) is chosen, see Tab. 8.1 for an overview.

The benefits of adding detuning are of course limited. To see this recall the cooperativities introduced in Sec. 8.2.3,

$$C_{\pm} = C_{\text{cl}} \frac{\kappa^2}{\kappa^2 + 4(-\Delta_c \pm \omega_m)^2} \leq C_{\text{cl}} = \frac{4g^2}{\kappa\gamma}, \quad (8.62)$$

which are related to the rates of the TMS and BS interaction. First we note that a fundamental limit of both cooperativities is set by the classical cooperativity C_{cl} , which we cannot overcome with a detuned drive. We also see that in the bad-cavity regime (e.g., [14]) the Lorentzian goes to unity, so a detuning of the drive will have no (beneficial) effect on the dynamics. On the other hand, if we consider the sideband-resolved regime (e.g., realized in [116]), where $\omega_m \gg \kappa$, we see that the difference between C_+ and C_- can become appreciable, $C_+ \ll C_-$ (or vice versa, depending on the detuning). This can indeed be used for an enhancement of the steady state squeezing of both preparation and retrodiction.

8.2.6 Conclusion and generalization

We applied the formalism developed in Chap. 7 to an optomechanical system in the weak-coupling limit. We were able to show that in the regime of large cooperativity, $C_q > 1$, and sufficiently high detection efficiency it is possible to prepare conditional states and retrodict effect operators ideally with arbitrary precision by continuously observing the sidebands of a properly detuned drive. While optomechanical systems [14, 90] are ideal for retrodiction because they facilitate large cooperativities, the formalism can in principle be applied to any continuously measured system.

We can now imagine the following experimental situation to prepare and measure conditional squeezed states. First the system is driven with a blue-detuned laser $\Delta_c = \omega_m$ to enhance the TMS interaction and aid preparation. To prepare a conditional squeezed state we need to observe the red sideband of the laser, $\Delta_{\text{lo}} = -\omega_m$, which for a blue drive is the cavity resonance. After the preparation is complete, the drive is red-detuned, $\Delta_c = -\omega_m$, to enhance BS coupling. To retrodict a squeezed effect operator we need to observe the blue sideband (of the drive), which again happens to be the cavity resonance.

Although we assume that the system is linear and stable resulting in Gaussian steady states and effect operators, we can use the scheme also for the verification of non-steady and thus non-Gaussian states. For example, one could prepare a mechanical oscillator in its ground state through sideband or feedback cooling [33, 117–119], then coherently add excitations to prepare a Fock state (or other non-Gaussian state), and afterwards perform time-continuous homodyne detection to realize a quadrature measurement on that state through retrodiction. Creation of a Fock state could be achieved, e.g., conditionally by photon-counting as shown in [120], or deterministically as suggested in [121]. Repetition of the retrodictive POVM measurement on identically prepared initial states enables reconstruction of the marginals. By changing the measured quadrature one can reconstruct the full Wigner function of the state [122]. Of course this requires a POVM with sufficient resolution

which crucially depends on large quantum cooperativity and high detection efficiency.

CONCLUSION AND OUTLOOK

The goal of this thesis was to explore possible approaches to use continuous measurements for the preparation and verification of nontrivial quantum states.

In the first part I consider a simple interferometric feedback scheme that generates an effective many-body interaction with collective dissipation between N local quantum systems. By generalizing a known feedback protocol to multiple systems in Chap. 4 I was able to show that the scheme can deterministically generate many-body entangled states. Since all feedback is local, and the scheme only requires coherent transmission and interferometry of light, it may allow for scalable, robust, and long-range generation of entangled states of matter. These are a necessity for many quantum information and communication protocols, and also for building a “quantum internet” [123, 124]. In Chap. 5 I employed the setup to generate an effective Ising Hamiltonian between an array of non-interacting qubits. I found that it is indeed possible to simulate an Ising interaction with arbitrary range and geometry, and inherent collective dissipation. Doing so showed that the large number of parameters of the model allow to easily tweak the dynamics, but also make it difficult to fully gauge the full scope of the Feedback Master Equation (FME). For example, a lot of the parameters are redundant, which could be avoided by finding a good parametrization. Another open problem is to identify the complete class of Liouvillians and corresponding steady states that are attainable by the setup, which would be beneficial to determine the limits of both preparation and simulation.

In the second part I investigated the question of how continuous measurements of a system can be used to infer information about its past state. In Chap. 6 I showed how to interpret a record of continuous measurements of a system as an instantaneous Positive-Operator Valued Measure (POVM) measurement on its initial state using retrodiction. In Sec. 8.2 I apply retrodiction to an optomechanical system in the weak-coupling limit. Here I was able to show that with large cooperativity, $C_q > 1$, and efficient detection it is possible to retrodict effect operators with sub-shot noise precision, just like it is possible to prepare conditional squeezed states. This makes it possible to use continuous measurements for state tomography in the usual way [125, 126] to verify the prepared state. While optomechanical systems facilitate large cooperativities [14, 90], and are thus ideal for retrodiction, the formalism can in principle be applied to any other continuously measured system. In Sec. 7.5.1 I was able to show that a stable linear system will make any initial state collapse to a Gaussian steady state, and that an analogous result holds for effect operators. However, although I considered only such stable systems retrodiction can also be used for the verification of non-steady and thus non-Gaussian states, as I discussed in Sec. 8.2.6.

I hope these results demonstrate that continuous measurements in conjunction with local feedback indeed constitute a powerful tool for the preparation and verification of quantum states.

Part III

APPENDIX

HOMODYNE DETECTION

Homodyne detection is a way to extract phase information from an optical signal. Since it plays an essential role in all schemes presented in this thesis let us recapitulate how it works.

A.1 INTENSITY VS. QUADRATURE MEASUREMENT

Consider an optical field with time-dependent Creation and Annihilation Operators (CAOs) $\hat{a}^\dagger(t), \hat{a}(t)$ as defined in Eq. (3.3). The field can be directly measured using photodetectors that convert incoming photons into free electrons through the photoelectric effect [127]. By applying a voltage these electrons generate a current $I(t)$ which is (ideally) proportional to the intensity of the incoming light, $I(t) \propto \langle \hat{a}^\dagger(t)\hat{a}(t) \rangle$, i. e., the number of incoming photons per unit time¹². The expectation value $\langle \hat{A} \rangle = \text{Tr}\{\hat{A}\rho(t)\}$ is always taken with respect to the state of the field. This gives us the modulus of the amplitude of the electric field as square root of the intensity, but no information about its phase.

¹² Note that $\hat{a}(t)$ has dimension $s^{-1/2}$.

Homodyne detection instead yields expectation values of quadrature operators of light [128], i. e., $\langle \hat{x}_\theta \rangle$ with $\hat{x}_\theta \propto \hat{a}e^{-i\theta} + \hat{a}^\dagger e^{i\theta}$. The goal of homodyning is to convert phase fluctuations into intensity fluctuations, which can be detected using regular photodetectors. This is done by superposing the incoming light (in the following referred to as *signal*) with a strong coherent field of the same frequency (the *local oscillator*) on a BS. The intensity of the superposed field then depends on (phase-dependent) interference between signal and local oscillator. Depending on the transmittivity τ of the BS one can distinguish between *balanced* ($|\tau|^2 = 1/2$) and *imbalanced* ($|\tau|^2 \lesssim 1$) homodyne detection. The former requires only one photodetector while the latter requires two, but balanced homodyne detection is more robust to technical noise such as intensity fluctuations of the laser [2]. In the following we consider in

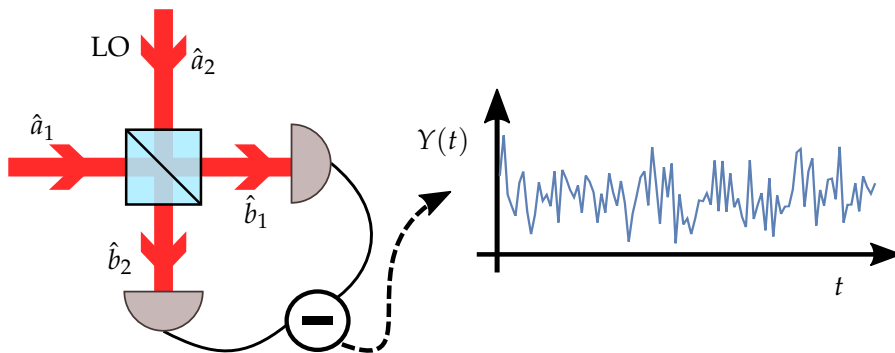


Figure A.1: A homodyne detector. The signal, \hat{a}_1 , is combined with a local oscillator, \hat{a}_2 , on a balanced Beam Splitter (BS). The intensity of both outputs is measured, and the difference yields the homodyne signal.

detail only balanced homodyne [7, 128]. A typical setup is depicted in Fig. A.1 where \hat{a}_1 belongs to the signal mode and \hat{a}_2 to the local oscillator.

A.2 BEAM SPLITTER

To better understand homodyne detection we recall the workings of a Beam Splitter (BS). It is a passive linear optical element so its outputs are linear superpositions of its inputs [128]. If two input modes come with CAOs $\hat{a}_1^\dagger, \hat{a}_1$ and $\hat{a}_2^\dagger, \hat{a}_2$ then its output modes will satisfy $\hat{b}_1 = \tau\hat{a}_1 + r\hat{a}_2$ and $\hat{b}_2 = r\hat{a}_1 + \tau\hat{a}_2$, where $\tau = |\tau|e^{i\theta_\tau}$ is the transmittivity and $r = |r|e^{i\theta_r}$ is the reflectivity. We assume ideal optics without dissipation or scattering so energy is conserved. This requires $\hat{a}_1^\dagger\hat{a}_1 + \hat{a}_2^\dagger\hat{a}_2 = \hat{b}_1^\dagger\hat{b}_1 + \hat{b}_2^\dagger\hat{b}_2$, which yields the conditions $|\tau|^2 + |r|^2 = 1$ and $\tau r^* + \tau^* r = 0$.

For balanced homodyne detection we assume $|\tau| = |r| = 1/\sqrt{2}$ and $\Delta_\theta := \theta_r - \theta_\tau = \pi/2$. The photodetectors measuring the outputs produce

$$I_1(t) = \langle \hat{b}_1^\dagger(t)\hat{b}_1(t) \rangle \quad (\text{A.1})$$

$$= \langle |\tau|^2 \hat{a}_1^\dagger(t)\hat{a}_1(t) + |r|^2 \hat{a}_2^\dagger(t)\hat{a}_2(t) \rangle \quad (\text{A.2})$$

$$+ \langle \tau^* r \hat{a}_1^\dagger(t)\hat{a}_2(t) + \tau r^* \hat{a}_2^\dagger(t)\hat{a}_1(t) \rangle$$

$$= \frac{1}{2} \langle \hat{a}_1^\dagger(t)\hat{a}_1(t) + \hat{a}_2^\dagger(t)\hat{a}_2(t) \rangle \quad (\text{A.3})$$

$$+ \frac{i}{2} \langle \hat{a}_1^\dagger(t)\hat{a}_2(t) - \hat{a}_2^\dagger(t)\hat{a}_1(t) \rangle$$

and analogously

$$I_2(t) = \frac{1}{2} \langle \hat{a}_1^\dagger(t)\hat{a}_1(t) + \hat{a}_2^\dagger(t)\hat{a}_2(t) \rangle \quad (\text{A.4})$$

$$- \frac{i}{2} \langle \hat{a}_1^\dagger(t)\hat{a}_2(t) - \hat{a}_2^\dagger(t)\hat{a}_1(t) \rangle.$$

Subtracting I_2 from I_1 removes the individual intensities and yields

$$Y(t) := I_1(t) - I_2(t) = -i \langle \hat{a}_1^\dagger(t)\hat{a}_2(t) - \hat{a}_2^\dagger(t)\hat{a}_1(t) \rangle. \quad (\text{A.5})$$

We consider the case where the local oscillator is in a coherent state with amplitude $\alpha = |\alpha|e^{i\theta}$, which is an eigenstate of \hat{a}_2 with $\hat{a}_2|\alpha\rangle_2 = \alpha|\alpha\rangle_2$, and θ is called *homodyne angle*. Assuming the signal mode is in some state ρ_1 we find the *measurement* or *homodyne current*

$$Y(t) = -i \text{Tr} \left\{ \left(\hat{a}_1^\dagger(t)\hat{a}_2(t) - \hat{a}_2^\dagger(t)\hat{a}_1(t) \right) \rho_1(t) \otimes |\alpha\rangle\langle\alpha|_2 \right\} \quad (\text{A.6})$$

$$= -i |\alpha| \text{Tr} \left\{ \left(e^{i\theta} \hat{a}_1^\dagger(t) - e^{-i\theta} \hat{a}_1(t) \right) \rho_1(t) \right\} \quad (\text{A.7})$$

$$= \sqrt{2} |\alpha| \langle \hat{x}_\theta^1(t) \rangle, \quad (\text{A.8})$$

where the quadrature operator

$$\hat{x}_\theta^1(t) := \frac{1}{\sqrt{2}} \left(e^{i(\theta-\pi/2)} \hat{a}_1^\dagger(t) + e^{-i(\theta-\pi/2)} \hat{a}_1(t) \right) \quad (\text{A.9})$$

is defined with respect to the phase of the local oscillator, and both $\hat{x}_\theta^1(t)$ and the expectation value act only on the signal.

Heterodyne detection

If the homodyne angle varies periodically with time, i. e., if the local oscillator is *detuned* in frequency from the signal, and if this happens at a rate much faster than set by the measurement time, it is possible to measure two conjugate quadratures simultaneously with reduced certainty of each. This is known as *heterodyne detection* [2].

Normalization of the measurement current

The homodyne measurement yields a signal $I(t) \propto I_1(t) - I_2(t)$ proportional to the difference of the photodetector outputs. This has to be normalized $Y(t) = I(t)/\alpha$ so that for vacuum input its increment $\delta Y(t) = Y(t + \delta t) - Y(t)$ yields the variance of white noise,

$$\delta t \stackrel{!}{=} \overline{\delta Y(t)^2} = \overline{\delta I(t)^2} / \alpha^2 \quad \Rightarrow \quad \alpha = \sqrt{\overline{\delta I(t)^2} / \delta t}. \quad (\text{A.10})$$

The bar denotes an ensemble average. The short time δt must be large enough to justify assuming the noise is white so it should be larger than physical correlation times of the input. In practice it is bounded from below by the temporal resolution of the detectors.

A.3 DETECTION EFFICIENCY

In reality not all signal photons lead to the emission of a photoelectron. This is quantified by the detection efficiency $\eta \in [0, 1]$, which gives the ratio of signal photons that contribute to the photocurrent compared to all signal photons. Focusing only on the detector the main factors that decrease η are (i) reflection at the surface of the detector, (ii) recombination of photoelectron-hole pairs, and (iii) absorption in the bulk instead of the active region of the detector, which also depends on the wavelength of the incoming light [127]. The efficiency is further decreased by unavoidable electronic and optical losses, as well as by “dead time” of the detector which masks subsequent absorption events. Instead of worrying about so many technical intricacies it has proven useful to assume ideal lossless detectors, and to model all efficiency-reducing effects by a single optical loss channel that degrades the signal *before* the measurement in Fig. A.1. This is done by assuming a virtual BS of transmittivity η that scatters a portion of the light out of the signal mode and replaces it with quantum vacuum. This is depicted in Fig. A.2

We assume the incoming signal is in state $\rho_{\text{sig}}(t)$ with corresponding annihilation operator \hat{a}_{sig} . When it traverses the BS in Fig. A.2 these become $\rho_1(t) = \rho_{\text{sig}}(t) \otimes |0\rangle\langle 0|_{\text{vac}}$ and $\hat{a}_1 = \sqrt{\eta}\hat{a}_{\text{sig}} + \sqrt{1-\eta}\hat{a}_{\text{vac}}$, where \hat{a}_{vac} belongs to the incoming vacuum. Plugging these expressions into (A.7) leads to the lossy homodyne current

$$Y(t) = |\alpha| \sqrt{\eta} \text{Tr}\{\rho_{\text{sig}}(t) \hat{x}_\theta(t)\} \quad (\text{A.11})$$

$$= |\alpha| \sqrt{\eta} \langle \hat{x}_\theta^{\text{sig}}(t) \rangle, \quad (\text{A.12})$$

where the quadrature operator

$$\hat{x}_\theta^{\text{sig}}(t) := \frac{1}{\sqrt{2}} \left(e^{i(\theta-\pi/2)} \hat{a}_{\text{sig}}^\dagger(t) + e^{-i(\theta-\pi/2)} \hat{a}_{\text{sig}}(t) \right) \quad (\text{A.13})$$

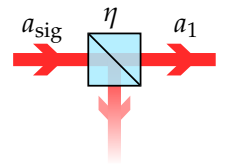


Figure A.2: Simple photon loss model.

is defined with respect to the local oscillator, and both $\hat{x}_\theta^{\text{sig}}(t)$ and the expectation value now only refer to the signal mode.

CUMULANT EQUATIONS OF MOTION

We will now derive the cumulant equations of motion for the quantum state of an arbitrary linear system as described in Chap. 7. We write N^{th} -order cumulants, i. e., of products of N canonical operators, as

$$V_{m_1, \dots, m_N}^{(N)} := \langle \hat{r}_{m_1} \dots \hat{r}_{m_N} \rangle_{\rho}^c \quad (\text{B.1})$$

where the superscript c stands for cumulant, and the indices $1 \leq m_k \leq 2M$ indicate that operator \hat{r}_{m_k} is at position k in the cumulant. We consider only symmetrically ordered cumulants, so the operator position does not matter, and the V are symmetric under permutations of indices. These general cumulants relate to the means and covariance matrix from the main text as

$$r_j = \langle \hat{r}_j \rangle_{\rho} = V_j^{(1)}, \quad (\text{B.2})$$

$$V_{jk} = \frac{1}{2} \langle \{ \hat{r}_j - r_j, \hat{r}_k - r_k \} \rangle_{\rho} = V_{jk}^{(2)}. \quad (\text{B.3})$$

If one is only interested in Gaussian states all cumulants of order $N \geq 3$ vanish identically. But for any non-Gaussian state *all* cumulants have to be taken into account [101].

Cumulants are obtained from the quantum characteristic function $\chi(\xi)$ with phase space variables $\xi \in \mathbb{R}^{2M}$, introduced in Sec. 7.2. This is defined as the expectation value of the symmetric Weyl operator $\mathcal{W}(\xi) = \exp(-i\xi^T \sigma \hat{r})$ [98–100],

$$\chi(\xi) := \langle \mathcal{W}(\xi) \rangle_{\rho} = \text{Tr}\{\mathcal{W}(\xi)\rho\}, \quad (\text{B.4})$$

where σ comprises the canonical commutation relations (7.1). Let us introduce the twisted derivative

$$\tilde{\partial}_j := \sum_{k=1}^{2M} \sigma_{jk} \frac{\partial}{\partial \xi_k}, \quad \tilde{\nabla} := \sigma \nabla, \quad (\text{B.5})$$

then χ serves as cumulant-generating function via

$$V_{m_1, \dots, m_N}^{(N)} = (-i\tilde{\partial}_{m_1}) \dots (-i\tilde{\partial}_{m_N}) \ln[\chi(\xi)]|_{\xi=0} \quad (\text{B.6a})$$

$$= (-i\tilde{\partial}_{m_1}) \dots (-i\tilde{\partial}_{m_N}) G(\xi)|_{\xi=0}, \quad (\text{B.6b})$$

with $G := \ln[\chi]$ or $\chi = \exp(G)$. The usual approach [95, Appendix 12] is to translate the master (or effect) equation into partial differential equations for the cumulants via (B.6).

B.1 FROM OPERATOR TO PARTIAL DIFFERENTIAL EQUATION

To find the correspondence between quantum and partial differential operators, consider the action of $\tilde{\nabla}$ on the Weyl operator. We single out one ξ_i ,

$$-i\xi_i^T \sigma \hat{r} = -i\tilde{\xi}_i \sum_k \sigma_{ik} \hat{r}_k - i \sum_{\substack{j,k \\ j \neq i}} \tilde{\xi}_j \sigma_{jk} \hat{r}_k =: \hat{A}_i + \hat{B}_{\neq i} \quad (\text{B.7})$$

so we can write

$$\mathcal{W}(\xi) := \exp(\hat{A}_i + \hat{B}_{\neq i}) \quad (\text{B.8})$$

$$= \exp(\hat{A}_i) \exp(\hat{B}_{\neq i}) \exp\left(-\frac{1}{2}[\hat{A}_i, \hat{B}_{\neq i}]\right) \quad (\text{B.9})$$

$$= \exp(\hat{B}_{\neq i}) \exp(\hat{A}_i) \exp\left(+\frac{1}{2}[\hat{A}_i, \hat{B}_{\neq i}]\right). \quad (\text{B.10})$$

We find

$$[\hat{A}_i, \hat{B}_{\neq i}] = -i\tilde{\zeta}_i \sum_{\substack{k \\ k \neq i}} \sigma_{ik} \tilde{\zeta}_k = -i\tilde{\zeta}_i (\sigma \tilde{\zeta})_i, \quad (\text{B.11})$$

where we used that σ is skew-symmetric and thus zero on the diagonal. Using this result to apply $\tilde{\nabla}$ to \mathcal{W} yields

$$-i\sigma \tilde{\nabla} \mathcal{W}(\xi) = \left(\hat{r} - \frac{1}{2}\xi\right) \mathcal{W}(\xi) = \mathcal{W}(\xi) \left(\hat{r} + \frac{1}{2}\xi\right), \quad (\text{B.12})$$

This gives us the important relations

$$\hat{r} \mathcal{W}(\xi) = \left(-i\sigma \tilde{\nabla} + \frac{1}{2}\xi\right) \mathcal{W}(\xi), \quad (\text{B.13a})$$

$$\mathcal{W}(\xi) \hat{r} = \left(-i\sigma \tilde{\nabla} - \frac{1}{2}\xi\right) \mathcal{W}(\xi), \quad (\text{B.13b})$$

from which we read off the replacement rules

$$\rho \hat{r} \rightarrow \left(-i\tilde{\nabla} + \frac{1}{2}\xi\right) \chi(\xi), \quad (\text{B.14a})$$

$$\hat{r} \rho \rightarrow \left(-i\tilde{\nabla} - \frac{1}{2}\xi\right) \chi(\xi). \quad (\text{B.14b})$$

The following combinations frequently appear in master equations

$$[\hat{r}, \rho] \rightarrow -\xi \chi(\xi), \quad [\hat{r}^\text{T}, \rho] \rightarrow -\xi^\text{T} \chi(\xi), \quad (\text{B.15})$$

$$\{\hat{r}, \rho\} \rightarrow -2i\tilde{\nabla} \chi(\xi), \quad \{\hat{r}^\text{T}, \rho\} \rightarrow -2i\tilde{\nabla}^\text{T} \chi(\xi). \quad (\text{B.16})$$

B.2 HAMILTONIAN

For a Hamiltonian with quadratic and linear terms,

$$\hat{H} = \frac{1}{2} \hat{r}^\text{T} H \hat{r} + \mathbf{h}^\text{T} \hat{r} \quad (\text{B.17})$$

with symmetric $H \in \mathbb{R}^{2M \times 2M}$ and $\mathbf{h} \in \mathbb{R}^{2M}$ we find

$$-i[\hat{H}, \rho] = -i\left(\frac{1}{2} \hat{r}^\text{T} H [\hat{r}, \rho] + \frac{1}{2} [\hat{r}^\text{T}, \rho] H \hat{r} + \mathbf{h}^\text{T} [\hat{r}, \rho]\right). \quad (\text{B.18})$$

The operator nature of \hat{r} and ρ prohibits us from commuting them, but otherwise we can treat H as a matrix, \hat{r} as a vector, and ρ as a scalar, which greatly simplifies the notation.

Using the replacement rules from the previous section we obtain

$$[\chi]_H = -\frac{i}{2} \left(-i\tilde{\nabla} - \frac{1}{2}\xi \right)^T H(-\xi) \quad (\text{B.19})$$

$$- \frac{i}{2} (-\xi)^T H \left(-i\tilde{\nabla} + \frac{1}{2}\xi \right) - i\mathbf{h}^T(-\xi)\chi(\xi)$$

$$= \frac{1}{2} \left(\tilde{\nabla}^T H \xi + \xi^T H \tilde{\nabla} + 2i\mathbf{h}^T \xi \right) \chi(\xi). \quad (\text{B.20})$$

Note that the first term requires use of the product rule since $\tilde{\nabla}$ acts on both ξ and χ , so to make this explicit we write

$$\left(\tilde{\nabla}^T H \xi \right) \chi(\xi) = \chi(\xi) \left(\tilde{\nabla}^T H \xi \right) + \xi^T H (\tilde{\nabla} \chi(\xi)). \quad (\text{B.21})$$

Here we see

$$\tilde{\nabla}^T H \xi = \sum_{j,k} \partial_j (\sigma^T H)_{jk} \xi_k = \sum_j (\sigma^T H)_{jj} = \text{Tr} \left[\sigma^T H \right] = 0, \quad (\text{B.22})$$

so the final expression reads

$$-i[\hat{H}, \rho] \rightarrow \left(\xi^T H \tilde{\nabla} + i\mathbf{h}^T \xi \right) \chi(\xi). \quad (\text{B.23})$$

To obtain the equations of motion of the cumulants, one has to take the derivative of Eq. (B.6), so

$$[dV_{m_1, \dots, m_N}^{(N)}]_H = (-i\tilde{\partial}_{m_1}) \dots (-i\tilde{\partial}_{m_N}) d \ln[\chi(\xi)]|_{\xi=0} \quad (\text{B.24})$$

$$= (-i\tilde{\partial}_{m_1}) \dots (-i\tilde{\partial}_{m_N}) \frac{1}{\chi} d\chi|_{\xi=0} \quad (\text{B.25})$$

$$= (-i\tilde{\partial}_{m_1}) \dots (-i\tilde{\partial}_{m_N}) e^{-G(\xi)} \left(\xi^T H \tilde{\nabla} + i\mathbf{h}^T \xi \right) e^{G(\xi)}|_{\xi=0} dt \quad (\text{B.26})$$

$$= (-i\tilde{\partial}_{m_1}) \dots (-i\tilde{\partial}_{m_N}) \left(\xi^T H (\tilde{\nabla} G(\xi)) + i\mathbf{h}^T \xi \right)|_{\xi=0} dt. \quad (\text{B.27})$$

The twisted derivatives act on ξ as $\tilde{\partial}_j \xi_k = \sum_l \sigma_{jl} \partial_l \xi_k = \sigma_{jk}$. We thus find, using the Einstein sum convention,

$$[dV_{m_1, \dots, m_N}^{(N)}]_H = \sum_{\tau \in \text{S}^{\text{cycl}}(N)} (\sigma H)_{m_{\tau(1)}, k} V_{k, m_{\tau(2)}, \dots, m_{\tau(N)}}^{(N)} dt \quad (\text{B.28})$$

$$+ (\sigma \mathbf{h})_{m_1} \delta_{N,1} dt$$

where τ runs through all cyclic permutations of $1, \dots, N$. Inspiration for this concise expression came from the fact that the covariance matrix ($N = 2$) evolves as

$$[\dot{V}]_H = \sigma H V + (\sigma H V)^T, \quad (\text{B.29})$$

i. e., a matrix product plus its transpose which is just an exchange of indices. In (B.28), which is at order N , the matrix product corresponds to the sum over k and the cyclic permutations reflect N possible transpositions (think of rotations about the diagonal of an $2M \times 2M$ matrix for $N = 2$ or rotations about the diagonal of the corresponding $2M \times \dots \times 2M$ -dimensional (hyper-)cube for $N \geq 3$).

B.3 LINDBLAD OPERATORS

For linear jump operators $\hat{L} = \Lambda \hat{\rho}$ with $\Lambda^\dagger \Lambda =: \Delta + i\Omega$ we find the Lindblad operators

$$\sum_j \mathcal{D}[\hat{L}_j] \rho = \sum_{j,k,l} \Lambda_{jk}^* \Lambda_{jl} \left(\hat{\rho}_l \hat{\rho}_k - \frac{1}{2} \{ \hat{\rho}_k \hat{\rho}_l, \rho \} \right) \quad (\text{B.30})$$

$$= \hat{\rho}^T \rho (\Lambda^\dagger \Lambda)^T \hat{\rho} - \frac{1}{2} \{ \hat{\rho}^T \Lambda^\dagger \Lambda \hat{\rho}, \rho \} \quad (\text{B.31})$$

$$= \frac{1}{2} \hat{\rho}^T \Delta [\rho, \hat{\rho}] + \frac{1}{2} [\hat{\rho}^T, \rho] \Delta \hat{\rho} - \frac{i}{2} \left(\hat{\rho}^T \Omega \{ \rho, \hat{\rho} \} + \{ \hat{\rho}^T, \rho \} \Omega \hat{\rho} \right) \quad (\text{B.32})$$

which becomes

$$[\dot{\chi}]_L = \left[\frac{1}{2} \left(-i\tilde{\nabla} - \frac{1}{2}\xi \right)^T \Delta \xi + \frac{1}{2} (-\xi)^T \Delta \left(-i\tilde{\nabla} + \frac{1}{2}\xi \right) - \left(-i\tilde{\nabla} - \frac{1}{2}\xi \right)^T \Omega \tilde{\nabla} - \tilde{\nabla}^T \Omega \left(-i\tilde{\nabla} + \frac{1}{2}\xi \right) \right] \chi(\xi) \quad (\text{B.33})$$

$$= \left[-\frac{1}{2} \xi^T \Delta \xi - \frac{i}{2} \tilde{\nabla}^T \Delta \xi + \frac{i}{2} \xi^T \Delta \tilde{\nabla} + 2i \tilde{\nabla}^T \Omega \tilde{\nabla} + \frac{1}{2} \xi^T \Omega \tilde{\nabla} - \frac{1}{2} \tilde{\nabla}^T \Omega \xi \right] \chi(\xi) \quad (\text{B.34})$$

$$= \left[-\frac{1}{2} \xi^T \Delta \xi + \xi^T \Omega \tilde{\nabla} + \frac{1}{2} \text{Tr}[\sigma \Omega] \right] \chi(\xi) \quad (\text{B.35})$$

where we used the product rule as in (B.21) to get

$$\tilde{\nabla}^T \Omega \xi = -\xi^T \Omega \tilde{\nabla} + \text{Tr}[\sigma \Omega]. \quad (\text{B.36})$$

We also used that Δ is symmetric so $-\tilde{\nabla}^T \Delta \xi + \xi^T \Delta \tilde{\nabla} = \text{Tr}[\sigma \Delta] = 0$, and Ω is skew-symmetric so $v^T \Omega v = 0$ for any vector v ; in particular

$$\tilde{\nabla}^T \Omega \tilde{\nabla} = 0. \quad (\text{B.37})$$

The contribution to the cumulant evolution will be given by

$$[dV_{m_1, \dots, m_N}^{(N)}]_L = (-i\tilde{\partial}_{m_1}) \dots (-i\tilde{\partial}_{m_N}) e^{-G(\xi)} \times \left[-\frac{1}{2} \xi^T \Delta \xi + \xi^T \Omega \tilde{\nabla} + \frac{1}{2} \text{Tr}[\sigma \Omega] \right] e^{G(\xi)} dt \quad (\text{B.38})$$

$$= (-i\tilde{\partial}_{m_1}) \dots (-i\tilde{\partial}_{m_N}) \times \left[-\frac{1}{2} \xi^T \Delta \xi + (\xi^T \Omega \tilde{\nabla} G(\xi)) + \frac{1}{2} \text{Tr}[\sigma \Omega] \right] \Big|_{\xi=0} dt \quad (\text{B.39})$$

$$= (\sigma \Delta \sigma^T)_{m_1 m_2} \delta_{N,2} dt + \frac{1}{2} \text{Tr}[\sigma \Omega] \delta_{N,0} dt + \sum_{\tau \in \mathcal{S}^{\text{cycl}}(N)} (\sigma \Omega)_{m_{\tau(1)}, k} V_{k, m_{\tau(2)}, \dots, m_{\tau(N)}}^{(N)} dt. \quad (\text{B.40})$$

B.4 MEASUREMENT TERMS

We assume linear measurement operators, $\hat{\mathbf{C}} = (A + iB)\hat{\mathbf{r}}$, which yield terms

$$(I) \sum_k (\hat{\mathbf{C}}_k \rho + \rho \hat{\mathbf{C}}_k^\dagger) dY_k = (\hat{\mathbf{C}}\rho + \rho \hat{\mathbf{C}}^\dagger)^T d\mathbf{Y} \quad (\text{B.41})$$

$$= (A(\hat{\mathbf{r}}\rho + \rho\hat{\mathbf{r}}) + iB(\hat{\mathbf{r}}\rho - \rho\hat{\mathbf{r}}))^T d\mathbf{Y} \quad (\text{B.42})$$

$$= (A\{\hat{\mathbf{r}}, \rho\} + iB[\hat{\mathbf{r}}, \rho])^T d\mathbf{Y} \quad (\text{B.43})$$

$$\rightarrow (I) [d\chi]_C = (-2iA\tilde{\nabla} - iB\tilde{\xi})^T d\mathbf{Y}\chi(\xi). \quad (\text{B.44})$$

Note that due to the stochastic nature of the Itô increment we need to implement the Itô table $dY_j dY_k = \delta_{jk} dt$ so we keep terms of up to second order,

$$(I) [dG]_C = [d\ln[\chi]]_C \quad (\text{B.45})$$

$$= \frac{1}{\chi} [d\chi]_C + \frac{1}{2} \left(-\frac{1}{\chi^2} \right) [d\chi]_C^2 \quad (\text{B.46})$$

$$=: [dG]_Y + [dG]_{\text{Itô}}. \quad (\text{B.47})$$

The linear term yields

$$(I) [dG]_Y = e^{-G(\xi)} (-2iA\tilde{\nabla} - iB\tilde{\xi})^T e^{G(\xi)} d\mathbf{Y} \quad (\text{B.48})$$

$$= (-2iA\tilde{\nabla}G(\xi) - iB\tilde{\xi})^T d\mathbf{Y}, \quad (\text{B.49})$$

which contributes to the cumulants

$$(I) [dV_{m_1, \dots, m_N}^{(N)}]_Y = (-i\tilde{\partial}_{m_1}) \dots (-i\tilde{\partial}_{m_N}) \times \quad (\text{B.50})$$

$$\times (-2iA\tilde{\nabla}G(\xi) - iB\tilde{\xi})^T d\mathbf{Y}|_{\xi=0}$$

$$= \left(2A_{jk} V_{k, m_1, \dots, m_N}^{(N+1)} - B_{jk} \sigma_{m_1 k} \delta_{N,1} \right) dY_j \quad (\text{B.51})$$

$$= \left(2V_{m_1, \dots, m_N, k}^{(N+1)} A_{kj}^T - (\sigma B^T)_{m_1 j} \delta_{N,1} \right) dY_j. \quad (\text{B.52})$$

If we replace the measurement signal with a Wiener increment by extracting the mean,

$$(I) d\mathbf{Y} = \langle \hat{\mathbf{C}} + \hat{\mathbf{C}}^\dagger \rangle dt + d\mathbf{W} \quad (\text{B.53})$$

$$= 2Ardt + d\mathbf{W} = 2AV^{(1)}dt + d\mathbf{W} \quad (\text{B.54})$$

we find

$$(I) [dV_{m_1, \dots, m_N}^{(N)}]_Y = \left(2V_{m_1, \dots, m_N, k}^{(N+1)} A_{kj}^T - (\sigma B^T)_{m_1 j} \delta_{N,1} \right) dW_j \quad (\text{B.55})$$

$$+ 2 \left(2V_{m_1, \dots, m_N, k}^{(N+1)} (A^T Ar)_k - (\sigma B^T Ar)_{m_1} \delta_{N,1} \right) dt.$$

The quadratic Itô correction contributes terms

$$[dG]_{\text{Itô}} = -\frac{1}{2} (-2iA\tilde{\nabla}G(\xi) - iB\tilde{\xi})^T (-2iA\tilde{\nabla}G(\xi) - iB\tilde{\xi}) dt \quad (\text{B.56})$$

$$= \frac{1}{2} \left(4(\tilde{\nabla}G(\xi))^T A^T A (\tilde{\nabla}G(\xi)) \right. \quad (\text{B.57})$$

$$\left. + \tilde{\xi}^T B^T B \tilde{\xi} + 4\tilde{\xi}^T B^T A (\tilde{\nabla}G(\xi)) \right) dt,$$

where the derivatives act only on the G right next to them. Evaluating the last two terms is straightforward and one finds

$$(-i\tilde{\partial}_{m_1}) \dots (-i\tilde{\partial}_{m_N}) [\xi^T B^T B \xi] |_{\xi=0} = -2(\sigma B^T B \sigma^T)_{m_1 m_2} \delta_{N,2}, \quad (\text{B.58})$$

and

$$\begin{aligned} & (-i\tilde{\partial}_{m_1}) \dots (-i\tilde{\partial}_{m_N}) [\xi^T B^T A (\tilde{\nabla} G(\xi))] |_{\xi=0} \\ &= \sum_{\tau \in \mathcal{S}^{\text{cycl}}(N)} (\sigma B^T A)_{m_{\tau(1)}, k} V_{k, m_{\tau(2)}, \dots, m_{\tau(N)}}^{(N)}. \end{aligned} \quad (\text{B.59})$$

To compute the remaining term we have to apply the product rule multiple times. This results in a sum over all possible sequences of derivatives acting either on the right or on the left $\tilde{\nabla} G$, so

$$\begin{aligned} & (-i\tilde{\partial}_{m_1}) \dots (-i\tilde{\partial}_{m_N}) 2[(\tilde{\nabla} G(\xi))^T A^T A (\tilde{\nabla} G(\xi))] |_{\xi=0} \\ &= -2 \sum_{n=0}^N \sum_{\substack{p \in \text{Bipart}(N) \\ |p|=n}} V_{m_{p(1)}, \dots, m_{p(n)}, j}^{(n+1)} (A^T A)_{jk} V_{k, m_{q(1)}, \dots, m_{q(N-n)}}^{(N-n+1)}. \end{aligned} \quad (\text{B.60})$$

where the sum runs over all possible bipartitions of $\{1, \dots, N\}$, such that one part contains n elements $p(1), \dots, p(n)$ while its complement contains $q(1), \dots, q(N-n)$. We extract the terms with $n=0$ and $n=N$ from the sum which each contain only one partition,

$$\begin{aligned} & -2 \left(V_j^{(1)} (A^T A)_{jk} V_{k, m_1, \dots, m_N}^{(N+1)} + V_{m_1, \dots, m_N, j}^{(N+1)} (A^T A)_{jk} V_k^{(1)} \right) \\ &= -4 V_{m_1, \dots, m_N, k}^{(N+1)} (A^T A r)_k, \end{aligned} \quad (\text{B.61})$$

and we see that this cancels exactly a term from (B.55). Combining the remaining measurement contributions we find

$$\begin{aligned} (\text{I}) \ [dV_{m_1, \dots, m_N}]_C &= \left(2V_{m_1, \dots, m_N, k}^{(N+1)} A_{kj}^T - (\sigma B^T)_{m_1 j} \delta_{N,1} \right) dW_j \\ &\quad - 2(\sigma B^T A r)_{m_1} \delta_{N,1} dt - (\sigma B^T B \sigma^T)_{m_1 m_2} \delta_{N,2} dt \\ &\quad + 2 \sum_{\tau \in \mathcal{S}^{\text{cycl}}(N)} (\sigma B^T A)_{m_{\tau(1)}, k} V_{k, m_{\tau(2)}, \dots, m_{\tau(N)}}^{(N)} dt \\ &\quad - 2 \sum_{n=1}^{N-1} \sum_{\substack{p \in \text{Bipart}(N) \\ |p|=n}} V_{m_{p(1)}, \dots, m_{p(n)}, j}^{(n+1)} (A^T A)_{jk} V_{k, m_{q(1)}, \dots, m_{q(N-n)}}^{(N-n+1)} dt. \end{aligned} \quad (\text{B.62})$$

B.5 COMBINED EVOLUTION

We put all terms from the previous sections together and find

$$\begin{aligned}
 \text{(I)} \quad & dV_{m_1, \dots, m_N}^{(N)} \\
 &= \sum_{\tau \in \mathcal{S}^{\text{cycl}}(N)} (\sigma(H + \Omega))_{m_{\tau(1)}, k} V_{k, m_{\tau(2)}, \dots, m_{\tau(N)}}^{(N)} dt + (\sigma \mathbf{h})_{m_1} \delta_{N,1} dt \\
 &+ \frac{1}{2} \text{Tr}[\sigma \Omega] \delta_{N,0} dt + (\sigma(\Delta - B^T B) \sigma^T)_{m_1 m_2} \delta_{N,2} dt \\
 &+ 2 \sum_{\tau \in \mathcal{S}^{\text{cycl}}(N)} (\sigma B^T A)_{m_{\tau(1)}, k} V_{k, m_{\tau(2)}, \dots, m_{\tau(N)}}^{(N)} dt - 2(\sigma B^T A \mathbf{r})_{m_1} \delta_{N,1} dt \\
 &- 2 \sum_{n=1}^{N-1} \sum_{\substack{p \in \text{Bipart}(N) \\ |p|=n}} V_{m_{p(1)}, \dots, m_{p(n)}, j}^{(n+1)} (A^T A)_{jk} V_{k, m_{q(1)}, \dots, m_{q(N-n)}}^{(N-n+1)} dt \\
 &+ 2V_{m_1, \dots, m_N, k}^{(N+1)} (A^T d\mathbf{W})_k - (\sigma B^T d\mathbf{W})_{m_1} \delta_{N,1}
 \end{aligned} \tag{B.63}$$

$$\begin{aligned}
 &= \sum_{\tau \in \mathcal{S}^{\text{cycl}}(N)} (Q + 2\sigma B^T A \delta_{N \neq 1})_{m_{\tau(1)}, k} V_{k, m_{\tau(2)}, \dots, m_{\tau(N)}}^{(N)} dt \\
 &+ \frac{1}{2} \text{Tr}[\sigma \Omega] \delta_{N,0} dt + (\sigma \tilde{\Delta} \sigma^T)_{m_1 m_2} \delta_{N,2} dt \\
 &- 2 \sum_{n=1}^{N-1} \sum_{\substack{p \in \text{Bipart}(N) \\ |p|=n}} V_{m_{p(1)}, \dots, m_{p(n)}, j}^{(n+1)} (A^T A)_{jk} V_{k, m_{q(1)}, \dots, m_{q(N-n)}}^{(N-n+1)} dt \\
 &+ (\sigma \mathbf{h} dt - \sigma B^T d\mathbf{W})_{m_1} \delta_{N,1} + 2V_{m_1, \dots, m_N, k}^{(N+1)} (A^T d\mathbf{W})_k.
 \end{aligned} \tag{B.64}$$

with

$$Q := \sigma(H + \Omega), \quad \tilde{\Delta} := \Delta - B^T B. \tag{B.65}$$

Specifically at first order this yields

$$\begin{aligned}
 \text{(I)} \quad & dr_m = dV_m^{(1)} = Q_{m,k} V_k^{(1)} dt + 2V_{m,k}^{(2)} (A^T d\mathbf{W})_k \\
 &+ (\sigma \mathbf{h} dt - \sigma B^T d\mathbf{W})_m
 \end{aligned} \tag{B.66}$$

which in vector form reads

$$\text{(I)} \quad dr_\rho = Q r_\rho dt + \sigma \mathbf{h} dt + (2V_\rho^{(2)} A^T - \sigma B^T) d\mathbf{W} \tag{B.67}$$

$$= M_\rho r_\rho dt + \sigma \mathbf{h} dt + (2V_\rho^{(2)} A^T - \sigma B^T) d\mathbf{Y}. \tag{B.68}$$

where we replaced the Wiener increment by the measurement current $d\mathbf{Y}$ as in Eq. (B.54), and introduced the drift matrix from Eq. (7.41),

$$M_\rho(t) = Q + 2\sigma B^T A - 4V_\rho^{(2)}(t) A^T A. \tag{B.69}$$

At second order we find for the (co)variances

$$\begin{aligned}
\text{(I)} \quad dV_{m_1, m_2}^{(2)} &= \sum_{\tau \in \mathcal{S}^{\text{cycl}}(2)} (Q + 2\sigma B^T A)_{m_{\tau(1)}, k} V_{k, m_{\tau(2)}}^{(2)} dt \\
&\quad + (\sigma \tilde{\Delta} \sigma^T)_{m_1 m_2} dt + 2V_{m_1, m_2, k}^{(3)} (A^T dW)_k \\
&\quad - 2 \sum_{\tau \in \mathcal{S}^{\text{cycl}}(2)} V_{m_{\tau(1)}, j}^{(2)} (A^T A)_{jk} V_{k, m_{\tau(2)}}^{(2)} dt \\
&= (Q + 2\sigma B^T A)_{m_1, k} V_{k, m_2}^{(2)} dt + (Q + 2\sigma B^T A)_{m_2, k} V_{k, m_1}^{(2)} dt \\
&\quad + (\sigma \tilde{\Delta} \sigma^T)_{m_1 m_2} dt + 2V_{m_1, m_2, k}^{(3)} (A^T dW)_k \\
&\quad - 2V_{m_1, j}^{(2)} (A^T A)_{jk} V_{k, m_2}^{(2)} dt - 2V_{m_2, j}^{(2)} (A^T A)_{jk} V_{k, m_1}^{(2)} dt
\end{aligned} \tag{B.70}$$

$$\begin{aligned}
&= (Q + 2\sigma B^T A)_{m_1, k} V_{k, m_2}^{(2)} dt + (Q + 2\sigma B^T A)_{m_2, k} V_{k, m_1}^{(2)} dt \\
&\quad + (\sigma \tilde{\Delta} \sigma^T)_{m_1 m_2} dt + 2V_{m_1, m_2, k}^{(3)} (A^T dW)_k \\
&\quad - 2V_{m_1, j}^{(2)} (A^T A)_{jk} V_{k, m_2}^{(2)} dt - 2V_{m_2, j}^{(2)} (A^T A)_{jk} V_{k, m_1}^{(2)} dt
\end{aligned} \tag{B.71}$$

which can be written more concisely as

$$\begin{aligned}
\text{(I)} \quad dV_{m_1, m_2}^{(2)} &= \left[M_\rho V_\rho^{(2)} + V_\rho^{(2)} M_\rho^T \right. \\
&\quad \left. + \sigma \tilde{\Delta} \sigma^T + 4V_\rho^{(2)} A^T A V_\rho^{(2)} \right]_{m_1, m_2} dt \\
&\quad + 2V_{m_1, m_2, k}^{(3)} (A^T dW)_k,
\end{aligned} \tag{B.72}$$

with an implicit sum over k in the last term, turning $V_\rho^{(3)}$ from a tensor into a matrix with the free indices m_1, m_2 . The evolution of cumulants of order $N \geq 3$ is given by

$$\begin{aligned}
\text{(I)} \quad dV_{m_1, \dots, m_N}^{(N)} &= \sum_{\tau \in \mathcal{S}^{\text{cycl}}(N)} (Q + 2\sigma B^T A)_{m_{\tau(1)}, k} V_{k, m_{\tau(2)}, \dots, m_{\tau(N)}}^{(N)} dt \\
&\quad - 2 \sum_{n=1}^{N-1} \sum_{\substack{p \in \text{Bipart}(N) \\ |p|=n}} V_{m_{p(1)}, \dots, m_{p(n)}, j}^{(n+1)} (A^T A)_{jk} V_{k, m_{q(1)}, \dots, m_{q(N-n)}}^{(N-n+1)} dt \\
&\quad + 2V_{m_1, \dots, m_N, k}^{(N+1)} (A^T dW)_k \\
&= \sum_{\tau \in \mathcal{S}^{\text{cycl}}(N)} M_{m_{\tau(1)}, k}^\rho V_{k, m_{\tau(2)}, \dots, m_{\tau(N)}}^{(N)} dt \\
&\quad - 2 \sum_{n=2}^{N-2} \sum_{\substack{p \in \text{Bipart}(N) \\ |p|=n}} V_{m_{p(1)}, \dots, m_{p(n)}, j}^{(n+1)} (A^T A)_{jk} V_{k, m_{q(1)}, \dots, m_{q(N-n)}}^{(N-n+1)} dt \\
&\quad + 2V_{m_1, \dots, m_N, k}^{(N+1)} (A^T dW)_k.
\end{aligned} \tag{B.73}$$

$$\tag{B.74}$$

It is worthy to note that generally all cumulants couple to the next higher order through the stochastic term. Thus the unconditional dynamics with dW averaged to zero will create a hierarchy that can be solved (e. g., for steady state) recursively from lower to higher orders.

B.6 BACKWARD ADDITION

To obtain the evolution equations of the cumulants associated with the effect operator we can compare the unnormalized master equation for ρ ,

$$\begin{aligned}
 \text{(I)} \quad d\rho(t) &= -i[\hat{H}, \rho(t)]dt + \sum_{j=1}^{N_L} \mathcal{D}[\hat{L}_j]\rho(t)dt \\
 &+ \sum_{k=1}^{N_C} \left(\hat{C}_k \rho(t) + \rho(t) \hat{C}_k^\dagger \right) dY_k(t).
 \end{aligned} \tag{B.75}$$

to the corresponding equation for \hat{E} ,

$$\begin{aligned}
 \text{(BI)} \quad -d\hat{E}(t) &= i[\hat{H}, \hat{E}(t)]dt + \sum_{j=1}^{N_L} \mathcal{D}^\dagger[\hat{L}_j]\hat{E}(t)dt \\
 &+ \sum_{k=1}^{N_C} \left(\hat{C}_k^\dagger \hat{E}(t) + \hat{E}(t) \hat{C}_k \right) dY_k(t).
 \end{aligned} \tag{B.76}$$

$$\begin{aligned}
 &= -i[-\hat{H}, \hat{E}(t)]dt + \sum_{j=1}^{N_L} \mathcal{D}[\hat{L}_j]\hat{E}(t)dt \\
 &+ \sum_{k=1}^{N_C} \left(\hat{C}_k^\dagger \hat{E}(t) + \hat{E}(t) \hat{C}_k \right) dY_k(t) \\
 &+ \sum_{j=1}^{N_L} \left(\hat{L}_j^\dagger \hat{E}(t) \hat{L}_j - \hat{L}_j \hat{E}(t) \hat{L}_j^\dagger \right) dt.
 \end{aligned} \tag{B.77}$$

We can immediately read off the following changes. The sign flip of \hat{H} causes $H \rightarrow -H$ and replacing the measurement operators \hat{C}_k by their adjoint entails $B \rightarrow -B$. We only need to work out the change $[d\chi_E]_{\text{bwd}}$ stemming exclusively from the sandwich terms in the last sum. Using the relations (B.14), (B.36) and (B.37) we obtain

$$-[d\hat{E}]_{\text{bwd}} = 2i\hat{r}^T \Omega \hat{E} \hat{r} dt \tag{B.78}$$

$$\rightarrow -[d\chi_E]_{\text{bwd}} = 2i \left(-i\tilde{\mathbf{V}}^T - \frac{1}{2}\tilde{\xi} \right)^T \Omega \left(-i\tilde{\mathbf{V}}^T + \frac{1}{2}\tilde{\xi} \right) \chi_E \tag{B.79}$$

$$= -\text{Tr}[\sigma \Omega] \chi_E dt - 2\tilde{\xi}^T \Omega (\tilde{\mathbf{V}} \chi_E) dt. \tag{B.80}$$

So the backward cumulants with $N \geq 1$ will have the additional term

$$-[dV_{m_1, \dots, m_N}^{(N)}]_{\text{bwd}} = -2 \sum_{\tau \in \text{S}^{\text{cycl}}(N)} \Omega_{m_{\tau(1)}, k} V_{k, m_{\tau(2)}, \dots, m_{\tau(N)}}^{(N)} dt. \tag{B.81}$$

The combined evolution of the backward cumulants thus reads

$$\begin{aligned}
(\text{BI}) \quad & -dV_{m_1, \dots, m_N}^{(N)} \\
& = - \sum_{\tau \in \mathcal{S}^{\text{cycl}}(N)} (Q + 2\sigma B^T A \delta_{N \neq 1})_{m_{\tau(1)}, k} V_{k, m_{\tau(2)}, \dots, m_{\tau(N)}}^{(N)} dt \\
& + \frac{1}{2} \text{Tr}[\sigma \Omega] \delta_{N,0} dt + (\sigma \tilde{\Delta} \sigma^T)_{m_1 m_2} \delta_{N,2} dt \\
& - 2 \sum_{n=1}^{N-1} \sum_{\substack{p \in \text{Bipart}(N) \\ |p|=n}} V_{m_{p(1)}, \dots, m_{p(n)}, j}^{(n+1)} (A^T A)_{jk} V_{k, m_{q(1)}, \dots, m_{q(N-n)}}^{(N-n+1)} dt \\
& - (\sigma h dt - \sigma B^T dW)_{m_1} \delta_{N,1} + 2V_{m_1, \dots, m_N, k}^{(N+1)} (A^T dW)_k.
\end{aligned} \tag{B.82}$$

Note that the difference between forward and backward equation amounts to nothing but a change in sign of the first line and of the first-order term in the last line. Specifically for the means we find

$$(\text{BI}) \quad -dr_E = -Qr_E dt - \sigma h dt + (2V_E^{(2)} A^T + \sigma B^T) dW \tag{B.83}$$

$$= M_E r_E dt - \sigma h dt + (2V_E^{(2)} A^T + \sigma B^T) dY, \tag{B.84}$$

with the backward drift matrix from Eq. (7.53),

$$M_E(t) := -Q - 2\sigma B^T A - 4V_E(t) A^T A. \tag{B.85}$$

For the covariance matrix we find

$$\begin{aligned}
(\text{BI}) \quad & -dV_{m_1, m_2}^{(2)} = \left[M_E V_E^{(2)} + V_E^{(2)} M_E^T \right. \\
& \quad \left. + \sigma \tilde{\Delta} \sigma^T + 4V_E^{(2)} A^T A V_E^{(2)} \right] dt \\
& \quad + 2V_{m_1, m_2, k}^{(3)} (A^T dW)_k,
\end{aligned} \tag{B.86}$$

Higher order ($N \geq 3$) cumulants evolve as

$$\begin{aligned}
(\text{BI}) \quad & -dV_{m_1, \dots, m_N}^{(N)} \\
& = - \sum_{\tau \in \mathcal{S}^{\text{cycl}}(N)} (Q + 2\sigma B^T A)_{m_{\tau(1)}, k} V_{k, m_{\tau(2)}, \dots, m_{\tau(N)}}^{(N)} dt \\
& - 2 \sum_{n=1}^{N-1} \sum_{\substack{p \in \text{Bipart}(N) \\ |p|=n}} V_{m_{p(1)}, \dots, m_{p(n)}, j}^{(n+1)} (A^T A)_{jk} V_{k, m_{q(1)}, \dots, m_{q(N-n)}}^{(N-n+1)} dt \\
& + 2V_{m_1, \dots, m_N, k}^{(N+1)} (A^T dW)_k.
\end{aligned} \tag{B.87}$$

$$\begin{aligned}
& = \sum_{\tau \in \mathcal{S}^{\text{cycl}}(N)} M_{m_{\tau(1)}, k}^E V_{k, m_{\tau(2)}, \dots, m_{\tau(N)}}^{(N)} dt \\
& - 2 \sum_{n=2}^{N-2} \sum_{\substack{p \in \text{Bipart}(N) \\ |p|=n}} V_{m_{p(1)}, \dots, m_{p(n)}, j}^{(n+1)} (A^T A)_{jk} V_{k, m_{q(1)}, \dots, m_{q(N-n)}}^{(N-n+1)} dt \\
& + 2V_{m_1, \dots, m_N, k}^{(N+1)} (A^T dW)_k.
\end{aligned} \tag{B.88}$$

OPTOMECHANICS: STEADY STATE VARIANCES AND MODE FUNCTIONS

In this chapter we provide some details and results of the calculations omitted in Sec. 8.2.

C.1 DRIVE ON RESONANCE, DETECT SIDEBANDS

C.1.1 Blue sideband, $\Delta_{\text{lo}} = +\omega_m$

On the blue sideband, for $\Delta_{\text{lo}} = +\omega_m$, we find

$$\begin{aligned}
 \text{(I) } d\rho(t) &= \mathcal{L}_{\text{th}}\rho(t) + \Gamma\mathcal{D}[\hat{a}^\dagger]\rho(t)dt + \Gamma\mathcal{D}[\hat{a}]\rho(t)dt \\
 &\quad + \sqrt{\eta\Gamma}\mathcal{H}[\hat{a}]\rho(t)dW_0(t) \\
 &\quad + \sqrt{\frac{\eta\Gamma}{2}}\mathcal{H}[\hat{a}^\dagger]\rho(t)dW_{c,2}(t) + \sqrt{\frac{\eta\Gamma}{2}}\mathcal{H}[i\hat{a}^\dagger]\rho(t)dW_{s,2}(t).
 \end{aligned} \tag{C.1}$$

Compared to the case of zero detuning the only difference are new measurement matrices,

$$A = \frac{\sqrt{\eta\Gamma}}{2} \begin{bmatrix} \sqrt{2} & 0 \\ 1 & 0 \\ 0 & 1 \end{bmatrix}, \quad B = \frac{\sqrt{\eta\Gamma}}{2} \begin{bmatrix} 0 & \sqrt{2} \\ 0 & -1 \\ 1 & 0 \end{bmatrix}. \tag{C.2}$$

In steady state we find $V_{xp}^{\text{ss}} = 0$ and

$$V_{xx}^{\text{ss}} = \frac{1}{6\eta C} \left(\sqrt{1 + 4\eta C((3 - 2\eta)C + 3\bar{n} + 1)} - 1 \right) + \frac{1}{6}, \tag{C.3}$$

$$V_{pp}^{\text{ss}} = \frac{1}{2\eta C} \left(\sqrt{1 + 4\eta C(C + \bar{n} + 1)} - 1 \right) - \frac{1}{2}. \tag{C.4}$$

The resulting drift matrix is diagonal $M_{\text{ss}} = -\text{diag}(\lambda_x, \lambda_p)$ with

$$\lambda_x = \frac{\gamma}{2}(\eta C(6V_{xx}^{\text{ss}} - 1) + 1) \tag{C.5}$$

$$= \frac{\gamma}{2}\sqrt{1 + 4\eta C((3 - 2\eta)C + 3\bar{n} + 1)}, \tag{C.6}$$

$$\lambda_p = \frac{\gamma}{2}(\eta C(2V_{pp}^{\text{ss}} + 1) + 1) \tag{C.7}$$

$$= \frac{\gamma}{2}\sqrt{1 + 4\eta C(C + \bar{n} + 1)}. \tag{C.8}$$

Computing the mode functions we find

$$f_{x|0}(t) = \sqrt{\frac{\eta\Gamma}{2}} e^{-\lambda_x t} (2V_{xx}^{\text{ss}} - 1), \quad f_{p|0}(t) = 0, \quad (\text{C.9})$$

$$f_{x|c,2}(t) = \sqrt{\frac{\eta\Gamma}{2}} e^{-\lambda_x t} \frac{2V_{xx}^{\text{ss}} + 1}{\sqrt{2}}, \quad f_{p|c,2}(t) = 0, \quad (\text{C.10})$$

$$f_{x|s,2}(t) = 0, \quad f_{p|s,2}(t) = \sqrt{\frac{\eta\Gamma}{2}} e^{-\lambda_p t} \frac{2V_{pp}^{\text{ss}} + 1}{\sqrt{2}}. \quad (\text{C.11})$$

The backward equations again yield $\bar{V}_{xp}^{\text{ss}} = 0$ and

$$\bar{V}_{xx}^{\text{ss}} = \frac{1}{6\eta C} \left(\sqrt{1 + 4\eta C((3 - 2\eta)C + 3\bar{n} + 1)} + 1 \right) - \frac{1}{6}, \quad (\text{C.12})$$

$$\bar{V}_{pp}^{\text{ss}} = \frac{1}{2\eta C} \left(\sqrt{1 + 4\eta C(C + \bar{n} + 1)} + 1 \right) + \frac{1}{2}. \quad (\text{C.13})$$

The resulting drift matrix is again diagonal, $\bar{M}_{\text{ss}} = -\text{diag}(\bar{\lambda}_x, \bar{\lambda}_p)$, with

$$\bar{\lambda}_x = \frac{\gamma}{2} (\eta C (6\bar{V}_{xx}^{\text{ss}} + 1) - 1) \quad (\text{C.14})$$

$$= \frac{\gamma}{2} \sqrt{1 + 4\eta C((3 - 2\eta)C + 3\bar{n} + 1)}, \quad (\text{C.15})$$

$$\bar{\lambda}_p = \frac{\gamma}{2} (\eta C (2\bar{V}_{pp}^{\text{ss}} - 1) - 1) \quad (\text{C.16})$$

$$= \frac{\gamma}{2} \sqrt{1 + 4\eta C(C + \bar{n} + 1)}. \quad (\text{C.17})$$

For the mode functions we find

$$\bar{f}_{x|0}(t) = \sqrt{\frac{\eta\Gamma}{2}} e^{-\bar{\lambda}_x t} (2\bar{V}_{xx}^{\text{ss}} + 1), \quad \bar{f}_{p|0}(t) = 0, \quad (\text{C.18})$$

$$\bar{f}_{x|c,2}(t) = \sqrt{\frac{\eta\Gamma}{2}} e^{-\bar{\lambda}_x t} \frac{2\bar{V}_{xx}^{\text{ss}} - 1}{\sqrt{2}}, \quad \bar{f}_{p|c,2}(t) = 0, \quad (\text{C.19})$$

$$\bar{f}_{x|s,2}(t) = 0, \quad \bar{f}_{p|s,2}(t) = \sqrt{\frac{\eta\Gamma}{2}} e^{-\bar{\lambda}_p t} \frac{2\bar{V}_{pp}^{\text{ss}} - 1}{\sqrt{2}}. \quad (\text{C.20})$$

Interestingly, considering the difference between variances,

$$\bar{V}_{xx}^{\text{ss}} - V_{xx}^{\text{ss}} = -\frac{1}{3} + \frac{1}{3\eta C} \approx -\frac{1}{3}, \quad (\text{C.21})$$

$$\bar{V}_{pp}^{\text{ss}} - V_{pp}^{\text{ss}} = 1 + \frac{1}{\eta C} \approx 1, \quad (\text{C.22})$$

we see that in case of large cooperativity, the backward position is better conditioned than the forward position while for the momentum it is the other way around.

c.1.2 Red sideband, $\Delta_{\text{lo}} = -\omega_m$

Comparing the master equation obtained by detecting the red sideband, $\Delta_{\text{lo}} = -\omega_m$,

$$\begin{aligned}
 \text{(I) } d\rho(t) &= \mathcal{L}_{\text{th}}\rho(t) + \Gamma\mathcal{D}[\hat{a}^\dagger]\rho(t)dt + \Gamma\mathcal{D}[\hat{a}]\rho(t)dt \\
 &+ \sqrt{\eta\Gamma}\mathcal{H}[\hat{a}^\dagger]\rho(t)dW_0(t) \\
 &+ \sqrt{\frac{\eta\Gamma}{2}}\mathcal{H}[\hat{a}]\rho(t)dW_{c,2}(t) + \sqrt{\frac{\eta\Gamma}{2}}\mathcal{H}[-i\hat{a}]\rho(t)dW_{s,2}(t),
 \end{aligned} \tag{C.23}$$

to the one for the blue sideband, we see that all measurement operators are replaced by their Hermitian conjugate. This means we have to replace $B \rightarrow -B$. We again find $V_{xp}^{\text{ss}} = 0$ and

$$V_{xx}^{\text{ss}} = \frac{1}{6\eta C} \left(\sqrt{1 + 4\eta C((3 - 2\eta)C + 3\bar{n} + 2)} - 1 \right) - \frac{1}{6}, \tag{C.24}$$

$$V_{pp}^{\text{ss}} = \frac{1}{2\eta C} \left(\sqrt{1 + 4\eta C(C + \bar{n})} - 1 \right) + \frac{1}{2}. \tag{C.25}$$

The diagonal drift matrix $M_{\text{ss}} = -\text{diag}(\lambda_x, \lambda_p)$ is strictly stable with

$$\lambda_x = \frac{\gamma}{2}(\eta C(6V_{xx}^{\text{ss}} + 1) + 1) \tag{C.26}$$

$$= \frac{\gamma}{2}\sqrt{1 + 4\eta C((3 - 2\eta)C + 3\bar{n} + 2)}, \tag{C.27}$$

$$\lambda_p = \frac{\gamma}{2}(\eta C(2V_{pp}^{\text{ss}} - 1) + 1) \tag{C.28}$$

$$= \frac{\gamma}{2}\sqrt{1 + 4\eta C(C + \bar{n})}, \tag{C.29}$$

and the mode functions read

$$f_{x|0}(t) = \sqrt{\frac{\eta\Gamma}{2}}e^{-\lambda_x t}(2V_{xx}^{\text{ss}} + 1), \quad f_{p|0}(t) = 0, \tag{C.30}$$

$$f_{x|c,2}(t) = \sqrt{\frac{\eta\Gamma}{2}}e^{-\lambda_x t}\frac{2V_{xx}^{\text{ss}} - 1}{\sqrt{2}}, \quad f_{p|c,2}(t) = 0, \tag{C.31}$$

$$f_{x|s,2}(t) = 0, \quad f_{p|s,2}(t) = \sqrt{\frac{\eta\Gamma}{2}}e^{-\lambda_p t}\frac{2V_{pp}^{\text{ss}} - 1}{\sqrt{2}}. \tag{C.32}$$

The backward equations again yield $\bar{V}_{xp}^{\text{ss}} = 0$ and

$$\bar{V}_{xx}^{\text{ss}} = \frac{1}{6\eta C} \left(\sqrt{1 + 4\eta C((3 - 2\eta)C + 3\bar{n} + 2)} + 1 \right) + \frac{1}{6}, \tag{C.33}$$

$$\bar{V}_{pp}^{\text{ss}} = \frac{1}{2\eta C} \left(\sqrt{1 + 4\eta C(C + \bar{n})} + 1 \right) - \frac{1}{2}. \tag{C.34}$$

The resulting drift matrix is again diagonal, $\bar{M}_{\text{ss}} = -\text{diag}(\bar{\lambda}_x, \bar{\lambda}_p)$, with

$$\bar{\lambda}_x = \frac{\gamma}{2}(\eta C(6\bar{V}_{xx}^{\text{ss}} - 1) - 1) \tag{C.35}$$

$$= \frac{\gamma}{2}\sqrt{1 + 4\eta C((3 - 2\eta)C + 3\bar{n} + 2)}, \tag{C.36}$$

$$\bar{\lambda}_p = \frac{\gamma}{2}(\eta C(2\bar{V}_{pp}^{\text{ss}} + 1) - 1) \tag{C.37}$$

$$= \frac{\gamma}{2}\sqrt{1 + 4\eta C(C + \bar{n})}. \tag{C.38}$$

For the mode functions we find

$$\bar{f}_{x|0}(t) = \sqrt{\frac{\eta\Gamma}{2}} e^{-\bar{\lambda}_x t} (2\bar{V}_{xx}^{\text{ss}} - 1), \quad \bar{f}_{p|0}(t) = 0, \quad (\text{C.39})$$

$$\bar{f}_{x|c,2}(t) = \sqrt{\frac{\eta\Gamma}{2}} e^{-\bar{\lambda}_x t} \frac{2\bar{V}_{xx}^{\text{ss}} + 1}{\sqrt{2}}, \quad \bar{f}_{p|c,2}(t) = 0, \quad (\text{C.40})$$

$$\bar{f}_{x|s,2}(t) = 0, \quad \bar{f}_{p|s,2}(t) = \sqrt{\frac{\eta\Gamma}{2}} e^{-\bar{\lambda}_p t} \frac{2\bar{V}_{pp}^{\text{ss}} + 1}{\sqrt{2}}. \quad (\text{C.41})$$

Considering the difference between variances,

$$\bar{V}_{xx}^{\text{ss}} - V_{xx}^{\text{ss}} = \frac{1}{3} + \frac{1}{3\eta C} \approx \frac{1}{3}, \quad (\text{C.42})$$

$$\bar{V}_{pp}^{\text{ss}} - V_{pp}^{\text{ss}} = -1 + \frac{1}{\eta C} \approx -1, \quad (\text{C.43})$$

we see that the situation is reversed compared to the blue sideband.

C.2 SUMMARY

Generally: $V_{xp}^{\text{ss}} = 0$ and “ \approx ” refers to $C, \bar{n}, \eta C \gg 1$.

C.2.1 Resonant detection, $\Delta_{\text{lo}} = 0$

$$V_{\text{ss}} := V_{xx}^{\text{ss}} = V_{pp}^{\text{ss}} \quad (\text{C.44})$$

$$= \frac{1}{8\eta C} \left(\sqrt{1 + 8\eta C(2C + 2\bar{n} + 1)} - 1 \right) \geq \frac{1}{2} \quad (\text{C.45})$$

$$\approx \frac{1}{2} \sqrt{\frac{C_q + 1}{\eta C_q}}, \quad (\text{C.46})$$

$$\bar{V}_{\text{ss}} = \frac{1}{8\eta C} \left(\sqrt{1 + 8\eta C(2C + 2\bar{n} + 1)} + 1 \right) \geq \frac{2C + 1}{4C} > \frac{1}{2} \quad (\text{C.47})$$

$$\approx \frac{1}{2} \sqrt{\frac{C_q + 1}{\eta C_q}}. \quad (\text{C.48})$$

$$\lambda = \bar{\lambda} = \frac{\gamma}{2} \sqrt{1 + 8\eta C(2C + 2\bar{n} + 1)} \quad (\text{C.49})$$

$$\approx \Gamma \sqrt{4\eta} \sqrt{\frac{C_q + 1}{C_q}}, \quad (\text{C.50})$$

At best prediction and retrodiction prepare and measure coherent states.

c.2.2 *Blue*, $\Delta_{10} = +\omega_m$

$$V_{xx}^{\text{ss}} = \frac{1}{6\eta C} \left(\sqrt{1 + 4\eta C((3 - 2\eta)C + 3\bar{n} + 1)} - 1 \right) + \frac{1}{6} \geq \frac{1}{2} \quad (\text{C.51})$$

$$\approx \frac{1}{3} \sqrt{\frac{(3 - 2\eta)C_q + 3}{\eta C_q}} + \frac{1}{6}, \quad (\text{C.52})$$

$$V_{pp}^{\text{ss}} = \frac{1}{2\eta C} \left(\sqrt{1 + 4\eta C(C + \bar{n} + 1)} - 1 \right) - \frac{1}{2} \geq \frac{1}{2} \quad (\text{C.53})$$

$$\approx \sqrt{\frac{C_q + 1}{\eta C_q}} - \frac{1}{2}, \quad (\text{C.54})$$

$$\bar{V}_{xx}^{\text{ss}} = \frac{1}{6\eta C} \left(\sqrt{1 + 4\eta C((3 - 2\eta)C + 3\bar{n} + 1)} + 1 \right) - \frac{1}{6} > \frac{1}{6} \quad (\text{C.55})$$

$$\approx \frac{1}{3} \sqrt{\frac{(3 - 2\eta)C_q + 3}{\eta C_q}} - \frac{1}{6}, \quad (\text{C.56})$$

$$\bar{V}_{pp}^{\text{ss}} = \frac{1}{2\eta C} \left(\sqrt{1 + 4\eta C(C + \bar{n} + 1)} + 1 \right) + \frac{1}{2} > \frac{3}{2} \quad (\text{C.57})$$

$$\approx \sqrt{\frac{C_q + 1}{\eta C_q}} + \frac{1}{2}. \quad (\text{C.58})$$

Prediction yields at best coherent states. Retrodictive squeezing requires $C_q > 1$ and $\eta > 1/2$:

$$\bar{V}_{xx}^{\text{ss}} < \frac{1}{2} \quad \Leftrightarrow \quad \eta > \frac{C + \bar{n} + 1}{2C} = \frac{C_q + 1}{2C_q} \quad (\text{C.59})$$

$$\lambda_x = \bar{\lambda}_x = \frac{\gamma}{2} \sqrt{1 + 4\eta C((3 - 2\eta)C + 3\bar{n} + 1)} \quad (\text{C.60})$$

$$\approx \Gamma \sqrt{\eta} \sqrt{\frac{((3 - 2\eta)C_q + 3)}{C_q}}, \quad (\text{C.61})$$

$$\lambda_p = \bar{\lambda}_p = \frac{\gamma}{2} \sqrt{1 + 4\eta C(C + \bar{n} + 1)} \quad (\text{C.62})$$

$$\approx \Gamma \sqrt{\eta} \sqrt{\frac{C_q + 1}{C_q}}. \quad (\text{C.63})$$

C.2.3 *Red*, $\Delta_{\text{lo}} = -\omega_m$

$$V_{xx}^{\text{ss}} = \frac{1}{6\eta C} \left(\sqrt{1 + 4\eta C((3 - 2\eta)C + 3\bar{n} + 2)} - 1 \right) - \frac{1}{6} > \frac{1}{6} \quad (\text{C.64})$$

$$\approx \frac{1}{3} \sqrt{\frac{(3 - 2\eta)C_q + 3}{\eta C_q}} - \frac{1}{6}, \quad (\text{C.65})$$

$$V_{pp}^{\text{ss}} = \frac{1}{2\eta C} \left(\sqrt{1 + 4\eta C(C + \bar{n})} - 1 \right) + \frac{1}{2} > \frac{3}{2} \quad (\text{C.66})$$

$$\approx \sqrt{\frac{C_q + 1}{\eta C_q}} + \frac{1}{2}, \quad (\text{C.67})$$

$$\bar{V}_{xx}^{\text{ss}} = \frac{1}{6\eta C} \left(\sqrt{1 + 4\eta C((3 - 2\eta)C + 3\bar{n} + 2)} + 1 \right) + \frac{1}{6} > \frac{1}{2} \quad (\text{C.68})$$

$$\approx \frac{1}{3} \sqrt{\frac{(3 - 2\eta)C_q + 3}{\eta C_q}} + \frac{1}{6}, \quad (\text{C.69})$$

$$\bar{V}_{pp}^{\text{ss}} = \frac{1}{2\eta C} \left(\sqrt{1 + 4\eta C(C + \bar{n})} + 1 \right) - \frac{1}{2} > \frac{1}{2} \quad (\text{C.70})$$

$$\approx \frac{1}{2} \sqrt{\frac{C_q + 1}{\eta C_q}} - \frac{1}{2}. \quad (\text{C.71})$$

Predictive squeezing requires $C_q > 1$ and $\eta > 1/2$:

$$V_{xx}^{\text{ss}} < \frac{1}{2} \quad \Leftrightarrow \quad \eta > \frac{C + \bar{n}}{2C} \approx \frac{C_q + 1}{2C_q} \quad (\text{C.72})$$

$$\lambda_x = \bar{\lambda}_x = \frac{\gamma}{2} \sqrt{1 + 4\eta C((3 - 2\eta)C + 3\bar{n} + 2)} \quad (\text{C.73})$$

$$\approx \Gamma \sqrt{\eta} \sqrt{\frac{(3 - 2\eta)C_q + 3}{C_q}}, \quad (\text{C.74})$$

$$\lambda_p = \bar{\lambda}_p = \frac{\gamma}{2} \sqrt{1 + 4\eta C(C + \bar{n})} \quad (\text{C.75})$$

$$\approx \Gamma \sqrt{\eta} \sqrt{\frac{C_q + 1}{C_q}}. \quad (\text{C.76})$$

C.3 DRIVE OFF-RESONANTLY

We now consider $\Delta_c \neq 0$. We start from Eq. (8.31) and again consider the three cases of resonant detection $\Delta_{\text{lo}} = 0$ and sideband detection $\Delta_{\text{lo}} = \pm\omega_{\text{eff}}$. Since the dissipation qualitatively does not change compared to the case of resonant driving we only consider what happens to the measurement operators. Recall the definition

$$\Gamma_{\pm} := g^2 \kappa |\eta_{\pm}|^2 = \frac{g^2 \kappa}{(\kappa/2)^2 + (-\Delta_c \pm \omega_m)^2}. \quad (\text{C.77})$$

c.3.1 Resonant detection, $\Delta_{\text{lo}} = 0$

After coarse-graining we again find a sine and cosine component of the photocurrent, which enter the master equation as

$$\sqrt{\frac{\eta}{2}} \mathcal{H} [\sqrt{\Gamma_+} \hat{a}^\dagger + \sqrt{\Gamma_-} \hat{a}] dW_c + \sqrt{\frac{\eta}{2}} \mathcal{H} [i\sqrt{\Gamma_+} \hat{a}^\dagger - i\sqrt{\Gamma_-} \hat{a}] dW_s. \quad (\text{C.78})$$

This yields measurement matrices

$$A = \sqrt{\eta} S_+ \mathbf{1}_2, \quad B = \sqrt{\eta} S_- \sigma, \quad (\text{C.79})$$

with

$$S_\pm := \frac{\sqrt{\Gamma_-} \pm \sqrt{\Gamma_+}}{2}, \quad (\text{C.80})$$

such that $2(S_-^2 + S_+^2) = \Gamma_- + \Gamma_+$ and $4S_- S_+ = \Gamma_- - \Gamma_+$, and in case of resonant driving ($\Delta_c \rightarrow 0$) one finds $S_- \rightarrow 0$ and $S_+ \rightarrow \sqrt{\Gamma}$. We also introduce the dimensionless quantities $s_\pm = S_\pm / \sqrt{\gamma}$. In steady state we then find $V_{xp}^{\text{ss}} = 0$ and equal variances

$$\begin{aligned} V_{xx}^{\text{ss}} &= V_{pp}^{\text{ss}} \\ &= \frac{1}{8\eta s_+^2} \left(-1 - (1 - \eta) 4s_- s_+ \right. \\ &\quad \left. + \sqrt{(1 - \eta)(4s_- s_+ + 1)^2 + \eta + 8\eta s_+^2 (2s_+^2 + 2\bar{n} + 1)} \right). \end{aligned} \quad (\text{C.81})$$

The diagonal drift matrix $M_{\text{ss}} = -\lambda \mathbf{1}_2$ is strictly stable with

$$\lambda = \frac{\gamma}{2} \sqrt{(1 - \eta)(4s_- s_+ + 1)^2 + \eta + 8\eta s_+^2 (2s_+^2 + 2\bar{n} + 1)}, \quad (\text{C.83})$$

and the mode functions are $f_{xs} = f_{ps} = 0$ and

$$\tilde{f}_{xc}(t) = \tilde{f}_{ps}(t) = \sqrt{\eta} e^{-\lambda t} (2S_+ V_{xx}^{\text{ss}} - S_-). \quad (\text{C.84})$$

Backward we find the same results except

$$\begin{aligned} \bar{V}_{xx}^{\text{ss}} &= \bar{V}_{pp}^{\text{ss}} \\ &= \frac{1}{8\eta s_+^2} \left(1 + (1 - \eta) 4s_- s_+ \right. \\ &\quad \left. + \sqrt{(1 - \eta)(4s_- s_+ + 1)^2 + \eta + 8\eta s_+^2 (2s_+^2 + 2\bar{n} + 1)} \right). \end{aligned} \quad (\text{C.85})$$

There is obviously no squeezing (symmetric variances) since

$$V_{xx}^{\text{ss}} \geq \frac{1}{2}, \quad \bar{V}_{xx}^{\text{ss}} \geq \frac{2s_+^2 + 1}{4s_+^2} > \frac{1}{2}. \quad (\text{C.87})$$

C.3.2 Blue sideband, $\Delta_{\text{lo}} = +\omega_{\text{eff}}$

After coarse-graining we again find a resonant as well as sine and cosine components oscillating at $2\omega_{\text{eff}}$,

$$\begin{aligned} & \mathcal{H} \left[\sqrt{\eta\Gamma^-} \hat{a} \right] dW_0(t) \\ & + \mathcal{H} \left[\sqrt{\frac{\eta\Gamma_+}{2}} \hat{a}^\dagger \right] dW_{c,2}(t) + \mathcal{H} \left[i \sqrt{\frac{\eta\Gamma_+}{2}} \hat{a}^\dagger \right] dW_{s,2}(t). \end{aligned} \quad (\text{C.88})$$

This yields measurement matrices

$$A = \frac{\sqrt{\eta}}{2} \begin{bmatrix} \sqrt{2\Gamma^-} & 0 \\ \sqrt{\Gamma_+} & 0 \\ 0 & \sqrt{\Gamma_+} \end{bmatrix}, \quad B = \frac{\sqrt{\eta}}{2} \begin{bmatrix} 0 & \sqrt{2\Gamma^-} \\ 0 & -\sqrt{\Gamma_+} \\ \sqrt{\Gamma_+} & 0 \end{bmatrix}. \quad (\text{C.89})$$

We introduce dimensionless parameters $C_\pm = \Gamma_\pm/\gamma$ which in case of a resonant drive ($\Delta_c \rightarrow 0$) become the classical cooperativity. In steady state we then find $V_{xp}^{\text{ss}} = 0$ and variances

$$\begin{aligned} V_{xx}^{\text{ss}} &= \frac{1}{2\eta(2C_- + C_+)} \left(-1 - (1 - 2\eta)C_- + (1 - \eta)C_+ \right. \\ & \left. + \sqrt{(C_- - C_+ + 1)^2 + 4\eta(3 - 2\eta)C_-C_+ + 4\eta C_+(\bar{n} + 1) + 8\bar{n}\eta C_-} \right) \end{aligned} \quad (\text{C.90})$$

$$\begin{aligned} V_{pp}^{\text{ss}} &= \frac{1}{2\eta C_+} \left(-1 - C_- + (1 - \eta)C_+ \right. \\ & \left. + \sqrt{(C_- - C_+ + 1)^2 + 4\eta C_+(C_- + \bar{n} + 1)} \right). \end{aligned} \quad (\text{C.91})$$

The diagonal drift matrix $M_{\text{ss}} = -\text{diag}(\lambda_x, \lambda_p)$ is strictly stable with

$$\lambda_x = \frac{\gamma}{2} \sqrt{(C_- - C_+ + 1)^2 + 4\eta(3 - 2\eta)C_-C_+ + 4\eta C_+(\bar{n} + 1) + 8\bar{n}\eta C_-}, \quad (\text{C.92})$$

$$\lambda_p = \frac{\gamma}{2} \sqrt{(C_- - C_+ + 1)^2 + 4\eta C_+(C_- + \bar{n} + 1)}, \quad (\text{C.93})$$

and the mode functions are

$$f_{x|0}(t) = \sqrt{\frac{\eta\Gamma^-}{2}} e^{-\lambda_x t} (2V_{xx}^{\text{ss}} - 1), \quad f_{p|0}(t) = 0, \quad (\text{C.94})$$

$$f_{x|c,2}(t) = \sqrt{\frac{\eta\Gamma_+}{2}} e^{-\lambda_x t} \frac{2V_{xx}^{\text{ss}} + 1}{\sqrt{2}}, \quad f_{p|c,2}(t) = 0, \quad (\text{C.95})$$

$$f_{x|s,2}(t) = 0, \quad f_{p|s,2}(t) = \sqrt{\frac{\eta\Gamma_+}{2}} e^{-\lambda_p t} \frac{2V_{pp}^{\text{ss}} + 1}{\sqrt{2}}. \quad (\text{C.96})$$

Backward we find $V_{xp}^{\text{ss}} = 0$ and

$$\begin{aligned} \bar{V}_{xx}^{\text{ss}} &= \frac{1}{2\eta(2C_- + C_+)} \left(1 + (1 - 2\eta)C_- - (1 - \eta)C_+ \right. \\ &\quad \left. + \sqrt{(C_- - C_+ + 1)^2 + 4\eta(3 - 2\eta)C_-C_+ + 4\eta C_+(\bar{n} + 1) + 8\bar{n}\eta C_-} \right) \end{aligned} \quad (\text{C.97})$$

$$\begin{aligned} \bar{V}_{pp}^{\text{ss}} &= \frac{1}{2\eta C_+} \left(1 + C_- - (1 - \eta)C_+ \right. \\ &\quad \left. + \sqrt{(C_- - C_+ + 1)^2 + 4\eta C_+(C_- + \bar{n} + 1)} \right). \end{aligned} \quad (\text{C.98})$$

The drift matrix is the same as in the forward case, and the mode functions are

$$\bar{f}_{x|0}(t) = \sqrt{\frac{\eta\Gamma_-}{2}} e^{-\lambda_x t} (2\bar{V}_{xx}^{\text{ss}} + 1), \quad \bar{f}_{p|0}(t) = 0, \quad (\text{C.99})$$

$$\bar{f}_{x|c,2}(t) = \sqrt{\frac{\eta\Gamma_+}{2}} e^{-\lambda_x t} \frac{2\bar{V}_{xx}^{\text{ss}} - 1}{\sqrt{2}}, \quad \bar{f}_{p|c,2}(t) = 0, \quad (\text{C.100})$$

$$\bar{f}_{x|s,2}(t) = 0, \quad \bar{f}_{p|s,2}(t) = \sqrt{\frac{\eta\Gamma_+}{2}} e^{-\lambda_p t} \frac{2\bar{V}_{pp}^{\text{ss}} - 1}{\sqrt{2}}. \quad (\text{C.101})$$

There is no predictive squeezing since

$$V_{xx}^{\text{ss}} \geq \frac{1}{2}, \quad V_{pp}^{\text{ss}} \geq \frac{1}{2}, \quad (\text{C.102})$$

but for retrodiction one finds

$$V_{xx}^E \geq \frac{2 + C_+}{4C_- + 2C_+} > 0, \quad \bar{V}_{pp}^{\text{ss}} \geq \frac{1}{2} + \frac{C_- + 1}{C_+} > \frac{1}{2}, \quad (\text{C.103})$$

and we see that a necessary requirement for $V_{xx}^E < \frac{1}{2}$ is $C_- > 1$.

c.3.3 Red sideband, $\Delta_{l0} = -\omega_{\text{eff}}$

After coarse-graining we again find a resonant as well as sine and cosine components oscillating at $2\omega_{\text{eff}}$,

$$\begin{aligned} &\mathcal{H} \left[\sqrt{\eta\Gamma_+} \hat{a}^\dagger \right] dW_0(t) \\ &+ \mathcal{H} \left[\sqrt{\frac{\eta\Gamma_-}{2}} \hat{a} \right] dW_{c,2}(t) + \mathcal{H} \left[-i\sqrt{\frac{\eta\Gamma_-}{2}} \hat{a} \right] dW_{s,2}(t), \end{aligned} \quad (\text{C.104})$$

which are related to the measurement operators of the red detection scheme through Hermitian conjugation and exchanging Γ_{\pm} . We thus find the measurement matrices

$$A = \frac{\sqrt{\eta}}{2} \begin{bmatrix} \sqrt{2\Gamma_+} & 0 \\ \sqrt{\Gamma_-} & 0 \\ 0 & \sqrt{\Gamma_-} \end{bmatrix}, \quad B = \frac{\sqrt{\eta}}{2} \begin{bmatrix} 0 & -\sqrt{2\Gamma_+} \\ 0 & \sqrt{\Gamma_-} \\ -\sqrt{\Gamma_-} & 0 \end{bmatrix}. \quad (\text{C.105})$$

In terms of $C_{\pm} = \Gamma_{\pm}/\gamma$ we find $V_{xp}^{\text{ss}} = 0$ and

$$V_{xx}^{\text{ss}} = \frac{1}{2\eta(C_- + 2C_+)} \left(-1 - (1 - \eta)C_- + (1 - 2\eta)C_+ \right. \\ \left. + \sqrt{(C_- - C_+ + 1)^2 + 4\eta(3 - 2\eta)C_-C_+ + 8\eta C_+(\bar{n} + 1) + 4\bar{n}\eta C_-} \right) \quad (\text{C.106})$$

$$V_{pp}^{\text{ss}} = \frac{1}{2\eta C_-} \left(-1 - (1 - \eta)C_- + C_+ \right) \quad (\text{C.107})$$

$$+ \sqrt{(C_- - C_+ + 1)^2 + 4\eta C_-(C_+ + \bar{n})}. \quad (\text{C.108})$$

The diagonal drift matrix $M_{\text{ss}} = -\text{diag}(\lambda_x, \lambda_p)$ is strictly stable with

$$\lambda_x = \frac{\gamma}{2} \sqrt{(C_- - C_+ + 1)^2 + 4\eta(3 - 2\eta)C_-C_+ + 8\eta C_+(\bar{n} + 1) + 4\bar{n}\eta C_-}, \quad (\text{C.109})$$

$$\lambda_p = \frac{\gamma}{2} \sqrt{(C_- - C_+ + 1)^2 + 4\eta C_-(C_+ + \bar{n})}, \quad (\text{C.110})$$

and the mode functions are

$$f_{x|0}(t) = \sqrt{\frac{\eta\Gamma_-}{2}} e^{-\lambda_x t} (2V_{xx}^{\text{ss}} + 1), \quad f_{p|0}(t) = 0, \quad (\text{C.111})$$

$$f_{x|c,2}(t) = \sqrt{\frac{\eta\Gamma_+}{2}} e^{-\lambda_x t} \frac{2V_{xx}^{\text{ss}} - 1}{\sqrt{2}}, \quad f_{p|c,2}(t) = 0, \quad (\text{C.112})$$

$$f_{x|s,2}(t) = 0, \quad f_{p|s,2}(t) = \sqrt{\frac{\eta\Gamma_+}{2}} e^{-\lambda_p t} \frac{2V_{pp}^{\text{ss}} - 1}{\sqrt{2}}. \quad (\text{C.113})$$

Backward we find $V_{xp}^{\text{ss}} = 0$ and

$$\bar{V}_{xx}^{\text{ss}} = \frac{1}{2\eta(C_- + 2C_+)} \left(1 + (1 - \eta)C_- - (1 - 2\eta)C_+ \right. \\ \left. + \sqrt{(C_- - C_+ + 1)^2 + 4\eta(3 - 2\eta)C_-C_+ + 8\eta C_+(\bar{n} + 1) + 4\bar{n}\eta C_-} \right) \quad (\text{C.114})$$

$$\bar{V}_{pp}^{\text{ss}} = \frac{1}{2\eta C_-} \left(1 + (1 - \eta)C_- - C_+ \right. \\ \left. + \sqrt{(C_- - C_+ + 1)^2 + 4\eta C_-(C_+ + \bar{n})} \right). \quad (\text{C.115})$$

The drift matrix is the same as in the forward case, and the mode functions are

$$\bar{f}_{x|0}(t) = \sqrt{\frac{\eta\Gamma_-}{2}} e^{-\lambda_x t} (2\bar{V}_{xx}^{\text{ss}} - 1), \quad \bar{f}_{p|0}(t) = 0, \quad (\text{C.116})$$

$$\bar{f}_{x|c,2}(t) = \sqrt{\frac{\eta\Gamma_+}{2}} e^{-\lambda_x t} \frac{2\bar{V}_{xx}^{\text{ss}} + 1}{\sqrt{2}}, \quad \bar{f}_{p|c,2}(t) = 0, \quad (\text{C.117})$$

$$\bar{f}_{x|s,2}(t) = 0, \quad \bar{f}_{p|s,2}(t) = \sqrt{\frac{\eta\Gamma_+}{2}} e^{-\lambda_p t} \frac{2\bar{V}_{pp}^{\text{ss}} + 1}{\sqrt{2}}. \quad (\text{C.118})$$

For prediction we find

$$V_{xx}^{\text{ss}} \geq \frac{1}{1 + C_+ + \sqrt{1 + C_+(6 + C_+)}} > 0, \quad V_{pp}^{\text{ss}} \geq \frac{1}{2}, \quad (\text{C.119})$$

with $V_{xx}^{\text{ss}} < 1/2$ whenever $\eta > (C_q^+ + 1)/(2C_q^+)$, where $C_q^+ = C_+/\bar{n}$. For retrodiction one finds no squeezing since

$$V_{xx}^E \geq \frac{1}{2} + \frac{1}{C_-} > \frac{1}{2}, \quad \bar{V}_{pp}^{\text{ss}} \geq \frac{1}{2} + \frac{C_- + 1}{C_+} > \frac{1}{2}. \quad (\text{C.120})$$

C.4 SUMMARY

Generally: $V_{xp}^{\text{ss}} = 0$ and “ \approx ” refers to $C_{\pm}, \bar{n}, \eta C_{\pm} \gg 1$. Also $C_q^{\pm} = C_{\pm}/(\bar{n} + 1) \approx C_{\pm}/\bar{n}$.

c.4.1 Resonant detection, $\Delta_{\text{lo}} = 0$

$$\begin{aligned} V_{\text{ss}} &:= V_{xx}^{\text{ss}} = V_{pp}^{\text{ss}} && (\text{C.121}) \\ &= \frac{1}{8\eta s_+^2} \left(-1 - (1 - \eta)4s_{-s_+} \right. \\ &\quad \left. + \sqrt{(1 - \eta)(4s_{-s_+} + 1)^2 + \eta + 8\eta s_+^2(2s_+^2 + 2\bar{n} + 1)} \right) \geq \frac{1}{2} && (\text{C.122}) \end{aligned}$$

$$\begin{aligned} \bar{V}_{\text{ss}} &= \frac{1}{8\eta s_+^2} \left(1 + (1 - \eta)4s_{-s_+} \right. \\ &\quad \left. + \sqrt{(1 - \eta)(4s_{-s_+} + 1)^2 + \eta + 8\eta s_+^2(2s_+^2 + 2\bar{n} + 1)} \right) \geq \frac{1}{2}, && (\text{C.123}) \end{aligned}$$

C.4.2 *Blue*, $\Delta_{lo} = +\omega_m$

$$V_{xx}^{ss} = \frac{1}{2\eta(2C_- + C_+)} \left(-1 - (1 - 2\eta)C_- + (1 - \eta)C_+ \right. \\ \left. + \sqrt{(C_- - C_+ + 1)^2 + 4\eta(3 - 2\eta)C_-C_+ + 4\eta C_+(\bar{n} + 1) + 8\bar{n}\eta C_-} \right), \quad (\text{C.124})$$

$$V_{pp}^{ss} = \frac{1}{2\eta C_+} \left(-1 - C_- + (1 - \eta)C_+ \right. \\ \left. + \sqrt{(C_- - C_+ + 1)^2 + 4\eta C_+(C_- + \bar{n} + 1)} \right), \quad (\text{C.125})$$

$$\bar{V}_{xx}^{ss} = \frac{1}{2\eta(2C_- + C_+)} \left(1 + (1 - 2\eta)C_- - (1 - \eta)C_+ \right. \\ \left. + \sqrt{(C_- - C_+ + 1)^2 + 4\eta(3 - 2\eta)C_-C_+ + 4\eta C_+(\bar{n} + 1) + 8\bar{n}\eta C_-} \right), \quad (\text{C.126})$$

$$\bar{V}_{pp}^{ss} = \frac{1}{2\eta C_+} \left(1 + C_- - (1 - \eta)C_+ \right. \\ \left. + \sqrt{(C_- - C_+ + 1)^2 + 4\eta C_+(C_- + \bar{n} + 1)} \right). \quad (\text{C.127})$$

$$V_{xx}^{ss} \geq \frac{1}{2}, \quad \bar{V}_{xx}^{ss} > 0, \quad (\text{C.128})$$

$$V_{pp}^{ss} \geq \frac{1}{2}, \quad \bar{V}_{pp}^{ss} > \frac{1}{2}, \quad (\text{C.129})$$

No predictive squeezing and retrodictive squeezing requires $C_q^- > 1$ and $\eta > 1/2$ with

$$\bar{V}_{xx}^{ss} < \frac{1}{2} \quad \Leftrightarrow \quad \eta > \frac{C_- + \bar{n} + 1}{2C_-} = \frac{C_q^- + 1}{2C_q^-}. \quad (\text{C.130})$$

c.4.3 *Red*, $\Delta_{10} = -\omega_m$

$$V_{xx}^{ss} = \frac{1}{2\eta(C_- + 2C_+)} \left(-1 - (1 - \eta)C_- + (1 - 2\eta)C_+ \right. \\ \left. + \sqrt{(C_- - C_+ + 1)^2 + 4\eta(3 - 2\eta)C_-C_+ + 8\eta C_+(\bar{n} + 1) + 4\bar{n}\eta C_-} \right) \quad (\text{C.131})$$

$$V_{pp}^{ss} = \frac{1}{2\eta C_-} \left(-1 - (1 - \eta)C_- + C_+ \right) \quad (\text{C.132})$$

$$+ \sqrt{(C_- - C_+ + 1)^2 + 4\eta C_-(C_+ + \bar{n})}, \quad (\text{C.133})$$

$$\bar{V}_{xx}^{ss} = \frac{1}{2\eta(C_- + 2C_+)} \left(1 + (1 - \eta)C_- - (1 - 2\eta)C_+ \right. \\ \left. + \sqrt{(C_- - C_+ + 1)^2 + 4\eta(3 - 2\eta)C_-C_+ + 8\eta C_+(\bar{n} + 1) + 4\bar{n}\eta C_-} \right) \quad (\text{C.134})$$

$$\bar{V}_{pp}^{ss} = \frac{1}{2\eta C_-} \left(1 + (1 - \eta)C_- - C_+ \right) \quad (\text{C.135})$$

$$+ \sqrt{(C_- - C_+ + 1)^2 + 4\eta C_-(C_+ + \bar{n})}. \quad (\text{C.136})$$

$$V_{xx}^{ss} > 0, \quad \bar{V}_{xx}^{ss} > \frac{1}{2}, \quad (\text{C.137})$$

$$V_{pp}^{ss} \geq \frac{1}{2}, \quad \bar{V}_{pp}^{ss} > \frac{1}{2}, \quad (\text{C.138})$$

No retrodictive squeezing and predictive squeezing requires $C_q^+ > 1$ and $\eta > 1/2$ with

$$V_{xx}^{ss} < \frac{1}{2} \quad \Leftrightarrow \quad \eta > \frac{C_+ + \bar{n}}{2C_+} = \frac{C_q^+ + 1}{2C_q^+}. \quad (\text{C.139})$$

BIBLIOGRAPHY

- [1] J. von Neumann. *Mathematische Grundlagen der Quantenmechanik*. Berlin, Heidelberg: Springer Berlin Heidelberg, 1996. DOI: 10.1007/978-3-642-61409-5.
- [2] H. M. Wiseman and G. J. Milburn. *Quantum Measurement and Control*. Cambridge: Cambridge University Press, 2010.
- [3] D. J. Wineland. *Superposition, entanglement, and raising Schrödinger's cat*. *Annalen der Physik* **525**, 739 (2013). DOI: 10.1002/andp.201300736.
- [4] S. Haroche. *Nobel Lecture: Controlling photons in a box and exploring the quantum to classical boundary*. *Reviews of Modern Physics* **85**, 1083 (2013). DOI: 10.1103/RevModPhys.85.1083.
- [5] V. P. Belavkin. *Quantum stochastic calculus and quantum nonlinear filtering*. *Journal of Multivariate Analysis* **42**, 171 (1992). DOI: 10.1016/0047-259X(92)90042-E. arXiv: math/0512362.
- [6] R. L. Hudson and K. R. Parthasarathy. *Quantum Ito's formula and stochastic evolutions*. *Communications in Mathematical Physics* **93**, 301 (1984). DOI: 10.1007/BF01258530.
- [7] H. M. Wiseman and G. J. Milburn. *Quantum theory of field quadrature measurements*. *Physical Review A* **47**, 642 (1993).
- [8] K. W. Murch et al. *Observing single quantum trajectories of a superconducting quantum bit*. *Nature* **502**, 211 (2013). DOI: 10.1038/nature12539. arXiv: 1305.7270.
- [9] N. Roch et al. *Observation of Measurement-Induced Entanglement and Quantum Trajectories of Remote Superconducting Qubits*. *Physical Review Letters* **112**, 170501 (2014). DOI: 10.1103/PhysRevLett.112.170501.
- [10] A. Kubanek et al. *Photon-by-photon feedback control of a single-atom trajectory*. *Nature* **462**, 898 (2009). DOI: 10.1038/nature08563.
- [11] E. Bimbard et al. *Homodyne Tomography of a Single Photon Retrieved on Demand from a Cavity-Enhanced Cold Atom Memory*. *Physical Review Letters* **112**, 033601 (2014). DOI: 10.1103/PhysRevLett.112.033601. arXiv: 1310.1228.
- [12] C. B. Møller et al. *Quantum back-action-evading measurement of motion in a negative mass reference frame*. *Nature* **547**, 191 (2017). DOI: 10.1038/nature22980. arXiv: 1608.03613.
- [13] H. Krauter et al. *Entanglement Generated by Dissipation and Steady State Entanglement of Two Macroscopic Objects*. *Physical Review Letters* **107**, 080503 (2011). DOI: 10.1103/PhysRevLett.107.080503. arXiv: 1006.4344.
- [14] M. Rossi et al. *Measurement-based quantum control of mechanical motion*. 2018. arXiv: 1805.05087. URL: <http://arxiv.org/abs/1805.05087>.

- [15] S. D. Barrett and P. Kok. *Efficient high-fidelity quantum computation using matter qubits and linear optics*. Physical Review A **71**, 060310 (2005). DOI: 10.1103/PhysRevA.71.060310. arXiv: quant-ph/0408040.
- [16] Y. L. Lim, A. Beige, and L. C. Kwek. *Repeat-until-success linear optics distributed quantum computing*. Physical Review Letters **95**, 1 (2005). DOI: 10.1103/PhysRevLett.95.030505. arXiv: quant-ph/0408043.
- [17] Y. L. Lim et al. *Repeat-until-success quantum computing using stationary and flying qubits*. Physical Review A **73**, 012304 (2006). DOI: 10.1103/PhysRevA.73.012304. arXiv: quant-ph/0508218.
- [18] K. G. H. Vollbrecht and J. I. Cirac. *Quantum simulations based on measurements and feedback control*. Physical Review A **79**, 042305 (2009). DOI: 10.1103/PhysRevA.79.042305. arXiv: 0811.1844.
- [19] H. M. Wiseman and G. J. Milburn. *Quantum theory of optical feedback via homodyne detection*. Physical Review Letters **70**, 548 (1993). DOI: 10.1103/PhysRevLett.70.548.
- [20] H. M. Wiseman. *Quantum theory of continuous feedback*. Physical Review A **49**, 2133 (1994). DOI: 10.1103/PhysRevA.49.2133.
- [21] M. Tsang. *Time-Symmetric Quantum Theory of Smoothing*. Physical Review Letters **102**, 250403 (2009). DOI: 10.1103/PhysRevLett.102.250403. arXiv: 0904.1969.
- [22] M. Tsang. *Optimal waveform estimation for classical and quantum systems via time-symmetric smoothing*. Physical Review A **80**, 033840 (2009). DOI: 10.1103/PhysRevA.80.033840. arXiv: 0909.2432.
- [23] M. Tsang. *Optimal waveform estimation for classical and quantum systems via time-symmetric smoothing. II. Applications to atomic magnetometry and Hardy's paradox*. Physical Review A **81**, 013824 (2010). DOI: 10.1103/PhysRevA.81.013824. arXiv: 0909.2432.
- [24] S. Gammelmark, B. Julsgaard, and K. Mølmer. *Past Quantum States of a Monitored System*. Physical Review Letters **111**, 160401 (2013). DOI: 10.1103/PhysRevLett.111.160401. arXiv: 1305.0681.
- [25] D. Tan et al. *Prediction and Retrodiction for a Continuously Monitored Superconducting Qubit*. Physical Review Letters **114**, 090403 (2015). DOI: 10.1103/PhysRevLett.114.090403. arXiv: 1409.0510.
- [26] S. J. Weber et al. *Quantum trajectories of superconducting qubits*. Comptes Rendus Physique **17**, 766 (2016). DOI: 10.1016/j.crhy.2016.07.007.
- [27] J. Zhang and K. Mølmer. *Prediction and retrodiction with continuously monitored Gaussian states*. Physical Review A **96**, 062131 (2017). DOI: 10.1103/PhysRevA.96.062131. arXiv: 1710.04950.
- [28] I. Guevara and H. Wiseman. *Quantum State Smoothing*. Physical Review Letters **115**, 180407 (2015). DOI: 10.1103/PhysRevLett.115.180407. arXiv: 1503.02799.

- [29] J. Lammers, H. Weimer, and K. Hammerer. *Open-system many-body dynamics through interferometric measurements and feedback*. Physical Review A **94**, 052120 (2016). DOI: 10.1103/PhysRevA.94.052120. arXiv: 1606.04475.
- [30] S. G. Hofer et al. *Time-continuous bell measurements*. Physical Review Letters **111**, 170404 (2013). DOI: 10.1103/PhysRevLett.111.170404. arXiv: 1303.4976.
- [31] E. Pardoux. *Équations du filtrage non linéaire de la prédiction et du lissage*. Stochastics **6**, 193 (1982). DOI: 10.1080/17442508208833204.
- [32] D. F. Kuznetsov. *Multiple Ito and Stratonovich Stochastic Integrals: Fourier-Legendre and Trigonometric Expansions, Approximations, Formulas*. Differential Equations and Control Processes **1** (2017).
- [33] S. G. Hofer and K. Hammerer. *Entanglement-enhanced time-continuous quantum control in optomechanics*. Physical Review A **91**, 033822 (2015). DOI: 10.1103/PhysRevA.91.033822. arXiv: 1411.1337.
- [34] S. G. Hofer. *Quantum Control of Optomechanical Systems*. PhD thesis. Universität Wien [Link], 2015.
- [35] M. A. Nielsen and I. L. Chuang. *Quantum Computation and Quantum Information*. Cambridge: Cambridge University Press, 2010, 702. DOI: 10.1017/CB09780511976667. arXiv: 1011.1669v3.
- [36] K. Jacobs. *Quantum Measurement Theory and its Applications*. Cambridge: Cambridge University Press, 2014, 554. DOI: 10.1017/CB09781139179027.
- [37] T. Heinosaari and M. Ziman. *Guide to mathematical concepts of quantum theory*. Acta Physica Slovaca. Reviews and Tutorials **58**, 188 (2008). DOI: 10.2478/v10155-010-0091-y. arXiv: 0810.3536.
- [38] T. Heinosaari and M. Ziman. *The Mathematical language of Quantum Theory*. Cambridge: Cambridge University Press, 2011. DOI: 10.1017/CB09781139031103.
- [39] S. Attal. *Lectures in Quantum Noise Theory*. Unpublished, available online [Link], 2018.
- [40] B. C. Hall. *Quantum Theory for Mathematicians*. Vol. 267. Graduate Texts in Mathematics. New York, NY: Springer New York, 2013. DOI: 10.1007/978-1-4614-7116-5.
- [41] M. M. Wolf. *Quantum channels & operations: Guided tour*. Lecture notes; available online [Link] (2012).
- [42] H. M. Wiseman and G. J. Milburn. *Squeezing via feedback*. Physical Review A **49**, 1350 (1994). DOI: 10.1103/PhysRevA.49.1350.
- [43] C. W. Gardiner, A. S. Parkins, and P. Zoller. *Wave-function quantum stochastic differential equations and quantum-jump simulation methods*. Physical Review A **46**, 4363 (1992). DOI: 10.1103/PhysRevA.46.4363.
- [44] M. J. Collett and C. W. Gardiner. *Squeezing of intracavity and traveling-wave light fields produced in parametric amplification*. Physical Review A **30**, 1386 (1984). DOI: 10.1103/PhysRevA.30.1386.

- [45] C. W. Gardiner and M. J. Collett. *Input and output in damped quantum systems: Quantum stochastic differential equations and the master equation*. Physical Review A **31**, 3761 (1985). DOI: 10.1103/PhysRevA.31.3761.
- [46] C. Gardiner. *Stochastic Methods: A Handbook for the Natural and Social Sciences*. 4th ed. Springer-Verlag Berlin Heidelberg, 2009.
- [47] C. Gardiner and P. Zoller. *Quantum Noise: A Handbook of Markovian and Non-Markovian Quantum Stochastic Methods with Applications to Quantum Optics*. 3rd ed. Springer Series in Synergetics. Springer, 2004.
- [48] L. K. Thomsen, S. Mancini, and H. M. Wiseman. *Spin squeezing via quantum feedback*. Physical Review A **65**, 618011 (2002). DOI: 10.1103/PhysRevA.65.061801. arXiv: quant-ph/0202028.
- [49] M. Aspelmeyer, T. J. Kippenberg, and F. Marquardt. *Cavity optomechanics*. Reviews of Modern Physics **86**, 1391 (2014). DOI: 10.1103/RevModPhys.86.1391. arXiv: 0712.1618.
- [50] M. E. Peskin and D. V. Schroeder. *An Introduction To Quantum Field Theory*. Westview Press, 1995.
- [51] D. B. Horoshko and S. Y. Kilin. *Direct Detection Feedback for Preserving Quantum Coherence in an Open Cavity*. Physical Review Letters **78**, 840 (1997). DOI: 10.1103/PhysRevLett.78.840.
- [52] H. M. Wiseman. *Using feedback to eliminate back-action in quantum measurements*. Physical Review A **51**, 2459 (1995). DOI: 10.1103/PhysRevA.51.2459.
- [53] M. A. Nielsen. *Conditions for a class of entanglement transformations*. Physical Review Letters **83**, 436 (1999). DOI: 10.1103/PhysRevLett.83.436. arXiv: quant-ph/9811053.
- [54] B. Kraus et al. *Preparation of entangled states by quantum Markov processes*. Physical Review A **78**, 042307 (2008). DOI: 10.1103/PhysRevA.78.042307. arXiv: 0803.1463v3.
- [55] V. Coffman, J. Kundu, and W. K. Wootters. *Distributed entanglement*. Physical Review A **61**, 52306 (2000). DOI: 10.1103/PhysRevA.61.052306. arXiv: quant-ph/9907047.
- [56] T. J. Osborne and F. Verstraete. *General monogamy inequality for bipartite qubit entanglement*. Physical Review Letters **96**, 1 (2006). DOI: 10.1103/PhysRevLett.96.220503. arXiv: quant-ph/0502176.
- [57] J. R. Johansson, P. D. Nation, and F. Nori. *QuTiP: An open-source Python framework for the dynamics of open quantum systems*. Computer Physics Communications **183**, 1760 (2012). DOI: 10.1016/j.cpc.2012.02.021. arXiv: 1211.6518.
- [58] J. R. Johansson, P. D. Nation, and F. Nori. *QuTiP 2: A Python framework for the dynamics of open quantum systems*. Computer Physics Communications **184**, 1234 (2013). DOI: 10.1016/j.cpc.2012.11.019. arXiv: 1211.6518.
- [59] H. Weimer. *Variational principle for steady states of dissipative quantum many-body systems*. Physical Review Letters **114**, 040402 (2015). DOI: 10.1103/PhysRevLett.114.040402. arXiv: 1409.8307.

- [60] H. Weimer. *Variational analysis of driven-dissipative Rydberg gases*. Physical Review A **91**, 063401 (2015). DOI: 10.1103/PhysRevA.91.063401. arXiv: 1501.07284.
- [61] M. B. Plenio and S. S. Virmani. *An Introduction to Entanglement Measures*. Quantum Information & Computation **7**, 1 (2007). arXiv: quant-ph/0504163.
- [62] G. Vidal and R. F. Werner. *Computable measure of entanglement*. Physical Review A **65**, 1 (2002). DOI: 10.1103/PhysRevA.65.032314. arXiv: quant-ph/0102117.
- [63] M. B. Plenio. *Logarithmic negativity: A full entanglement monotone that is not convex*. Physical Review Letters **95**, 5 (2005). DOI: 10.1103/PhysRevLett.95.090503. arXiv: quant-ph/0505071.
- [64] F. Ticozzi and L. Viola. *Stabilizing entangled states with quasi-local quantum dynamical semigroups*. Philosophical Transactions of the Royal Society A: Mathematical, Physical and Engineering Sciences **370**, 5259 (2012). DOI: 10.1098/rsta.2011.0485. arXiv: 1112.4860.
- [65] F. Ticozzi and L. Viola. *Steady-State Entanglement by Engineered Quasi-Local Markovian Dissipation*. 2013. arXiv: 1304.4270. URL: <http://arxiv.org/abs/1304.4270>.
- [66] R. P. Feynman. *Simulating physics with computers*. International Journal of Theoretical Physics **21**, 467 (1982). DOI: 10.1007/BF02650179. arXiv: quant-ph/9508027.
- [67] S. Lloyd. *Universal Quantum Simulators*. Science **273**, 1073 (1996). DOI: 10.1126/science.279.5354.1113h.
- [68] I. Buluta and F. Nori. *Quantum Simulators*. Science **326**, 108 (2009). DOI: 10.1126/science.1177838.
- [69] I. M. Georgescu, S. Ashhab, and F. Nori. *Quantum simulation*. Reviews of Modern Physics **86**, 153 (2014). DOI: 10.1103/RevModPhys.86.153. arXiv: 1308.6253.
- [70] A. A. Houck, H. E. Türeci, and J. Koch. *On-chip quantum simulation with superconducting circuits*. Nature Physics **8**, 292 (2012). DOI: 10.1038/nphys2251.
- [71] B. P. Lanyon et al. *Universal Digital Quantum Simulation with Trapped Ions*. Science **334**, 57 (2011). DOI: 10.1126/science.1208001. arXiv: 1109.1512.
- [72] K. Kim et al. *Quantum simulation of frustrated Ising spins with trapped ions*. Nature **465**, 590 (2010). DOI: 10.1038/nature09071.
- [73] D. Porras and J. I. Cirac. *Effective quantum spin systems with trapped ions*. Physical Review Letters **92**, 207901 (2004). DOI: 10.1103/PhysRevLett.92.207901. arXiv: quant-ph/0401102.
- [74] A. Hu, T. E. Lee, and C. W. Clark. *Spatial correlations of one-dimensional driven-dissipative systems of Rydberg atoms*. Physical Review A **88**, 053627 (2013). DOI: 10.1103/PhysRevA.88.053627. arXiv: 1305.2208.

- [75] C. Ates et al. *Dynamical phases and intermittency of the dissipative quantum Ising model*. Physical Review A **85**, 1 (2012). DOI: 10.1103/PhysRevA.85.043620. arXiv: 1112.4273v2.
- [76] T. E. Lee, H. Häffner, and M. C. Cross. *Antiferromagnetic phase transition in a nonequilibrium lattice of Rydberg atoms*. Physical Review A **84**, 031402 (2011). DOI: 10.1103/PhysRevA.84.031402. arXiv: 1104.0908.
- [77] M. Marcuzzi et al. *Universal nonequilibrium properties of dissipative rydberg gases*. Physical Review Letters **113**, 210401 (2014). DOI: 10.1103/PhysRevLett.113.210401. arXiv: 1406.1015.
- [78] M. Hoening et al. *Antiferromagnetic long-range order in dissipative Rydberg lattices*. Physical Review A **90**, 021603 (2014). DOI: 10.1103/PhysRevA.90.021603. arXiv: 1404.1281v1.
- [79] M. Idel and M. M. Wolf. *Sinkhorn normal form for unitary matrices*. Linear Algebra and Its Applications **471**, 76 (2015). DOI: 10.1016/j.laa.2014.12.031. arXiv: 1408.5728.
- [80] P. Zoller and C. W. Gardiner. *Quantum Noise in Quantum Optics: the Stochastic Schrödinger Equation*. 1997. arXiv: quant-ph/9702030. URL: <http://arxiv.org/abs/quant-ph/9702030>.
- [81] K. Jacobs and D. A. Steck. *A straightforward introduction to continuous quantum measurement*. Contemporary Physics **47**, 279 (2006). DOI: 10.1080/00107510601101934. arXiv: quant-ph/0611067.
- [82] P. Athanasios and S. U. Pillai. *Probability, Random Variables and Stochastic Processes*. 4th ed. Boston: McGraw-Hill, 2002.
- [83] L. Bouten, R. Van Handel, and M. R. James. *An Introduction to Quantum Filtering*. SIAM Journal on Control and Optimization **46**, 2199 (2007). DOI: 10.1137/060651239. arXiv: math/0601741.
- [84] H. M. Wiseman. *Quantum trajectories and quantum measurement theory*. Quantum and Semiclassical Optics: Journal of the European Optical Society Part B **8**, 205 (1996). DOI: 10.1088/1355-5111/8/1/015. arXiv: quant-ph/0302080.
- [85] S. M. Barnett, D. T. Pegg, and J. Jeffers. *Bayes' theorem and quantum retrodiction*. Journal of Modern Optics **47**, 1779 (2000). DOI: 10.1080/09500340008232431. arXiv: quant-ph/0106139.
- [86] S. M. Barnett et al. *Master Equation for Retrodiction of Quantum Communication Signals*. Physical Review Letters **86**, 2455 (2001). DOI: 10.1103/PhysRevLett.86.2455.
- [87] D. T. Pegg, S. M. Barnett, and J. Jeffers. *Quantum retrodiction in open systems*. Physical Review A **66**, 022106 (2002). DOI: 10.1103/PhysRevA.66.022106. arXiv: quant-ph/0208082.
- [88] M. Yanagisawa. *Quantum smoothing*. 2007. arXiv: 0711.3885. URL: <http://arxiv.org/abs/0711.3885>.
- [89] M. Tsang. *A Bayesian quasi-probability approach to inferring the past of quantum observables*. 2014. arXiv: 1403.3353. URL: <http://arxiv.org/abs/1403.3353>.

- [90] C. F. Ockeloen-Korppi et al. *Stabilized entanglement of massive mechanical oscillators*. Nature **556**, 478 (2018). DOI: 10.1038/s41586-018-0038-x. arXiv: 1711.01640.
- [91] S. J. Weber et al. *Mapping the optimal route between two quantum states*. Nature **511**, 570 (2014). DOI: 10.1038/nature13559. arXiv: 1403.4992.
- [92] T. Mikosch. *Elementary Stochastic Calculus, With Finance in View*. Vol. 6. Advanced Series on Statistical Science and Applied Probability. World Scientific Publishing Co. Pte. Ltd., 1998. DOI: 10.1142/9789812386335.
- [93] H. I. Nurdin and N. Yamamoto. *Linear Dynamical Quantum Systems*. Communications and Control Engineering. Springer International Publishing, 2017. DOI: 10.1007/978-3-319-55201-9.
- [94] M. Hillery et al. *Distribution functions in physics: Fundamentals*. Physics Reports **106**, 121 (1984). DOI: 10.1016/0370-1573(84)90160-1.
- [95] S. Barnett and P. Radmore. *Methods in Theoretical Quantum Optics*. Oxford University Press, 1997. DOI: 10.1093/acprof:oso/9780198563617.001.0001.
- [96] G. Adesso, S. Ragy, and A. R. Lee. *Continuous Variable Quantum Information: Gaussian States and Beyond*. Open Systems & Information Dynamics **21**, 1440001 (2014). DOI: 10.1142/S1230161214400010. arXiv: 1401.4679.
- [97] A. Ferraro, S. Olivares, and M. G. A. Paris. *Gaussian states in continuous variable quantum information*. 2005. arXiv: quant-ph/0503237. URL: <http://arxiv.org/abs/quant-ph/0503237>.
- [98] J. Eisert and M. M. Wolf. *Gaussian Quantum Channels*. In: *Quantum Information with Continuous Variables of Atoms and Light*. Published by Imperial College Press and distributed by World Scientific Publishing Co., 2007, 23. DOI: 10.1142/9781860948169_0002. arXiv: quant-ph/0505151.
- [99] X. Wang et al. *Quantum information with Gaussian states*. Physics Reports **448**, 1 (2007). DOI: 10.1016/j.physrep.2007.04.005. arXiv: 0801.4604.
- [100] T. Heinosaari, A. S. Holevo, and M. M. Wolf. *The semigroup structure of Gaussian channels*. Quantum Information and Computation **10**, 0619 (2010). arXiv: 0909.0408.
- [101] J. S. Ivan, M. S. Kumar, and R. Simon. *A measure of non-Gaussianity for quantum states*. Quantum Information Processing **11**, 853 (2012). DOI: 10.1007/s11128-011-0314-2. arXiv: 0812.2800.
- [102] E. Meeron. *Series Expansion of Distribution Functions in Multicomponent Fluid Systems*. The Journal of Chemical Physics **27**, 1238 (1957). DOI: 10.1063/1.1743985.
- [103] G.-C. Rota and J. Shen. *On the Combinatorics of Cumulants*. Journal of Combinatorial Theory, Series A **91**, 283 (2000). DOI: 10.1006/jcta.1999.3017.

- [104] S. Olivares. *Quantum optics in the phase space*. The European Physical Journal Special Topics **203**, 3 (2012). DOI: 10.1140/epjst/e2012-01532-4. arXiv: 1111.0786.
- [105] C. Weedbrook et al. *Gaussian quantum information*. Reviews of Modern Physics **84**, 621 (2012). DOI: 10.1103/RevModPhys.84.621. arXiv: 1110.3234.
- [106] M. G. Genoni, L. Lami, and A. Serafini. *Conditional and unconditional Gaussian quantum dynamics*. Contemporary Physics **57**, 331 (2016). DOI: 10.1080/00107514.2015.1125624. arXiv: 1607.02619.
- [107] D. Grimmer et al. *A classification of open Gaussian dynamics*. Journal of Physics A: Mathematical and Theoretical **51**, 1 (2018). DOI: 10.1088/1751-8121/aac114. arXiv: 1709.07891.
- [108] B. L. Schumaker. *Quantum mechanical pure states with gaussian wave functions*. Physics Reports **135**, 317 (1986). DOI: 10.1016/0370-1573(86)90179-1.
- [109] M. G. A. Paris et al. *Purity of Gaussian states: Measurement schemes and time evolution in noisy channels*. Physical Review A **68**, 012314 (2003). DOI: 10.1103/PhysRevA.68.012314. arXiv: quant-ph/0304059.
- [110] Z. Huang and M. Sarovar. *Smoothing of Gaussian quantum dynamics for force detection*. Physical Review A **97**, 042106 (2018). DOI: 10.1103/PhysRevA.97.042106. arXiv: 1712.00874.
- [111] R. Van Handel. *The Stability of Quantum Markov Filters*. Infinite Dimensional Analysis, Quantum Probability and Related Topics **12**, 153 (2009). DOI: 10.1142/S0219025709003549.
- [112] W. H. Zurek, S. Habib, and J. P. Paz. *Coherent states via decoherence*. Physical Review Letters **70**, 1187 (1993). DOI: 10.1103/PhysRevLett.70.1187.
- [113] Y. Chen. *Macroscopic quantum mechanics: theory and experimental concepts of optomechanics*. Journal of Physics B: Atomic, Molecular and Optical Physics **46**, 104001 (2013). DOI: 10.1088/0953-4075/46/10/104001. arXiv: 1302.1924.
- [114] T. A. Palomaki et al. *Coherent state transfer between itinerant microwave fields and a mechanical oscillator*. Nature **495**, 210 (2013). DOI: 10.1038/nature11915. arXiv: 1206.5562.
- [115] T. A. Palomaki et al. *Entangling Mechanical Motion with Microwave Fields*. Science **342**, 710 (2013). DOI: 10.1126/science.1244563.
- [116] C. F. Ockeloen-Korppi et al. *Quantum Backaction Evading Measurement of Collective Mechanical Modes*. Physical Review Letters **117**, 140401 (2016). DOI: 10.1103/PhysRevLett.117.140401. arXiv: 1608.06152.
- [117] A. D. O'Connell et al. *Quantum ground state and single-phonon control of a mechanical resonator*. Nature **464**, 697 (2010). DOI: 10.1038/nature08967. arXiv: 1602.03841.
- [118] J. D. Teufel et al. *Sideband cooling of micromechanical motion to the quantum ground state*. Nature **475**, 359 (2011). DOI: 10.1038/nature10261. arXiv: 1103.2144.

- [119] J. Chan et al. *Laser cooling of a nanomechanical oscillator into its quantum ground state*. *Nature* **478**, 89 (2011). DOI: 10.1038/nature10461. arXiv: 1106.3614.
- [120] S. Hong et al. *Hanbury Brown and Twiss interferometry of single phonons from an optomechanical resonator*. *Science* **358**, 203 (2017). DOI: 10.1126/science.aan7939. arXiv: 1706.03777.
- [121] F. Khalili et al. *Preparing a Mechanical Oscillator in Non-Gaussian Quantum States*. *Physical Review Letters* **105**, 070403 (2010). DOI: 10.1103/PhysRevLett.105.070403. arXiv: 1001.3738.
- [122] H. Miao et al. *Probing macroscopic quantum states with a sub-Heisenberg accuracy*. *Physical Review A* **81**, 012114 (2010). DOI: 10.1103/PhysRevA.81.012114. arXiv: 0905.3729.
- [123] R. J. Schoelkopf and S. M. Girvin. *Wiring up quantum systems*. *Nature* **451**, 664 (2008). DOI: 10.1038/451664a.
- [124] H. J. Kimble. *The quantum internet*. *Nature* **453**, 1023 (2008). DOI: 10.1038/nature07127. arXiv: 0806.4195.
- [125] D.-G. Welsch, W. Vogel, and T. Opatrný. *II Homodyne Detection and Quantum-State Reconstruction*. In: *Progress in Optics*. 1999, 63. DOI: 10.1016/S0079-6638(08)70389-5. arXiv: 0907.1353.
- [126] M. Paris and J. Řeháček, eds. *Quantum State Estimation*. Vol. 649. *Lecture Notes in Physics*. Berlin, Heidelberg: Springer Berlin Heidelberg, 2004. DOI: 10.1007/b98673.
- [127] B. E. A. Saleh and M. C. Teich. *Fundamentals of Photonics*. *Wiley Series in Pure and Applied Optics*. New York, USA: John Wiley & Sons, Inc., 1991. DOI: 10.1002/0471213748.
- [128] R. Loudon. *The Quantum Theory of Light*. 3rd ed. Oxford: Oxford University Press, 2000.

CURRICULUM VITAE

PERSONAL DATA

Name Jonas Lammers
Born 6 February 1989 in Hannover, Germany
Nationality German
Address Podbielskistr. 176, 30177 Hannover

EDUCATION

Since 2013 Ph. D. in Theoretical Physics
 Leibniz Universität Hannover
 Thesis: *State Preparation and Verification in Continuously Measured Quantum Systems*
 Supervisor: Prof. Dr. K. Hammerer

2012–2013 Study Abroad
 Department of Applied Mathematics
 University of Bristol, UK

2011–2013 M. Sc. Physics
 Leibniz Universität Hannover
 Thesis: *Distribution of the Proper Delay Times of an Andreev Quantum Dot*
 Supervisors: Prof. Dr. R. F. Werner (Hannover) and Prof. Dr. F. Mezzadri (Bristol)

2008–2011 B. Sc. Physics
 Leibniz Universität Hannover
 Thesis: *Zero-Point Energies in Quantum Field Theory and the Cosmological Constant*
 Supervisor: Prof. Dr. M. Zagermann

2004–2005 Study Abroad
 Dondero High School
 Royal Oak, Michigan, USA

2000–2007 Abitur, Hölty Gymnasium Wunstorf

PUBLICATIONS

- [1] J. Lammers and K. Hammerer. *Quantum state retrodiction in Gaussian systems and its application in optomechanics*. In preparation (2018).
- [2] J. Lammers, H. Weimer, and K. Hammerer. *Open-system many-body dynamics through interferometric measurements and feedback*. *Physical Review A* **94**, 052120 (2016). DOI: 10.1103/PhysRevA.94.052120. arXiv: 1606.04475.